From Drought Deficits to Climate Resilience:

Coupled Surface-Groundwater Modelling and Nature-Based Solutions for Drought Assessment and Mitigation

Estifanos Addisu Yimer

Thesis submitted in fulfilment of the requirements for the award of the degree of Doctor of Engineering Sciences (Doctor in de Ingenieurswetenschappen)

Department of Water and Climate
Faculty of Engineering
Vrije Universiteit Brussel

September 2025

Alle rechten voorbehouden. Niets van deze uitgave mag worden vermenigvuldigd en/of openbaar gemaakt worden door middel van druk, fotokopie, microfilm, elektronisch of op welke andere wijze ook, zonder voorafgaande schriftelijke toestemming van de auteur.

All rights reserved. No part of this publication may be produced in any form by print, photoprint, microfilm, electronic or any other means without permission from the author.

Printed by
Crazy Copy Center Productions
VUB Pleinlaan 2, 1050 Brussel
Tel: +32 2 629 33 44
crazycopy@vub.be
www.crazycopy.be

ISBN: 9789493461086
NUR CODE: 943
THEMA: RBK

PhD Jury Composition

Prof. Dr. Ann Van Griensven	Promotor Department of Water and Climate Vrije Universiteit Brussel (VUB), Belgium
Prof. Dr.Ir Jiri Nossent	Co-promotor Department of Water and Climate Vrije Universiteit Brussel (VUB), Belgium
Prof. Dr. Marijke Huysmans	Secretary Department of Water and Climate Vrije Universiteit Brussel (VUB), Belgium
Prof. Dr. Tine Tysmans	Chair Department of Mechanics of Materials and Constructions Vrije Universiteit Brussel (VUB), Belgium
Prof. Dr. Iris De Graeve	Vice-Chair Department of Electrochemical and Surface Engineering Vrije Universiteit Brussel (VUB), Belgium
Prof. Anne Van Loon	External Examiner Water & Climate Risk Group Vrije Universiteit Amsterdam, the Netherlands
Dr.Ir. Syed Mustafa	External Examiner Hydrology and Quantitative Water Management Group Wageningen University & Research, the Netherlands

Acknowledgements

Difficult to write 4 years of my journey in one page but let me try. Guess what its almost 3 am trying to think of all the names so that I will not forget anyone. If I forget your name, please don't take it personally :). Everything starts with God, I would like to give this achievement to the almighty God, his mother St. Mary and all the saints who guided my way to accomplish this PhD thesis.

Next, no one beleived in me more than my parents ever since I was a kid. Both used to say and still says, our boy will be a great academician in the future. So, this PhD thesis is dedicated to my parents, Ato. Addisu Yimer Yenew and Wro. Woinetu Chane Melese. Their prayers day and night keeps my way always positive and successful. Next comes my wonderful brother (Hailemariam) and his amazing wife (Fani) who gave us a hand with my daughter Dania so that I can get focused on writing this thesis. My other siblings; Tigist , Sinkinesh, and Ayenew played a vital role that I would like to acknowledge. I love you all! The whole family in Ethiopia deserves a recognition whose constant support didn't vanish although facing a difficult time in war and unstable economic condition. I hope the situation will get better and war will disappear from the face of the globe.

My beautiful wife Dr. Nuhamin Eshetu is the driving force behind the happy face, successful research career and completion of this PhD thesis, hence, I want to take this chance to thank you sincerely. I love you for being by my side in the highs and lows for the past 10 years. Your gift is multifold but giving birth to our adorable Dania is beyond everything. This enlightens every day of our life though with all the challenge of having a baby while doing a PhD. Our daughter Dania is our bond and this PhD is a witness for our strength to pass difficult times together. Can you imagine, during the PhD, COVID was also a big impact which would have been difficult without you. You are a miracle to the family Nuhueye and surprise surprise, a new addition to the family is also on the way, for those who don't know, let our happiness be yours. I also would like to thank my father (Eshetu) and mother (Keli) in laws. Keli's genuine prayer is top notch and Eshetu's wonderful conversations, great cuisines he creates (enjoy the follow up PhD reception fully made by the great hands of him), prayers and fatherly advice.

I would like to thank the jury members: prof. Marijke Huysmans, prof. Anne Van Loon and Dr.ir. Syed Mustafa for taking their time to read my thesis document and giving their valuable feedback. I also want to thank prof. Dr. Tine Tysmans for chairing my defense.

Nothing would have not been possible without the genuine trust that I got from Ann, who decided to hire me as PhD researcher despite knowing me a bit. What a motherly personality you have and I want to thank you for believing on me and giving me the freedom to explore different topics throughout this journey. Great time we had with you and your beautiful family in Brussels, Antwerp, Mekness, Fez, Paris, Aarhus, Vienna, Berlin, Korea, etc. Speaking of supervisors, I can not thank enough Jiri for firstly supervising my master's thesis and then asking Ann if she can hire me. Your supportive and positive guidance helped me to excel. Your son was born when I was doing my master's thesis and he is growing faster than my salary:). The conversation I have with Hilde is priceless and thank you for your kind support.

When I arrived in the department nearly five years ago, there were only few people (Ghert, Inne, Afnan, Albert, Annabel, Cas, Monica, Yi, Luke, etc.) whose welcoming gesture is highly appreciated. All of them left, but here I am the last survivor :). If any acronym deserves the phrase "A great place to work and such a multinational and diverse environment" is HYDR. I had a wonderful time with all of you guys who already left, still around or recently joined. In multiple occasions, I enjoyed the beers we shared (with all the department people), the in-depth discussion we had about academic life, personal life (Afnan, Lien, Abedulla, Paul, Sofie, etc.,), jokes we laughed over, etc. A wonderful list of researchers that I collaborated and I want to thank personally are, Lorenzo (my Italian buddy), Alitane, Hans and Bert from RMI (thank you for your advice during my internship and also during the whole PhD), Ryan (from Colorado State University - without your gwflow, my life would have been MODFLOW :)), Lien (a great friend and down to earth personality on top of collaborating with me in four major papers), Abedulla (a great humorous guy with golden heart) and Erasto (disciplined and great researcher). All my master's students that I supervised are also part of my happy memory of my PhD journey. A wonderful people like Zainab and Elga (with the whole family) whom I collaborated in multiple occasions and gained experience that I admire a lot and thank you for that.

My wonderful friends Yaredo and Tedo are the pillars for having a wonderful childhood and also till now here in Belgium. Wherever we go, we head together. You guys means a lot with your genuine and supportive attitude. I can not list all my friends but here is to those who were there every way: Sol, Ade, Girume, Zeme, Luwalawi (Kemem), and Kalebo. This list continues in Belgium and France: Yidnek, Sam, Sami Netherlands, Bese, Alazar, Liyu, Mahdi, etc., thank you for the special moments we had and still are having. Friday will not be Friday without my football buddies and our time in De Spuye afterwards (Bura, Lula, Tadi, Gecho, Eyob, Tare, etc.,). My football team at VUB where we have plenty of happy moments while winning and also loosing (Joachim, Amaury, Etienne, Greta, Mateusz, Harry, Boud, etc.). The wider Ethiopian community in Leuven, Brussels, Ghent, Antwerpen, etc., who are there for my family and I deserve a huge recognition. Thank you all!

Estifanos Addisu Yimer

September, 2025

Leuven, Belgium

Abstract

Geohydrological modelling is crucial for understanding how water balance components react to changing environments. Researchers usually prefer to model surface and groundwater processes separately due to the difficulty of coupling those water systems. In doing so, groundwater-surface water interactions will be ill-represented. Thus, coupled models are required mainly in groundwater-dominated watersheds with shallow aquifers where the streams and aquifers interact constantly. The widely applied soil water assessment tool (SWAT) was recently modified with versatile options representing detailed processes (SWAT+). Despite improvements, groundwater representation is still conceptual. Thus, recent advancements have introduced a groundwater flow module (gwflow) for SWAT+, making it fully physically based and distributed. In this thesis, the newly coupled SWAT +gwflow model is modified to account for groundwater-soil interaction and produced aiding tools for model development, calibration and post-processing. The enhanced model is then tested and validated in the Scheldt basin - specifically the Kleine Nete, Grote Nete, Demer, Dijle and Zenne, Dender, Upper Scheldt, and the Leie as well as to some selected representative watersheds across the globe.

Models are vital to evaluate the extent to which climatic extremes affect surface and groundwater reserves. As hydroclimatic extremes are becoming more frequent and intense, investigating how these events evolve spatially and temporally is crucial. Specifically, drought has complex patterns and occurring mechanisms affecting several layers of watershed water balance components. Thus, in this research, the SWAT+gwflow model setup for the Scheldt basin is used to evaluate the impact of climate change on streamflow and groundwater droughts. There are two major drought analysis methodologies, one which is a standardized index based which fits a given variable (e.g., precipitation, streamflow, groundwater head, etc.) to a probability distribution function and then transforming it to cumulative distribution function and ultimately converting it to standardized normal distribution function making it spatially and temporally comparable. This method fails to provide information on the amount of deficit. As policymakers are keen to know how much the decline in a given water balance component is due to drought, threshold-based drought analysis is the widely used method. Therefore, this research compares the two methods, generates a methodology to find an appropriate distribution function, and ultimately uses an attribution analysis using the Inter-Sectoral Impact Model Intercomparison Project (ISIMIP) factual (with climate change) and counterfactual (without climate change - detrended data) data

to evaluate and assess if climate change is a key player and to what extent it aggravates hydrological drought events.

In recent years, nature-based solutions (NbS) for hydroclimatic extreme mitigation/ adaptation measures have been gaining momentum. These measures opt for natural means of increasing the landscape's water holding capacity, allowing groundwater systems to recharge, decreasing runoff, reducing sediment load, etc. Drought is the least studied hazard compared to floods, regarding NbS as a mitigation measure. Also, there is a lack of framework for suitability mapping of NbS locations for drought mitigation. Therefore, in this last work package, an extensive literature review is made to assess NbS targeting drought, henceforth, a new framework for finding locations with the highest possible advantage on recharging aquifers is investigated.

The results indicated that the standalone SWAT+ model is unable to capture the geohydrological water balance components and river discharge (Nash-Sutcliffe efficiency (NSE) below 0.5). However, the coupled model with the inclusion of groundwater-soil interaction has improved geohydrological simulations by providing reasonable annual average water balance and monthly streamflow values. Next, the regional groundwater-surface modelling of the Scheldt basin indicated successful application of the coupled model with calibration and validation of streamflow, showing NSE ranging between 0.6 and 0.9. The seven watersheds inside the regional Scheldt basin mostly have shallow aquifers, making the modelling practice convenient with the SWAT+gwflow model setups. Furthermore, an investigation of the Kleine Nete watershed to simulate agricultural water drainage flux has added to the coupled model's ability to capture complex geohydrological conditions. In the agricultural water drainage assessment, finding the locations of ditches was critical, hence, a novel methodology was developed that considers groundwater levels along with classical remote sensing and decision classification methods. Finally, the development of an open-source Python script for the coupled model input preparation (model development), calibration, and post-processing eased the coupled model's application among the wider SWAT community.

Next, by using the calibrated and validated coupled models for the seven watersheds, an attribution study was made to evaluate the extent of climate change impact on rivers and groundwater and hydrological drought in general. Factual and counterfactual data from the Inter-Sectoral Impact Model Intercomparison Project (ISIMIP) is used to force the models. The impact assessment on the rivers has indicated that the low flows decreased between 3.5 and 14%. The cumulative deficit showed the highest impact on the Upper Scheldt catchment. Furthermore, the Upper Scheldt and Leie basins experienced an average increase in streamflow deficit of about 10 m^3/s during drought periods. The use of three detrended datasets has indicated uncertainty of deficit values, but all agree that the impact of climate change on the rivers is evident. The groundwater attribution on the Kleine Nete indicated that the groundwater level has decreased considerably in recent years (2010 onwards). Overall, from 1970 onwards, there was an average of a 10 cm significant decline

in groundwater head, with some locations having a maximum decline ranging between 0.1 and 1.5 meters, which shows the uncertainty spread. The groundwater drought assessment has indicated an increase in maximum drought deficit and duration due to climate change. The deficit is mainly high for short-term (1 to 3 months) and yearly impact but revives at a 24-month timescale. This is attributed to the shallow nature of the aquifer water table, which declines in shorter time and revives at longer timescales. These highlight the need to apply necessary mitigation or adaptation measures to reduce the impact climate change causes on the Kleine Nete or, in general, unconfined groundwater reserves.

After highlighting that drought is partly attributed to climate change and the need for mitigation/adaptation measures is found to be evident, NbS mainly targeting drought are investigated. A literature review made on NbS and drought indicated the following major findings: few NbS studies focus on drought compared to other hazards such as floods, most NbS implementations are located in Europe, effectiveness is not well quantified for implemented NbS and finally, for achieving considerable drought mitigation, large-scale NbS are needed. With this in mind, the next research focuses on finding large-scale NbS, which requires framework development, and applying the framework at a regional scale, with Flanders as a case study area. The main findings from this work were the following: The new mapping framework addresses drought-specific needs and climate scenarios, and the results for Flanders underscore the highly suitable potential for detention basins (2552.2 km²) and managed aquifer recharge areas (2538.7 km²), emphasizing the adaptability and scalability of the framework for addressing drought in the region, detention basins compensate partly for the high groundwater demand, and finally, regional application yields actionable insights for decision-makers.

This dissertation emphasizes that the physical and distributed nature and modification we applied to the gwflow module have enhanced geohydrological simulations in groundwater-dominated watersheds, such as the Scheldt basin. Additionally, climate change impacts on surface and groundwater are analyzed by estimating deficit values that policymakers can use to assess extremes and their possible impact. Finally, resilience against drought with NbS is assessed by locating potential NbS areas based on several conditions. Thus, water managers can utilize this research to apply necessary mitigation measures to tackle the hazard by looking into its impact at several layers of the Scheldt River basin.

This PhD dissertation is structured around four major parts. The first focuses on model development, including model modification, verification, and tool development. Secondly, using the tools and modifications made in the first part, the model is further used for assessing processes such as drainage impact on geohydrology, groundwater–surface water interactions and groundwater–soil interactions in the Scheldt basin (model application). Thirdly, the calibrated and validated model is used to investigate drought in the region. Finally, solutions for drought mitigation are explored, focusing mainly on nature-based solutions.

List of abbreviations

SWAT	Soil and Water Assessment Tool
SWAT+	Soil and Water Assessment Tool Plus
gwflow	Groundwater Flow Module
NbS	Nature-based Solutions
NSE	Nash-Sutcliffe Efficiency
PBIAS	Percent Bias
RMSE	Root Mean Square Error
MAE	Mean Absolute Error
GIS	Geographic Information System
HRU	Hydrologic Response Unit
LSU	Landscape Unit
ET	Evapotranspiration
DEM	Digital Elevation Model
GUI	Graphical User Interface
DHRU	Disaggregated Hydrologic Response Unit
QSWATMOD	QGIS-based SWAT-MODFLOW Interface
SWATMOD-Prep	SWAT-MODFLOW Preparation Tool
IPPC	Input Preparation, Post-Processing, and Calibration Tool
DTC	Decision Tree Classification
RS	Remote Sensing
GPR	Ground Penetrating Radar
UASs	Unmanned Aerial Systems
SPEI	Standardized Precipitation Evapotranspiration Index
SSI	Standardized Streamflow Index
SSMI	Standardized Soil Moisture Index
SWI	Standardized Water-level Index
GOF	Goodness of Fit
K-S	Kolmogorov-Smirnov Test
A-D	Anderson-Darling Test
S-W	Shapiro-Wilk Test
TB	Threshold-Based Method
SIB	Standardized Index-Based Method

ISIMIP	Inter-Sectoral Impact Model Intercomparison Project
MAR	Managed Aquifer Recharge
RWH	Rainwater Harvesting
GI	Green Infrastructure
EBA	Ecosystem-Based Adaptation
VMM	Vlaamse Milieumaatschappij (Flemish Environment Agency)
CIW	Coördinatiecommissie Integraal Waterbeleid (Coordination Commission for Integrated Water Policy)
MK	Mann-Kendall Test
GLHYMPS	Global Hydrogeology Maps
SCS	Soil Conservation Service
MODFLOW	Modular Finite-Difference Groundwater Flow Model
VIC	Variable Infiltration Capacity
ABCD	A Basin-scale Continuous Hydrologic Model
SWIM	Soil and Water Integrated Model
ECOMAG	Ecological Model for Applied Geophysics
IUCN	International Union for Conservation of Nature
EC	European Commission
OECD	Organisation for Economic Co-operation and Development
UN	United Nations
WWAP	World Water Assessment Programme
FAO	Food and Agriculture Organization
USC	Upper Scheldt Catchment
PET	Potential Evapotranspiration
PEST	Parameter ESTimation Tool
PSO	Particle Swarm Optimization

Contents

Acknowledgements **iv**

Acknowledgements **v**

Abstract **vii**

List of Abbreviations **ix**

List of Abbreviations **xi**

Contents **xiii**

List of Figures **xvii**

List of Tables **xxvii**

1 Introduction **1**
1.1 General Background 1
1.2 Research objectives and questions 4
1.3 Scientific novelty of the research 5
1.4 Outline of the thesis 6
1.5 Study areas 7

2 Background **9**
2.1 Geohydrological modelling 9
2.1.1 The Soil Water Assessment Tool (SWAT) 11
2.1.2 SWAT+gwflow 14
2.1.3 Overview of SWAT+ input preparation, calibration and postprocessing tools 17
2.1.4 Agricultural water drainage unit identification techniques 18
2.2 Drought 19
2.3 Nature-based solutions 24

3 Model development **29**
3.1 Modifying the gwflow module to account for groundwater-soil interactions for accurate representation of groundwater-surface water dynamics 30
3.1.1 Summary 30
3.1.2 Introduction 31
3.1.3 Study area and data 32
3.1.4 Methodology 34
3.1.5 Results 38
3.1.6 Conclusion 42
3.2 An open source SWAT+gwflow input preparation, post-processing and calibration tool development 44
3.2.1 Summary 44
3.2.2 Introduction 45
3.2.3 Study area 45
3.2.4 Design and Implementation 45
3.2.5 SWAT+gwflow input generation 49
3.2.6 SWAT+gwflow calibration using Particle Swarm Optimization (PSO) 52
3.2.7 SWAT+gwflow post–processing 53
3.2.8 Results 53
3.2.9 Conclusion 58

4 Model application **59**
4.1 Groundwater level-based filtering to improve the accuracy of locating agricultural water drainage locations 60
4.1.1 Summary 60
4.1.2 Introduction 61
4.1.3 Study area and data 61
4.1.4 Methodology 63
4.1.5 Results 66
4.1.6 Discussion 75
4.1.7 Conclusion 76
4.2 The impact of extensive agricultural water drainage on the hydrology of the Kleine Nete watershed, Belgium 78
4.2.1 Summary 78
4.2.2 Introduction 79
4.2.3 Study area and data 80
4.2.4 Methodology 83
4.2.5 Results 86
4.2.6 Discussion 96
4.2.7 Conclusion 98
4.3 Regional evaluation of groundwater-surface water interaction in the Scheldt basin using SWAT+gwflow 100
4.3.1 Summary 100
4.3.2 Introduction 101

4.3.3 Study area and data . . . 101
4.3.4 Methodology . . . 103
4.3.5 Results . . . 106
4.3.6 Conclusion . . . 121

5 Drought assessment in the Scheldt basin 123
5.1 A coupled SWAT+gwflow model application for comprehensive drought analysis in the Scheldt Basin . . . 124
5.1.1 Summary . . . 124
5.1.2 Introduction . . . 125
5.1.3 Study area and Data . . . 125
5.1.4 Methodology . . . 125
5.1.5 Results . . . 127
5.1.6 Discussion . . . 136
5.1.7 Conclusion . . . 140
5.2 Attributing climate change impact on streamflow decrease at regional scale using coupled surface – groundwater model . . . 141
5.2.1 Summary . . . 141
5.2.2 Introduction . . . 142
5.2.3 Study area and data . . . 143
5.2.4 Methodology . . . 143
5.2.5 Results . . . 145
5.2.6 Discussion . . . 162
5.2.7 Conclusion . . . 164
5.3 Is climate change aggravating groundwater drought? A case study in a groundwater dominated watershed . . . 165
5.3.1 Summary . . . 165
5.3.2 Introduction . . . 166
5.3.3 Study area . . . 168
5.3.4 Methodology . . . 168
5.3.5 Results . . . 168
5.3.6 Discussion . . . 180
5.3.7 Conclusion . . . 182

6 Nature-based solutions for drought mitigation 185
6.1 The underexposed nature-based solutions: a critical state-of-art review on drought mitigation . . . 186
6.1.1 Summary . . . 186
6.1.2 Introduction . . . 187
6.1.3 Methodology . . . 187
6.1.4 Result . . . 189
6.1.5 Discussion and Conclusion . . . 206
6.2 Framework for mapping large–scale Nature-Based Solutions for drought mitigation: regional application in Flanders . . . 210

6.2.1 Summary 210
6.2.2 Introduction 211
6.2.3 Study area 211
6.2.4 Methodology 212
6.2.5 Result 222
6.2.6 Discussion 230
6.2.7 Conclusion 233

7 Conclusion and Recommendation **235**
7.1 Conclusion 235
7.2 Recommendations 240

8 Appendix **244**

List of Outputs **257**

Bibliography **263**

List of Figures

1.1 Major chapters of the thesis, excluding introduction and literature review (background) . . . 3
1.2 Research objectives of the three main categories of the thesis (geohydrological modelling and its application, drought assessment, and finally, nature-based solutions for drought mitigation). . . . 5
1.3 Study areas used for the different parts of the thesis. IPPC stands for Input Preparation, Post Processing and calibration tool . . . 8

2.1 The different sources and sinks to and from the control volume. The control volume is the smallest unit where computation is made inside the gwflow module . . . 16
2.2 The widely adopted drought analysis methodologies (standardized index and threshold based) . . . 20
2.3 Yearly average maximum temperature and yearly total precipitation for Belgium with the trend line and significance level (p-value). . . . 23

3.1 Major parts of Chapter 3 which focus on model and tool development . . . 29
3.2 Study area used for evaluating the impact of groundwater-soil interaction on general geohydrology . . . 32
3.3 The elevation of the impermeable layer base is taken as a reference for the unconfined aquifer. It was accessed on September 30th, 2021, from https://www.dov.vlaanderen.be/portaal/. The other colors correspond to different geological units, however, the focus of this study lies on the impermeable layer and the yellow unit (Brussel sand), which corresponds to the unconfined aquifer. The dotted line corresponds to mTAW = National Topographic Reference). The plot is not in to scale, and the transect is for A–A, as seen in (Fig. 3.2). . . . 33
3.4 The different hydraulic conductivity zones according to the GLHYMS dataset. Originally, there were 24 zones, which has three dominant zones. Hence, to reduce computation time and avoid overfitting, only the three zones' hydraulic conductivity and specific yield parameters are calibrated . 35

3.5 Water yield and net recharge for the condition of including the gwsoil mechanism (A and C) and not including the gwsoil mechanism (B and D) . 40
3.6 The geographical locations of the 12 watersheds 46
3.7 The delineation and river networks as generated by the SWAT+gwflow model used in the 12 study watersheds. The elevation is reported with a common legend to enable comparison between watersheds 47
3.8 The schematic representation of the IPPC tool development 48
3.9 The proper layout of folders and files for the SWAT+gwflow input generation process 49
3.10 The inputs that need to be modified inside the script (from lines 393 to 475) — continued on next page 50
3.10 (continued) The inputs that need to be modified inside the script (from lines 393 to 475) 51
3.11 The final structure of the folder after the script finishes running (which adds several other folders that contain useful files for the successful coupling of the SWAT+ and gwflow module) 52
3.12 The user needs to modify the inputs for the post-processing script to work correctly (lines 114 to 128) 53
3.13 The streamflow outputs from the SWAT+gwflow model after model calibration. 55
3.14 Examples of post-processing outputs (groundwater head) created with the Python script 56
3.15 Examples of post-processing outputs (recharge) created with the Python script 57

4.1 Major parts of Chapter 4 which focues on model application 59
4.2 Location and spatial elevation variation of the two study areas. 62
4.3 A flow chart showing the methodology we followed to identify tile/ditch network in the respective case study areas. 63
4.4 The soil moisture difference before and after a significant rainfall event (a) and shapefile of agricultural fields (b). The agricultural field shapefile is used to clip the soil moisture difference shapefile, as the aim is to find drainage units in agricultural plots. These plots are for the first study area (Ontario, Canada). 67
4.5 The actual location of tile drains (ground truth data) (a) and the result from the remote sensed-based approach intersected with the ground truth area (b). The accuracy is estimated based on this intersected shapefile. 68
4.6 The result of the RS-based approach for the Kleine Nete watershed where the blue patches denote potential drained areas while the pink lines are the ditch network (ground truth data). (For interpretation of the references to color in this figure legend, the reader is referred to the web version of this article 69

4.7 Potential tile drain locations for the first case study area after filtering pixels corresponding to agricultural land with (a) soils of low drainage capacity and (b) gentle slopes ($\leq$4%). 71
4.8 The land use (a), soil drainage class (b), slope class (c), and the result of the DTC filtering (d) for the Kleine Nete watershed. The green patches at the least bottom plot (d) stand for potential drained areas according to the DTC methodology. 73
4.9 The groundwater table depth (a) and potential drainage unit locations (b) after the RS result is combined with a groundwater-based filtering technique where locations with a water table depth of less than 1.2 m are considered possible tile drain locations. These plots are for the first case study area (Ontario, Canada). 74
4.10 The annual average groundwater depth (a), the actual ditch network (black lines), along with the water table depth (b) for the second case study area (Kleine Nete watershed). The locations with shallow groundwater are located in the vicinity of the ditch network, hence, including groundwater-based filtering to identify ditches in agricultural fields is crucial 75
4.11 The Kleine Nete watershed, groundwater observation wells (L1 to L7), homogeneous hydraulic conductivity zones, and mesh with the size of 200 m by 200 m resulting in 129 rows and 171 columns (a). The change in volume for each grid cell is taken as a governing equation in the gwflow groundwater module. The next plot (b) shows the major land use types inside the watershed, followed by the elevation variation (c), and finally, the aquifer thickness (d) according to the global dataset is shown. 82
4.12 Schematic overview of the ditch system modeled in the SWAT+gwflow model setup. 84
4.12 The simulated and observed daily streamflow at the catchment outlet during the validation period for the standalone model 87
4.13 Daily simulated and observed streamflow values according to SWAT+gwflow 1 modeling approach 88
4.14 Scatter plot for the modeled and measured groundwater head for calibration strategy 1 (using only streamflow) and calibration strategy 2 (using both streamflow and groundwater head). The plot is for well locations 3 (a), 4 (b), 5 (c), and 7 (d). The closer the dots/stars are near the bisector line, the better the model simulation 88
4.15 Timeseries plot for the modeled and measured groundwater head for calibration strategy 2 (using both streamflow and groundwater head). The plot is for well locations 3 , 4 , 5 , and 7 (from top to bottom). 89
4.16 The calibrated hydraulic conductivity values based on two calibration strategies (based on streamflow – SWAT+gwflow 1 and based on stream-flow and hydraulic head – SWAT+gwflow 2). For zone numbers, refer to Fig. 4.11 91
4.17 Daily simulated and observed streamflow values according to SWAT+gwflow 2 modeling approach. 92

4.18 Water balance value differences due to the two calibration strategies we followed 92
4.19 The simulated and observed hydraulic head values at L7 (refer to Fig. 1 for well name) for the calibration and validation period. The plot is for the two calibration strategies; calibrating the coupled model for only streamflow and calibrating the coupled model for both streamflow and groundwater head. 94
4.20 The variation of water table depth according to calibration strategy 1 (SWAT+gwflow 1) and strategy 2 (SWAT+gwflow 2) 95
4.21 The average water table depth and volume of groundwater before and after the application of the drainage unit in the modeling scheme 96
4.22 The seven catchments, their boundaries, their respective river network, and validation gauging stations used for model evaluation (they are not used to calibrate the coupled model) 102
4.23 The locations of observation wells inside the Kleine Nete watershed that are used for calibration and validation 104
4.24 The parameter that adjusts soil moisture for percolation to occur (perco), soil evaporation compensation factor (esco), plant uptake compensation factor (epco), and Soil available water capacity (awc) (top) and surface runoff lag coefficient (sur_lag) (bottom) calibrated parameters 107
4.25 The minimum, average, and maximum hydraulic conductivity (a) and specific yield (b), recharge delay (c), and water table depth (d) 108
4.26 Comparison between streamflow model output and measured values for calibration and validation periods for the Kleine Nete, Grote Nete, Demer, Dender, and upper Scheldt catchments 112
4.27 The basin average water balance components, precipitation (P), surface runoff (Surq), evapotranspiration (ET), saturated excess flow (satex), and the average of the seven watersheds (in mm) 114
4.28 The boundary groundwater flow at catchment boundary (a) and recharge (b) and groundwater transferred to the soil profile (c) given in mm 115
4.29 Groundwater-surface water interaction (GW-SW) in the seven watersheds from 1975 to 2021. The values are negative as they are sinks (taken out of the groundwater) and given in mm's 116
4.30 Groundwater-surface water interaction in the seven watersheds during summer time (1st August 2007). The numbers stand for minimum, quartiles (three or four quartiles), and maximum values of GW-SW interactions. As for the Leie, the third quartile and maximum values are the same. As indicated in the previous figure, the USC and Leie watersheds constitute significant baseflow 119

5.1 Major parts of Chapter 5 which focuses on drought assessment 123
5.2 Spatial plots of distribution functions for shortterm (left) and longterm (right) meteorological droughts respectively 127

5.3 Spatial plots of distribution functions for shortterm (left) and longterm (right) streamflow droughts respectively 128
5.4 Overall rejection frequency plots using groundwater head for Kleine Nete, 25% represents limit of rejection frequency 129
5.5 Summary of short-term meteorological drought events for all catchments (obtained at SPEI < -1.5) 131
5.6 Summary of meteorological drought events for all catchments using Threshold based method 132
5.7 Summary of agricultural drought events for all catchments using Threshold based method 133
5.8 Summary of short-term streamflow drought events for all catchments (SSI < -1.5, 1-month accumulation period) 134
5.9 Summary of streamflow droughts using the TB method for all catchments . 135
5.10 Summary of groundwater droughts using TB method for different sites within Kleine Nete 136
5.11 Differences in water balance components (precipitation, evapotranspiration, lateral flow, surface runoff, percolation, and soil moisture) between factual and counterfactual scenarios across watersheds in the Scheldt basin. Results are presented for three climate attribution models 148
5.12 Differences between observed and counterfactual mean precipitation (mm), averaged across three climate attribution datasets, for various watersheds in the Scheldt basin. Shaded areas represent associated uncertainty ranges, while solid lines indicate mean values. Dashed lines show the observed (blue) and counterfactual (red) trends. P-values indicate the statistical significance of these trends, with values below 0.05 considered significant . 149
5.13 Differences between observed and counterfactual mean evapotranspiration (mm), averaged across three climate attribution datasets for various watersheds in the Scheldt basin. Shaded areas represent associated uncertainty ranges, while solid lines indicate mean values. Dashed lines show the observed (blue) and counterfactual (red) trends. P-values indicate the statistical significance of these trends, with values below 0.05 considered significant 150
5.14 Differences between observed and counterfactual mean soil moisture (mm), averaged across three climate attribution datasets, for various watersheds in the Scheldt basin. Shaded areas represent associated uncertainty ranges, while solid lines indicate mean values. Dashed lines show the observed (blue) and counterfactual (red) trends. P-values indicate the statistical significance of these trends, with values below 0.05 considered significant 151
5.15 Seasonal differences in precipitation (mm), summed for each season across the years 1970–2020, between factual and counterfactual simulations for three individual climate attribution datasets. Seasons are defined as follows: Winter (December–February), Spring (March–May), Summer (June–August), and Autumn (September–November) 152

5.16 Seasonal differences in evapotranspiration (mm), summed for each season across the years 1970–2020, between factual and counterfactual simulations for three individual climate attribution datasets. Seasons are defined as follows: Winter (December–February), Spring (March–May), Summer (June–August), and Autumn (September–November) 153
5.17 Seasonal differences in runoff (mm), summed for each season across the years 1970–2020, between factual and counterfactual simulations for three individual climate attribution datasets. Seasons are defined as follows: Winter (December–February), Spring (March–May), Summer (June–August), and Autumn (September–November) 154
5.18 Long-term mean difference (deficit) in streamflow from model simulations using factual and counterfactual climate data, averaged across three climate attribution models. Shaded areas represent uncertainty ranges, and the dashed red line indicates no difference 155
5.19 Flow Duration Curves comparing factual and counterfactual quantiles across different flow regimes and climate attribution models. Exceedance probabilities of 20%, 50%, and 99% represent low, medium, and high flows, respectively, highlighting changes in flow under climate change scenarios 157
5.20 Cumulative streamflow deficit (m^3/s) of factual and counterfactual discharges, summed for each drought event across various watersheds in the Scheldt basin and analyzed using three climate attribution models 159
5.21 Drought duration (in months) of factual and counterfactual drought events across various watersheds in the Scheldt basin and analyzed using three climate attribution models 160
5.22 Streamflow deficit difference (m^3/s) of factual and counterfactual discharges for each drought event, across various watersheds in the Scheldt basin and analyzed using three climate attribution models 161
5.23 Comparison of measured and (factual) simulated groundwater head data (m) at five wells (L1 to L5). Each subplot represents one well, with coloured dots indicating the different climate attribution models. The 1:1 dashed line represents perfect agreement, highlighting deviations between measured and simulated factual values 170
5.24 Comparison of annual average mean factual and counterfactual groundwater heads (m) from 1970 to 2015, averaged for three climate attribution models. Each subplot represents a different well, showing both factual (blue line) and counterfactual (orange line) simulations. Shaded bands around each line indicate the range of uncertainty in the simulations 171
5.25 Comparison of measured, factual and counterfactual groundwater heads (m), with their uncertainty range. Each subplot represents a different well, showing both factual (purple) and counterfactual (light orange) simulations. Shaded bands indicate the range of uncertainty in the simulations 172

5.26 Differences between annual average mean factual and counterfactual groundwater head values (m) from 1970 to 2015 for wells L1 to L5. Each subplot represents a different well, with the purple line indicating the anomaly (factual minus counterfactual values) and the grey shading representing the uncertainty band across different climate datasets. The red dashed line denotes the trend in anomaly values, and the p-value indicates the statistical significance of the trend over time 173
5.27 Scatter plots comparing factual and counterfactual groundwater head values (m) for five wells (L1 to L5), illustrating the alignment between simulated groundwater heads under factual and counterfactual scenarios. Each subplot represents one well, with coloured dots representing different climate datasets. The dashed 1:1 bisector line indicates perfect agreement between factual and counterfactual values 174
5.28 Annual average seasonal differences (cm) between factual and counterfactual groundwater head simulations for 1970-2015 for the three climate attribution dataset and displayed for each well (L1 to L5). Each panel represents one season (winter, spring, summer, and autumn) 175
5.29 Boxplots of maximum deficit (m) for factual (red) and counterfactual (black) scenarios, for the three climate attribution datasets and displayed for various drought accumulation periods (1M = 1 month, 24M = 24 months, etc.). 178
5.30 Heatmaps showing the yearly drought duration differences (in months) between factual and counterfactual scenarios for drought events at a 1-month accumulation period across three climate attribution models and five wells (L1 to L5). 179

6.1 Major parts of Chapter 6 which focuses on drought mitigation/adaptation measures via nature-based solutions 185
6.2 The percentage of NbS applications targeting drought or other hydroclimatic extremes at global, regional (Europe), and local levels (Belgium) . . . 190
6.3 The number of nature-based solutions targeting drought at different scales and their spatial distribution 191
6.4 The widely applied nature based solutions (NbS) at a global scale (except in Europe). The bigger the text's size, the wider the NbS application. 192
6.5 The widely applied nature based solutions (NbS) at European scale (except in Belgium). The bigger the size of the text, the more widely the NbS application. 195
6.6 The widely applied nature based solutions (NBS) in Belgium. The bigger the size of the text, the more widely the NBS application. 197
6.7 The number of literature that corresponds to small scale, large scale, and without scale mentioned 200
6.8 Comparison of reviewed literature regarding content - Applied or Theoretical, Methods (Focus on Experiments and Modelling) 201

6.9 (A) Land cover, topography and river network of the Flemish region, (B) Location of Flanders in Europe, (C) River basins in Flanders 212
6.10 : Flowchart for identifying suitable locations for DB and MAR. 215
6.11 :Suitable areas for detention basins (DB) in the Flemish region, initially identified with Boolean constraint mapping based on 15 criteria and refined through PCA by reducing the criteria to 14 224
6.12 :Suitable areas for managed aquifer recharge (MAR) in the Flemish region, initially identified with Boolean constraint mapping based on 15 criteria and refined through PCA by reducing the criteria to 12 224
6.13 :Comparison of suitable areas for detention basins (DB) in the Flemish Region: multi-criteria decision-making (approach 2) vs. Boolean constraint mapping (approach 1) 226
6.14 :Comparison of suitable areas for managed aquifer recharge (MAR) in the Flemish Region: multi-criteria decision-making (approach 2) vs. Boolean constraint mapping (approach 1) 227
6.15 Climate change impact on the decrease in average lowest groundwater levels in Flanders (VMM and Sumaqua) for 2050, with suitable detention basin locations outlined using two methods (Boolean constraint mapping and AHP) 228
6.16 Climate change impact on the decrease in average lowest groundwater levels in Flanders (VMM and Sumaqua) for 2050, with suitable locations for managed aquifer recharge outlined using two methods (Boolean constraint mapping and AHP) 228
6.17 Comparison between estimated yearly groundwater use and potential yearly recharge due to detention basins with three different scenarios for 2050 and 2100 per basin 229
6.18 Estimated decrease in groundwater volume (m^3) due to climate change for 2050 and 2100 per basin 230

8.1 Overall rejection frequency plots for meteorological drought for all catchments, horizontal line at 25% represents limit of rejection frequency. . 245
8.2 Overall rejection frequency plots for soil moisture drought for all catchments, horizontal line at 25% represents limit of rejection frequency. 246
8.3 Overall rejection frequency plots for all catchments using streamflow, horizontal line at 25% represents limit of rejection frequency. 247
8.4 Correlation analysis between SSI-1 and SPEI at different accumulation periods on the x-axis 247
8.5 Summary of long-term meteorological drought events for all catchments (i.e. 6-month accumulation period). 248
8.6 Summary of long-term streamflow drought events using SIB for all catchments (12-month accumulation period). 249
8.7 Meteorological drought events estimated starting from 1970 using the $80th$ percentile threshold to observe onsets preceding hydrological drought events. 249

8.8 Groundwater drought events estimated starting from 1975 using the $80th$ percentile threshold. Location of groundwater head simulated (Herentals) is the closest to the outlet of the streamflow and hydrological subbasin to be spatially consistent. 250
8.9 Differences between observed and counterfactual mean runoff (mm), averaged across three climate attribution datasets, for various watersheds in the Scheldt basin. Shaded areas represent associated uncertainty ranges, while solid lines indicate mean values. Dashed lines show the observed (blue) and counterfactual (red) trends. P-values indicate the statistical significance of these trends, with values below 0.05 considered significant. . 251
8.10 Figure 5: Differences between observed and counterfactual mean percolation (mm), averaged across three climate attribution datasets, for various watersheds in the Scheldt basin. Shaded areas represent associated uncertainty ranges, while solid lines indicate mean values. Dashed lines show the observed (blue) and counterfactual (red) trends. P-values indicate the statistical significance of these trends, with values below 0.05 considered significant. 252
8.11 Long-term mean streamflow (m^3/s) from model simulations using factual and counterfactual climate data, averaged over three climate attribution models. Shaded areas represent uncertainty ranges, and the dashed line represents observed streamflow data for comparison across various watersheds in the Scheldt basin. 253
8.12 Relative differences (deficits) between factual and counterfactual quantiles for low flows, analyzed across three climate attribution dataset and various watersheds in the Scheldt basin. This is to show the low flows (less than 20%). 254
8.13 Heatmaps showing the yearly drought duration differences (in months) between factual and counterfactual scenarios for drought events at a 12-month accumulation period across three climate attribution models and five wells (L1 to L5). Each panel represents one well, with colours indicating the magnitude of the drought duration difference: blue shades represent shorter drought durations in the factual scenario, while red shades represent longer drought durations in the factual scenario. 255
8.14 Heatmaps showing the yearly drought duration differences (in months) between factual and counterfactual scenarios for drought events at a 24-month accumulation period across three climate attribution models and five wells (L1 to L5). Each panel represents one well, with colours indicating the magnitude of the drought duration difference: blue shades represent shorter drought durations in the factual scenario, while red shades represent longer drought durations in the factual scenario. 256

List of Tables

3.1 Comparison of model performance metrics for SWAT+ and SWAT+*gwflow* 39
3.2 Comparison of water balance components with and without `gwsoil`. . . . 41
3.3 The twelve study areas descriptions (catchment name, country where it is located, area, annual average precipitation, and groundwater characteristics) 46
3.4 Nash-Sutcliffe efficiency (NSE) of the calibration and validation periods in the five watersheds (non-Belgian). Belgian catchments are discussed in Yimer et al. (2023b). 54

4.1 Warm-up, calibration, and validation periods. 83
4.2 Model performance for calibration and validation periods 92
4.3 Inputs and Outputs to the watershed (mm) 93
4.4 The root mean square error (RMSE) and mean absolute error (MAE) for the calibration period based on SWAT+gwflow 1 (top) and SWAT+gwflow 2 (bottom) calibration strategies. 94
4.5 The list of model inputs required to set up the SWAT+ and the coupled SWAT+gwflow model 103
4.6 The number of sub-basins, HRUs, channels, calibration and validation periods, area, groundwater discretization, number of homogeneous hydraulic conductivity zones, and dominant zones used for calibrating the model (e.g. 10 zones are used instead of 165 zones for calibrating the upper Scheldt basin) 105
4.7 The Nash-Sutcliffe efficiency (NSE) for the analyzed catchments for the calibration and validation periods (at daily and monthly streamflow values). This result is based on the gauging station near the catchment outlet (top) and other internal stations (bottom). The asterisk (*) indicates that validation gauging stations are unavailable or not used. Refer to Fig. 4.22 for the locations of the validation gauging stations. 110
4.8 Watershed Soil Water Balance and Groundwater Balance Error 113

6.1 Small-scale and Large-scale Solutions 189
6.2 The number of projects that are implemented and ongoing for the different decades 191

6.3 The number of projects which are successfully implemented, ongoing, or with no status information 191
6.4 Fundamental scale for comparing criteria relative to each other, adapted from Saaty (1980) 219

Chapter 1

Introduction

1.1 General Background

Hydroclimatic extremes are prevailing across the globe, and their severity and duration are amplifying over time. Their impact is seen at the surface (Bhaga et al., 2020), soil (Zhu et al., 2021), and subsurface (Van Lanen and Peters, 2000) levels. For example, according to OECD (2020), droughts are becoming more intense with prolonged duration. The recent consecutive drought events in Belgium are notable examples. Floods sometimes accompany drought events (e.g., July of 2021). This shows the complex nature of interacting hydroclimatic extremes (Barendrecht et al., 2024). Hence, modelling and analysis tools are needed to capture the complexity.

These events are assessed using models to explore their impact on watershed geohydrology. Several modeling efforts are made to capture geohydrological functioning and water balance components. However, these efforts are hindered by the inability of models to capture inherent surface-groundwater interactions (Bailey et al., 2016). This interaction is vital for comprehensively assessing catchment geohydrology. According to (Wang and Chen, 2021), modelling surface and subsurface processes separately can ease the modelling practice (input preparation, computationally, complexity-wise, etc.). Thus, surface water models are developed to represent the surface processes and then are separately fed to groundwater models. For example, the modular groundwater flow model (MODFLOW) has been used to investigate groundwater quantity and quality with diverse applications across the globe (Harbaugh, 2005). There are also surface water modelling practices that use conceptual, data-driven, and physically based models (Gülbaz and Kazezyilmaz-Alhan, 2017; Sun et al., 2015; Warsta et al., 2013). In both cases, the inherent relationship between groundwater and surface water is not represented. Thus, modelling community is pushing toward the development of coupled models.

One of the widely applied model is the soil water assessment tool (SWAT), which re-

cently was updated to have an advanced representation of hydrological processes labeled as SWAT+ (Bieger et al., 2017). The model was applied to watersheds in tropical (Memarian et al., 2014), temperate (Holder et al., 2019), cold (Zare et al., 2022), and arid (Rocha et al., 2023) environments. Its versatile use is seen for watershed water balance assessment (Uniyal et al., 2015), scenario analysis (e.g., climate change (Bhatta et al., 2019)), management practices (Epelde et al., 2015) and reservoir operations (Jordan et al., 2022).

However, model has shortcomings, such as the conceptual representation of groundwater systems, which leads to unrealistic designation of groundwater processes and affects the overall water balance (Bailey et al., 2020b). For example, SWAT+ assumes that aquifers are one unit per subbasin, which is unrealistic. Also, it assumes that groundwater heads do not vary spatially, hindering a clear picture of recharge variability across watersheds. In addition, conceptual representations bring empirical parameters that often need to be calibrated without considering their physical meaning.

Due to these shortcomings, a new groundwater module (gwflow) was developed and merged into the SWAT+ model structure to replace the conceptual representation of the groundwater processes. The coupled model was applied in different basins across the globe, with its application seen to improve geohydrological simulations in tile-intensive watersheds (Bailey et al., 2022), groundwater-surface water interaction-dominated catchments (Bailey et al., 2023), etc. However, the coupled model still has a limitation in accounting for groundwater-soil interaction where groundwater reaching the soil profile is not considered. This can lead to inappropriate water balance estimations in geohydrological modelling and further skews model applications. Therefore, this dissertation modfied the coupled SWAT+gwflow model to designate this process accurately. In addition, the model's ability to efficiently and accurately represent groundwater–surface water interactions at a regional scale is missing, hence, the regional Scheldt basin is used to validate the model.

Geohydrological models are useful for evaluating the past, current, and future status of water quantity and quality. Specifically, they are used to assess the impact of land use, climate, human factors, etc., on water resources. The primary outcome of models is to inform policymakers about the mechanism by which a given water resource is deteriorating in quality and/or reducing in quantity, possible mitigation/adaptation measures to curb the impact, evaluation of water management scenarios, etc.

For example, SWAT+gwflow can be used to model shallow groundwater-dominant watersheds, where the impact of agricultural water drainage on the availability of this vital freshwater resource is immense. However, the locations of the drainage units (tile, ditch, etc.) are not well known, as historical agricultural expansion practices do not document the whereabouts of these units (Valayamkunnath et al., 2020). Thus, developing a novel methodology for locating agricultural water drainage areas and investigating their impact using the SWAT+gwflow model is an additional value of this dissertation.

Additional use of geohydrological modes is to investigate hydroclimatic extremes, among which drought is still underexplored, and its challenges persist across watersheds. Its spatial and temporal uncertainty and complex patterns make it difficult to predict its impact on water resources (Vicente-Serrano et al., 2010). Some scholars attribute an increase in severity and frequency of drought to be the consequence of climate change (Chiang et al., 2021). Hence, the extent of climate change's impact on rivers and aquifers is evaluated using the coupled SWAT+gwflow model for the regional Scheldt basin. In doing so, comprehensive drought analysis methods and tools are produced to advance our understanding of drought at different spatial and temporal scales.

To combat the impact of drought on surface and groundwater resources, adaptation and/or mitigation measures are needed. In recent years, nature-based solutions have been getting more attention from the wider community in their ability to reduce the impact of extremes on ecology, water resources, and communities (Gómez Martín et al., 2021). Since NbS are emerging concepts with widespread acceptance, evaluating their use for drought management has not been explored in depth. Therefore, in this thesis, an extensive literature review has been made to find NbS applications targeting drought. Furthermore, NbS suitability mapping framework is developed, which is finally used to find suitable areas for detention basins and managed aquifer recharge areas with Flanders (the northern part of Belgium) as a case study area.

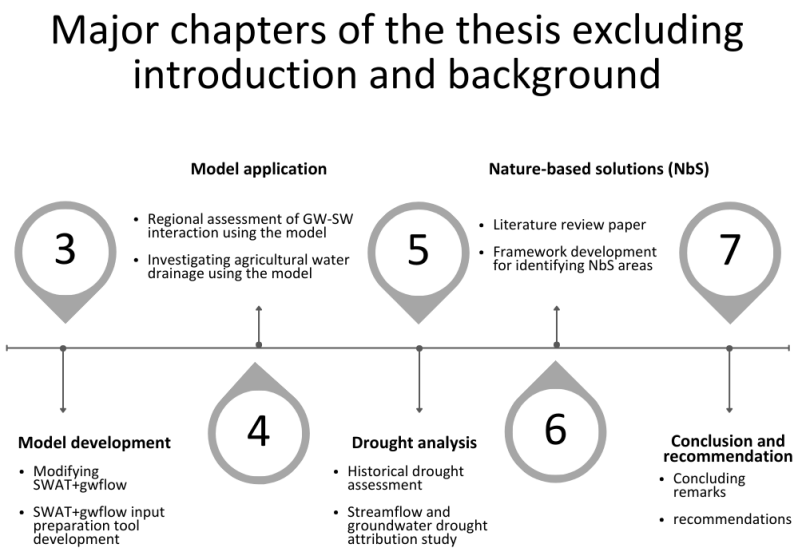


Figure 1.1: Major chapters of the thesis, excluding introduction and literature review (background)

1.2 Research objectives and questions

The main objective of the thesis is to investigate drought using a fully coupled surface-groundwater model and ultimately assess nature-based solutions for mitigating the impact of drought. However, to reach the last milestone, we attained several objectives. (Fig. 1.2).

1. **Objective 1**. A newly coupled geohydrological model (SWAT+gwflow) is modified to account for groundwater-soil interaction, which, in the end, is used to simulate water balance components in the Dijle watershed, Belgium (Chapter 3). This latter is also used to evaluate surface water-groundwater interactions (SW-GW) at the regional Scheldt basin (Chapter 4)

2. **Objective 2**. The lack of input preparation, post-processing, and calibration tool (IPPC) for the SWAT+gwflow model leads to the development of an automation toolkit for enhanced model application (Chapter 3). This tool avoids the long manual GIS operations that need to be done to prepare input files.

3. **Objective 3**. Having the modified SWAT+gwflow model and the tool from the previous objectives, assessing the use of the coupled model for further use such as investigating the impact of agricultural water drainage (Chapter 4), evaluating SW-GW interactions at the regional scale (Chapter 4), assessing climate change impact on streamflow and groundwater reserve is done (Chapter 5).

4. **Objective 4**. For the SWAT+gwflow model to evaluate agricultural water drainage, finding the locations where the drainage units are placed is vital. Thus, a new methodology is primarily formed to enhance the accuracy of locating those drainage units.

5. **Objective 5**. Developing an inventory of historical droughts (meteorological, agricultural, and hydrological) in the regional Scheldt basin is also the objective of this thesis which makes it one of its kind. Hence, using the coupled model, the Scheldt basin historical droughts are investigated (Chapter 5).

6. **Objective 6**. Assessing whether climate change is a main player in streamflow and groundwater drought in the Scheldt basin is examined using the coupled model, where it's forced with factual (with climate change) and counterfactual (detrended – without climate change) data.

7. **Objective 7**. In the end, an extensive literature review on the use of nature-based solutions (NbS) for drought mitigation is assessed. In addition, a novel framework is developed to find suitable detention basins and managed aquifer recharge areas to mitigate the impact of drought on water resources (Chapter 6).

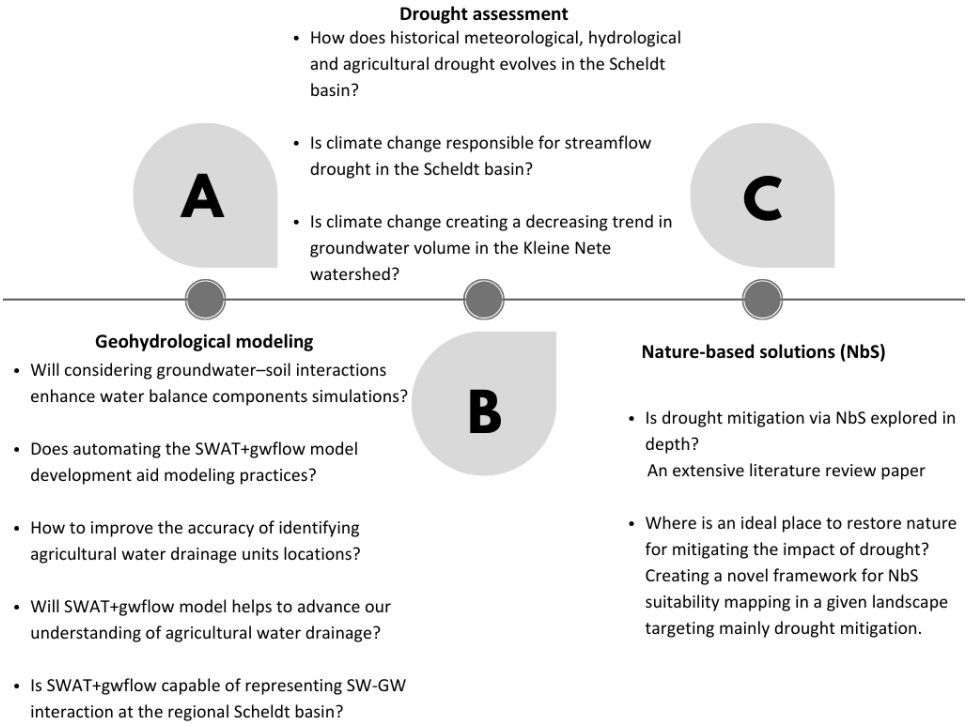


Figure 1.2: Research objectives of the three main categories of the thesis (geohydrological modelling and its application, drought assessment, and finally, nature-based solutions for drought mitigation).

1.3 Scientific novelty of the research

- The modification that was adopted on the SWAT+gwflow to account for groundwater-soil interaction is vital to capture the geohydrology of watersheds, mainly those in groundwater-dominated areas or shallow aquifers (e.g., catchments in Flanders).
- The model was applied and validated at a regional scale for the first time, increasing the model's reliability in representing geohydrology in different climatic, geological, and land use contexts. Additionally, its application for assessing intensively drained agricultural areas is validated, showcasing its adaptability for scenario analysis and implications for policy-making.
- Before applying the model for assessing agricultural water drainage in the Kleine Nete watershed, finding areas that apply drainage was challenging, and this research designed a methodology that identifies those locations and assesses their impact using SWAT+gwflow. The methodology was validated using an additional study area in

Ontario, Canada's highly drained agricultural area, indicating its global application potential.

- There is no tool for input preparation, post-processing and calibration for the newly developed SWAT+gwflow model, making it useful for the wider SWAT+ user community.
- Inventory and comprehensive assessment of historical meteorological, agricultural, and hydrological droughts is missing in the Scheldt basin, hence, the historical drought assessment using a calibrated and validated SWAT+gwflow model is vital. Additionally, analyzing and finding an appropriate probability distribution function to further be used for the three different drought types shows the scientific added value of this research.
- Climate change attribution studies at catchment scale and representing both the surface and groundwater hydrology are rare, hence, the use of SWAT+gwflow model in the Scheldt basin to evaluate the extent of climate change impact on the geohydrology is vital addition of this research to attribution analysts.
- A comprehensive literature review on nature-based solutions (NbS) was conducted to target drought. Additionally, a novel framework was also designed to find suitable detention basins and managed aquifer recharge locations to withstand extreme drought events in a given landscape.

1.4 Outline of the thesis

This doctoral thesis is organized based on a series of international peer-reviewed journal articles, either published, in review or draft stage. The thesis is structured as follows (Fig. 1.1):

In chapter 2, A literature review is conducted to show the state-of-the-art geohydrological modeling, input preparation, post-processing and calibration tools for the SWAT+ model, groundwater-surface water interactions, agricultural water drainage identification techniques, the impact of water drainage on geohydrology, drought analysis methods, drought attribution to climate change, and nature-based solutions for hydroclimatic extremes. This chapter identifies research gaps, which are later investigated in depth in the following chapters.

In chapter 3, This chapter has two major parts. Firstly, the SWAT+gwflow model is modified to account for groundwater-soil interactions, hereafter validated using the Dijle watershed located in Belgium as a case study area. Secondly, the SWAT+gwflow model input preparation, post-processing, and calibration (IPPC) tool is developed to ease the model's application. This chapter is based on two peer-reviewed published papers.

In chapter 4, The modified SWAT+gwflow model and the IPPC tool from the previous chapter are used to perform a detailed assessment of geohydrology. Firstly, extensive agricultural water drainage is investigated using the coupled model. For this assessment, finding the locations of the agricultural drainage units is vital. Thus, a novel methodology is created to identify agricultural water drainage areas by combining remote sensing and groundwater levels. The coupled model is also used to evaluate groundwater-surface water interactions at a regional scale (the Scheldt basin). This chapter aims to validate the coupled model, which will ultimately be used to perform drought analysis in the next chapter. This chapter is based on three peer-reviewed published papers.

In chapter 5, The calibrated and validated coupled model from the previous chapter is used to perform drought analysis. Firstly, historical droughts (meteorological, agricultural and hydrological) inside the Scheldt basin are investigated using the coupled model outputs. Secondly, using factual (with climate change) and counterfactual (without climate change), the impact of climate change on rivers and groundwater systems is assessed. This chapter is based on three draft papers.

In chapter 6, Drought-specific nature-based solutions are assessed. Firstly, an extensive literature review is conducted to find research gaps. Next, a framework to find suitable areas for detention basins and managed aquifer recharge areas is developed. This framework is applied in Flanders and is assessed to see if local water demand can be met with the possible detention basin areas outlined by the framework. This chapter is based on two peer-reviewed published papers.

The key findings of this doctoral research are summarized in chapter 7 and recommendations for future research are indicated.

1.5 Study areas

For Chapter 3, we modified the SWAT+gwflow model, and to verify the modification, the Dijle watershed located in Belgium is used as a case study area. In the same chapter, the input preparation, post-processing, and calibration tool is tested using watersheds from Belgium, Spain, Morocco, Italy, and Denmark). For subsequent use of the model, seven watersheds inside the Scheldt basin are used (Chapters 4 and 5). However, when developing the novel methodology to identify agricultural water drainage unit locations, we used Kleine Nete and one additional catchment from Ontario, Canada. (Fig. 1.3).

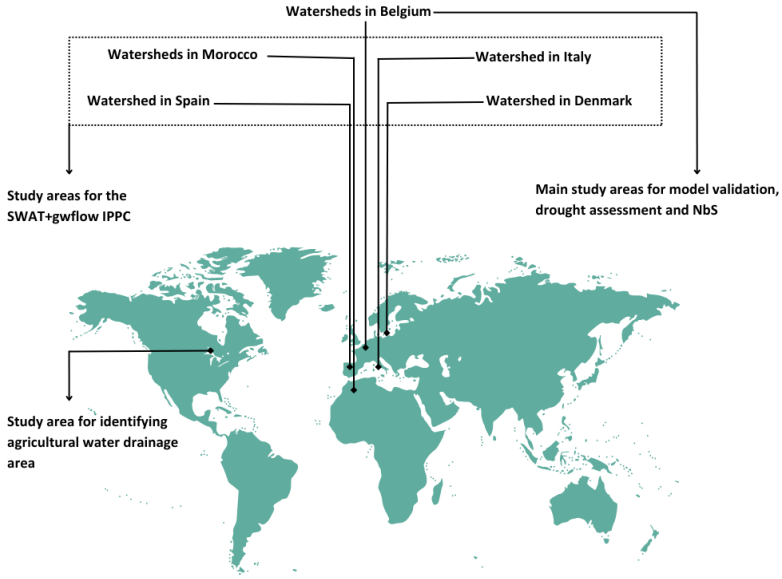


Figure 1.3: Study areas used for the different parts of the thesis. IPPC stands for Input Preparation, Post Processing and calibration tool

Chapter 2

Background

This section provides an overview of the four aspects of the thesis: geohydrological modelling, drought analysis, climate change attribution, and nature-based solutions. It dives into the state-of-the-art working mechanisms, how they are analyzed, and their limitations in accordance with the objectives of this thesis.

2.1 Geohydrological modelling

The complex nature of watersheds requires tools to evaluate the current trends (increasing or decreasing) of water system reserves (groundwater and surface water). Numerical models are widely used to represent geohydrological processes and provide insights for improved water management. These models are generally classified based on their model structure into conceptual and physical-based models, or on their level of discretization, into lumped and (semi-)distributed models (Pechlivanidis et al., 2011). There exists a vast literature that focuses on conceptual hydrological models (Raimonet et al., 2017; Woo et al., 2019; Choi et al., 2009; Essou et al., 2016; Vu et al., 2012). Models have limitations as they are usually simplistic, and their underlying concepts underestimate the spatially distributed nature of hydrological processes (Martina et al., 2011; Pellicer-Martínez et al., 2015; Sreedevi et al., 2021). In Raimonet et al. (2017), conceptual models are indicated to have significant pitfalls but are sometimes preferred over "complex" model setups due to reduced input requirement, relatively less uncertainty in the model parameter estimation process, comparatively low computation time, etc. (Al-Safi et al., 2020; Blöschl and Montanari, 2010; Ibrahim et al., 2015; Nguyen et al., 2018; Sun et al., 2015). These disadvantages of both lumped and distributed models can sometimes be overcome using semi-distributed models that offer a good balance between lumped, oversimplified conceptual models and fully distributed physically based models (Pechlivanidis et al., 2011).

An additional categorization of geohydrological models can be done based on whether they simulate either surface water or groundwater using standalone "single models" or both us-

ing "coupled models" (Wang and Chen, 2021). Surface water models mostly feature a simplified representation of groundwater (e.g., Soil and Water Assessment Tool, SWAT, Variable Infiltration Capacity, VIC, ensemble of surface water hydrology study by Huang et al. (2017), etc.), while groundwater models require recharge simulated from other surface water models (e.g., Modular Finite Difference Groundwater Flow, MODFLOW) (Aliyari et al., 2019). These single models, however, are preferably coupled when the groundwater-surface water interactions play a significant role. The benefits of coupling different models are evident, especially when considering the regional scale where human and environmental processes fully interact (Barthel and Banzhaf, 2016).

Groundwater (GW) and surface water (SW) have long been treated as separate components of the water system. However, they are in fact interconnected representations of a single resource that naturally influence one another and have an impact on water quantity, quality and pollutant diffusion (Fleckenstein et al., 2010). Due to growing pressures on water resources and water availability, the need for an integrated water management approach, considering GW and SW as a single entity has increased (Tigabu et al., 2020; Devito et al., 1996; Bailey et al., 2023). Furthermore, there has been an increasing interest into the interface between GW and SW, the hyporheic zone, because of its habitat potential for various organisms and as an area of biogeochemical cycling of nutrients and contaminants (Van der Velde et al., 2009). Additionally, significant spatial and temporal variability between GW and SW water fluxes can occur and complicate their coupling (Bailey et al., 2016). An improved multidisciplinary understanding of GW-SW interactions is thus required to conquer these challenges and further improve hydrological models that integrate both components (Bailey et al., 2020a).

Different levels of integration exist when coupling models, ranging from sequential or loose coupling, in which models operate autonomously, to fully embedded or integrated models (Siad et al., 2019). It is to be noted that both fully and loosely coupled models have limitations that need to be considered before using them for different applications. Coupled models require higher computational time and costs, and they are more complex. These potentials and problems are especially true for fully coupled models, which currently have been tested only in academic studies and whose potential in practical case studies is still to be demonstrated (Barthel and Banzhaf, 2016). For these reasons, loosely coupled models are considered a better alternative in practice (Wang and Chen, 2021), even if the regional geohydrological processes might be oversimplified (Barthel and Banzhaf, 2016).

Consequently, groundwater–surface water interaction has been mostly explored at a point or on a local scale, while regional scale (103 to 105 km^2) studies are rare. Since coupled models have a complex computational requirements, which need more data and computer resources, the number of coupled model applications in regional studies is very limited (Barthel and Banzhaf, 2016). For example, Bauer et al. (2006) used a conceptual coupled model with three components (overland flow, groundwater flow, and unsaturated zone) to simulate a data-scarce area like the Okavango Delta in Botswana. One of the most common

coupling combinations is the SWAT–MODFLOW coupling, dating back to 1999 (Wang and Chen, 2021). A large-scale application of SWAT–MODFLOW coupling application has been performed by Bailey et al. (2016) to model a basin in Oregon, USA. Similarly, Aliyari et al. (2019) updated the SWAT–MODFLOW codes to improve irrigation representation and tested it in a large basin in Colorado, USA. Deb et al. (2019) showed that the coupled SWAT–MODFLOW produced improved runoff simulations better than the standalone SWAT model, especially during dry periods, in two basins of Southeast Australia. Moreover, the MODFLOW model was also combined with the VIC model to investigate the impacts of climate change in a basin in Northwest USA (Sridhar et al., 2018). In general, however, the major challenges from these applications are either that they are too simplified, they require detailed data, or they are challenging to run for fine resolution due to computational requirement.

Based on the coupling scheme between GW and SW models two different approaches can be distinguished to design an integrated hydrological model, i.e. a fully coupled and loosely coupled approach. Here, the fully coupled approach refers to a design where the equations describing surface and subsurface flow are solved simultaneously in a physics-based model. On the other hand the loosely coupled approach refers to a design where coupling is achieved by using the model output of one model as input into the other model. According to Barthel and Banzhaf (2016) fully coupled models seem to be the best approach at first sight since such holistic description of the hydrological cycle can connect different processes over various spatial and temporal scales. However, they state that many authors agree such an approach is constrained by data availability and opt that loosely coupled models with a simple coupling approach might still be suitable even with oversimplification of the regional system Sridhar et al. (2018). Thus, there has been ongoing effort to find compromising point between these modelling approaches, mainly by the soil water assessment tool (SWAT) team at Texas A&M.

2.1.1 The Soil Water Assessment Tool (SWAT)

The Soil and Water Assessment Tool (SWAT), developed in the early 1990's, is a conceptual, continuous model developed to predict the impact of land management practices on water resources, sediment, agricultural and chemical yields (Arnold et al., 1998). SWAT is physically based, using data on climate, soil properties, topography, land use and management practices and vegetation to model the physical processes related to water movement, nutrient cycling, sediment movement, etc. (Bieger et al., 2017).

Over the past two decades it has become one of the most widely used hydrological models, applied to several basins across the world. Up till now, the model's capabilities have expanded significantly due to continuous development by the SWAT development group and collaborating scientists from all over the world due to it's open-source code (Chawanda et al., 2020). The SWAT model user community has user groups, extensive documentation which ensures transparency, reproducibility and comparability with other studies, making it an ideal model for use globally. The foundational strength of the SWAT model include its

combination of land processes and detailed management practices with channel processes as well as it's computational efficiency (Arnold et al., 2018; Yen et al., 2019). Additionally, it has a strong technical model support and there exist various interface tools and software for pre– and postprocessing of data and the construction, calibration, and parameterization of the SWAT model (Arnold et al., 2012). Nevertheless, the model struggled to clearly identify pollution sources and transport processes due to its spatial simplicity, which is an important step in several applications that consider water quality. Therefore, the SWAT code has undergone many modifications over the years to face these and future challenges resulting in SWAT+, an entirely revised and restructured model. SWAT+ uses the same basic algorithms to calculate processes in the model, but is far more flexible in its spatial representation of these processes and their interactions. Furthermore, the structure of the input files and organization have changed significantly.

SWAT+ allows the simulation of several physical processes in a watershed. To facilitate modelling, a watershed can be portioned into several hydrologic response units (HRUs). HRUs are unique combinations of landuse, soil type and elevation bands. Subsequently, HRUs are divided into upland and low land areas, labelled as landscape units (LSUs), one of the key improvements of SWAT+ compared to SWAT (Bieger et al., 2017; Arnold et al., 2018; Yimer et al., 2023a). Next, processes are lumped at subbasins level which ultimately forms the watershed. LSUs represent the land areas within the subbasin and are subdivided into hydrologic response units (HRUs). SWAT+ simulates the water balance of the watershed at the HRU level and aggregates the HRU output at the LSU level which can subsequently be routed to other spatial objects, e.g. channels, ponds, reservoirs, etc.,. SWAT+ is specifically designed for long-term, large-scale, continuous simulations of land–water processes, including climate variability, land use change, and management impacts. This is realized by a connect file that specifies the output for each spatial object, making it easier to connect managed flow systems. Total flow for HRUs and LSUs is obtained by summing up the surface runoff, lateral flow, and tile flow and does not include seepage which is assumed to recharge underlying aquifers (Dile et al., 2022).

SWAT+ simulates the hydrological cycle based on the water balance. Precipitation can be intercepted and held by vegetation or reach the soil surface. At the surface, water can infiltrate into the soil profile or flow overland as surface runoff, where it moves relatively fast to a stream channel and contributes to short-term stream response. On the other hand, infiltrated water can be stored in the soil, evaporated or percolate deeper as recharge for aquifers where it can contribute to return flow. Return flow or base flow is defined as the volume of streamflow originating from groundwater. These fluxes can be calculated according to different methods such as e.g. the soil conservation service (SCS) curve number method for surface runoff, the Green & Ampt method for infiltration, etc. (Dile et al., 2022).

For each subbasin SWAT simulates a shallow and deep aquifer. The shallow aquifer is an unconfined aquifer that directly contributes to flow in the main channel of the subbasin. The deep aquifer, on the other hand, is a confined aquifer and contributes to streamflow

outside of the watershed. The percolating water is partitioned between these two aquifers as recharge, which is calculated as,

$$w_{\text{rchrg},i} = \left(1 - \exp\left(-\frac{1}{\delta_{\text{gw}}}\right)\right) \cdot w_{\text{seep}} + \exp\left(-\frac{1}{\delta_{\text{gw}}}\right) \cdot w_{\text{rchrg},i-1} \tag{2.1}$$

where $w_{\text{rchrg},i}$ represents the amount of recharge entering the aquifers on day i (mm), δ_{gw} the delay time of the overlying geologic formations (days), w_{seep} the total amount of water exiting the soil profile through the bottom on day i and $w_{\text{rchrg},i-1}$ the amount of recharge entering the aquifers on day $i-1$. Partitioning between the aquifers is achieved by means of an aquifer percolation coefficient. Furthermore, base flow is only allowed to enter the main channel of the subbasin when a certain threshold, specified by the user, is achieved. Finally, groundwater flow in to the main channel is calculated according to,

$$\frac{dQ_{\text{gw}}}{dt} = \alpha_{\text{gw}} \left(w_{\text{rchrg,sh}} - Q_{\text{gw}}\right) \tag{2.2}$$

where Q_{rchrg} represents the groundwater flow into the main channel on day $i(mm)$, $w_{\text{rchrg},sh}$ the amount of recharge entering the aquifers on day i and α_{gw} the baseflow recession constant. Here, the baseflow recession constant or proportionality constant is a direct index of the groundwater flow response to changes in recharge.

Apart from the hydrological processes, SWAT+ determines the channel routing of the calculated water load, sediments, nutrients and pesticides. During this step, velocity and discharge of the channel flow is calculated taking into account evaporation losses as well as transmission losses through the channel bed. Additionally, water losses related to human use or agriculture can be incorporated. The channel flow can be supplemented by direct rainfall or point source discharge. Routing is done using the Muskingum routing method or a variable storage coefficient method (Bieger et al., 2017; Dile et al., 2022).

SWAT and SWAT+ have been frequently applied worldwide to asses climate change impacts, pollutant losses, water supply, sediment dynamics, water management and conservation practices. However, due to a simplified representation of groundwater processes, both models are rather limited in groundwater–driven catchments (Deb et al., 2019; Gassman et al., 2007; Peterson and Hamlett, 1998; Spruill et al., 2000; Srivastava et al., 2006). Calculations in SWAT(+) at HRU level allow for an efficient calculation scheme with a trade-off in spatial resolution due to its semi-distributed features. Therefore, SWAT(+) has often been coupled to a groundwater model such as MODFLOW (Perkins and Sophocleous, 1999; Bailey et al., 2016; Kim et al., 2008; Galbiati et al., 2006; Guzman et al., 2015; Sophocleous et al., 1999), a modular groundwater flow model developed by the U.S. Geological Survey.

According to Wang and Chen (2021), the coupling between SWAT and MODFLOW can be divided into three main stages. The coupling had first been proposed by Sophocleous et al. (1999) which led to the development of a combined SWAT/MODFLOW model

named SWATMOD. This model was capable of simulating surface water, groundwater and aquifer-stream interactions continuously and was applied to the Rattlesnake Creek basin in south-central Kansas (Sophocleous et al., 1999).

In the second stage a new integrated SWAT/MODFLOW model, called SWAT-MODFLOW, was developed by Kim et al. (2008) with the introduction of an innovative HRU-cell conversion interface. This way, daily flow data could be exchanged between HRUs (SWAT) and cells (MODFLOW), including recharge, evapotranspiration, river-aquifer interaction and pumping rates. Consequently, the model was applied to the Musimcheon Basin in South Korea and showed better simulation results than the standalone SWAT model.

One of the remaining challenges in coupling SWAT to MODFLOW is that HRUs are not geographically located as opposed to cells in MODFLOW. Therefore, Bailey et al. (2016) developed a new integrated SWAT-MODFLOW model where a HRU disaggregation (DHRU) technique was introduced. DHRUs further divide the original HRUs in contiguous areas within the subbasin, which allows HRU calculations to be geo-located and can represent recharge spatially for linkage to MODFLOW grid cells. Additionally, Bailey et al. (2017) developed a graphical user interface (GUI) named SWATMOD-Prep based on the SWAT-MODFLOW code to couple a SWAT watershed with a MODFLOW groundwater model. The GUI serves as a guide for the coupling of an existing SWAT model with a new single layer MODFLOW model. Nevertheless, the model has disadvantages, mainly not allowing the coupling between SWAT and an existing MODFLOW model. Finally, this downside has been resolved by Park et al. (2019), who introduced a new, QGIS-based GUI for SWAT-MODFLOW models named QSWATMOD. It allows a new MODFLOW model to be created or an existing model to be used. Consequently, plus the fact that it is based on the open-source QGIS platform, it is more accessible to the hydrologic modelling community. Furthermore, a variety of options are available to link the SWAT river network with MODFLOW river cells to account for groundwater-surface water interactions. However, there are disadvantages that characterize the coupling of SWAT with MODFLOW, e.g. long runtimes and extensive modifications to modelling codes and additional source files still persist, leading to the development of SWAT+gwflow as explained in the following section.

2.1.2 SWAT+gwflow

Similar to the SWAT code, SWAT+ uses simplified steady–state equations to represent the groundwater flow component, including groundwater discharge to streams, variation in the groundwater table and storage, and water exchange between aquifers and streams. This simplified representation has some limitations. Groundwater discharge to streams and recharge are the sole components influencing groundwater head, whereas stream seepage to aquifers is not accurately represented in the standalone SWAT+ model. Furthermore, groundwater is analyzed separately from the neighboring aquifers at every aquifer unit (there is no interaction among sub-basins in the groundwater). These limitations might lead to erroneous results while simulating nutrient loads or water availability in basins with

groundwater dominance (Bailey et al., 2022, 2020b). To tackle these limitations, Bailey et al. (2020a) created a new physically based and spatially distributed groundwater flow module of SWAT+ called gwflow.

SWAT+gwflow is suitable for catchments with unconfined aquifers, and it uses the Dupuit –Forchheimer approximation, where the vertical hydraulic gradient is assumed to be negligible. The standalone SWAT+ model has a simplified representation of groundwater hydrology where linear reservoir approximations are used, leading to misrepresentation of the hydrologic processes (Deb et al., 2019; Gassman et al., 2007; Peterson and Hamlett, 1998; Spruill et al., 2000; Srivastava et al., 2006). As the aquifers in Flanders are mostly unconfined, the SWAT+gwflow model has more valuable features to benefit from than the standalone SWAT+ model. It should be noted that the new module (gwflow) is a physically based and fully distributed model with essential model outputs such as recharge, groundwater–surface water interaction fluxes, groundwater–soil fluxes, saturated excess flow, pumping, etc.

This new coupled model has the advantage over the other applications in that it is based on global datasets for aquifer properties, such as depth to the base of the unconfined aquifer, and that the implemented coupling requires less computation time. On the other hand, it still maintains the heterogeneous and physical hydrogeology of the watershed systems.

This module, when activated, replaces the existing aquifer module of SWAT+ due to the limitations of the groundwater representation inside the standalone model. In this module, the aquifer is represented by a single layer, and the user chooses the size of the square grid cells used to discretize the aquifer into volumetric control volumes (Fig. 2.1). At the level of each grid cell (i.e., a small volume of aquifer), the stored groundwater volume is updated at a daily time step based on groundwater inflows and outflows.

$$\frac{\Delta V}{\Delta t} = (Q_{\text{rech}} + Q_{\text{sw}\rightarrow\text{gw}}) - (Q_{\text{gwet}} + Q_{\text{gw}\rightarrow\text{sw}} + Q_{\text{satex}} + Q_{\text{pump}}) \pm Q_{\text{north}} \pm Q_{\text{south}} \pm Q_{\text{west}} \pm Q_{\text{east}} \tag{2.3}$$

Where V is the grid cell groundwater volume in m³, t is the time step in days, and Q is the volumetric groundwater flux in m³/day. Q_{rech} (1) and $Q_{\text{sw}\rightarrow\text{gw}}$ (2) are source fluxes, and they are recharge and streamflow to aquifers, respectively. Q_{gwet} (3), $Q_{\text{gw}\rightarrow\text{sw}}$ (4), Q_{satex} (5), and Q_{pump} (6) are sink fluxes, which are groundwater removed by means of evapotranspiration, groundwater discharge to surface water bodies (mainly streams), saturation excess flow that occurs when the groundwater table is above the ground surface, and groundwater depletion through pumping, respectively. The fluxes $Q_{\text{north}}, Q_{\text{south}}, Q_{\text{west}}$, and Q_{east} represent lateral flow (Fig. 2.1) to or from surrounding grid cells, calculated using Darcy's Law, depending on the groundwater head values of the cells.

Furthermore, the recharge flux is transferred to each cell from the HRUs at every time step, and the amount transferred depends on the intersection fraction of each grid cell with an

HRU (Bailey et al., 2020b, 2022). By implementing an expression for groundwater storage into Eq. 2.3 that relates to groundwater head h and specific yield S_y, Eq. 2.4 solves h for every grid cell using an explicit scheme expressed by:

$$h^{n+1} = h^n + \Big(Q_{\text{rech}} + Q_{\text{sw}\rightarrow\text{gw}} - Q_{\text{gwet}} - Q_{\text{gw}\rightarrow\text{sw}} - Q_{\text{satex}} - Q_{\text{pump}} \pm Q_{\text{north}} \pm Q_{\text{south}} \pm Q_{\text{west}} \pm Q_{\text{east}}\Big) \cdot \frac{\Delta t}{S_y \Delta x \Delta y} \tag{2.4}$$

The gwflow module is coupled with SWAT+ in such way that recharge from each HRU is passed to the water table and each grid cell that intersects with a specific HRU will receive the percolating water as recharge. The amount of water that has passed from the HRUs to the grids is multiplied by the grid size so that it can be passed to the control volume in m^3/s. The lateral flow to and outside of neighboring cells is estimated based on the Darcy's law, where a higher/lower hydraulic gradient forces groundwater to be added/removed to cells. As for evapotranspiration (ET) from the groundwater system, the depth at which ET is extinct determines the amount of water that leaves the aquifer. The surface-groundwater interaction is simulated based on Darcy's law where the river stage and groundwater head in the vicinity of the streams determines the amount of water transferred to and from the aquifer and vice versa. Finally, the saturated excess flow occurs only if the water table lies above the ground surface. Note that, when gwflow module is used, the old/simplified groundwater module parameters will not be active.

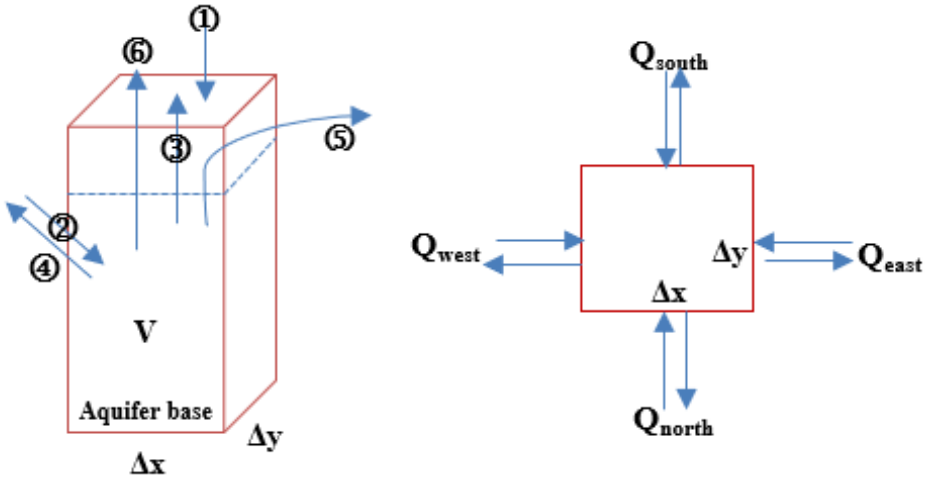


Figure 2.1: The different sources and sinks to and from the control volume. The control volume is the smallest unit where computation is made inside the gwflow module

2.1.3 Overview of SWAT+ input preparation, calibration and postprocessing tools

One of the main strengths of SWAT is the large community of users, whose efforts contributed to the establishment of protocols, tools, and scripts to simplify and homogenize the application of the model. For example, calibration protocols with clear metrics and thresholds to evaluate hydrological model performances were established in the highly cited papers of Moriasi et al. (2007, 2015). The model's success is also to be attributed to the intuitive Graphical User Interfaces that ease the model setup, calibration, and simulations. Watershed delineation, for example, is typically performed in SWAT with the ARCSWAT (Winchell et al., 2007) or QSWAT(+) (Dile et al., 2022) interfaces. Climate data, management, and other setup options are then included and edited in the SWAT(+) Editor. Calibration and sensitivity analysis are instead performed with tools such as SWAT–CUP (Abbaspour et al., 2015), IPEAT(+) (Yen et al., 2019), R-SWAT (Nguyen et al., 2022), and SWAT+ Toolbox. Moreover, SWAT Check helps the user to individuate potential problems in their models (White et al., 2014). Software such as the SWAT + AW was also created to enhance the reproducibility of the studies (Chawanda et al., 2020). To ease the coupling of SWAT with MODFLOW to improve the representation of groundwater, the QSWATMOD (Park et al., 2019) and the SWATMOD-Prep (Bailey et al., 2017) interfaces were developed.

Even though SWAT and MODFLOW have been extensively coupled in many studies, their integration requires significant modification of the modeling codes and the addition of multiple source files, leading to long time for the setup and running of simulations (Bailey et al., 2020b). The gwflow module was developed to solve these issues, and since its introduction, it has been applied in various studies (Bailey et al., 2023, 2022; Yimer et al., 2023b,c,a). Nevertheless, interfaces that aid the input creation, post-process, and calibration are not available for SWAT+gwflow.

Preparing inputs for gwflow involves multiple GIS routines, making it a potentially time-consuming process. Therefore, automating input preparation becomes crucial for the geo-hydrological modeling community. Additionally, the coupled model has advanced in representing various interactions such as wetland-groundwater, floodplain-groundwater, and reservoir-groundwater. These interactions necessitate additional inputs beyond what is typically required for the coupled model, underscoring the need for scripts accommodating such exchanges.

The SWAT+gwflow inputs constitute the following major files: gwflow.input, gwflow.hrucell, gwflow.cellhru and gwflow.rivercell. The gwflow.input is the central file containing the module's basic information (which processes to simulate the hydraulic conductivity and specific yield zones, aquifer thickness, ground surface elevation, etc).

2.1.4 Agricultural water drainage unit identification techniques

Soil and land transformations to boost agricultural land productivity are common practices. Soil amelioration (physical and chemical), land forming (to improve water distribution in the field), soil and water conservation, and irrigation are some of the watershed modification techniques (Tilahun and Seyoum, 2020). These strategies (and many others) are applied to increase farm productivity (Smedema et al., 2000). Since the beginning of civilization in Mesopotamia and Iran (before 4000 BCE), subsurface drainage has been the most popular conservation method (Kalita et al., 2007). Around the middle of $19th$ century, drainage systems started to emerge when the impact of salinity was becoming apparent (Valipour et al., 2020). It can be said that the advancement of drainage science originated in France under the direction of Henry Darcy, who founded what is known as Darcy's law (Valipour et al., 2020). Hooghoudt (1940) came up with the analytical solution for groundwater flow to drains, and other researchers, such as Ernst (1962) and Kirkham (1972), followed.

Drainage in agricultural fields will help to prevent or reduce waterlogging, where the water table is maintained at a depth of 1–2 m beneath the ground surface by tile drainage, thus enabling crop productivity (Sloan et al., 2016). They can be made from clay, ceramic, or corrugated plastic (Roy, 2014). A drainage system also helps to control over salinity in irrigated areas. According to Ritzema et al. (2008), around 8.4 million ha of area is affected by soil salinity, whereas 5.5 million ha of land is waterlogged. This is amplified in arid and semiarid areas with high evaporation (Chávez et al., 2015). This salinization of agricultural fields is increasing at an alarming rate, hence, lands are being abandoned (Ritzema et al., 2008). Freshwater flushing to remove salt from root zone in irrigated farms is a reliable and widely applied method that ultimately improves soil quality (Christen and Skehan, 2001; Guo et al., 2018).

These artificial drainage systems have hydrological and environmental impacts (Yimer et al., 2023b). Drainage systems can alter the water quantity and quality in surface and groundwater systems (Rozemeijer et al., 2010). Thus, drainage ditches can transport nutrients and other agricultural pollutants to downstream water bodies (Smith et al., 2008). Recent studies on tile drainage have directed their attention toward assessing the impact of drainage units on the water quality of surface and groundwater systems (Allred et al., 2018; Bailey et al., 2022; Behrendt et al., 2000; Fausey et al., 1995; Kalita et al., 2007; Williams et al., 2015). Freshwater is scarce due to drought (Yimer et al., 2022), hence, the drained water can be useful to cope with dry spell months.

According to Valayamkunnath et al. (2020), it is difficult to investigate its impact on the hydrology and water quality due to the lack of tile-drainage location map. Thus, finding the location of drainage units is vital for the farmers to increase their economic benefits through sustained crop productivity. It is also essential to measure the density and spacing between tile lines (Stillman et al., 2006), but knowing their location is still challenging, hence, considerable efforts are made to identify and map drainage units.

Existing techniques to identify drainage units include manual operations such as digging and non-invasive methods such as remote sensing-based approaches (RS)(Thayn et al., 2011), decision tree classification (DTC), ground penetrating radar (GPR), thermal detection, Unmanned Aerial Systems (UASs) (Tilahun and Seyoum, 2020; Allred et al., 2020) etc. The RS approach is based on the assumption that the remotely sensed images before and after a major rainfall event can differentiate drained and undrained fields (Northcott et al., 2000; Gökkaya et al., 2017; Thayn et al., 2011). The DTC follows the hierarchal identification of drainage units based on land use, soil drainage class, and slope (Naz et al., 2009). The shortcoming of the invasive methods is the expense related to the digging-out process (Allred et al., 2018). As for the GPR technique, extensive effort is required until the buried units are identified (Allred et al., 2004). Tile spacing and line identification advancements using high-resolution imagery (UASs) are emerging (Allred et al., 2021; Koganti et al., 2020; Tilahun and Seyoum, 2020). Although the RS and DTC approaches are considerably cheaper and more efficient, they can also provide low accuracy in determining the location of the drainage units (Naz and Bowling, 2008; Reynolds, 2014; Thompson, 2010). For example, RS-based techniques rely on the availability of cloud-free imagery to implement the methodology successfully. Similarly, the DTC method does not necessarily infer the existence of drainage units. Therefore, proper, cost-effective, accurate, and efficient mapping techniques are needed to locate drainage units (Tilahun and Seyoum, 2020). On top of this, all the drain locating techniques neglect the primary cause of drain application: groundwater level reaching the root zone. Hence, accounting for this major variable and applying additional filtering on the RS technique can potentially improve the accuracy of the traditional approaches.

2.2 Drought

Geohydrological models are quite versatile in producing outputs that can be used to evaluate natural hazards (e.g., drought, floods, etc.) and human-induced water scarcity. However, what is drought? How does it occur? What is its impact on water systems, society, biodiversity, etc.? How to assess it? These questions will be explored in depth in this section.

What is drought and its impact?

Drought has affected millions of people across the globe, with an estimated human loss of 650,000 and economic loss tripling from 1970 to 2019 (UN, 2022). Droughts, as defined according to Europea (2007) is significant temporary reductions in the average availability of water, which deviate significantly from the typical levels of natural water availability and are classified as natural occurrences. Water scarcity is defined as a situation in which there are not enough water resources to meet average long-term demands. It describes the long–term water imbalances, in which the amount of water available is less than the amount needed, indicating that the amount of water needed surpasses what can be sustainably extracted (Europea, 2007).

Drought analysis methods

In conducting integrated drought analysis, two main approaches are often used: the threshold-based method (TB) and the standardized index-based method (SIB) (Fig. 2.2). The Threshold Based Method, which is still used in drought analysis today, was first presented by Yevjevich (1967) and then further developed into an explicit drought definition approach by Zelenhasić and Salvai (1987). The threshold-based method uses two ways of calculating the threshold to determine whether a given time series of a hydrometeorological variable is under drought or not. The constant threshold method uses a given percentile (usually between the 70^{th} and 95^{th} percentile) of the time series as used in Sung and Chung (2014) while the variable threshold takes monthly percentiles of the same range to account for the seasonal variation. While both methods are used to conduct drought analysis in a comprehensive manner, the variable threshold method has been used more recently (Van Huijgevoort et al., 2012; Van Loon et al., 2014).

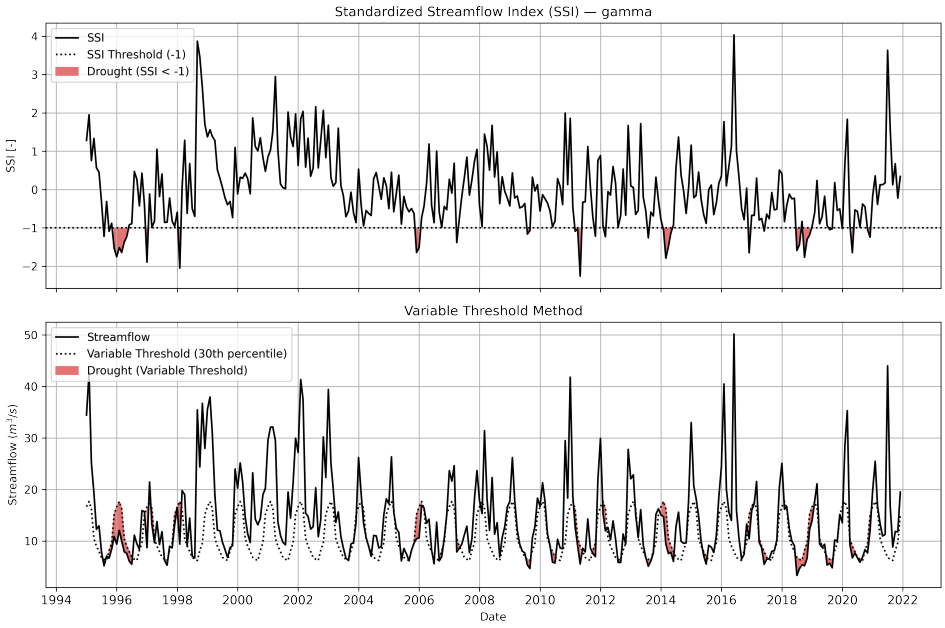


Figure 2.2: The widely adopted drought analysis methodologies (standardized index and threshold based)

The other method is the standardized index–based method, which involves the computation of drought indices for the different types of drought and then computing drought severity, duration, and intensity to characterize drought events (Mishra et al., 2010). This method mainly involves taking the time series of hydrometeorological variables from outputs of a

model or from meteorological stations at different time scales (1, 3, 6, 9, 12, etc. months). This is followed by fitting statistical distributions to determine overall anomalies. A wide range of indices, derived from various variables, have been established to detect and measure instances of drought. These consist of, for instance, the Standardized Precipitation Evapotranspiration Index (SPEI) (Vicente-Serrano et al., 2010), Standardized Streamflow Index (SSI) (Modarres, 2007), Standardized Soil Moisture Index (SSMI) (Hao et al., 2014), Standardized Water-level Index (SWI) (Bhuiyan, 2004), etc.

When conducting drought analysis using SIB method, the choice of the statistical distributions used to fit the hydrometeorological variable is critical as it can lead to inaccuracies (Yimer et al., 2022). Due to this, Goodness of Fit (GOF) tests including the Kolmogorov-Smirnov (K–S) test, Anderson-Darling (A–D) test, and Shapiro-Wilk (S–W) test were conducted for SPEI in Yimer et al. (2022). These tests were also conducted for both SPEI and SPI in Stagge et al. (2015). A common conclusion reached by both studies was that the S–W test efficiently differentiates among the candidate distributions for the normality testing of the final derived drought index. In addition, the S–W test produces results similar to those of the K–S and A–D tests with more sensitivity and the K–S test was found to be the least sensitive to suggested distributions. More importantly, the S–W test can be quickly and easily implemented as opposed to K–S and A–D tests, negating the requirement for Monte Carlo simulations of critical test values (Yimer et al., 2022).

Drought severity is defined as cumulative sum of index deficits below the threshold (commonly -1 for SIB and below predetermined threshold for TB method) during drought event and drought duration is the number of consecutive time steps (months, weeks, days depending on the index) that the index remains below the threshold. Finally, drought intensity is the quotient of drought severity and duration which shows the average deficit relative to the duration.

The use of geohydrological models for drought analysis

Many drought indices are derived from the results of hydrological models (Maskey and Trambauer, 2015). While some observational data for drought monitoring and historical drought analysis may be available, these data are typically restricted to a small number of locations and are typically insufficient to represent the spatial variability of droughts (Maskey and Trambauer, 2015). This is certainly the situation in which using a distributed or semi-distributed hydrological model is quite beneficial (Maskey and Trambauer, 2015). Additionally, a hydrological model is a tool for prediction and can therefore be very helpful for assessing, tracking, operational forecasting of drought (Maskey and Trambauer, 2015).

Another aspect of drought that could be studied by using a coupled geohydrological model such as the SWAT+gwflow is drought propagation (Yimer et al., 2023a). Drought propagation is studied to represent how drought conditions change and spread throughout different hydrological systems (Wossenyeleh et al., 2021). In the terrestrial portion of the hydrologi-

cal cycle, the term "drought propagation" is defined as the shift in the drought signal and entails translating abnormal meteorological conditions into hydrological drought (Van Loon, 2015). Droughts, essentially happen in a specific order, for instance, precipitation deficit causes meteorological drought, which next affects soil moisture. Finally a delayed occurrence of a hydrological drought (streamflow and/or groundwater drought) are caused by low soil recharge into water features like lakes and streams (Mishra et al., 2010). Although soil moisture drought mostly occurs concurrently with meteorological drought, streamflow drought and groundwater drought are relatively delayed (Van Loon, 2015). Hence, the need to understand the relationships between meteorological drought and hydrological drought in terms of lag–time is evident. The simplicity and ease of interpretation makes the threshold–based method suitable for studying drought propagation as it is also applied in several studies (For example, Heudorfer and Stahl (2017); Odongo et al. (2023); Van Loon (2013); Wossenyeleh et al. (2021).

Drought attribution to climate change

Drought is an abnormal deviation in water balance components (precipitation, streamflow, groundwater level, etc.) from normal conditions (Van Loon, 2015; Zhou et al., 2024). This can affect agricultural products (such as crops), humans, ecology, and more (Blauhut et al., 2016; Cohen et al., 2021). Recent extreme hydroclimatic events, in particular, indicate an increase in drought severity and duration in various regions around the globe (Chiang et al., 2021; Spinoni et al., 2014; Vicente-Serrano et al., 2022). Most scholars agree that the major factor in the worsening of this phenomenon is climate change. However, some question whether climate change is the only factor involved (Chiang et al., 2021; Frame et al., 2020; Perkins-Kirkpatrick et al., 2022; Van Oldenborgh et al., 2021).

Climate variability, land cover changes, and catchment characteristics changes can affect hydrological processes in river basins (Ahmed et al., 2022; De Niel and Willems, 2019). Detection and attribution of changes in natural systems offer a robust tool for understanding the complex causes of climate change, enabling the development of more effective mitigation and adaptation strategies (Didovets et al., 2024; Mondal and Mujumdar, 2012). The detection of changes examines the system change without identifying the reasons for that change, whereas attribution assesses the relative contributions of the causal factors to that change (Ahn et al., 2016; Mondal and Mujumdar, 2012). The used methods can be divided into data-based and simulation-based approaches (Gelfan et al., 2023). This can involve comparing observed discharge with detrended climate data, without climate change, or by excluding human influence in anthropogenic affected systems (Didovets et al., 2024). Studying detection is complicated by challenges such as high runoff variability, urbanization, deforestation, interactions among drivers, and short streamflow records (De Niel and Willems, 2019; Gelfan et al., 2023).

For all these analyses, a tool to simulate the geohydrological components is required. This is where geohydrological models play a role. Simulated streamflow, groundwater head,

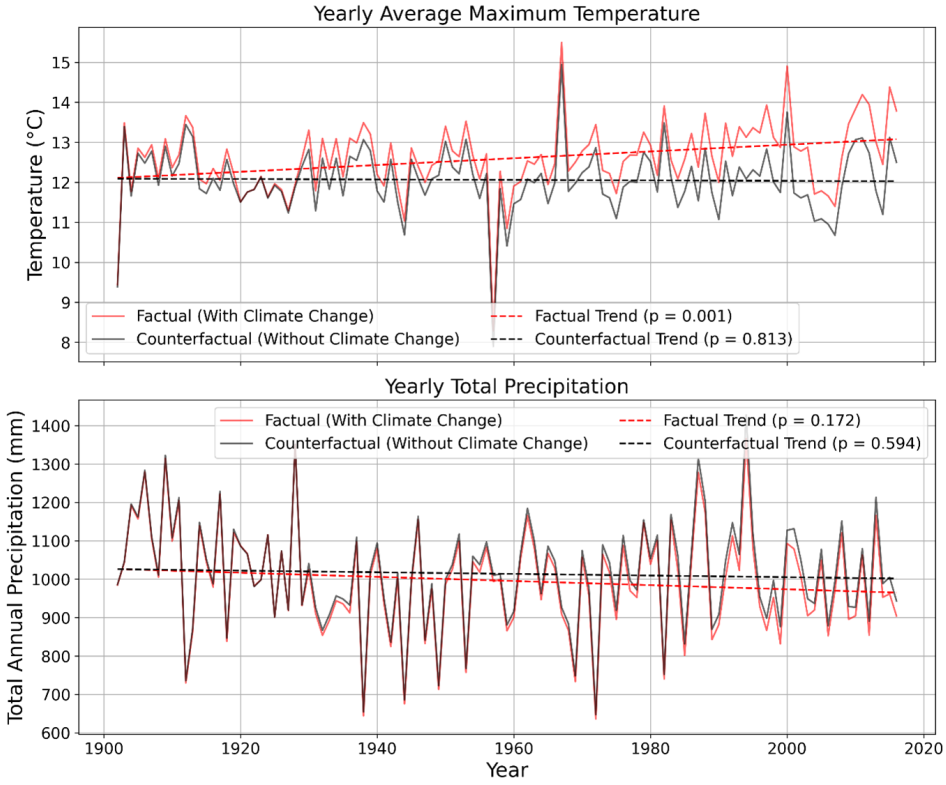


Figure 2.3: Yearly average maximum temperature and yearly total precipitation for Belgium with the trend line and significance level (p-value).

runoff, evapotranspiration (ET), percolation, and soil moisture are primarily used to perform spatiotemporal analysis of drought in watersheds (Guevara Ochoa et al., 2020). In drought attribution studies, the use of models is essential if the objective is to investigate hydrological and agricultural drought (Ding et al., 2021; Sun et al., 2023; Wang et al., 2023). De Niel and Willems (2019) fitted a panel analysis model for Flanders, Belgium, attributing changes in river peak flows. They found that catchment characteristics explain more of the changes than climate variability or land cover changes. Similarly, a Bayesian statistical framework was used to attribute changes in peak river flows in the UK (Brady et al., 2019). When a genetic programming model is applied at a basin scale in India, it attributes observed changes to human–induced climate change (Mondal and Mujumdar, 2012). The ABCD hydrologic model was also applied in the Connecticut River Basin, USA, where it was found that climate factors were the largest contributors to observed changes (Ahn et al., 2016). Didovets et al. (2024) studied six upstream countries in Asia using the Soil and Water Integrated Model (SWIM), a semi–distributed hydrological model. They found that

changes in discharge could be attributed to climate change in some catchments. Additionally, four river basins in different locations were studied using ECOMAG–based models, with high confidence that the observed changes can be attributed to climate drivers (Gelfan et al., 2023).

Models alone cannot fully evaluate attribution studies. Therefore, different scenario dataset are needed to simulate factual (with climate change) and counterfactual (without climate change) conditions (Fig. 2.3). The Inter-Sectoral Impact Model Intercomparison Project (ISIMIP) provides four detrended datasets to help understand and disentangle the effects of climate change and natural variability (Mengel et al., 2021). Each method comes with its own associated uncertainty, so it is crucial to show this to policymakers when discussing potential declines in groundwater head (Nkwasa et al., 2024).

2.3 Nature-based solutions

What is nature-based solution?

Climate change affects the Earth in many ways, including heavy storms, floods, wildfires, sea level rises, and severe droughts (Cortinovis et al., 2022). The latter is considered one of the most expensive climate disasters globally as they leave chronic and long-term impacts on the ecosystem, agriculture (Yimer et al., 2023a), and human society (Cook et al., 2018; WWAP (United Nations World Water Assessment Programme) and UN-Water, 2018). Cook et al. (2018) define drought broadly as an "anomalous moisture deficit relative to some normal baseline". More specifically, three types of droughts can be distinguished: meteorological, agricultural, and hydrological. Meteorological droughts are due to the lack of precipitation, while agricultural droughts occur as the precipitation deficit continues through time and affects soil moisture. As the deficit persists and even affects the streamflow and storage in aquifers and reservoirs, hydrological droughts arise (Cook et al., 2018; Debele et al., 2019; Wilhite and Glantz, 1985).

Droughts occurred more frequently with increased intensity and duration in the last years on a global scale (OECD, 2020; Yimer et al., 2022). The total population affected by drought is now estimated at 1.8 billion, including both the socio–economic and mortality impacts. Also, in the future, the frequency of droughts is projected to increase in most regions, except in the high northern latitudes, east of Australia, and east of Eurasia. These regions are expected to experience no significant change or even a decrease in frequency (WWAP (United Nations World Water Assessment Programme) and UN-Water, 2018). So, droughts are not only occurring in the already dryer areas, as is sometimes supposed, but they also threaten regions that are usually not facing water scarcity, such as Belgium. The predicted longer duration and frequency of droughts can be alleviated by staking nature-based solutions (WWAP (United Nations World Water Assessment Programme) and UN-Water, 2018). Enlarging and maximizing the water storage capacities

and retaining the water in the aquifers (slower release of water) is one way to cope with droughts using NBS (OECD, 2020; WWAP (United Nations World Water Assessment Programme) and UN-Water, 2018). As aquifers have a large potential storage capacity, the available groundwater in the aquifers and additional water can function as a buffer in periods of high seasonal variations in the water supply. The extra water falling in wet periods can be stored on the (sub)surface and contribute to the water availability in dry periods later (Keesstra et al., 2018; WWAP (United Nations World Water Assessment Programme) and UN-Water, 2018). However, the potential of natural water storage in the subsurface (of aquifers) is not yet recognized. The water resources management plans should include surface or subsurface storage opportunities or a combination of those in the face of the increasing water variability (WWAP (United Nations World Water Assessment Programme) and UN-Water, 2018).

There has been growing research on the potential of NBS for climate change adaptation in the last decade (Seddon et al., 2020). They can contribute to achieving sustainable cities under climate change impacts, which is considered one of the most significant challenges that urban areas will face in the future (Kabisch et al., 2017; Seddon et al., 2020). NBS create benefits in two ways: they create opportunities to cope with the causes and consequences of climate change, but at the same time, they support biodiversity and, therefore, also the chain of ecosystem services needed to sustain human life (Seddon et al., 2020). Based on a study by Eggermont et al. (2015), three types of NBS can be distinguished according to their number of services and stakeholder groups, maximization degree of the delivery of key services, and level and type of engineering. The first type refers to restoring natural or protected ecosystems using minimum interventions to maintain existing ecosystem services. In contrast, the second type uses effective management practices to reach sustainability and multi–functionality while gaining more selected ecosystem services. Finally, the third type uses a maximum level of intervention and even creates new ecosystems to deliver the key services (Eggermont et al., 2015; Kooijman et al., 2021).

The NBS concept was developed, elaborated, and popularized by different organizations, such as the International Union for Conservation of Nature (IUCN) and the European Commission (EC), with different definitions and conceptualizations according to their perspectives (Cohen-Shacham et al., 2016). Mackinnon et al. (2008) first mentioned the principle of NBS in "Biodiversity, Climate Change, and Adaptation: Nature–Based Solutions" from the World Bank Portfolio to stress the importance of biodiversity conservation for climate change adaptation (Mackinnon et al., 2008). A year later, the IUCN put the concept in a broader context and defined NBS as "actions to protect, sustainably manage and restore natural and modified ecosystems in ways that address societal challenges effectively and adaptively, to provide both human well-being and biodiversity benefits. They are underpinned by benefits that flow from healthy ecosystems and target major challenges as climate change, disaster risk reduction, food, and water security and are critical to economic development (Cohen-Shacham et al., 2016; Kooijman et al., 2021). Then, the European Commission defined NBS as "...nature–based solutions to societal challenges as solu-

tions that are inspired and supported by nature, which are cost-effective, simultaneously provide environmental, social, and economic benefits and help build resilience. Such solutions bring more, and more diverse, nature and natural features and processes into cities, landscapes, and seascapes, through locally adapted, resource-efficient and systemic interventions" (European Commission, 2015).

The principles of NBS do not differ much from other existing concepts of Green Infrastructure (GI) and Ecosystem-Based Adaption (EBA). Furthermore, in the case of urban NBS, the concept is often used interchangeably (Dorst et al., 2019). Therefore, the literature suggests looking at NBS as 'an umbrella concept' (Kooijman et al., 2021), also covering other concepts such as sustainability and ecosystem-related approaches to address societal challenges (Cohen-Shacham et al., 2016; Dorst et al., 2019; Irfanullah, 2021). Yet, it creates the potential to attach segregated knowledge and expertise of the previous and current approaches in urban green planning. A more performance-based urban planning approach makes it easier to reach a sustainable solution for urban areas (Dorst et al., 2019).

NBS are multifunctional solutions that mimic complex systems and processes of nature (European Commission, 2015; Nelson et al., 2020). Therefore, NBS implementation is challenging for green urban planners, with different barriers limiting the broader and successful adoption. To improve the future performance of NBS, it is essential to study the barriers that hinder their implementation. Also, the requirements to overcome these barriers must be well–investigated, as what is usually presented in the planning phase does not always correspond to what is realized in practice (Frantzeskaki et al., 2020). According to Frantzeskaki et al. (2020), three gaps are differentiated for implementing NBS in cities: skills gaps, governance gaps, and knowledge gaps. Nelson et al. (2020) also state many barriers, including knowledge gaps of effectiveness, lack of awareness, low costs and benefits expertise, poor stakeholder engagement and inequity, lack of policy and economic instruments, and insufficient financing.

NBS are designed to fix many societal challenges, and they are mainly promoted to create resilience in the (urban) environment and cope with the negative impacts of climate change, such as extreme weather disasters (floods, droughts, etc.) (Cortinovis et al., 2022). When mimicking the natural processes in urban infrastructure, they also provide many additional benefits (Raymond et al., 2017). Examples are carbon sequestration, water quality, land conservation, food production, biodiversity and ecosystem services, and recreation (European Commission, 2015). They contribute co-benefits to urban residents, such as improved health and well-being and the local green economy (Kabisch et al., 2017). Some indirect co–benefits may also include the learning (e.g., outdoor classrooms), where awareness is raised about the potential benefits, stakeholder inclusion, and energy savings (Davies et al., 2021).

NbS suitability mappinge

An important first step in using Nature–Based Solutions (NBS) in river landscapes is to assess their suitability in different locations (Mubeen et al., 2021). The success of these solutions greatly depends on where they are implemented and using them in the wrong areas could worsen the situation (Ahmadisharaf et al., 2016). Many authors agree that Geographic Information Systems (GIS) can be helpful in identifying appropriate locations for NBS (Baldwin et al., 2022; Gallagher et al., 2019; Hosseinzadeh et al., 2023; Mubeen et al., 2021; Muthanna et al., 2018). GIS provides valuable insights and tools for decision-makers, urban planners, and resource managers to prioritize and implement nature-based strategies that can effectively combat drought impacts (Mubeen et al., 2021).

Numerous suitability analysis studies have been conducted for flood risk reduction and stormwater management. These studies include research by (Ahmadisharaf et al., 2016), (Baldwin et al., 2022), (Hosseinzadeh et al., 2023), (Liu et al., 2023), (Mubeen et al., 2021), (Senes et al., 2021). (Mubeen et al., 2021) used the GIS-Multi-Criteria Analysis (MCA) methodology to map the suitability of four large-scale NBS types, including detention basins, river widening, floodplain restoration, and retention ponds for flood risk reduction in catchments. (Ahmadisharaf et al., 2016) used a multi-criteria decision-making site selection framework in ArcGIS for detention basins, with similar criteria such as slope, land use, distance to channels, social hotspots, and permeability. (Liu et al., 2023) added thematic layers to locate suitable small detention basins using Multi-Criteria Evaluation (MCE) and consider river density, distance from buildings, vegetation cover index, and specific elevation factors for small dam construction in the Mataniko catchment, Honiara. (Baldwin et al., 2022) focused on identifying suitable NBS sites called “FloodWise” practices using ArcGIS software, specifically in rural areas of North Carolina. Criteria considered included slope restrictions, filtering of specific agricultural land uses and crops, and soil characteristics, as well as buffers from existing infrastructure, the presence of floodplains, and the historical vulnerability of croplands to inundation data layers. (Senes et al., 2021) described a methodology for locating Green Infrastructure (GI) for stormwater management using GIS and identified slope, land use, and soil type as main criteria. In contrast to the studies mentioned above, exclusion areas were defined for GI implementation to protect groundwater wells and avoid areas vulnerable to groundwater pollution. However, none of these studies included any aquifer-related characteristics or hydrometeorological criteria which are critical criteria for drought studies. Overall, flood risk reduction studies consider surface characteristics and management criteria but do not include drought-related criteria.

In contrast, not many studies perform a drought-specific suitability analysis, especially for the above-mentioned types of NBS: detention basins and retention ponds, wetland restoration, afforestation, river widening, green infrastructure, and floodplain restoration. However, for other straightforward drought-mitigating types of NBS, such as Managed Aquifer Recharge (MAR) implementation (Fuentes and Vervoort, 2020; Pedrero et al., 2011; Rahman et al., 2013; Sardar et al., 2022; Soliman et al., 2022; Talozi et al., 2023) and rainwater harvesting (RWH) (Kahinda et al., 2008; Mbilinyi et al., 2007; Rejani et al., 2017; Sayl

et al., 2020; Suni et al., 2023), numerous researchers have performed suitability mapping in the past decade. These studies have mainly focused on (semi)-arid regions, including Mediterranean and African countries, Southeast Asia, and Australia. Unlike the site selection for flood risk and stormwater management practices, the suitability mapping for MAR and RWH takes into account various key criteria to assess drought impacts, such as aquifer thickness (Rahman et al., 2013; Talozi et al., 2023), groundwater flow zones (Rahman et al., 2013), specific groundwater quality criteria (Rahman et al., 2013; Soliman et al., 2022), groundwater depth (Fuentes and Vervoort, 2020; Pedrero et al., 2011; Rahman et al., 2013; Talozi et al., 2023), and many hydrogeological characteristics (Fuentes and Vervoort, 2020; Sardar et al., 2022; Soliman et al., 2022; Talozi et al., 2023). Some hydrometeorological aspects, such as precipitation characteristics, are also considered (Kahinda et al., 2008; Mbilinyi et al., 2007; Rejani et al., 2017; Sardar et al., 2022; Soliman et al., 2022; Talozi et al., 2023). Despite the large number of studies in the (semi)-arid regions, having to cope with insufficient water resources and droughts, these studies are lacking for currently temperate climate regions in, for example, West Europe.

Although flood and drought management have distinct primary objectives, they share a common aspect: water retention plays a crucial role in both cases (Teschemacher et al., 2020). Consequently, flood-effective NBS, such as detention basins, retention ponds, and wetlands, will also be beneficial against drought. They not only create a buffer in wet periods, but they also create a source of stored water which can be used to meet the water demand in a dry period (Teschemacher et al., 2020). Among the evident drought-specific NBS, it is clear from the various studies that MAR has emerged as a significant method with promising results. The measure enables the restoration or preservation of groundwater levels during periods of excess surface water, concurrently offering a water reservoir that can support ecological processes and irrigation requirements during periods of drought while minimizing water losses due to evapotranspiration (Dillon and Arshad, 2016; Rawluk et al., 2013). It contributes to the long-term sustainability of water resources, is typically used on a larger scale, and can store significantly larger volumes of water (Wendt et al., 2021). Concluding, the suitability assessment of detention and retention basins, wetlands, and managed aquifer recharge to mitigate future drought events will have wide applicability effective against multiple hazards.

Chapter 3

Model development

In this chapter, three major outcomes of the research are presented, namely: model modification, SWAT+gwflow model input preparation, post-processing and calibration tool development (IPPC), and finally, applying the modified model using an exemplary groundwater-driven watershed, Dijle-Belgium.

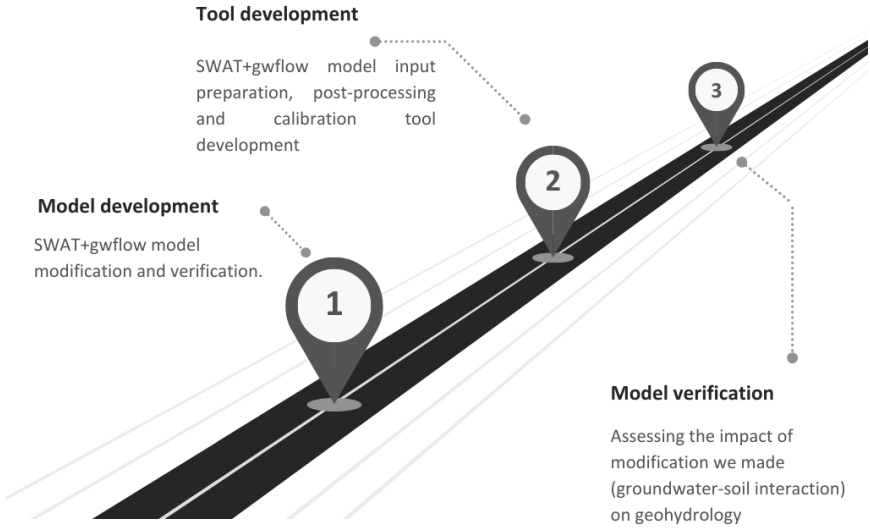


Figure 3.1: Major parts of Chapter 3 which focus on model and tool development

3.1 Modifying the gwflow module to account for groundwater-soil interactions for accurate representation of groundwater-surface water dynamics

3.1.1 Summary

Recent water availability and scarcity problems have highlighted the importance of surface–groundwater interactions. Thus, groundwater models are coupled with surface water models. However, this solution is complex, needing code modifications and long computation times. Recently, a new groundwater module (gwflow) was developed directly inside the SWAT code to tackle these issues. This research assesses gwflow's capabilities in representing surface–groundwater system interactions in the Dijle catchment (892.54 km^2), a groundwater-driven watershed in Belgium. Additional developments were made in SWAT+gwflow to represent the interaction between the groundwater and soil (gwsoil). The model was calibrated for monthly mean streamflow at the catchment outlet (1983 to 1996) and validated for two periods (validation 1: 1975 to 1982 and validation 2: 1997 to 2002).

It was found that the SWAT+gwflow model is better at representing the total flow (NSE of 0.6) than the standalone SWAT+ (NSE of 0.4). This was confirmed during two validation periods where the standalone model scored unsatisfactory monthly NSE (0.6 and 0.1), while the new model's NSE was 0.7 and 0.5. Additionally, the SWAT+gwflow model simulations better depict the groundwater via baseflow and attain proper water balance values. Thus, in a highly groundwater-driven catchment, the simplified representation of groundwater systems by the standalone SWAT+ model has pitfalls. In addition, the modification made to the gwflow module (gwsoil) improved the model's performance, which, without such adjustment, overestimates the streamflow via saturation excess flow. When including the gwsoil mechanism, thereby providing a more accurate representation of water storage and movement, groundwater is transferred to the soil profile, increasing the overall soil water content and thereby increasing lateral flow. This novel modification can also have implications for other distributed hydrological models to consider such exchanges in their modeling scheme.

This section is published as: **Yimer, E. A.**, Bailey, R. T., Piepers, L. L., Nossent, J., and Van Griensven, A.: Improved Representation of Groundwater–Surface Water Interactions Using SWAT+gwflow and Modifications to the gwflow Module, Water, 15, 3249, 2023. https://doi.org/10.3390/w15183249

3.1.2 Introduction

Geohydrological systems can be modeled using either surface water, groundwater, or coupled models (Siad et al., 2019). However, separate representation of surface and groundwater processes has limitations, as it neglects the interaction between these vital processes (Larocque and Broda, 2016). This interlink is essential for the sustainable existence of surface water bodies (Alley et al., 1999), and in some studies it accounts for the vast majority of the hydrological cycle (Moore, 2010). This led to an extensive coupling approach to understand the mechanism whereby these two separate but interlinked systems operate (Abbott et al., 1986; Ewen et al., 2000; Maré et al., 2007; Scibek et al., 2007). Therefore, as new challenges arise regarding water quantity and quality, together with many other water management practices, a more holistic approach towards hydrological modeling is necessary (Stefania et al., 2018; Chapman et al., 2007; Fleckenstein et al., 2010; Kalbus et al., 2006; Levy and Xu, 2011; Oxtobee and Novakowski, 2002; Woessner, 2000).

Hydrological models such as the Soil and Water Assessment Tool (SWAT) can account for the groundwater component of the hydrological system within the aquifer module, but with important limitations. The groundwater head is calculated at the hydrologic response units (HRU) level; hence, the water table is not spatially distributed. Hydraulic conductivity and specific yield do not vary spatially, as each aquifer system is assumed to be homogeneous. Therefore, SWAT is not suited to simulating the spatiotemporal variation of groundwater variables. Another limitation is that the groundwater head only changes with recharge and return flow, whereas many other groundwater flows exist (e.g., groundwater extraction through pumping). In addition, return flow is calculated only for steady-state conditions. This component only occurs when groundwater storage surpasses a certain threshold, while in reality this is determined by hydraulic gradients. Also, seepage caused by hydraulic gradients is not simulated (Bailey et al., 2020a; Kim et al., 2008; Putthividhya and Laonamsai, 2017). Due to these reasons, and since the standalone SWAT model has major limitations for applications on groundwater-dominated catchments (Deb et al., 2019; Gassman et al., 2007; Peterson and Hamlett, 1998; Spruill et al., 2000; Srivastava et al., 2006), there has been an effort to replace this simplified representation of groundwater hydrology in SWAT.

This led to the coupling of SWAT and MODFLOW (Perkins and Sophocleous, 1999; Bailey et al., 2020a; Kim et al., 2008; Galbiati et al., 2006; Guzman et al., 2015; Sophocleous et al., 1999). The coupled SWAT–MODFLOW framework combines the SWAT software modeling tool with MODFLOW (Harbaugh, 2005), where the latter is embedded as a subroutine, replacing the groundwater module in SWAT. The main issue with integrating SWAT and MODFLOW is the complex model code modification and long computation time requirement. Due to this, Bailey et al. (2020a) recently developed a new physical-based groundwater flow module (gwflow) as part of the SWAT+ modeling code. SWAT+ is the new and restructured version of SWAT (Bieger et al., 2017). The gwflow module is based on the Dupuit–Forchheimer assumption of horizontal flow in unconfined aquifers. Therefore, this module should be used in cases where the groundwater system is composed of an unconfined aquifer. Hence, this module could replace the current SWAT+ aquifer module

for unconfined aquifers and allow for spatially distributed groundwater simulations such as groundwater head (i.e., water table elevation), groundwater storage, groundwater discharge to streams, etc.

However, one critical limitation of the gwflow module is that groundwater–soil interactions are not represented, leading to incorrect water balance at the HRU level. These are vital interactions whenever the water table is higher than the bottom of the soil profile. Hence, in this chapter, this limitation/research gap is assessed, the source code of the coupled SWAT+gwflow model is modified, and a comparison before and after applying this modification is presented. Furthermore, we aimed to apply the coupled model (SWAT+gwflow) to a groundwater-influenced catchment located in a temperate climate and investigate how the baseflow is represented. Subsequently, a model output comparison was performed between the standalone SWAT+ and the one modified with the gwflow module.

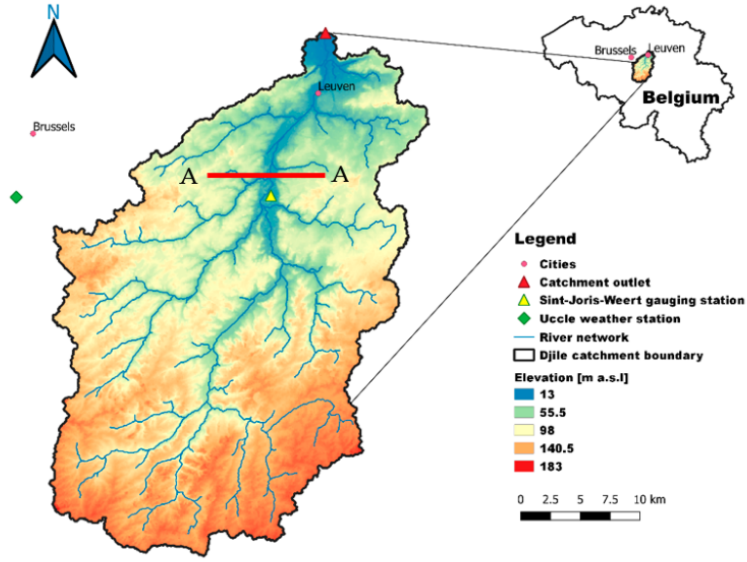


Figure 3.2: Study area used for evaluating the impact of groundwater-soil interaction on general geohydrology

3.1.3 Study area and data

Study area

Located in the center of Belgium, the Dijle catchment (Fig. 3.2) has an average length of 86 km and an area of 892.54 km^2. It is a part of the larger Scheldt basin (21,863 km^2) situated in Belgium, France, and the Netherlands. The Dijle River springs near Houtain–Le–Val in Wallonia and flows towards the North–East. In Court-Saint-Etienne, Thyle and Orne's

rivers are added to its river flow. In addition, the Train river originating from Wallonia ends up in the Dijle. At the border between Flanders and Wallonia, the Dijle has an average flow rate of 4.5 m³/s.

In general, the catchment is homogeneous regarding soil type, whereas more than 90% is covered by silt-textured luvisols (Van Oost et al., 2012). Substantial soil textures that can be found in the Dijle catchment are silt, sandy loam, and loamy sand. The area is known to have a spatial transition in texture from North–West to South–East, giving a pattern of sand and sandy loam in the Northern part and silt regions in the southwestern part. The sandy aquifer (traditionally known as "Brussels sand") is dominant with a lower im-permeable layer called Kortrijk, which acts as the base of the unconfined aquifer (Fig. 3.2). The Dijle catchment has a mean elevation of 40 meters and an average slope of 2% (Batelaan and De Smedt, 2007).

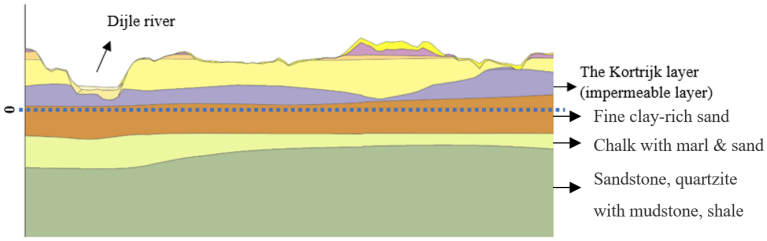


Figure 3.3: The elevation of the impermeable layer base is taken as a reference for the unconfined aquifer. It was accessed on September 30th, 2021, from https://www.dov.vlaanderen.be/portaal/. The other colors correspond to different geological units, however, the focus of this study lies on the impermeable layer and the yellow unit (Brussel sand), which corresponds to the unconfined aquifer. The dotted line corresponds to mTAW = National Topographic Reference). The plot is not in to scale, and the transect is for A–A, as seen in (Fig. 3.2).

Data

The weather data is obtained from the Royal Meteorological Institute of Belgium (RMI) for variables such as precipitation (mm), relative humidity (decimal fraction), solar radiation (MJ/m²), temperature (°C), and wind speed (m/s) from 1970 until 2011 at the Uccle gauging station. Although this weather station is not situated inside the catchment area, the weather data can be used for this study, as the weather variables are approximately constant spatially across Belgium. The average precipitation from a gridded dataset (10 points inside the watershed) indicated similar daily average precipitation values as the Uccle station. By the time this research was conducted, the gridded dataset was not available, hence, the Uccle station weather data was used. The other inputs for developing the SWAT+ model are soil and land use maps obtained from the Food and Agriculture Organization (FAO, year: 2010) and the European Space Agency (ESA, year: 2020, resolution: 200m), respectively. Finally, the Digital Elevation Model (DEM) of 50m by 50m was reassembled from 90m by

90m DEM acquired from USGS (last accessed, September 30, 2021 https://earthexplorer.usgs.gov/) and is used to delineate the catchment. The streamflow data runs from 1975 to 2002 for both the catchment outlet (Wilsele) and Sint–Joris–Weert (SJW) gauging station.

3.1.4 Methodology

The methodology comprised two main parts: the first was modeling the catchment with the standard SWAT+ model, and the second was to use the new "gwflow" module as a replacement for the simplistic representation of the groundwater module in the SWAT+ model. This enabled us to assess the potential of the new module (gwflow) to simulate the groundwater hydrology of the Dijle catchment better than the standalone model.

As gwflow is embedded as a subroutine within the SWAT+ Fortran code, the inputs for the standalone SWAT+ model are also inputs for the gwflow model setup. For the SWAT +gwflow module, SWAT+ version 60.5.2 is coupled with the gwflow module. In addition, an aquifer thickness raster (vertical distance from the ground surface to bedrock, i.e., the thickness of unconsolidated sediments) was downloaded from https://data.isric.org/ (Shangguan et al. (2017), last accessed on 21 September 2022). To check the validity of the global dataset, the depth to the impermeable layer, called the Kortrijk layer (Fig. 3.3), was also taken from a previous study conducted by Wossenyeleh, (2021) [40]. The permeability of the aquifer material was obtained from https://dataverse.scholarsportal.info/ (Huscroft et al. (2018), last accessed on 21 September 2022). This helped us to classify the aquifer into distinct zones, where each zone has its own corresponding hydraulic conductivity (K_{aqu}) and specific yield (S_y) values (Bailey et al., 2020a).

The SWAT+ model setup starts by delineating the catchment where the Wilsele gauging station is taken as the catchment outlet, and this resulted in a total catchment area of 892.54 km² with 1496 HRUs, 21 subbasins, and 162 channels. The streamflow data at Wilsele is downloaded from Waterinfo (last accessed, September 21, 2022 https://www.waterinfo.be/) for the same time window as the other weather inputs. The Penman-Monteith was chosen as the potential evapotranspiration (PET) calculation method, whereas the Muskingum method was selected for flow routing. We used SWAT+ version 60.5.2 for the model setup.

It is worth noting that the global datasets that we used to prepare the gwflow inputs have a mismatch with the locally available data. Hence, we have made simplifications that ease the sensitivity and calibration process. For instance, the number of different hydraulic conductivity zones according to the global dataset is 24; however, previous studies on this catchment [40] have shown the dominance of one zone (called "Brussels sand"), and we also have noticed from the global dataset that the hydraulic conductivity values for most zones were similar. Hence, we calibrated only the dominant zones (Fig. 3.4). If we take the 24 zones as independent zones, we will need to perform sensitivity analysis for 24 zones (a total of 48 parameters, which is 24 for hydraulic conductivity and 24 for specific yield). Note that this number does not account for the other model parameters. This will increase

computation time, create difficulty while calibrating the model at the latter stages, and may lead to overfitting. However, this simplification will not reduce model performance, which is checked at later stages in the result section. This type of simplification is well-known in hydrological modeling as a parsimonious representation (Wossenyeleh et al., 2021; Atkinson et al., 2002; Basu et al., 2010; Sivapalan, 2003).

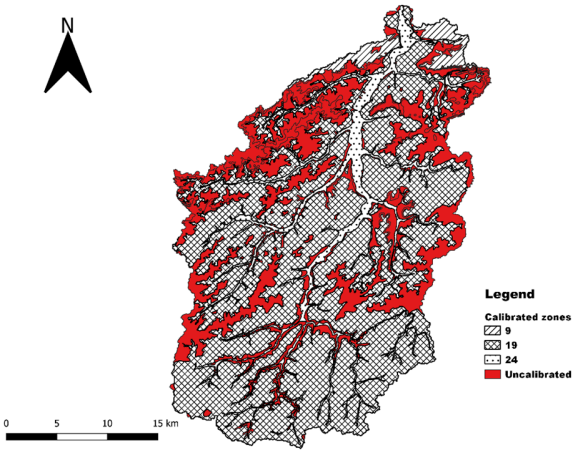


Figure 3.4: The different hydraulic conductivity zones according to the GLHYMS dataset. Originally, there were 24 zones, which has three dominant zones. Hence, to reduce computation time and avoid overfitting, only the three zones' hydraulic conductivity and specific yield parameters are calibrated

Modification to the gwflow module to account for groundwater-soil interaction

In the original water balance equation of the gwflow module (Bailey et al., 2020a), the interaction between SWAT+ HRU soil profiles and gwflow grid cells occurs only through the passing of deep percolation from the soil profile to groundwater, i.e., the water table elevation, and corresponding groundwater storage, simulated for each grid cell does not interact with nor affect the hydrological processes of the soil profile. This could lead to situations where the gwflow module simulates a water table within the soil profile, with all inherent groundwater calculations such as lateral flow, while at the same time, the HRU in the same vicinity as the grid cell is simulating percolation and soil lateral flow. This leads to duplicate processes, but by different equations. To remedy this flaw, in this study, we modify the gwflow module to allow the transfer of groundwater to the soil profile for grid cells where the water table rises into the soil profile (Eq. 3.1). This is particularly important for groundwater-dominated catchments (i.e., high baseflow fractions) where the water table is shallow. For each cell, for each time step, the simulated water table elevation (i.e., groundwater head) is compared to the elevation of the soil profile bottom of the HRU to which it is connected spatially. If the water table elevation wt_elev (m) is above the elevation of the soil profile bottom soilelev (m), then the volume of groundwater to transfer

to the soil profile Qgw_soil is calculated as:

$$Q_{\text{gw}\rightarrow\text{soil}} = (\text{wt}_{\text{elev}} - \text{soil}_{\text{elev}}) \cdot A_{\text{hru}} \cdot S_y \tag{3.1}$$

Where A_{hru} is the area (m^2) of the HRU within the spatial area of the grid cell, and S_y is the specific yield of the aquifer. This volume of water is added to the HRU soil layers that are at or below the elevation of the water table. The inclusion of this transfer term can yield higher rates of recharge during a model simulation, due to added water to the soil profile that subsequently can move downward to the water table. Therefore, when presenting and discussing model results or estimating recharge rates for a watershed or portion of a watershed, the "net" recharge should be estimated by subtracting the transfer volume from the simulated recharge volume, i.e.,

$$\text{true recharge} = Q_{\text{rech}} - Q_{\text{gw}\rightarrow\text{soil}}.$$

We further modified the module to include municipal pumping, which is added as another sink term in the water balance equation. The starting and ending date of pumping and the daily pumping rate are inputs for wells located inside any case study area, with any number of pumping periods possible for each well. For this study, it's considered zero.

Sensitivity, calibration, and water balance analysis

The sensitivity and calibration analysis for the SWAT+*gwflow* model setup is performed using the Parameter Estimation Tool, PEST. For the standalone SWAT+ modeling work, sensitivity and calibration analyses were done based on two approaches. The first uses the SWAT+ toolbox developed by Celray James Chawanda (last accessed February 21, 2022). This tool applies the variance–based Sobol method.

The second approach involves calibrating the standalone SWAT+ model using the PEST tool, to compare the two model setups using a consistent calibration methodology. The time window from 1983 to 1996 is used for calibration, with the first three years considered as a warm-up period. The remaining data is divided into two validation periods: 1975–1982 as "Validation 1" and 1997–2002 as "Validation 2." Sensitivity and calibration are performed using monthly streamflow data at the outlet of the catchment.

A comparison is made between the daily and monthly simulated and measured streamflow data at the catchment outlet. Additionally, the calibrated model is tested using streamflow data from another gauging station located at Sint–Joris–Weert (SJW), approximately 14 km upstream of the catchment outlet. Although sensitivity and calibration occur in parallel when using PEST, a limited number of parameters were used to ensure comparability with the standalone SWAT+ model.

The soil water balance for the standalone SWAT+ model (Eq. 3.2) is calculated using precipitation (P), surface runoff (Surq), lateral discharge (Latq), percolation (Pr), and evapotranspiration (ET). For the SWAT+*gwflow* model, the same variables are considered (Eq. 3.2), with the addition of groundwater transferred to the soil (gwsoil), in cases where the water table intersects the soil profile:

$$\text{Change in soil moisture storage}_{\text{SWAT+}} = P - \text{Surq} - \text{Latq} - \text{Pr} - \text{ET} + \text{error} \tag{3.2}$$

$$\text{Change in soil moisture storage}_{\text{SWAT+gwflow}} = P + \text{gwsoil} - \text{Surq} - \text{Latq} - \text{Pr} - \text{ET} + \text{error} \tag{3.3}$$

The groundwater balance is calculated for SWAT+*gwflow* (Eq. 4.11) using recharge (rech, equal to percolation Pr), groundwater evapotranspiration (gwet), groundwater flow to streams (gwsw), stream seepage to groundwater (swgw), saturation excess flow (satex), groundwater transfer to soil (gwsoil), groundwater pumping (pump), and flow across the catchment boundary (bound):

$$\begin{aligned}\text{Change in groundwater storage} = {} & \text{rech} - \text{gwet} - \text{gwsw} + \text{swgw} \\ & - \text{satex} - \text{gwsoil} - \text{pump} + \text{bound} + \text{error}\end{aligned} \tag{3.4}$$

The sum of the groundwater balance at each daily time step is compared with the difference in total groundwater volume before and after each day, to ensure closure of the aquifer system water balance.

When using the SWAT+ toolbox, the Nash-Sutcliffe Efficiency (NSE) was used as an objective function. In contrast, PEST minimizes the sum of squared residuals (SSR). The conventional performance metrics, namely NSE and Percent Bias (PBIAS), are used to evaluate the simulation of streamflow at both the catchment outlet and SJW gauging station. Additionally, water balance closure was verified. The closer the NSE (Eq. 4.5) is to 1, and PBIAS (Eq. 4.6) is to 0, the better the model performance.

$$\text{NSE} = 1 - \frac{\sum_{t=1}^{T}(Q_m^t - Q_o^t)^2}{\sum_{t=1}^{T}(Q_o^t - \overline{Q_o})^2} \tag{3.5}$$

$$\text{PBIAS} = \frac{\sum_{t=1}^{T}(Q_o^t - Q_m^t) \times 100}{\sum_{t=1}^{T} Q_o^t} \tag{3.6}$$

Where Q_m^t is the simulated streamflow at time t, Q_o^t is the observed streamflow at time t, and $\overline{Q_o}$ is the mean observed streamflow.

3.1.5 Results

Sensitivity analysis, calibration, validation, and water balance
The sensitivity analysis based on both the SWAT+ toolbox and PEST revealed that the curve number, usually the most sensitive parameter in the SWAT+ model, is not sensitive. Instead, the percolation coefficient (perco), which is a coefficient that adjusts the soil moisture for percolation to take place, is the most sensitive one. This is evident as the catchment is more groundwater–driven. The sensitivity analysis hides the importance of the other parameters due to the super–sensitive nature of perco. However, when the other parameters, except perco are compared, it is found that the other groundwater-related parameters also play a role that indicates the importance of appropriate representation of the groundwater hydrology to simulate the general hydrological processes in highly groundwater-dominated catchments.

The sensitivity analysis has a similar result as Wossenyeleh et al., (2021) where the hydraulic conductivity of the "Brussels sand" (Kaqu19) is a very sensitive parameter. Nevertheless, according to their result, river conductance, which is equivalent to streambed conductivity (bed_k) in SWAT+gwflow is not sensitive, contrary to the result of our sensitivity analysis. However, the study by Wossenyeleh et al., (2021) is only a tiny part of the catchment (only the Doode Bemde wetland area), while our study area encompasses the whole catchment.

The calibrated model parameters values closely match with the finding of Wossenyeleh et al., (2021), where according to SWAT+gwflow, "Brussels sand (zone 19)" hydraulic conductivity is 9.6 m/day while they estimated it to be 8 m/day. The values are between the range of values suggested by Possemiers et al. (2012) and Vandersteen et al. (2014). In addition, the hydraulic conductivity of the river valley represented as zone 24 is 3.1 m/day, while Wossenyeleh et al., (2021) estimated it to be 3 m/day. As for the specific yield, the result indicated that the "Brussels sand" has a specific yield of 0.4, which has a difference of 0.25 compared with Wossenyeleh et al., (2021). According to Bear (1972), Carsel and Parrish (1988) and Loheide II and Gorelick (2005), the specific yield of sandy aquifers can reach up to 0.385, hence, our result is also in 0.005 difference with their suggestion, hence, the specific yield is in an acceptable range.

The quaternary formation (the river valley), the specific yield is 0.026 and 0.03, according to SWAT+gwflow and Wossenyeleh et al., (2021), respectively. Here, it is vital to mention that in Wossenyeleh et al., (2021), the model setup was using MODFLOW forced with recharge obtained from another hydrological model (WetSpaSS). However, for SWAT+gwflow model setup, the recharge is directly transferred from the soil profile, which does not require setup, calibration, and validation of other hydrological models to get recharge values. This is one added value of the new coupled model compared to independently developed models.

The calibration has resulted in an NSE of 0.4 and 0.6 for the standalone SWAT+ and the SWAT+gwflow, respectively. The SWAT+gwflow simulation result corresponds to satisfactory, according to Moriasi et al. (2007). This indicates that the simplified representation of the groundwater system by the standalone SWAT+ model reduces the performance of simulating geohydrological water balance components in groundwater-dominated catchments. The daily streamflow simulation using SWAT+gwflow has also resulted in a high NSE (0.5) during the calibration period.

The result of the first validation period (1975 to 1982) suggested that the standalone SWAT+ has a lower NSE (unsatisfactory) while the SWAT+gwflow simulation managed to show a higher similarity between measured and simulated streamflow data with an NSE of 0.7 (Tab. 3.1), which is good according to Moriasi et al., (2007). The SWAT+gwflow is also successfully applied to research conducted by Bailey et al. (2020a),Bailey et al. (2022), and Yimer et al. (2023b). The result indicated that the SWAT+ model could not adequately represent the Dijle catchment, while the SWAT+gwflow has improved the hydrological simulation. It is to be noted that the calibration using either PEST or the global optimization tool (SWAT+ toolbox) resulted in an NSE of 0.4 for the standalone model setup.

The modeled streamflow at the SJW gauging stations mimics the measured monthly mean streamflow where the NSE is 0.5, 0.7, and 0.4 for the calibration period, the first and second validation periods, respectively. The respective PBIAS values are 11.16%, 6.12%, and 15.41%. Hence, the calibrated model managed to accurately estimate streamflow in another location (inside the catchment). It is to be noted that when `gwsoil` interaction is not considered, the streamflow simulation has deteriorated with an NSE of 0.1. This result has shown the importance of accounting for such exchanges in the modeling scheme.

Table 3.1: Comparison of model performance metrics for SWAT+ and SWAT+*gwflow*

	Time step	**NSE**		**PBIAS [%]**		**Watershed soil water balance**	**GW balance error (mm)**
		SWAT+	*gwflow*	SWAT+	*gwflow*	SWAT+ / *gwflow*	*gwflow*
Calibration	Daily	-0.1	0.5	1.7	-0.9	2.6% / 0.17%	–1.12
	Monthly	0.4	0.6	1.6	-1.0	–	–
Validation 1	Daily	0.1	0.5	-5.6	-11.0	3.1% / 0.21%	1.72
	Monthly	0.6	0.7	-5.6	-10.9	–	–
Validation 2	Daily	-0.3	0.4	11.0	6.4	11.4% / 0.17%	1.22
	Monthly	0.1	0.5	11.0	4.9	–	–

The water balance closes for both the watershed as a whole and the groundwater system. It closes with less than 11.4% error for both SWAT+ and SWAT+gwflow during calibration

and validation periods. There are numerous error–producing aspects in the water balance components. For example, model structural issues, model parameters, calibration procedures, model inputs, rounding off etc., are the major sources of errors. Mainly, the groundwater balance error is due to the rounding off, where currently, the code only prints out four digits (note that it is less than 2 mm for all periods we assessed).

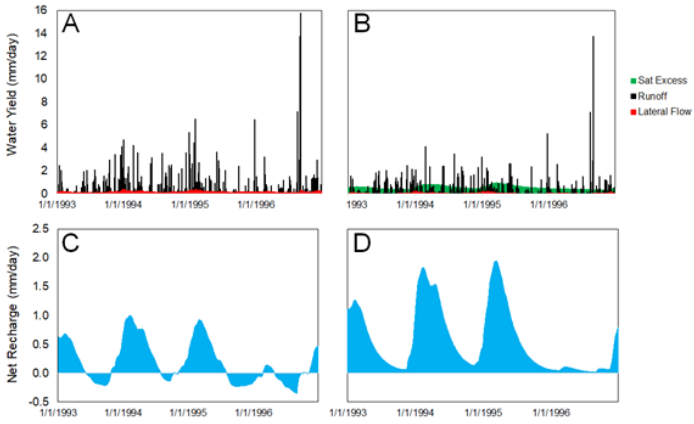


Figure 3.5: Water yield and net recharge for the condition of including the gwsoil mechanism (A and C) and not including the gwsoil mechanism (B and D)

The average annual hydrologic fluxes (mm/yr) within the watershed system and precipitation fractions are listed in Table 2. For the simulation period, on average ET accounts for 67% of precipitation, and surface runoff, soil lateral flow, and net recharge account for 10%, 5%, and 12%, respectively. When neglecting the gwsoil mechanism (i.e., turning off this feature in the SWAT+ code), hydrologic flux rates change dramatically (Tab. 3.2). This condition yields a very high rate of saturation excess flow (164 mm), as groundwater head is allowed to rise to the ground surface, i.e., there is no interaction with the soil profiles of the HRUs. This high rate of saturation excess flow, when combined with surface runoff (66.4 mm) and soil lateral flow (10.6 mm) and accounting for stream seepage to groundwater (4.5 mm), results in a total water yield of 237 mm, which greatly overestimates streamflow at the gauging site. Net recharge (Fig. 3.5) is also much higher in this condition (204 mm), as groundwater is not removed from the aquifer and placed in the soil profile. The high recharge rates result in high groundwater head, which in many places of the watershed reaches the ground surface, resulting in saturation excess flow.

The components of water yield (surface runoff, soil lateral flow, saturation excess flow) are shown in (Fig. 3.5), with saturation excess flow being zero, due to the inclusion of the gwsoil term, and hence the groundwater head as simulated by the gwflow module not allowed to rise to the ground surface and induce saturation excess flow, but instead ground-

water is incorporated into the soil profile and managed by the HRU soil processes of runoff and soil lateral flow. For this condition, therefore, soil lateral flow acts as a pathway for groundwater to reach the stream network, and hence can be considered as baseflow. This allows an accurate depiction of baseflow, as shown by the streamflow comparison in (Fig. 3.5). The inclusion of the gwsoil mechanisms results in net recharge (Fig. 3.5) that, when averaged over the entire watershed, is usually positive, but can be negative as groundwater is transferred to the soil profile, but no recharge occurs.

In contrast, when including the gwsoil mechanism, thereby providing a more accurate representation of water storage and movement, groundwater is transferred to the soil profile, increasing the overall soil water content and thereby increasing surface runoff and soil lateral flow to 83.6 mm and 43.2 mm, respectively, increases of 26% and 300%. ET also increases (from 544 mm to 559 mm) as more water is stored in the soil layers. Net recharge is now 103 mm, or approximately half of the volume simulated when the gwsoil mechanism is excluded from the model, as groundwater is transferred to the soil profile.

These results indicate the importance of including the gwsoil mechanism into the SWAT+ modeling code, and in general including groundwater-soil interactions in integrated hydrologic models. This mechanism provides a realistic movement of water in the shallow subsurface, allowing water in the soil profile, whether percolating from above or resulting from high groundwater levels, to be subject to the appropriate hydrologic process (recharge, soil lateral flow, ET, runoff) within the watershed system.

Table 3.2: Comparison of water balance components with and without `gwsoil`.

	Values (mm's)		**Percentage of precipitation (%)**	
	Without `gwsoil`	**With `gwsoil`**	**Without `gwsoil`**	**With `gwsoil`**
Inputs to Watershed				
Precipitation	838.9	838.9	–	–
Boundary inflow	-5.5	-26.5	–	–
Lake seepage to groundwater	0.4	0.3	–	–
Outputs from Watershed				
Surface ET	544.4	559.0	65	67
Surface runoff	66.4	83.6	8	10
Soil lateral flow	10.6	43.2	1	5
Stream seepage to groundwater	-4.5	-4.4	–	–
Saturation excess flow	164.2	0.0	20	0
Groundwater ET	0.2	0.0	–	–
Internal Flow				
Recharge to the water table	204.8	837.2	–	–
Groundwater transfer to soil	0.0	733.9	0	87
Net recharge	204.8	103.3	24	12

3.1.6 Conclusion

Coupled geohydrological models are required to investigate groundwater-surface water interactions. However, due to the difficulty in code modification and computation time, several approaches are made. For example, recently, a new module (called gwflow) was developed to replace the simplified representation of the groundwater system in SWAT. This paper aimed to assess whether a groundwater-driven catchment (Dijle) can be better represented with either the "standard" SWAT+ model or the newly developed SWAT+gwflow model. In addition, the gwflow module is modified to ac-count for groundwater–soil interactions (gwsoil). Consequently, the effect on water balance values and total and baseflow representation is investigated.

First, we modeled the catchment using the standalone SWAT+ model, and during the calibration period (1983 to 1996), the NSE is 0.4, while this decreased considerably (less than zero) during the two validation periods (1975 to 1982 and 1997 to 2002). From this, it is apparent that the standalone model could not adequately represent the hydrology of this groundwater-driven catchment. This is attributed to the simplified representation of the groundwater component of the SWAT+ model. Contrary to this, the simulation improved considerably when we modeled the catchment using SWAT+gwflow. For instance, the NSE has increased to 0.6, 0.7, and 0.5 during the calibration, the first and second validation periods, respectively. Furthermore, we com-pared the streamflow model output at another gauging station (Sint–Joris–Weert), and it was captured with an NSE of 0.5, 0.7, and 0.4 during the calibration and the first and second validation periods, respectively.

Comparison made before and after modifying the module (accounting gwsoil) interaction revealed that streamflow simulation has deteriorated when gwsoil interaction is neglected (NSE of 0.1) while the NSE has improved (NSE = 0.6) when such exchanges are included in the modeling scheme. This is due to overestimation of streamflow, which occurs as groundwater is allowed to rise to the ground surface, resulting in high rates of saturation excess flow (164 mm). In contrast, when the gwsoil mechanism is operational, shallow groundwater is transferred to the soil profile, wherein the additional water is subject to ET, surface runoff, and soil lateral flow (increased by 300%). On top of this, the comparison also indicates a significant difference among the water balance variables and baseflow values, suggesting the importance of including gwsoil interaction in the hydrological modeling. This has implication for other coupled models to consider adding this interaction in their modeling scheme.

In general, the new groundwater module (gwflow) has an advantage over the standalone SWAT+ groundwater module. This is important for a highly groundwater-driven catchment where the baseflow plays a significant role. The new coupled model, along with the modification we made has four major advantages, including; a better representation of the baseflow, appropriate soil water (water balance) and streamflow values, detailed groundwater model output mapping, and finally, the coupled model does not require recharge from another surface water model to force the groundwater system which is the case for

independent surface and groundwater modeling approaches. To conclude, this coupled model has implication for other geohydrological models that has simplified representation of groundwater systems to replace it with physically based and spatially distributed modules to better capture the geohydrology. Furthermore, the coupled model has importance for proper aquifer management in an integrated (coupled) scheme. However, further research is required to represent wetlands in SWAT+gwflow and identify and assess tile drain units. We believe that the latter may play a significant role in improving models on groundwater-dominated catchments where groundwater is likely to enter near the root zone, driving the application of tile drains.

3.2 An open source SWAT+gwflow input preparation, post-processing and calibration tool development

3.2.1 Summary

The Soil and Water Assessment Tool (SWAT/SWAT+) modelling suite is widely applied for integrated hydrological studies. Due to the simplified representation of the groundwater hydrology in SWAT/SWAT+, this is frequently coupled with groundwater models such as the Modular Groundwater Flow model (MODFLOW) and the recent gwflow. For SWAT+gwflow, however, the preparation of the inputs has to be done manually using GIS routines which are mostly cumbersome and difficult for large watersheds. Additionally, the application is hampered as there are no tools for post-processing and calibration compared to the standalone versions of the models. Therefore, this research aims to tackle these issues by presenting an open source, Python-based script to prepare, post-process and calibrate using Particle Swarm Optimization (PSO) any SWAT+gwflow model setups. To show its range of applicability in different contexts, the script is used for twelve case studies in Belgium, Denmark, Italy, Morocco and Spain.

The input preparation lasted between 3 to 10 minutes, which is more efficient than manual input preparation. Additionally, the post-processing enables the SWAT+gwflow user community to produce and examine water balance components easily. Finally, calibration using PSO is made possible for the coupled model. In the watersheds we investigated, calibration resulted in NSE values between 0.4 and 0.97. Free and open-source scripts allow users to apply geohydrological models easily and ensure the reproducibility of modeling works.

This section is under review as: **Yimer, E. A.**, José Pablo Terán Orsini, Lorenzo Villani, Abdennabi Alitanea, Zakaria Ammari, Brian Omondi Oduor, Anandita Agarwal, Ryan T. Bailey, Jiri Nossent,Ann van Griensven: An open source SWAT+gwflow input generation, post-processing and calibration tool for comprehensive assessment of water resources.

3.2.2 Introduction

Even though SWAT and MODFLOW have been extensively coupled in many studies, their integration requires significant modification of the modeling codes and the addition of multiple source files, leading to long time for the setup and running of simulations (Bailey et al., 2020a). The gwflow module was developed to solve these issues, and since its introduction, it has been applied in various studies (Bailey et al., 2023, 2022; Yimer et al., 2023b,a,c). Nevertheless, interfaces that aid the input creation, post-process, and calibration are not available for SWAT+gwflow. This paper presents an open–source, Python-based script to prepare, post–process, and calibrate any SWAT+gwflow model setups and test and evaluate its applicability in 12 different study watersheds.

3.2.3 Study area

The study areas are 12 watersheds located in Belgium, Denmark, Italy, Spain, and Morocco (Fig. 3.7). The main characteristics of the watersheds are reported in Table 1. The catchment area varies from the smallest Cidacos watershed (477 km^2) to the largest Upper Scheldt (5976 km^2). According to the maps of Beck et al. (2018), climates can be mostly categorized as temperate, either with or without summer dry season. An exception is represented by the Gudenå watershed climate in Denmark, which is classified as cold. Annual average precipitation ranges from 300 to almost 1000 mm. Shallow unconfined aquifers are present in the Belgian and Danish watersheds, where slopes are negligible. Elevations are higher in the Moroccan, Italian, and Spanish watersheds (Fig. 3.7).

3.2.4 Design and Implementation

The methodology comprises three major parts: starting with the SWAT+gwflow input preparation, continuing to calibrate any SWAT+gwflow model setup, and finally, post-processing (Fig. 3.8). The script was developed in Python version 3.8. The following packages (with corresponding version or higher) are required for the script:

- Pandas 1.5.2
- Geopandas 0.12.2
- Gdal 3.6.1
- Numpy 1.23.5
- Shapely 2.0.0
- Matplotlib 3.6.2 & Matplotlib_scalebar 0.8.1
- Pyswarms 1.3.0
- Pathlib 1.0.1
- Shutil 1.7.0

Table 3.3: The twelve study areas descriptions (catchment name, country where it is located, area, annual average precipitation, and groundwater characteristics)

#	Catchment name	Country	Area (km^2)	Annual avg. precipitation (mm)	Groundwater characteristics
1	Kleine Nete	Belgium	551	821	Shallow groundwater table with unconfined aquifer
2	Grote Nete	Belgium	509	828	Shallow groundwater table with unconfined aquifer
3	Demer	Belgium	2204	785	Mix of confined and unconfined aquifers
4	Dender	Belgium	1352	903	Mix of confined and unconfined aquifers
5	Dijle and Zenne	Belgium	2428	873	Mix of confined and unconfined aquifers but mainly composed of Brussel sand aquifer system with shallow groundwater table
6	Leie	Belgium and France	3794	–	Mix of confined and unconfined aquifers
7	Upper Scheldt	Belgium and France	5976	931	Mix of confined and unconfined aquifers
8	Gudenå	Denmark	2625	800–850	Shallow unconfined aquifers
9	Bruna	Italy	836	786	Mostly confined aquifers
10	R'Dom	Morocco	1970	300–500	Shallow aquifer (Plio-Villafranchian sandstone, conglomerate sand and lacustrine limestone) and deep aquifer (Lias dolomitic limestone)
11	Mikkes	Morocco	1368	365–965	Two aquifers and one aquitard. The first aquifer is unconfined and thin. The second aquifer is unconfined upstream and becomes confined under marls downstream
12	Cidacos	Spain	477	400–800	Mainly alluvial aquifer of about 61 km^2 of extension and up to 20 m deep with mainly gravel and sand with low degree of cementation at the bottom and silt and clay in the surface layers

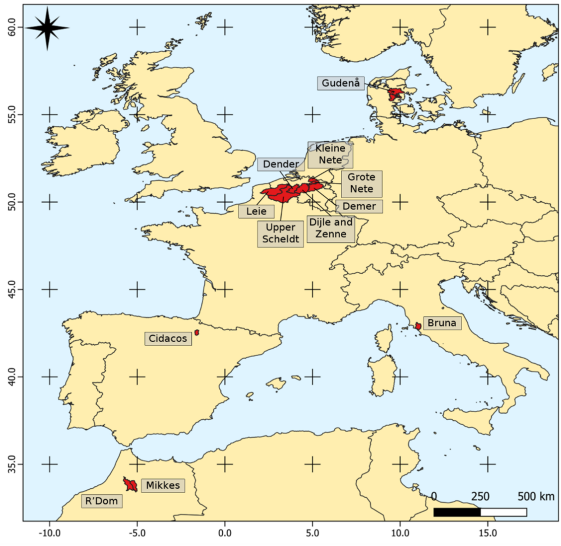


Figure 3.6: The geographical locations of the 12 watersheds

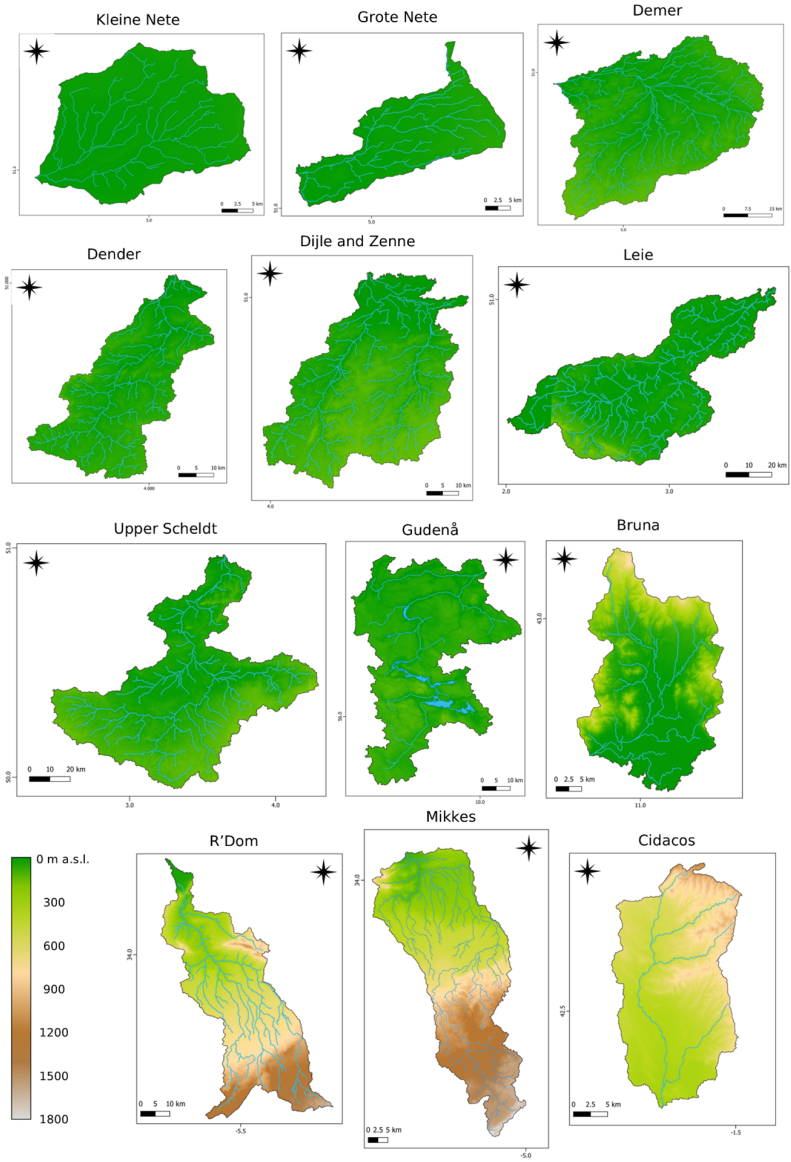


Figure 3.7: The delineation and river networks as generated by the SWAT+gwflow model used in the 12 study watersheds. The elevation is reported with a common legend to enable comparison between watersheds

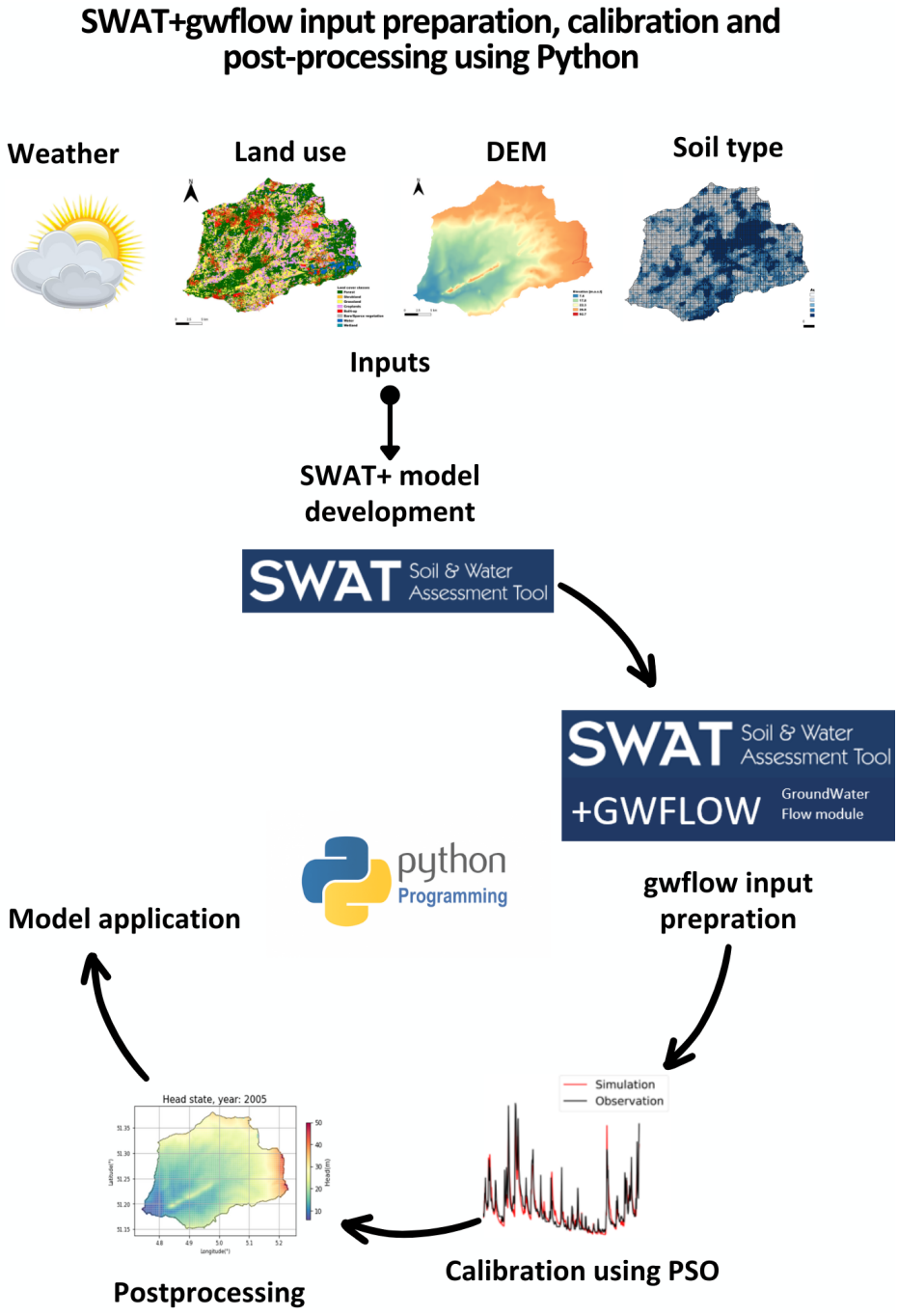


Figure 3.8: The schematic representation of the IPPC tool development

3.2.5 SWAT+gwflow input generation

The SWAT+gwflow inputs constitute the following major files: gwflow.input, gwflow.hrucell, gwflow.cellhru and gwflow.rivercell. The gwflow.input is the central file containing the module's basic information (which processes to simulate the hydraulic conductivity and specific yield zones, aquifer thickness, ground surface elevation, etc). The latest version of the SWAT+gwflow model has a new structure for the gwflow.input file, zones, aquifer thickness, recharge delay, ground surface elevation, etc., are in an array format contrary to the previous version, which was listed in a table format.
It is ideal to have a general folder in which the script and all data are stored. All required data must be stored in this folder (they can be inside their own folders). The following structure is recommended:

- Folder with global and local raster files and shapefiles with information about the basin and aquifer (sub-basins, DEM, aquifer thickness, aquifer conductivity, lakes, etc.)
- Folder with original SWAT+ output files folder (files inside the TxtInOut folder of the standalone SWAT+ model should be copied in this folder).
- `gwflow` executable file (`SWAT+gwflow.exe`)
- Excel file with simulation years and day of output, an example is provided with the script.

Figure 3.9 below shows a proper layout of the general folder, while Figure **??** represents a part of the code regarding the inputs that need to be modified by the user.

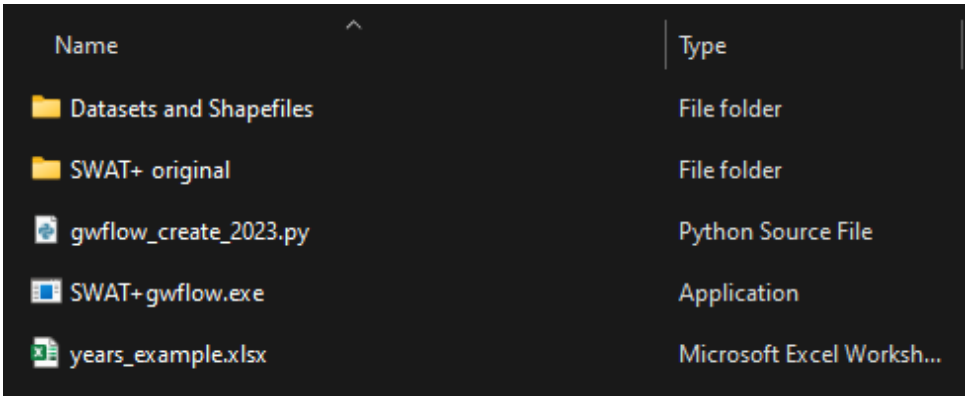


Figure 3.9: The proper layout of folders and files for the SWAT+gwflow input generation process

It is necessary to first indicate some information before running the script, such as the geographical projection of the project, the name of the SWAT+ original folder, and names of specific shapefiles and raster files, among others. This is done from lines 393 until 425.

Further on, the initial values for the gwflow module must be indicated from lines 431 until 475 (e.g., grid cell size, type of boundary conditions, simulation of tile drains, simulation of groundwater-wetland interaction, initial specific yield, initial streambed conductivity, groundwater extinction depth).

Mostly, the parts to carefully look into are from lines 393 to 451, where the other parts can be calibrated at a later stage as they are initial values. Once all file names, initial conditions, and values are provided as indicated in the previous paragraphs, it is possible to run the script.

```
#%% Filenames
# EPSG code and file names

# Define projection code. Must be written as string EPSG:CODE
EPSG='EPSG:31370'
#SWAT+ original folder (TxtInOut by default)
swat_folder='SWAT+ original'
# GIS Filenames (Basin shapefile, global rasters, etc)
# Filename and directory of basin shapefile
basin_file='subs1.shp'
# Raster file of aquifer thickness GLOBAL
thick_raster_file='BDTICM_M_250m_ll.tif'
# Shapefile of aquifer thickness LOCAL, if not used, leave equal to 0
thick_file_local=0
thickness_attribute_name='Avg_Thick' #Specify the attribute name for thickness in the shapefile
# DEM raster filename
dem_raster='DEM_filled.tif'
# Conductivity GeoDataBase filename
conductivity_file='GLHYMPS.shp'
#River network shapefile filename
river_filename='rivs1.shp'
# HRU shapefile filename
hrus_filename='hrus2.shp'
#Excel simulation years file
years_file='years_example.xlsx'
# Observation locations shapefile filename - If not existent, leave as empty string
obs_file=''
# Tile cell locations shapefile filename and attribute name if tile groups exist - If not existent, leave as empty string
tiles_file=''
tile_group_att='group'

# Lakes shapefile
lakes_file="HydroLAKES_polys_v10.shp"
# Floodplains shapefile
floodplain_file=''
# Reservoirs shapefile
reservoir_file= ''
```

```
# Initial values for SWAT+gwflow module
# Basic information
cell_size=300 #Grid cell size (units depending on projection)
WTI_flag=1 #Water table initiation flag (1 = water table depth is specified)
WT_depth=2 #Water table depth (m) at start of simulation
Boundary_conditions=1 #Boundary conditions (1=constant head; 2=no flow)
GW_soiltransfer=1 #Groundwater --> soil transfer is simulated (0 = n; 1 = yes)
Saturation_excess=1 #Saturation excess flow is simulated (0 = no; 1 = yes)
External_pumping=0 #external groundwater pumping (0=off; 1=on)
Tiledrain_flow_sim=0 #Tile drain flow is simulated (0 = no; 1 = yes)
Reservoir_exchange=0 #groundwater-reservoir exchange (0=off; 1=on)
Wetland_exchange=0 #groundwater-wetland exchange (0=off; 1=on)
Floodplain_exchange=0 #groundwater-floodplain exchange (0=off; 1=on)
Canal_seepage=0 #canal seepage to groundwater (0=off; 1=on)
GW_ET_flag=1 #Groundwater ET flag (0 = groundwater ET not simulated; 1 = groundwater ET simulated)
HRU_recharge=1 #Recharge is passed from HRUs (0 = no; 1 = yes)
recharge_delay=32.36 #Recharge delay (days) between soil profile and water table
GW_nutrient_sim=0 #Groundwater nutrient transport is simulated (0 = no; 1 = yes)
timestep_balance=0.25 #Time step (days) to solve groundwater balance equation

#Reservoir shapefile attribute names and properties - Only necessary if GW-floodplain is on
reservoir_thickness=2.00 #reservoir bed thickness (m)
reservoir_bed_K=0.00000999 #Reservoir bed conductivity (m/day)
```

Figure 3.10: The inputs that need to be modified inside the script (from lines 393 to 475)
— continued on next page

```
#Initial values for the model
init_sy=0.2 #Initial specific yield 'Sy'
init_n=0.25 #Initial porosity 'n'
streambed_k=0.000027563836 #Streambed hydraulic conductivity (m/day)
streambed_thick=1.88600367 #Streambed thickness (m)
EXDP=1.00 #Groundwater ET extinction depth (m)
ET_fix=0.0 #Fixed Vegetation ET
init_N=3.0 #Initial NO3 concentration
init_P=0.05 #Initial P concentration
row_det=100 #Cell row for detailed sources/sink output
col_det=150 #Column row for detailed sources/sink output
rv_depth=5.0 #Vertical distance (m) of streambed below the DEM value
tile_depth=1.22 #Depth (m) of tiles below ground surface
tile_area=50 #Area (m2) of groundwater inflow (circumference*length) * flow length
tile_k=5.0 #Hydraulic conductivity (m/day) of the drain perimeter
tile_groups=0 #Tile cell groups (flag: 0=no; 1=yes)
tile_groups_number=0 #Number of tile cells groups
denit_constant=-0.0001 #First-order rate constant for denitrification (1/day)
disp_coef=5.00 #Dispersion coefficient (m2/day)
nit_sorp=1.00 #Sorption retardation coefficient for Nitrate
pho_sorp=1.00 #Sorption retardation coefficient for Phosphorus
transport_steps=1 #Number of transport time steps per flow time step
```

Figure 3.10: (continued) The inputs that need to be modified inside the script (from lines 393 to 475)

The following folders will be produced in the same directory as the script:

- `GIS_plots`: Contains basic spatial plots showing aquifer thickness, elevation variation, hydraulic conductivity zones, etc.
- `grids`: Folder with all produced grids.
- `inputs_files`: Contains the GWFlow inputs (`gwflow.input`, `gwflow.cellhru`, `gwflow.hrucell`, `gwflow.rivcells`, `file.cio`, `rout_unit.con`, `object.cnt`, and `codes.bsn` files).
- `SWAT+ gwflow`: Folder with a copy of the original, plus the new and modified input files, and the gwflow executable.
- `supplementary`: Folder with intermediate files that result from geoprocessing.

A snapshot of the original and new folders (in red rectangle) is shown in Figure 3.11. Finally, the script copies the files from the folder `input_files` into the `SWAT+ gwflow` folder and runs the gwflow executable. The new version of the SWAT+gwflow module contains additional interactions such as groundwater–wetland, groundwater–floodplain, and groundwater–reservoir interactions. All these are included in the script to allow the users to have the full potential of using the coupled model. The user has to specify either `0` or `1` if any of the three interactions are to be simulated (in lines 439 to 441). In addition, the user has to provide the reservoir, wetland, and floodplain shapefiles so that the grids connecting with those entities can be taken from the intersection and the interactions can be simulated.

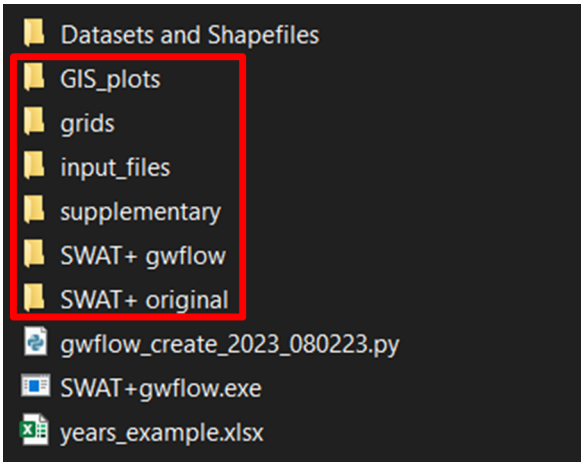


Figure 3.11: The final structure of the folder after the script finishes running (which adds several other folders that contain useful files for the successful coupling of the SWAT+ and gwflow module)

3.2.6 SWAT+gwflow calibration using Particle Swarm Optimization (PSO)

The calibration for any SWAT+gwflow model setup is now possible by selecting the variables to calibrate using Particle Swarm Optimization (PSO). PSO is a global optimization tool widely used in many fields. It has already been successfully applied in hydrological modelling with SWAT (Hui et al., 2020; Zhang et al., 2009). Other tools for the application of PSO calibration in hydrological modelling exist (e.g. (Zambrano-Bigiarini and Rojas, 2013)), but they are not specific for SWAT+gwflow. For now, the script works for optimizing the model for streamflow and groundwater head, but for multiple locations (multi–site calibration). In the next version, it is planned to include calibrating the model for ET, soil moisture, nutrients (e.g. nitrate, phosphate, etc.), etc.

There are two Python scripts that need to be used to calibrate the coupled model (`PSO_user.py` and `PSO_gwflow.py`). The first one is for the user to provide the working directory, number of distinct hydraulic zones to calibrate, simulation period, observed file name, objective function (e.g., *Nash-Sutcliffe efficiency*, *root mean square error*, etc.), number of particles, number of iterations, time step (monthly or daily), a parameter table, and parameter bounds. The parameter table contains all the parameters that are included in SWAT+, along with a column to specify `'y'` if you want to calibrate the parameter or `'n'` otherwise. The second script will initiate the calibration procedure and stop once the objective function value cannot increase or decrease further.

3.2.7 SWAT+gwflow post–processing

The model outputs of the `SWAT+gwflow` model setup can be easily explored using the post-processing script, which requires: the year of simulation, the projection of the different raster and vector layers, and the day/month to produce the map. Note that some outputs need to be activated for the script to work smoothly. For example, inside the `print.prt` file, the user needs to activate `hru_wb` (for the annual average value). Also, the years for which the user wants to generate spatial plots must be specified at the bottom of the `gwflow.input` file. Once the necessary information, as shown in Figure 3.12, is filled in correctly, the spatial maps showing different water fluxes (e.g., groundwater–surface water interactions, recharge, groundwater–soil interactions, saturated excess flow, groundwater ET, groundwater head, etc.) will be produced.

The folder SWAT+ gwflow will be generated while the previous script runs, and the post–processing script can be used to produce the different maps before or after calibrating the model. The user can also run the post–processing script after running different scenarios (running at different time windows, turning on and off different model outputs, etc.).

```
#%%File names
output_folder='SWAT+ gwflow'
basin_file='subs1.shp'
hru_file='hrus2.shp'

Run Cell | Run Above | Debug Cell
#%% Simulation years
init_year=2000
final_year=2009

Run Cell | Run Above | Debug Cell
#%%Plot date
plot_year=2005
plot_month=2
#PLOT TYPE: For annual plots (State, flux & mass) type 1, for monthly state (head, concentrations) type 2
plot_type=1
#EPSG
epsg='epsg:31370'
```

Figure 3.12: The user needs to modify the inputs for the post-processing script to work correctly (lines 114 to 128)

3.2.8 Results

The results for the five watersheds except for the Belgian are reported in this section. A more in–depth analysis of the specific results of the seven watersheds from Belgium can be found in (Yimer et al., 2023c). Furthermore, examples of visualization outputs created with the tool are shown.

SWAT+gwflow input generation

The input generation took much less time than the manual GIS routine, between 3 and 10 minutes. Note that the bigger the watershed, the finer the grid cell size, and the more detailed the Hydrologic Response Units (HRUs) are, the more time it can take to prepare the SWAT+gwflow inputs. Hence, the user should take into account these factors, but the issue won't be more on the input generation, rather, it will affect the running of the coupled model.

Streamflow calibration using PSO

Results of the SWAT+gwflow application at the 12 watersheds indicated the successful mimicking of the streamflow at the catchment outlets of the respective watersheds. The baseflow was captured reasonably, which makes the appropriate representation of the groundwater (Fig. 3.13). Calibration resulted in NSE (Tab. 3.4) values between 0.4 and 0.97 (only unsatisfactory for the Denmark watershed). The Gudenå watershed is dominated with extensive water drainage via tiles/ditch (Sechu et al., 2023), and their inclusion is expected to improve the geohydrological simulations. The underestimation of the streamflow by the coupled model is an indication for the unaccounting of the water removed by the drainage system. The advantage of using PSO lies on the global search strategy it follows which is contrary to Parameter ESTimation tool (PEST), which is based on local optimization (Doherty, 2016), thus, the integration of PSO with SWAT+gwflow is vital.

Post-processing results

The users can retrieve monthly or yearly average spatial plots for recharge, groundwater head, groundwater-soil interaction, groundwater saturated excess flow, groundwater–surface water interaction, etc. For demonstration, we hereby present the groundwater head and recharge for five watersheds (Fig. 3.14,3.15)

Table 3.4: Nash-Sutcliffe efficiency (NSE) of the calibration and validation periods in the five watersheds (non-Belgian). Belgian catchments are discussed in Yimer et al. (2023b).

Catchment	Calibration	Validation
Gudenå	0.55	0.40
Bruna	0.94	0.85
R'Dom	0.75	0.58
Mikkes	0.91	0.50
Cidacos	0.97	0.84

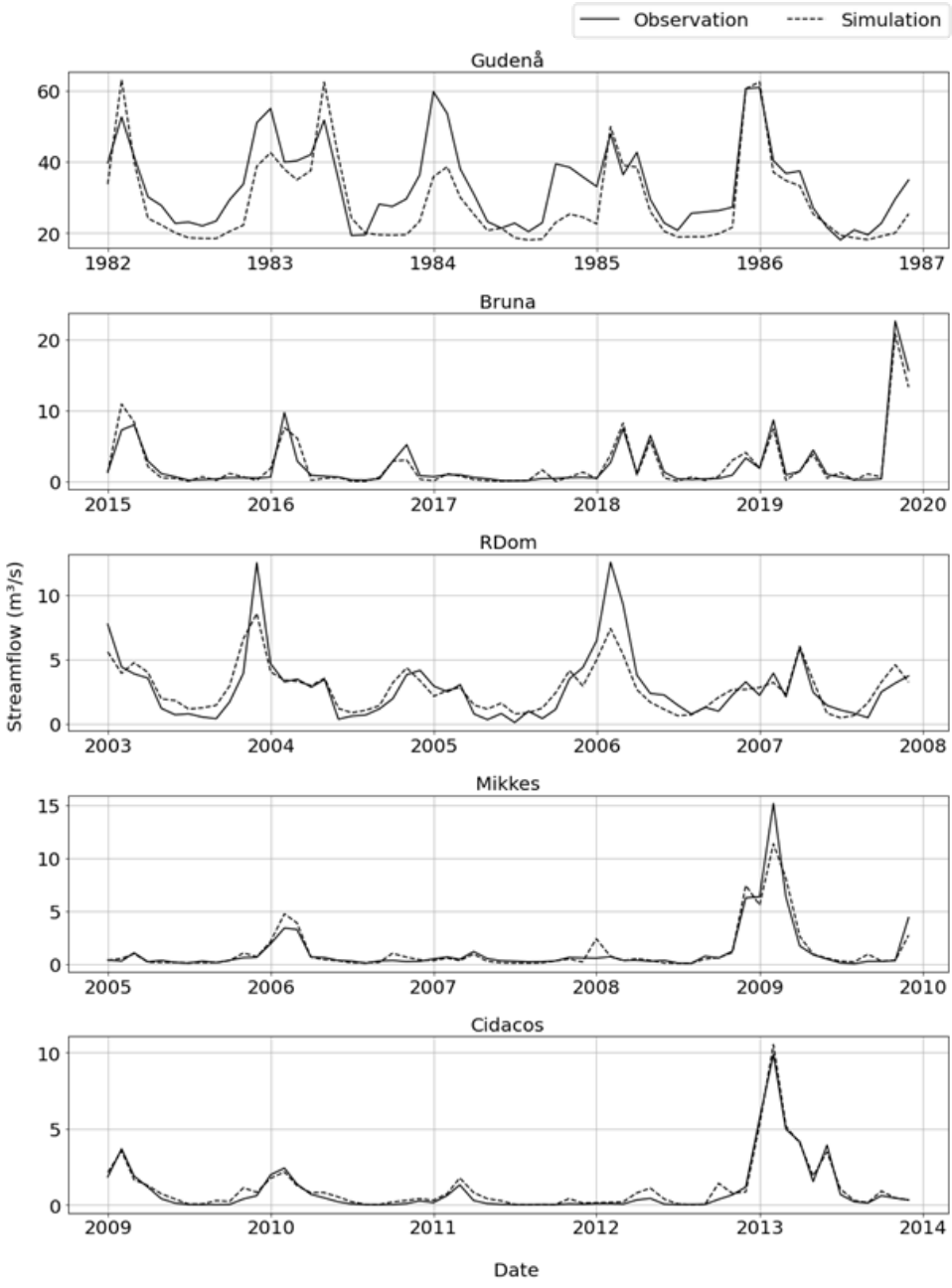


Figure 3.13: The streamflow outputs from the SWAT+gwflow model after model calibration.

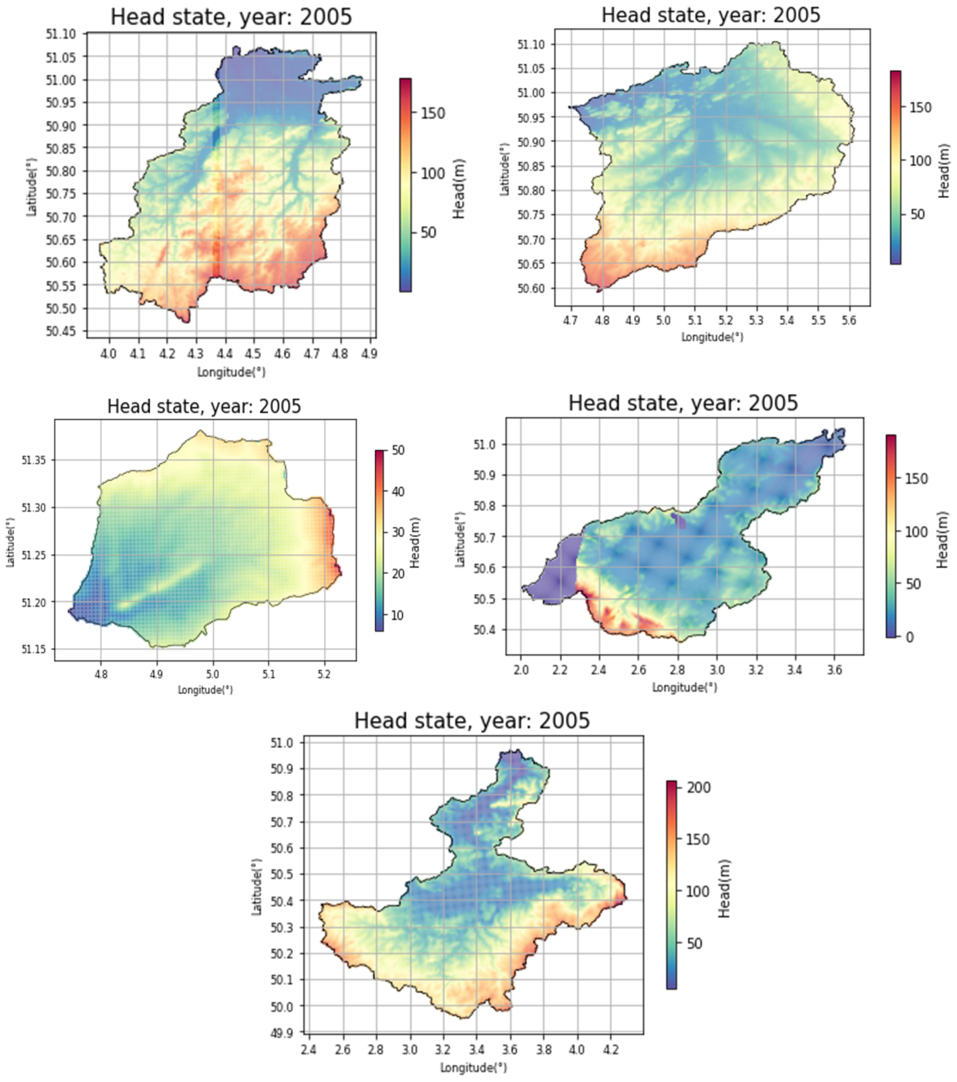


Figure 3.14: Examples of post-processing outputs (groundwater head) created with the Python script

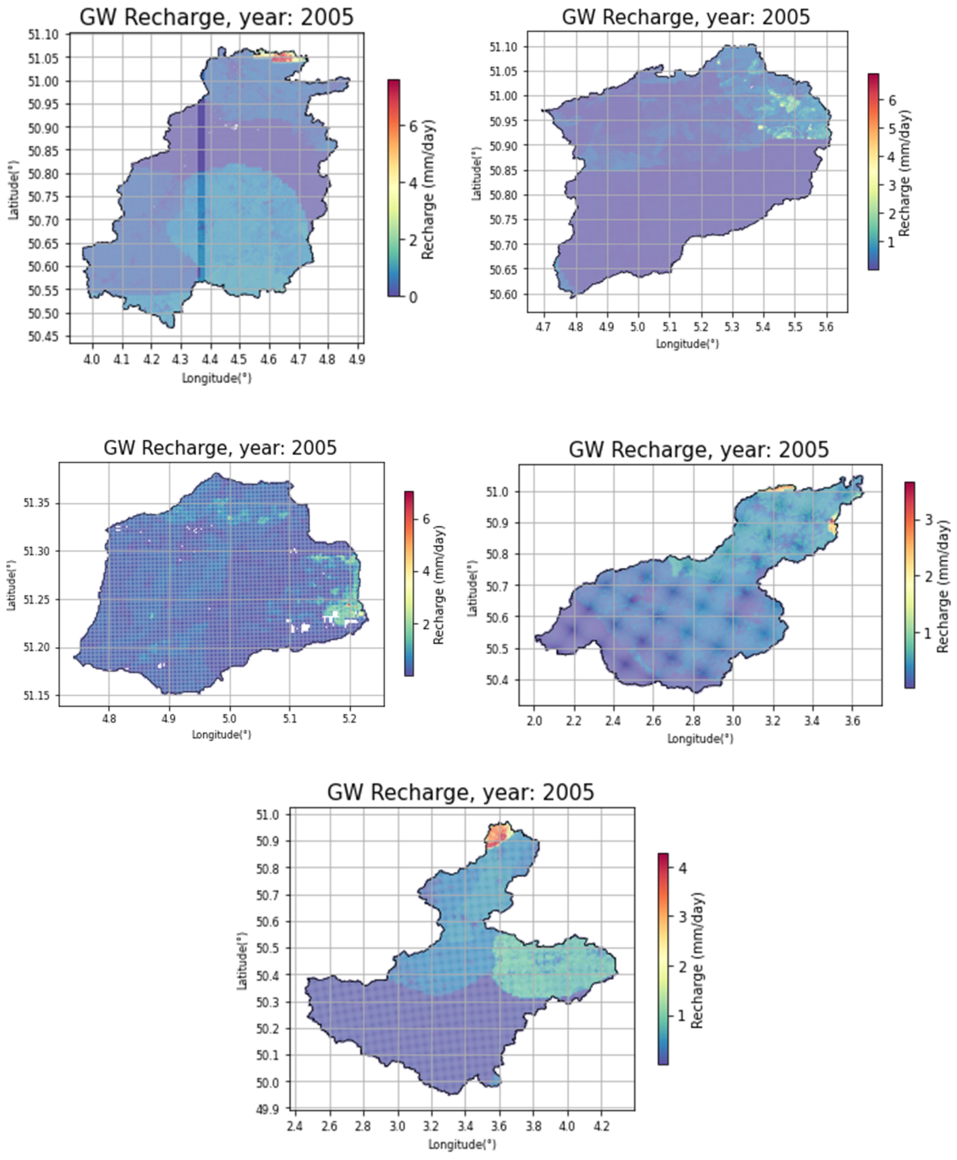


Figure 3.15: Examples of post-processing outputs (recharge) created with the Python script

3.2.9 Conclusion

The SWAT+gwflow input generation, calibration using Particle Swarm Optimization (PSO) tool and post–processing can be done using the open source and user–friendly Python–based script. The script fully automates the complex task of geoprocessing and formatting the numerous data files required for integrating SWAT+ with the SWAT+gwflow module, which allows the user to prepare the inputs efficiently (less than 10 minutes for the watersheds that we investigated), and to more easily test various setup conditions and scenarios. Moreover, the software quickly produces output visualization in a format ready for presentation, which saves time for the user that would otherwise require extra steps for this purpose.

The calibration script can also be used to optimize model parameters of the standalone SWAT+ model on top of calibrating the coupled SWAT+gwflow model. Application for 12 diverse watersheds located across the globe indicated the practicability of the coupled groundwater-surface water model (SWAT+gwflow), with satisfactory performances for all the watersheds, except for the Denmark watershed.

The integration of the multiple purposes of this script enhances the functionality SWAT +gwflow, significantly increasing its accessibility. This improvement enables a wider range of users to incorporate this module into their hydrological models, greatly enhancing the accuracy of their simulations in those cases where groundwater plays a critical role in the catchment's hydrological processes.

Chapter 4

Model application

This chapter is a result of three major papers. Firstly, the Kleine Nete catchment is modeled using SWAT+gwflow to evaluate the extent at which agricultural water drainage can affect the waterbalance components. For this analysis, first finding the location of agricultural water drainage units inside the watershed is vital, hence, we developed a novel generic methodology that better helps locate drainage units in agricultural landscape. Finally, seven watershed inside the Scheldt basin are modeled with the aim to capture the streamflow, groundwater-surface water interactions and general waterbalance components.

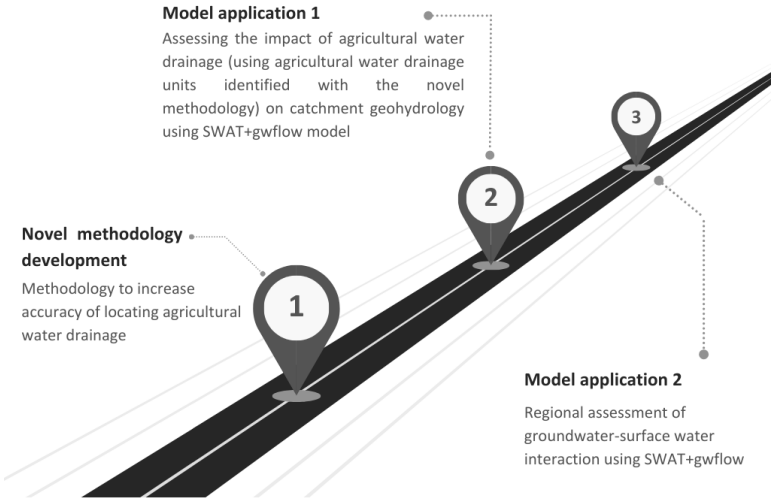


Figure 4.1: Major parts of Chapter 4 which focues on model application

4.1 Groundwater level-based filtering to improve the accuracy of locating agricultural water drainage locations

4.1.1 Summary

Remote sensing (RS) using satellites circling around the Earth has great potential for monitoring surface processes with reduced cost and greater access. This study uses three approaches to identify possible drainage unit locations: existing benchmark techniques and a novel complementary approach based on groundwater table depth. The study area comprises a site in Ontario, Canada, and the Kleine Nete catchment, Belgium. First, a change detection method based on the interpretation of RS imagery is used to retrieve soil moisture differences. Based on the retrieved soil moisture differences, it is possible to distinguish between drained and undrained fields. Secondly, the decision tree classification (DTC) method based on filtering pixels corresponding to agricultural fields with a slowly draining soil class along with a gentle slope was applied to identify drainage units. Finally, a novel filtering technique based on groundwater table depth is applied as a complementary identification tool to the former approach.

The remote sensing method resulted in 87.8% accuracy in the first study area, while the decision tree classification achieved 96.7% accuracy. Although the RS approach was not successful in following the ditch network, the DTC was able to indicate ditch networks with up to 58% accuracy. However, the additional filtering using groundwater level measurements increased the drainage unit identification accuracy in the first study area (corresponds to finding an additional 19.4 km^2 area of drains). A final quantitative assessment for the second study area revealed a close follow-up of the ditch network to the shallow groundwater table maps. In general, it can be concluded that both the remote sensing and the DTC method have tremendous potential to identify drainage units, although with limitations in particular cases, such as low accuracy. Moreover, it can be advised that a local visit to the study area is required to investigate what type of drainage system is used. Next, the novel use of groundwater level-based filtering further improves the drainage identification procedure. Finally, combining several data and techniques allows for accurately identifying drainage units, which is ultimately useful for the sustainable management of drained water from agricultural fields.

This section is published as: **Yimer, E.A.**, Yadollahi, S., Riakhi, F.-E., Alitane, A., Weerasinghe, I., Wirion, C., Nossent, J., van Griensven, A., 2023. A groundwater level-based filtering to improve the accuracy of locating agricultural tile drain and ditch networks. International Journal of Applied Earth Observation and Geoinformation 122, 103423. https://www.sciencedirect.com/science/article/pii/S1569843223002479

4.1.2 Introduction

According to Valayamkunnath et al. (2020), due to the lack of tile-drainage existence and/or a location map, it is difficult to investigate its impact on the hydrology and water quality. Thus, finding the location of drainage units is vital for the farmers to increase their economic benefits through sustained crop productivity.

Existing techniques to identify drainage units include manual operations such as digging and non–invasive methods such as remote sensing-based approaches (RS), decision tree classification (DTC), ground penetrating radar (GPR), thermal detection, etc. The RS approach is based on the assumption that the remotely sensed images before and after a major rainfall event can differentiate drained and undrained fields (Gökkaya et al., 2017). The DTC follows the hierarchal identification of drainage units based on land use, soil drainage class, and slope (Naz et al., 2009). The shortcoming of the invasive methods is the expense related to the digging–out process (Allred et al., 2018). As for the GPR technique, extensive effort is required until the buried units are identified (Allred et al., 2004).

Although the RS and DTC approaches are considerably cheaper and more efficient, they can also provide low accuracy in determining the location of the drainage units (Naz and Bowling, 2008; Reynolds, 2014; Thompson, 2010). For example, RS-based techniques rely on the availability of cloud–free imagery to implement the methodology successfully. Similarly, the DTC method does not necessarily infer the existence of drainage units. Therefore, proper, cost–effective, accurate, and efficient mapping techniques are needed to locate drainage units (Tilahun and Seyoum, 2020). On top of this, all the drain locating techniques neglect the primary cause of drain application: groundwater level reaching the root zone. Hence, accounting for this major variable and applying additional filtering on the RS technique can potentially improve the accuracy of the traditional approaches.

Therefore, the existing drain identification techniques are first applied (RS and DTC) and evaluated. Henceforth, this research applied a novel approach to improve the accuracy of the identification of drainage units. For this, case studies from Canada and Belgium are used to show the performance of the three methods.

4.1.3 Study area and data

Study area

The study areas are located in the south of Ontario, Canada, and the northeast of Belgium (i.e., the Kleine Nete watershed) (Fig. 4.2). The Ontario case study covers an area of 1130 km^2, which is part of the Great Lakes–St. Lawrence River watershed. This area was selected due to the high density of agricultural land and the availability of tile–drainage data. More than half of the fields in this region are tile–drained to grow crops such as corn, wheat, and soybean - https://www150.statcan.gc.ca/t1/tbl1/en/tv.action?pid=3810011201, (last accessed 30 April 2021). Notably, 13% of the farms in Ontario are irrigated (Karásek

and Nováková, 2020). The average annual rainfall amounts to 922 mm, with February being the driest month (61 mm) and May the wettest (94 mm).

The Kleine Nete catchment is a subbasin of the Nete catchment, located in northeast Belgium, and occupies an area of about 552 km^2, as shown in Fig. 4.2 Generally, the catchment's watercourses are shallow with low hydraulic head and flow rates, known as lowland streams. The rivers are primarily fed by rainwater and seepage. While most rivers are unnavigable and natural, artificial canals are also present within the catchment (Boerema et al., 2014). Elevation in the area ranges from 5 to 48 m above sea level. The catchment is characterized by predominantly sandy soils (about 89%), with 6.1% dunes, 3.6% sandy loam, and 1.3% clay (Nossent, 2012). The region experiences a temperate climate with warm summers and cold winters with occasional snowfall. Based on long-term weather data from 1960 to 1991, Dams et al. (2009) reported a mean annual precipitation of 828 mm and a mean annual potential evapotranspiration of 664 mm. Temperatures average around 5°C in winter and 14°C in summer (Woldeamlak, 2007). The dominant land cover in the catchment is agriculture, representing 45.1% of the area—comprising 26.5% grasslands and 18.7% croplands. Forests cover 42.7%, built-up areas 9.6%, water bodies 1.9%, and wetlands only 0.1%. This classification is based on the European Space Agency (ESA) WorldCover map for the year 2020 - https://esa-worldcover.org/en (last accessed 24 June 2022).

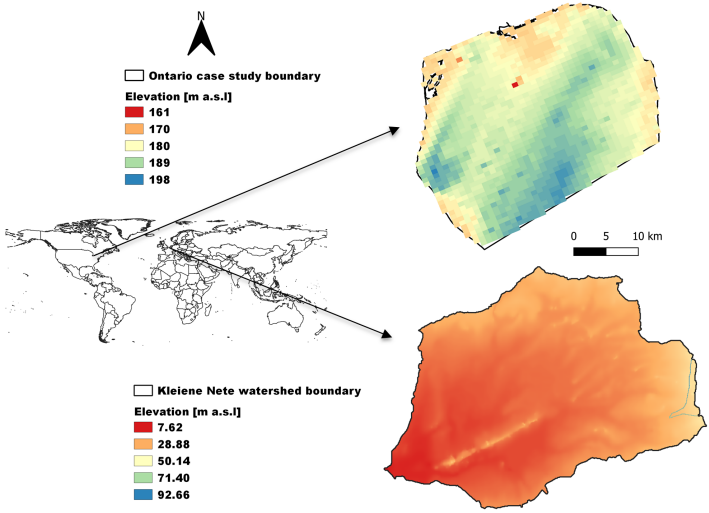


Figure 4.2: Location and spatial elevation variation of the two study areas.

4.1.4 Methodology

The methodology we followed started by applying existing methodologies, such as a remote sensing (RS) based approach and a decision tree classification (DTC) technique to identify drainage units. Next, a novel approach to improve drainage unit identification based on groundwater table depth follows. Finally, the RS and groundwater level-based filtering techniques are combined (Fig. 4.3). The accuracy is assessed using ground truth data in all the approaches.

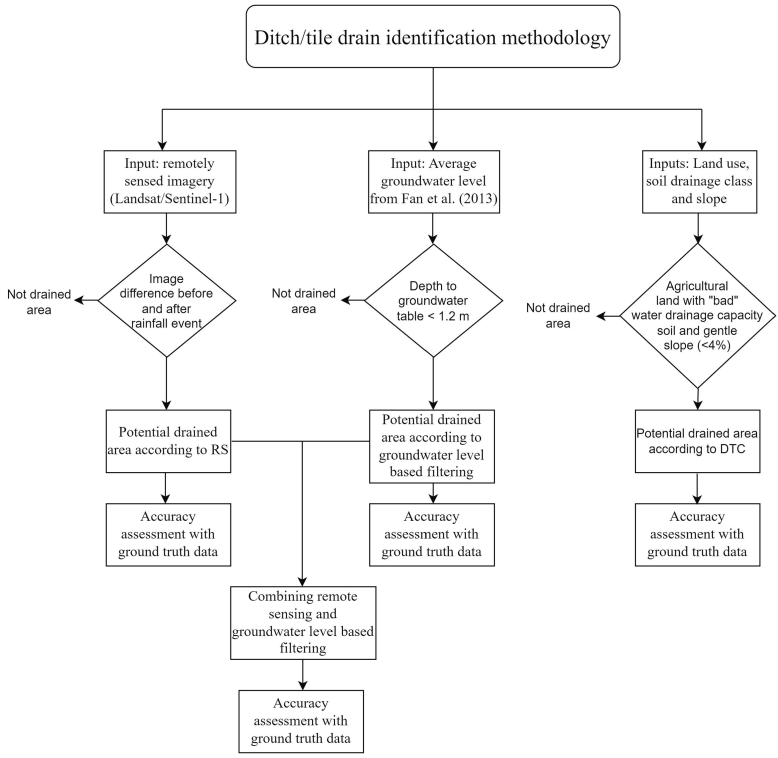


Figure 4.3: A flow chart showing the methodology we followed to identify tile/ditch network in the respective case study areas.

Drainage unit identification using remotely sensed imagery

The method here involves estimating soil moisture based on surface reflectance measured with satellite sensors (change detection technique). Henceforth, the difference between the soil moisture before and after a significant rainfall event can indicate how fast water is being drained. This implies the existence of a drainage system beneath an agricultural

field. This approach has been successfully applied using data from the European Remote Sensing (ERS) Scatterometer over West Africa (Wagner et al., 1999) and Sentinel–1 data over Spain (Gao et al., 2017).

Ontario case study
Two active weather stations (Windsor and Harrow) are used to derive average rainfall between 2020 and 2021, where rainfall events above 2.5 mm are used. In total, there are 150 rainfall events of more than 2.5 mm in the study area. For nine of these dates, there are Sentinel 1 data for the day of rainfall and the next day that can be used to see the change in soil moisture. The C-band SAR instruments on the Sentinel–1 satellites provide data in a dual or single polarization. Sentinel–1 data comes with VV and VH polarizations with fine spatial (10 m) and temporal resolution (12 days). Signals acquired in the VV polarization are used to construct soil moisture estimates in this study, as previous research has demonstrated that VH data has drawbacks in estimating soil moisture owing to volume scattering, which is highly dependent on the geometrical configuration and features of the vegetation (Karjalainen et al., 2008). The Sentinel–1 satellite data used for this study runs from the $1^{s}t$ of January 2020 to the end of September 2021. The raw data was further processed using the Sentinel-1 Toolbox (https://github.com/wajuqi/Sentinel-1-preprocessing-using-Snappy, last accessed 24^{th} of June 2022) according to the following steps:

- Applying orbit file
- Thermal noise removal
- Radiometric calibration
- Speckle filtration
- Terrain correction

To validate the result for the Ontario study area, a publicly available dataset showing tile drain locations is used and can be accessed at the following link (https://geohub.lio.gov.on.ca/maps/ontarioca11::tile-drainage-area, last accessed 24^{th} of June 2022).

Kleine Nete case study
Initially, rainfall data at Herentals station was collected from the Waterinfo website (https://www.waterinfo.be/, last accessed $24^{th}$of June 2022). This data was analyzed, where the 30^{th} of October 2018 corresponds to the day with significant rainfall of 25.95 mm. Then, dry and wet Landsat 8 Surface Reflectance images were acquired from the United States Geological Survey website (https://earthexplorer.usgs.gov/), which correspond to the images taken before and after the significant rainfall event on the 14^{th} of October and 15^{th} of November 2018, respectively. The images have 9% and 1.2% cloud cover, and both are captured at path number 198 and row number 024. The acquired images comply with the requirement of having less vegetation cover, as they are captured during winter months when vegetation and foliage cover are less in Belgium (Roelens et al., 2018). According to

Woo et al. (2019), choosing days with rainfall events of at least 2.54 mm during the ten days following the 25 mm rainfall event is advisable. Besides, Naz et al. (2009) recommended that no precipitation should occur for at least three days before the date of the wet image acquisition. This is to allow sufficient time for the surplus of water to drain and for the soil albedo to develop adequately. Note that the soil albedo, which represents the amount of reflected light from the soil, is related to soil moisture. Wetter soils located relatively far from the drains will have a darker color and lower albedo, while the artificially drained soils have brighter colors due to high reflectance and, thus, higher albedo. These requirements are met in the wet image used for this study.

Due to the presence of clouds in the dry and wet images, the CloudMasking plugin of the Quantum Geographic Information System (QGIS) version 3.16.14 was used to generate a cloud mask using two filters. With the Blue Band filter, the threshold used is 14000, which is the default for Landsat 8 blue band, where every pixel lower than the threshold is masked. With the QA Band filter, clouds and their shadows, cirrus, dilated clouds, and aerosols have specific bit numbers which, when selected, the plugin marks their corresponding pixels (ht tps://smbyc.github.io/CloudMasking/, last accessed 24 June 2022). This method uses the shortwave infrared (SWIR) part of the electromagnetic spectrum, which is band 6, having a wavelength ranging between 1.57 and 1.65 μm. The created cloud mask is then applied only to band 6 of each optical image. The masked areas in these images became *no data* areas, which are then filled by interpolating the neighboring 10 pixels using the Geospatial Data Abstraction Library (GDAL) Fill No Data tool. Band 6 of the wet image is then subtracted from band 6 of the dry image to locate the potentially artificially drained areas in the agricultural zones of the Kleine Nete (Gökkaya et al., 2017). In the resulting difference map, the potentially drained areas appear lighter as they have lower soil moisture, hence higher reflectance, while darker colored areas indicate potentially undrained locations. The map is finally classified into potentially drained areas for locations with a value equal to or lower than 0, as performed by Gökkaya et al. (2017) in their study. For this study area, ground truth data is obtained from the Belgian National Geographical Institute (NGI) (https://www.geopunt.be/, last accessed 24 June 2022).

Drainage unit identification using decision tree classification (DTC)

For the DTC method, the agricultural areas are first outlined and then intersected with soil classes with "bad drainage". "Bad drainage" for the Ontario soil map stands for; I - Imperfectly, P - Poorly, and VP - Very Poorly. As for the Belgian map, moderate poor to very poor are considered. The resulting shapefile is then again intersected with the slope shapefile, where 4% is taken to identify possible drainage units for both case studies. For this method, soil and land use maps are obtained from https://geohub.lio.gov.on.ca/map s/ontarioca11::soil-survey-complex and https://open.canada.ca/en/open-maps for the first case study (last accessed 24^{th} of June 2022). For the second study area, the soil map is adapted from Nossent (2012), while the land use map is taken from European Space Agency (ESA). The slope in both cases is estimated using a digital elevation model (DEM)

having a 30 m resolution and is acquired from https://earthexplorer.usgs.gov/, last accessed 24^{th} of June 2022.

Novel drainage unit identification methodology

The methods discussed above do not consider the primary cause of the drain application, which is the rise of groundwater level to the root zone. Hence, we propose to apply a filtering technique to the outcome of the RS method. The additional filtering will allow capturing additional areas as tile/ditch drains in a given area that were not detected or neglected by the former methods. For this methodology, local observation wells or a global dataset can be used to map groundwater depth from the ground surface. For this study, global water table depth data was acquired from Fan et al. (2013). According to Fan et al. (2013), the dataset combines more than a million government archives, literature, and reports and fills missing values with a groundwater model output (1 km resolution). Note that the more data is included in the analysis, the better is the map produced by Fan et al. (2013). For our study areas (Belgium and Canada), the information is readily available, hence, the accuracy of the water table information for those areas is high. Since drains are mostly applied at a depth of 0.6 to 1.2 m, a groundwater depth of less than 1.2 m is considered a potential drain location. This new approach will follow after the RS technique, which is expected to increase the detection accuracy.

The remote sensing approach has the advantage of showing areas with soil moisture variation before and after a rainfall event, hence, in those areas, there must be a system taking the water away. Therefore, remote sensing is more physically meaningful. On the other hand, the decision tree classification is based on the assumption that farmers will put a drainage system if a pixel corresponds to a gentle slope and soil with low water drainage capacity, which is not always the case (due to financial limitations, lack of knowledge, etc.). It is to be noted that, even if the groundwater depth is shallow, the agricultural land owner might not necessarily drain the water, hence, combining RS and groundwater level-based filtering is vital. On top of this, the mere use of groundwater depth can be beneficial to identify locations that require extensive drainage and understand and consequently set policies for sustainable management of agricultural lands and groundwater.

4.1.5 Results

Accuracy of the remote sense-based approach

For both case studies, the soil moisture content difference $[m^3/m^3]$ before and after a significant rainfall event shows areas with clear patches of negative values, corresponding to areas where the water drains quickly and follows agricultural plots. The estimated drainage area that intersects with the ground truth data divided by the total ground truth area is considered the method's accuracy (Gökkaya et al., 2017). For the first case study, the modeled area with tile drains is around 375.8 km^2, while the real tile drain area is around 428 km^2, leading to an accuracy of 87.8% (Fig. 4.4).

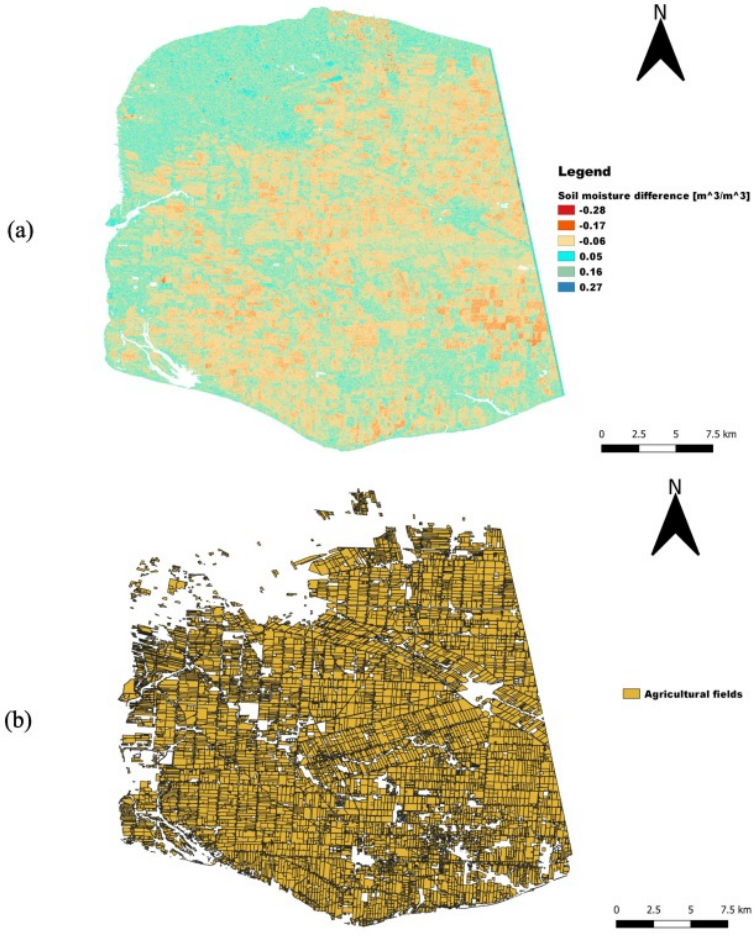


Figure 4.4: The soil moisture difference before and after a significant rainfall event (a) and shapefile of agricultural fields (b). The agricultural field shapefile is used to clip the soil moisture difference shapefile, as the aim is to find drainage units in agricultural plots. These plots are for the first study area (Ontario, Canada).

The soil moisture difference is masked with the agricultural area shapefile, and pixels with negative soil moisture difference, which stand for areas with drainage units, are filtered (Fig. 4.5). This resulted in a shapefile that later intersected with the actual tile drainage map, which allows us to estimate the accuracy of the remote sensing approach (Fig. 4.5).



Figure 4.5: The actual location of tile drains (ground truth data) (a) and the result from the remote sensed-based approach intersected with the ground truth area (b). The accuracy is estimated based on this intersected shapefile.

For the second study area (Kleine Nete), it is observed that drainage is present across different parts of the catchment, with strong drainage at the center and the south of the catchment (Fig. 4.6). The validation of this method led to an accuracy of only 17.3%. But in general, this method was able to characterize artificial drains across the catchment as the estimated drainage locations are spread nearby and in proximity to the ditch lines. Furthermore, the

threshold used to classify the resulting difference image into drained and undrained areas might influence the accuracy (Gökkaya et al., 2017). The choice of this threshold is based on the principle that drained areas will dry faster after the rain event; hence their reflectance will be high, and when a dry image is deducted, the difference will be smaller. On the other hand, after a rainfall event, the reflectance of undrained areas will be smaller, and the difference between wet and dry images will be higher.

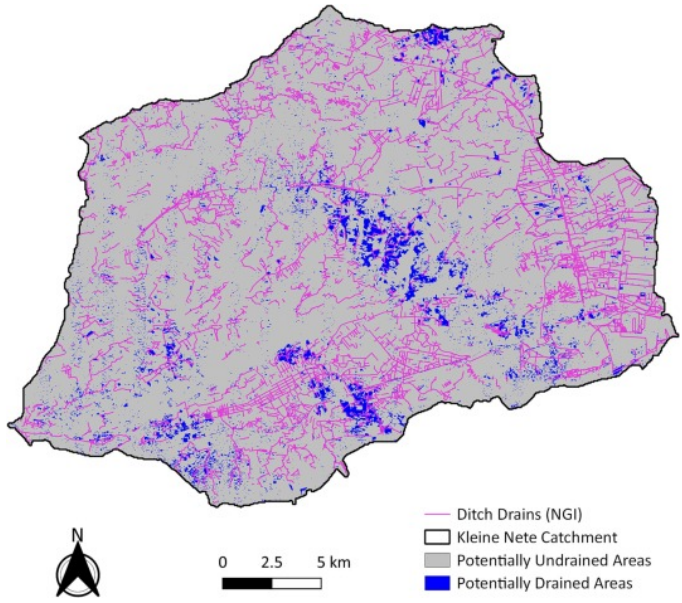


Figure 4.6: The result of the RS-based approach for the Kleine Nete watershed where the blue patches denote potential drained areas while the pink lines are the ditch network (ground truth data). (For interpretation of the references to color in this figure legend, the reader is referred to the web version of this article

However, some features in the catchment might have similar spectral reflectance to those classified as drained areas, while they are not as shown by the validation map leading to overestimating the drained locations (Naz et al., 2009). Often, the spectral reflectance of soil and crop residues are alike in the near-infrared (NIR) part of the electromagnetic spectrum. Hence, differentiating soil moisture conditions from crop residues using this method is difficult and might lead to the underestimation of drained areas (Naz et al., 2009; Streck et al., 2002). It is to be noted that the drainage system applied in this watershed is a ditch network, contrary to the Ontario case study where tile drains are used. This is one limitation of the RS–based approach, where it can not identify the drainage type.

Accuracy of the decision tree classification (DTC) approach

The DTC approach follows a hierarchical tactic where pixels corresponding to agricultural plots with soil having lower water drainage capacity and a gentle slope are identified as potentially drained areas. Therefore, the agricultural land is intersected with lower drainage classes, and then finally, this intersected shapefile is clipped with a slope of less than 4%. These result in potential drainage unit locations, with nearly 96.8% and 58% of the ditch network lying in the modeled results for the first (Fig. 4.7) and second (Fig. 4.8) study areas, respectively.

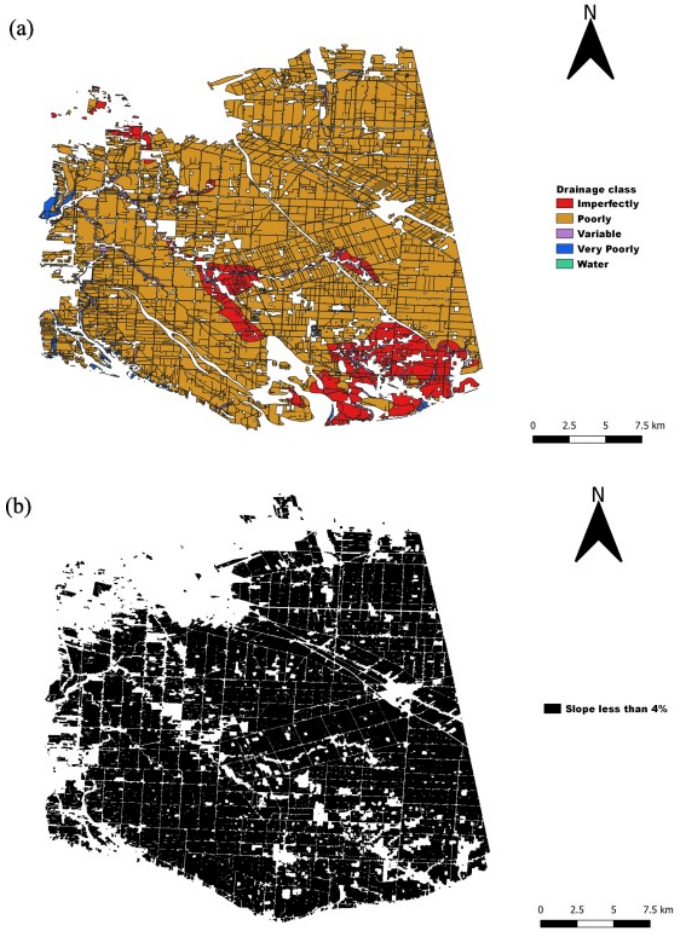


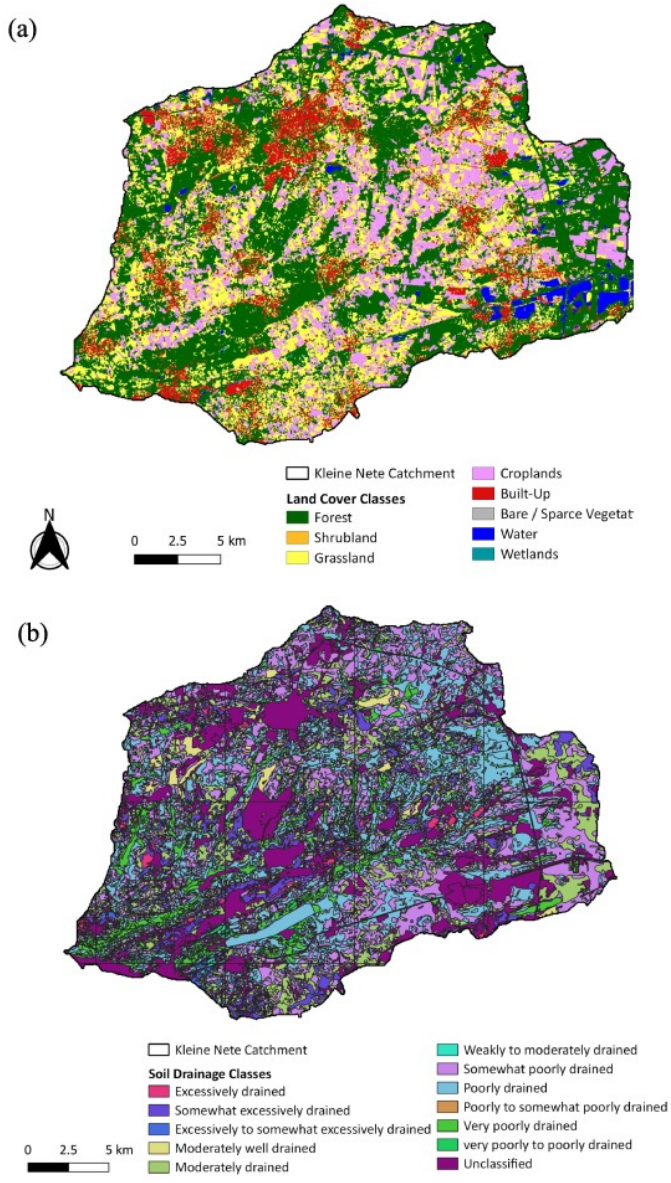


Figure 4.7: Potential tile drain locations for the first case study area after filtering pixels corresponding to agricultural land with (a) soils of low drainage capacity and (b) gentle slopes ($\leq$4%).

For the second drainage area, the area is dominated by a gentle slope (mainly less than 4%), hence, the results presented in Fig. 4.8 are for a slope with less than or equal to 4%. The quantitative validation of the DTC approach led to accuracies of 52%, 54%, 57%, and 58% due to changing the slope thresholds to equal or lower than 0.5%, 1%, 2%, and 4%, respectively. The inclusion of higher slope classes improved the accuracy of the mapping, making the DTC capable of characterizing more drained areas compared to the RS method. For instance, a slope threshold of 4% led to more characterization of drained areas compared to that of 1%.

However, the criteria used in the DTC might not reflect the current practices of the farmers (Gökkaya et al., 2017). Also, according to the fieldwork conducted by Gökkaya et al., (2017), it was observed that farmers could drain the soils irrespective of their drainage type to improve the crops growing conditions.

However, in both approaches (RS and DTC), the primary cause of drainage unit identification is not given attention, i.e., groundwater levels are not used as an additional filtering criterion for situations where groundwater level reaches up to 1.2 m from the ground surface. Hence, we propose and later apply a novel framework for using groundwater level as a criterion to identify drainage units.


(a)
Kleine Nete Catchment
Land Cover Classes
Forest
Shrubland
Grassland
Croplands
Built-Up
Bare / Sparce Vegetat
Water
Wetlands
N
0 2.5 5 km
(b)
Kleine Nete Catchment
Soil Drainage Classes
Excessively drained
Somewhat excessively drained
Excessively to somewhat excessively drained
Moderately well drained
Moderately drained
Weakly to moderately drained
Somewhat poorly drained
Poorly drained
Poorly to somewhat poorly drained
Very poorly drained
very poorly to poorly drained
Unclassified
0 2.5 5 km

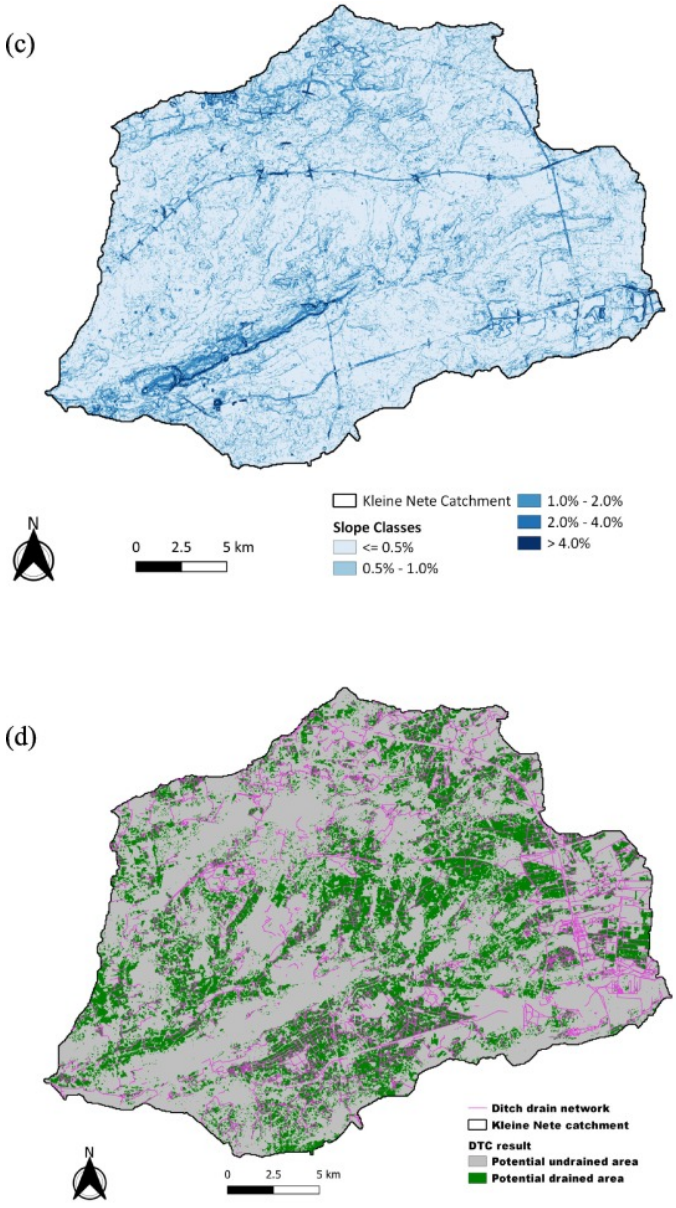


Figure 4.8: The land use (a), soil drainage class (b), slope class (c), and the result of the DTC filtering (d) for the Kleine Nete watershed. The green patches at the least bottom plot (d) stand for potential drained areas according to the DTC methodology.

Result of groundwater level-based filtering combined with the remote-sensing approach

The annual average groundwater depth from the global dataset indicated the prevalence of shallow groundwater in both case studies. Tile drains are mostly dug up to a level where oxygen deficiency will not suffocate the root zone. This depth is mainly in the range of 0.6 to 1.2 m, and we considered pixels with groundwater depth of less than 1.2 m to be potential tile drain locations. However, outlining these potential locations is not accurate unless this approach is combined with the remote sensing methodology, since the mere existence of shallow groundwater does not necessarily imply that farmers have put tile drains. Nevertheless, the drained-away water observed from the remote sensing approach combined with shallow groundwater depth increases the likelihood of having tile drains underneath. This is the basis for our hypothesis, where the accuracy of tile identification can be increased if we combine the RS and water table depth approach. Due to the combination of these two approaches, it is possible to identify an additional area of 19.4 km^2 that was not identified by the sole RS approach; hence, it can create a substantial difference for a much bigger area (Fig. 4.9).

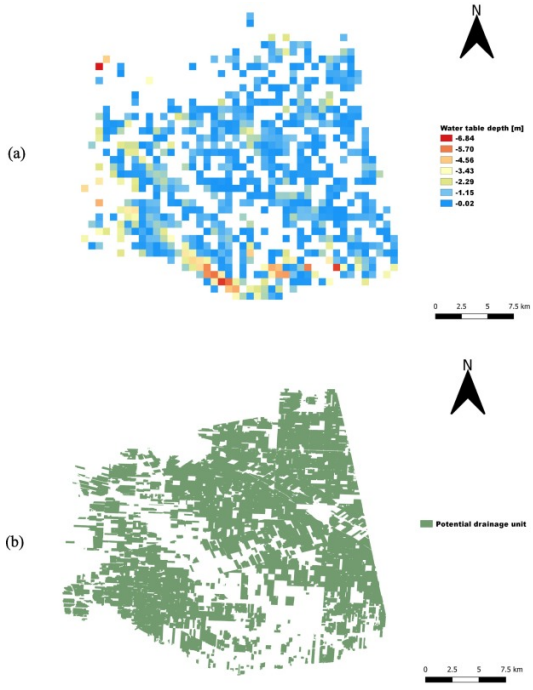


Figure 4.9: The groundwater table depth (a) and potential drainage unit locations (b) after the RS result is combined with a groundwater-based filtering technique where locations with a water table depth of less than 1.2 m are considered possible tile drain locations. These plots are for the first case study area (Ontario, Canada).

The Kleine Nete case study has a very distinct water table depth variation where places that are shallow and require drainage units have branching patterns. This is partly in line with the ditch network provided by the Belgian National Geographical Institute (Fig. 4.10).

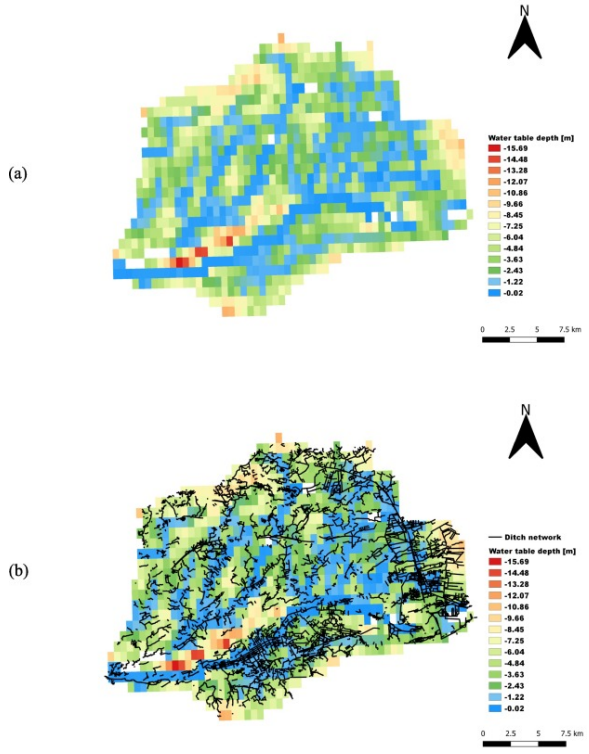


Figure 4.10: The annual average groundwater depth (a), the actual ditch network (black lines), along with the water table depth (b) for the second case study area (Kleine Nete watershed). The locations with shallow groundwater are located in the vicinity of the ditch network, hence, including groundwater-based filtering to identify ditches in agricultural fields is crucial

4.1.6 Discussion

Agricultural water drainage has a massive environmental impact by affecting the water quality of surface water bodies (Alexander et al., 2008; Goolsby and Battaglin, 2001) and ultimately affecting the aquatic ecosystem (Blann et al., 2009; Cooper, 1993). Therefore, finding the location of the drainage unit is vital to mitigate the impact that drained water can have on those systems. However, assessing the impact is difficult due to the lack of data on the locations of these units (Valayamkunnath et al., 2020). Combining remote sensing and groundwater level-based filtering can outline tile/ditch networks in data-scarce

regions. Henceforth, these maps can be utilized to perform impact studies on surface water, groundwater bodies, and the environment (Carluer and De Marsily, 2004; Du et al., 2005; Koch et al., 2013; Mitsch et al., 2001; Muenich et al., 2016; Tomer et al., 2008).

The remote sensing-based approach (RS) has indicated low accuracy in the second case study area, possibly due to some features in the catchment might have similar spectral reflectance to those classified as drained areas (Naz et al., 2009). The spectral reflectance of soil and crop residues are often alike in the near-infrared (NIR) part of the electromagnetic spectrum. Hence, differentiating soil moisture conditions from crop residues using this method is difficult and might lead to the underestimation of drained areas (Naz et al., 2009, Streck et al., 2002). The RS approach application by Gökkaya et al., (2017) and Naz et al., (2009) indicated a lower accuracy compared to our result, hence, accuracy variations are also seen across different study areas. Therefore, a global study to investigate these differences further is required. Furthermore, the first case study area is dominated by agriculture, while the second case study area is a combination of crops, forests, urban areas, bare soil, etc. Hence, the contrasting land use in these two case study areas can also play a role in increasing/decreasing the accuracy of the RS methodology. When only one type of land use is dominant (e.g., agricultural area in the first case study), the soil moisture estimation from RS will be easy and follows a clear pattern as complex water routes (e.g., canals, urban drainage systems, pavements, etc.) are absent. Finally, cloud coverage on the RS imagery can also decrease the accuracy of locating ditch networks, thus, methods other than interpolation to fill missing values should be devised.

The decision tree classification (DTC) approach outlined drainage units better than the RS-based methodology. However, the criteria used in the DTC might not reflect the farmers' current practices (Gökkaya et al., 2017; Sugg, 2007). Also, according to the fieldwork conducted by Gökkaya et al., (2017), it was observed that farmers could drain the soils irrespective of their drainage type to improve the crops growing conditions. Contrarily, the RS approach can indicate the existence of drains due to the physical reasoning via the inclusion of the soil moisture condition (indirect indication of water drainage) in the RS identification technique (Varner et al., 2003; Verma et al., 1996). Therefore, coupling the RS-based approach with groundwater level–based filtering can improve and consolidate the drainage unit identification procedure. Hence, we applied additional filtering using groundwater level, which managed to capture an additional 19.4 km^2 area that was not identified by the RS approach. Due to the availability of global groundwater level datasets (Fan et al., 2013), applying our proposed methodology is feasible, mainly for regions that lack drainage unit location maps. Note that local groundwater level measurements are preferable over global datasets to ensure accurate drainage unit filtering.

4.1.7 Conclusion

Agricultural fields are mostly drained due to the excess water reaching the root zones of crops. However, knowing where these drainage units are installed to conserve drained water is critical with climate change and water scarcity. Nevertheless, identifying the lo-

cation of these drainage units is yet challenging. This study presents agricultural drainage unit identification using remotely sensed data (RS), a decision tree classification (DTC) approach, and a novel methodology that uses a filtering technique based on a groundwater table depth. Two case studies were selected for the analysis: Ontario, Canada (case study 1) and the Kleine Nete watershed, Belgium (case study 2). For researchers in the field of hydrology and water quality, knowing the location of a network of tile/ditch drainage can be crucial to know and mitigate the environmental impact of drained water.

The result of the RS approach indicated a very good agreement between the ground truth data and the modeled drainage unit locations with an accuracy of 87.8% (case study 1). However, the second case study resulted in a different pattern, but as per our site visit, the area is not well known to have subsurface drains; instead, it is dominated by a ditch network. Hence, a field visit to the local study area helps to understand and explain the scientific results of this type. The DTC methodology resulted in 96.75% and 58% accuracy for the first and second case studies, respectively. This is a considerable improvement compared to the RS approach.

Finally, since the RS approach indicates the actual soil moisture status (draining water), we applied an additional filtering technique to the RS resulting maps. This approach relies on the idea that the major factor for drainage unit application is the emergence of a water table into the root zone. To the best of our knowledge, this critical factor is not considered in any of the methodologies. Thus, filtering areas with water table depth (less than 1.2 m) data can indicate which areas require/already have drainage units and can improve the accuracy of the RS technique. The formulated hypothesis is correct as the accuracy of the RS technique for the first case study has increased, corresponding to an increase of around 19.4 km^2 of a drained area previously not identified by the sole RS approach. As for the second case study, the qualitative assessment indicated the close follow-up of the shallow groundwater table and the ditch network (ground truth data). Hence, we strongly recommend the use of groundwater table information while applying drainage unit identification methodologies.

The contrasting land use type between the two study areas, where one is dominated by agriculture and the other contains a variety of land use types, indicated the complexity of the soil moisture variation in the latter case. Therefore, the degree of accuracy is also related to the complexity level of study areas. Finally, the inability of any of the methodologies to differentiate between tile and ditch drains is one research question that needs to be tackled in the future by looking into soil moisture attribute that is inherent to variation due to the two different drainage systems.

4.2 The impact of extensive agricultural water drainage on the hydrology of the Kleine Nete watershed, Belgium

4.2.1 Summary

Agricultural water drainage can significantly lower groundwater levels and affect catchment hydrology. Therefore, building models with and without these features can indicate an adverse impact on the geohydrological process. Therefore, the standalone Soil Water Assessment Tool (SWAT+) model was initially developed to simulate streamflow at the Kleine Nete catchment outlet. Next, a physically based and spatially distributed groundwater module (gwflow) was integrated into the SWAT+ model and calibrated for stream discharge at the catchment outlet. Finally, the same model was calibrated for both streamflow and groundwater heads. These final model parameters are used to investigate the basin-wide hydrologic fluxes with and without including agricultural drainage systems in the model scheme.

The result suggested that the standalone SWAT+ model poorly represented the stream discharge and attained low NSE values of 0.18 and 0.37 during the calibration and validation periods, respectively. Integrating the gwflow module to SWAT+ improved the model representation of stream discharge (NSE = 0.91 and 0.65 for calibration and validation periods, respectively) and groundwater heads. However, calibrating the model for only streamflow resulted in a high root mean square error (above 1 m) for groundwater head, and the seasonality is not captured. On the other hand, calibrating the coupled model for streamflow and hydraulic head reduced the root mean square error (below 0.5 m) and captured the seasonality of groundwater level fluctuations. Finally, drainage application resulted in a 50% (from 33.04 mm to 16.59 mm) reduction in groundwater saturation excess flow and an 18.4 mm increment in drainage water to streams. To conclude, the new SWAT+gwflow model is more appropriate than the standalone SWAT+ model for the case study. Furthermore, calibrating the SWAT+gwflow model for streamflow and groundwater head has improved the model simulation, with implications for general coupled models where representing surface and groundwater in the calibration strategy is beneficial.

This section is published as: **Yimer, E. A.**, Riakhi, F.-E., Bailey, R. T., Nossent, J., & van Griensven, A. (2023). The impact of extensive agricultural water drainage on the hydrology of the Kleine Nete watershed, Belgium. Science of The Total Environment, 885, 163903. https://doi.org/10.1016/j.scitotenv.2023.163903

4.2.2 Introduction

Agricultural drainage is a common practice to improve crop productivity, and it improves soil moisture and maintains the root zone adequately aerated. In relatively flat lands with low or medium soil infiltration capacity or locations characterized by intensive rainfall, the water supply in the root zone can go beyond the soil's infiltration capacity. The soil surface endures repeated instances of waterlogging, thus, drainage systems are often applied (Oosterbaan, 1994). Hence, extensive applications of water drainage system in agricultural plots are seen in Europe where $1/3^{rd}$ of northwestern Europe is drained (Gramlich et al., 2018). Specifically, until 1984, nearly 60,000 ha were drained in Belgium, where the provinces of West– and East–Flanders took the bigger portion due to low–lying areas and widespread arable land (Dierickx and Feyen, 1987). Therefore, ditches and subsurface drainage systems were applied to collect surface runoff and excess groundwater to avoid root zone saturation, thus preventing soil waterlogging.

However, these drainage systems could negatively affect the catchment hydrology, as Hasselquist et al. (2018) reported, as they caused a reduction in groundwater levels and increased the unsaturated zone depth. The impact is mainly two ways, one is the impact on water storage (volume of freshwater decreases). Second, the excess water removed by the ditches affects the water quality of streams, ultimately affecting the environment. The drained water can contain fertilizers, pesticides, and excess nutrients such as phosphorus and nitrogen. This can lead to eutrophication, contaminate river water, create adverse ecological effects, etc.

Furthermore, the lack of steep slopes in lowland areas led to the dominance of groundwater outflow to streams via riverbeds or through ditch drains when there is an increase in groundwater levels (Van der Velde et al., 2009). This makes low-laying catchments rich in surface water networks of rivers and ditch drains, where surface and groundwater interactions are strongly present. Attempts to investigate these interactions included coupling the Soil Water Assessment Tool (Arnold et al., 1998) with the Modular groundwater Flow model (MODFLOW) (Kim et al., 2008). An example of such coupled model application at different spatial scales in Denmark indicated the usefulness of accounting groundwater systems to capture the impact of drainage from agricultural land (Frederiksen and Molina-Navarro, 2021). However, the model coupling requires extensive code modification to SWAT and significantly extended simulation time (Bailey et al., 2020a).

Besides, there are several attempts to investigate the impact of agricultural drainage on general geohydrology using SWAT (Bauwe et al., 2016; Green et al., 2006; Guo et al., 2018; Ikenberry et al., 2017; Koch et al., 2013; Mehan et al., 2019; Moriasi et al., 2013; Schilling et al., 2019; Singh et al., 2005). Few studies have been implemented to investigate the impact of drainage in fields smaller than 10 km^2 (Gramlich et al., 2018; Muma et al., 2016; Tuohy et al., 2016). However, drainage simulations in SWAT are based on lumped and 1–dimensional procedures aimed at identifying the depth of the drains from each Hydrologic Response Unit (HRU). Also, the model applies simplistic steady–state groundwater

equations to account for the groundwater component, and it does not generate groundwater heads which are critical in evaluating model performance and in compelling the hydrologic interactions in a drained catchment (Bailey et al., 2022; Hansen et al., 2013; Rozemeijer et al., 2010).

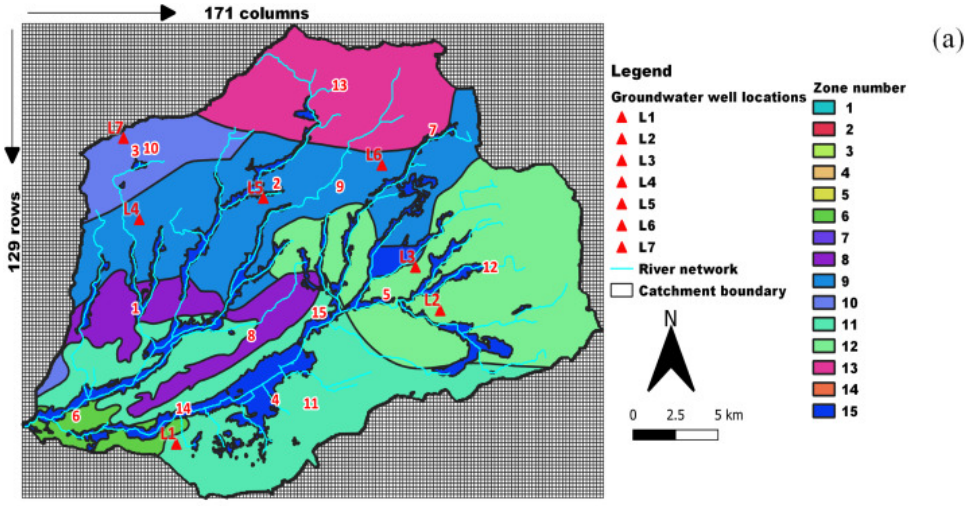
Therefore, Bailey et al. (2020a) developed a new groundwater flow module (gwflow) that is physically based and spatially fully distributed and is integrated with SWAT+ (the revised and restructured version of SWAT). This coupled model simulates several groundwater and surface water fluxes at a catchment scale. In addition, the gwflow module can explicitly include agricultural drains in the modeling scheme, enabling the estimation of the total amount of drained water.

To utilize the gwflow capabilities and since the amount of drained water from agricultural fields is unknown in most basins, the Kleine Nete watershed is chosen which is a ditch–dominated watershed (as indicated in the drainage unit identification paper). Hence, the main objective of this study is to assess drainage's influence on catchment hydrology using a physically based and spatially distributed modeling approach. The sub–objectives include finding a calibration strategy that suits this coupled model. Also, the standalone SWAT+ model is evaluated for a groundwater-influenced watershed, and henceforth, a comparison is made between the standalone SWAT+ and SWAT+gwflow model setups. In addition, the developed models are assessed against stream discharge and groundwater heads, and the changes in hydrologic fluxes due to drainage are evaluated. The research is intended to highlight the need to investigate drained water from agricultural fields for sustainable use and management of groundwater, which can ultimately affect the environment.

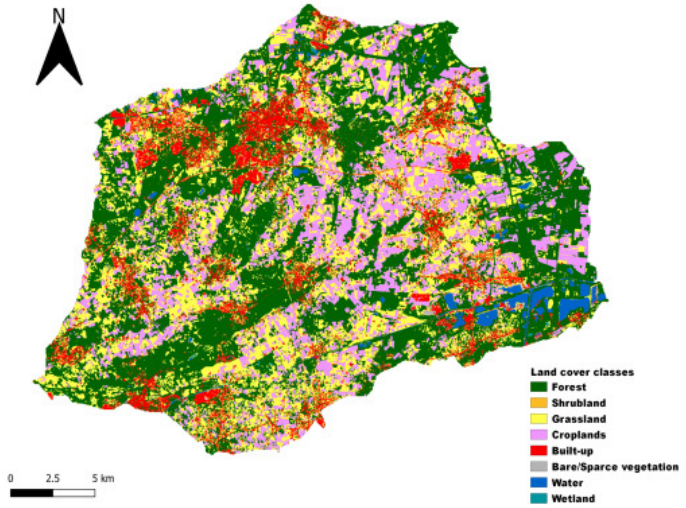
Therefore, based on the identified drainage locations from the previous section, the impact of those drainage units on catchment geohydrology is further explored in this section. This and the following section are ways of testing or validating the newly coupled SWAT+gwflow model in different geohydrological, climatic and human influence setting.

4.2.3 Study area and data

The study area for this analysis is the Kleine Nete watershed, located in northeast of Belgium (Fig. 4.11).The catchment mainly comprises agricultural land, grasslands, croplands, forests, and built-up areas. The elevation variation in the catchment is very low. The aquifer thickness varies from 9 to around 27 meters.


171 columns
129 rows
Legend
Groundwater well locations
L1
L2
L3
L4
L5
L6
L7
River network
Catchment boundary
Zone number
1
2
3
4
5
6
7
8
9
10
11
12
13
14
15
N
0 2.5 5 km

(a)


N
Land cover classes
Forest
Shrubland
Grassland
Croplands
Built-up
Bare/Sparce vegetation
Water
Wetland
0 2.5 5 km

(b)

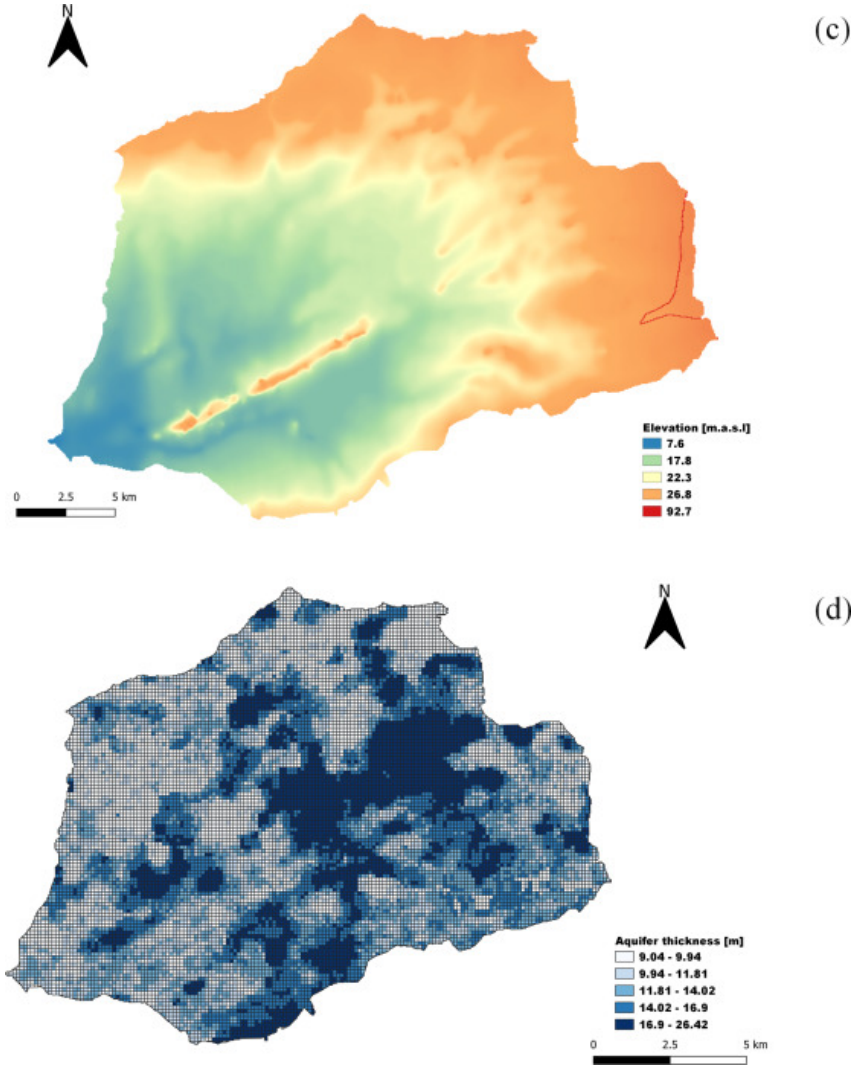


Figure 4.11: The Kleine Nete watershed, groundwater observation wells (L1 to L7), homogeneous hydraulic conductivity zones, and mesh with the size of 200 m by 200 m resulting in 129 rows and 171 columns (a). The change in volume for each grid cell is taken as a governing equation in the gwflow groundwater module. The next plot (b) shows the major land use types inside the watershed, followed by the elevation variation (c), and finally, the aquifer thickness (d) according to the global dataset is shown.

4.2.4 Methodology

The methodology we followed starts with developing the SWAT+ model for our study area, followed by implementing the gwflow module. Henceforth, we compare alternative calibration schemes using only streamflow as a calibration target, followed by both streamflow and groundwater head. Finally, we compare the simulated watershed fluxes with and without the ditch network using the later model configuration.

Table 4.1: Warm-up, calibration, and validation periods.

Warm-up	Calibration	Validation
01/01/2005 to 31/12/2009	01/01/2010 to 31/12/2014	01/01/2015 to 31/12/2021

To account for drainage, the explicit equation of the groundwater head is modified to Eq. 4.1, where Q_{drain} is the drained flow rate in m^3/day, representing the amount of groundwater removed by drains from each grid cell at a daily time step when the simulated groundwater head h is greater than the drain elevation z_{drain} [m]. Darcy's Law is used to compute Q_{drain} at every grid cell that represents a drain, as shown in Eq. 4.2 (Bailey et al., 2022). Here, K_{drain} is the hydraulic conductivity (m/day) of the drain, P_{drain} is the distance in meters along which groundwater head is lost (estimated by dividing the aquifer drain inflow area by the filter sediment thickness), and z_{drain} is obtained by subtracting the drain depth [m] from the land surface elevation [m] in every grid cell having a drain (Fig. 4.12). Furthermore, when Q_{drain} is extracted from the groundwater storage of a specific cell, it is then supplied to the nearby SWAT+ channels of that cell. The drain water estimation is made at grid cells that intersect with the ditch network shapefile provided by the Belgian National Geographical Institute (NGI) (last accessed June 2022).

$$h^{n+1} = h^n + \left[\left(Q_{\text{rech}} + Q_{\text{sw}\to\text{gw}}\right) - \left(Q_{\text{gwet}} + Q_{\text{gw}\to\text{sw}} + Q_{\text{satex}} + Q_{\text{pump}} + Q_{\text{drain}}\right) \pm Q_{\text{north}} \pm Q_{\text{south}} \pm Q_{\text{west}} \pm Q_{\text{east}}\right] \frac{\Delta t}{S_y \Delta x \Delta y} \tag{4.1}$$

$$Q_{\text{drain}} = K_{\text{drain}} \cdot P_{\text{drain}} \cdot \left(h - z_{\text{drain}}\right) \tag{4.2}$$

In addition to evaluating the model on its use for evaluating agricultural water drainage, the SWAT+gwflow model has not been evaluated on a regional scale, thus, investigating the coupled model's ability to represent the GW–SW in teraction at such a large–scale, in combination with the use of a global aquifer property dataset for model development is vital.

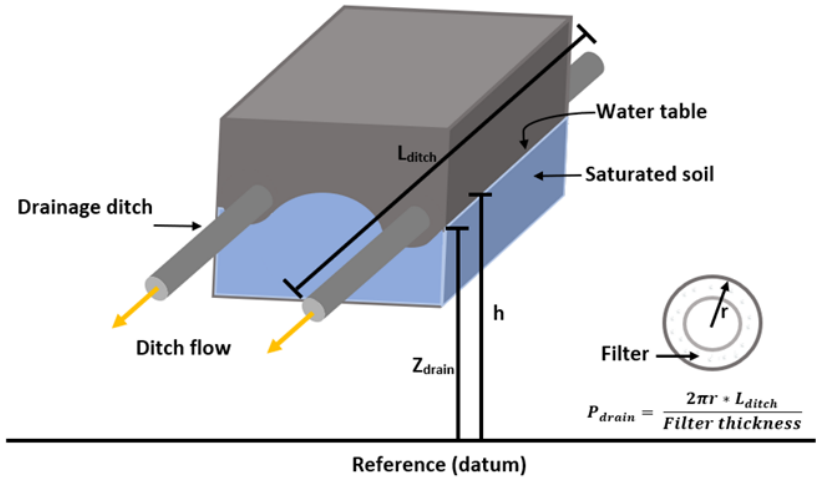


Figure 4.12: Schematic overview of the ditch system modeled in the SWAT+gwflow model setup.

Calibration, validation, and evaluation of the SWAT+ and SWAT+gwflow model output

Sensitivity analysis can identify the set of parameters that mostly influence the model outputs, which can further be used for model calibration (Nossent et al., 2011). In this study, the global, variance-based Sobol' sensitivity analysis (SA) is used for the standalone SWAT+ model, where the variance contributed from a parameter or the interaction of more than two parameters to the unconditional variance in the model outcomes is quantified, and represented as Sobol' sensitivity indices (SIs) (Nossent et al., 2011; Sobol', 1990).

The first–order Sobol sensitivity index is calculated as:

$$S_i = \frac{V_{X_i}\left(\mathbb{E}_{X_{\sim i}}(Y|X_i)\right)}{V(Y)} \tag{4.3}$$

The total variance of the model output Y is expressed as:

$$V(Y) = V_{X_i}\left(\mathbb{E}_{X_{\sim i}}(Y|X_i)\right) + \mathbb{E}_{X_i}\left(V_{X_{\sim i}}(Y|X_i)\right) \tag{4.4}$$

where V_{X_i} and $\mathbb{E}_{X_i}$ represent the variance and expectation over the factor X_i, respectively, while $V_{X_{\sim i}}$ and $\mathbb{E}_{X_{\sim i}}$ denote the variance and expectation over all factors except X_i. The term $V_{X_i}(\mathbb{E}_{X_{\sim i}}(Y|X_i))$ measures the first-order effect of X_i, and $\mathbb{E}_{X_i}(V_{X_{\sim i}}(Y|X_i))$ represents the residual.

The total sample size tested for this study is 1012 samples, using 22 parameters, during the simulation period from 01/01/2005 to 31/12/2021 with a warm-up period of 5 years. The

sensitivity analysis (SA) is performed using SWAT+Toolbox version 0.7.6 (https://swat.tamu.edu/software/plus/, last accessed in June 2022) on the selected parameters that are expected to influence catchment discharge and groundwater flow. A comparison with the study of Nossent (2012) is also conducted.

According to Gupta et al. (2003), the observation data used during the calibration period should contain sufficient information about the catchment behavior to ensure proper parameter optimization representing hydrological processes. To fulfill this, the average yearly precipitation is calculated from available weather stations, which is then used to classify each simulation year into wet or dry years, following the approach by (Bayat et al., 2013). Based on this analysis, the calibration period is selected to include wet and normal years, with 2013 and 2014 showing relatively normal to dry conditions. The validation period covers a mix of wet, normal, and dry years. For the total simulation period of 17 years, the warm-up, calibration, and validation periods are summarized in Tab. 4.1. The SWAT+Toolbox is chosen for calibration due to its global optimization capabilities, which help avoid local optimum solutions.

For calibrating the SWAT+*gwflow* models, the automated software PEST (Parameter ESTimation) was used. PEST is an independent software that computes the parameter values based on the model's input and output files **?**. The parameters used for PEST optimization are predicted to affect stream discharge, recharge, groundwater, and drainage flow. We first calibrated the model for streamflow at the catchment outlet. Next, we calibrated the model for both streamflow (at the catchment outlet) and groundwater head values.

For model evaluation, statistical indices, such as the Nash–Sutcliffe Efficiency (NSE) and the percent bias (PBIAS) expressed by Eq. 4.5 and 4.6, are used to compare modeled and observed discharge. Where Q_{oi} and Q_{si} are the observed and simulated discharge, respectively, and $\bar{Q}$ is the average observed streamflow value.

$$\mathrm{NSE} = 1 - \frac{\sum_{i=1}^{n}(Q_{oi} - Q_{si})^2}{\sum_{i=1}^{n}(Q_{oi} - \bar{Q})^2} \tag{4.5}$$

$$\mathrm{PBIAS} = \frac{\sum_{i=1}^{n} Q_{oi} - Q_{si}}{\sum_{i=1}^{n} Q_{oi}} \times 100 \tag{4.6}$$

Regarding the evaluation of the groundwater head, visual assessment is used to contrast observed and simulated data at the seven monitoring wells. Statistical indicators such as the root mean square error (RMSE) and the mean absolute error (MAE), shown by Eq. 4.7 and 4.8, are also used for model performance evaluation. Where H_{oi} and H_{si} are the observed and simulated groundwater head [m], and n is the sample size. The unit of RMSE and MAE is meters, and these statistics quantify the average magnitude of the residuals. While RMSE assigns a higher weight to larger errors (an error is a difference between the model prediction and actual observed data value), the MAE gives the same weight to all the errors.

$$\text{RMSE} = \sqrt{\frac{1}{n}\sum_{i=1}^{n}(H_{oi} - H_{si})^2} \tag{4.7}$$

$$\text{MAE} = \frac{1}{n}\sum_{i=1}^{n}|H_{oi} - H_{si}| \tag{4.8}$$

To have an idea about the internal processes, the absolute error of the water balance is calculated from a soil profile point of view based on Eq. 4.9. Where the inputs are precipitation (Pr), and the outputs include surface runoff (surq), lateral flow (latq), percolation (perco), and evapotranspiration (Et). All the water components are in units of mm.

$$\Delta SW = Pr - surq - latq - perco - Et \tag{4.9}$$

4.2.5 Results

Standalone SWAT+ model output result

The result of the SA shows that the model parameters that have the highest influence on the model output include the plant uptake factor EPCO, the curve number for moisture condition II called CN2, and the soil evaporation compensation factor ESCO. These parameters were also sensitive in the SWAT model developed by Nossent (2012) for the Kleine Nete catchment. However, CN2 was the highest sensitive parameter in their study, which is not the case in this study. This could be due to the new interactions in SWAT+ (because of the gwflow module) or the different simulation periods and the input data used for this study. CN2 is a crucial parameter for flow simulations which is computed for every HRU, and quantifies the contribution of every flux affecting the stream discharge. Besides, its values are affected by soil permeability and land use types. ESCO is the second sensitive parameter as it accounts for evaporation in the cracks of soil layers and upward water flow through the capillary rise. Furthermore, the parameters EPCO and REVAPMN have approximately the same least sensitivity. EPCO controls the compensated amount of water to be transpired by the plants when inadequate water is available in the upper soil layer. Besides, REVAPMN allows water percolation from shallow to deep aquifers (Nossent, 2012). These parameters influence the groundwater component. The highly sensitive parameter FLOMN controls the aquifer storage and sets a minimum threshold to permit return flow. This process is significant for surface and subsurface flows.

It is observed that the standalone model overestimates the high flows during the calibration and validation periods, as is confirmed by the negative PBIAS (calibration: -15.4% and validation: -5.15%). Furthermore, the model fails to represent the catchment hydrological processes during wet years, as during the years 2016 and 2021, the second high peak event is not captured by the model (Fig. 4.12). Moreover, the NSE (calibration: 0.18 and validation: 0.37) values indicate unsatisfactory model performance during both the calibration and validation periods (Moriasi et al., 2015).

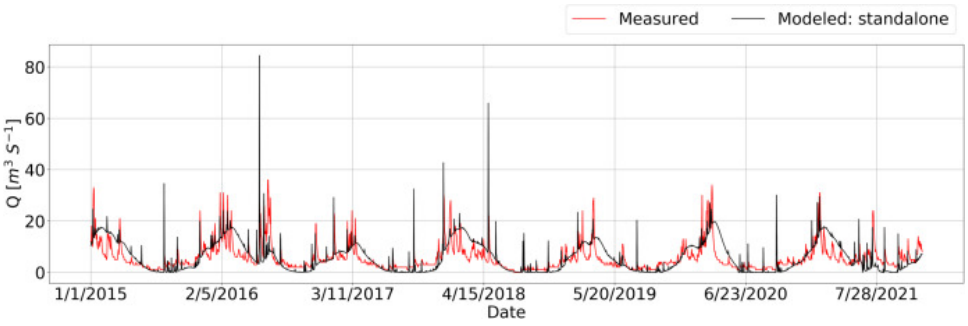


Figure 4.12: The simulated and observed daily streamflow at the catchment outlet during the validation period for the standalone model

Regarding the low flows, they are over- and underestimated by the model, and their trend is not well captured. This confirms the limitation of SWAT+ in representing the groundwater flow component for a groundwater–driven watershed, as it uses a simplified approach and assumptions to represent the groundwater fluxes (Deb et al., 2019; Gassman et al., 2007; Peterson and Hamlett, 1998; Spruill et al., 2000; Srivastava et al., 2006). Hence, coupled models are vital where integrating the gwflow module is necessary to tackle standalone SWAT+ model limitations.

Result of the SWAT+gwflow model by including ditch (calibration using only streamflow data)

In general, the high and low flows and their seasonal variability are well captured by the model compared to the standalone SWAT+ model (Fig. 4.13). During the validation period, the model underestimated the high and low flows during most simulation years, as confirmed by the positive PBIAS (calibration: -2.1% and validation: 19.7%). According to Moriasi et al. (2015), the model performance is very good during the calibration and good during the validation periods, as statistically shown by the NSE values (calibration: 0.91 and validation: 0.72). While the PBIAS value during the calibration is very good (-2.1%), it is unsatisfactory during the validation (19.7%). However, it is concluded that using SWAT+gwflow to estimate stream discharge at the outlet of a groundwater–driven catchment is competent compared to the standalone SWAT+ model.

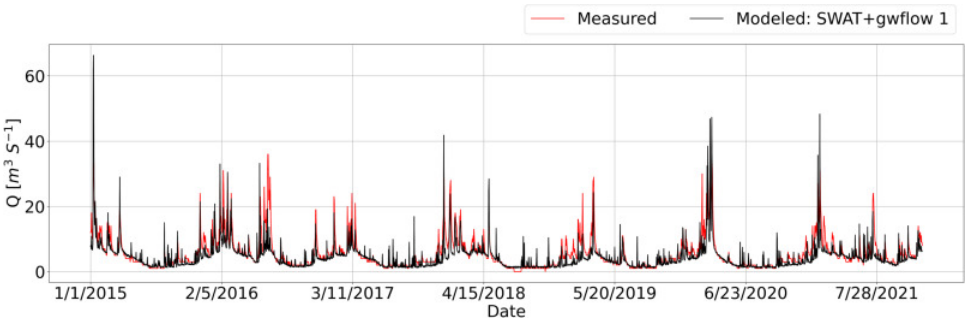


Figure 4.13: Daily simulated and observed streamflow values according to SWAT+gwflow 1 modeling approach

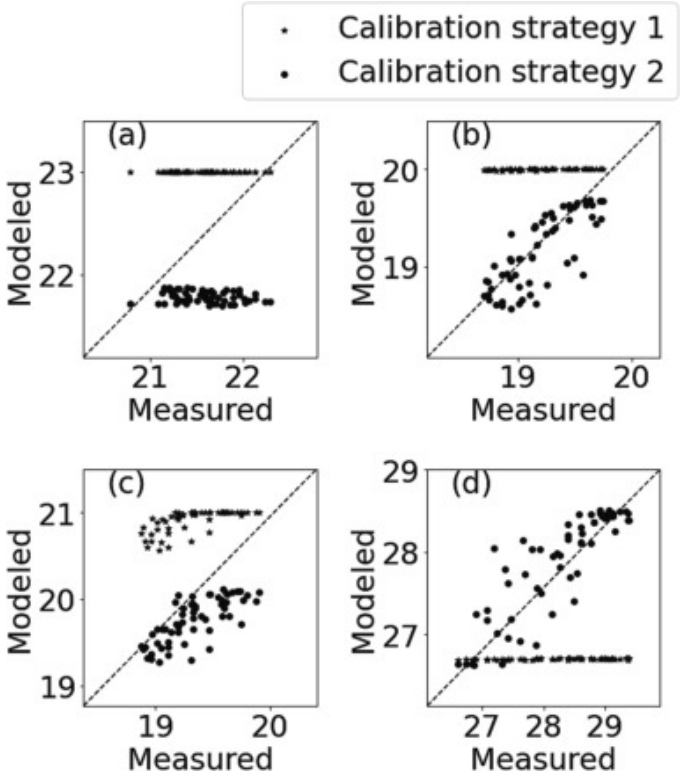


Figure 4.14: Scatter plot for the modeled and measured groundwater head for calibration strategy 1 (using only streamflow) and calibration strategy 2 (using both streamflow and groundwater head). The plot is for well locations 3 (a), 4 (b), 5 (c), and 7 (d). The closer the dots/stars are near the bisector line, the better the model simulation

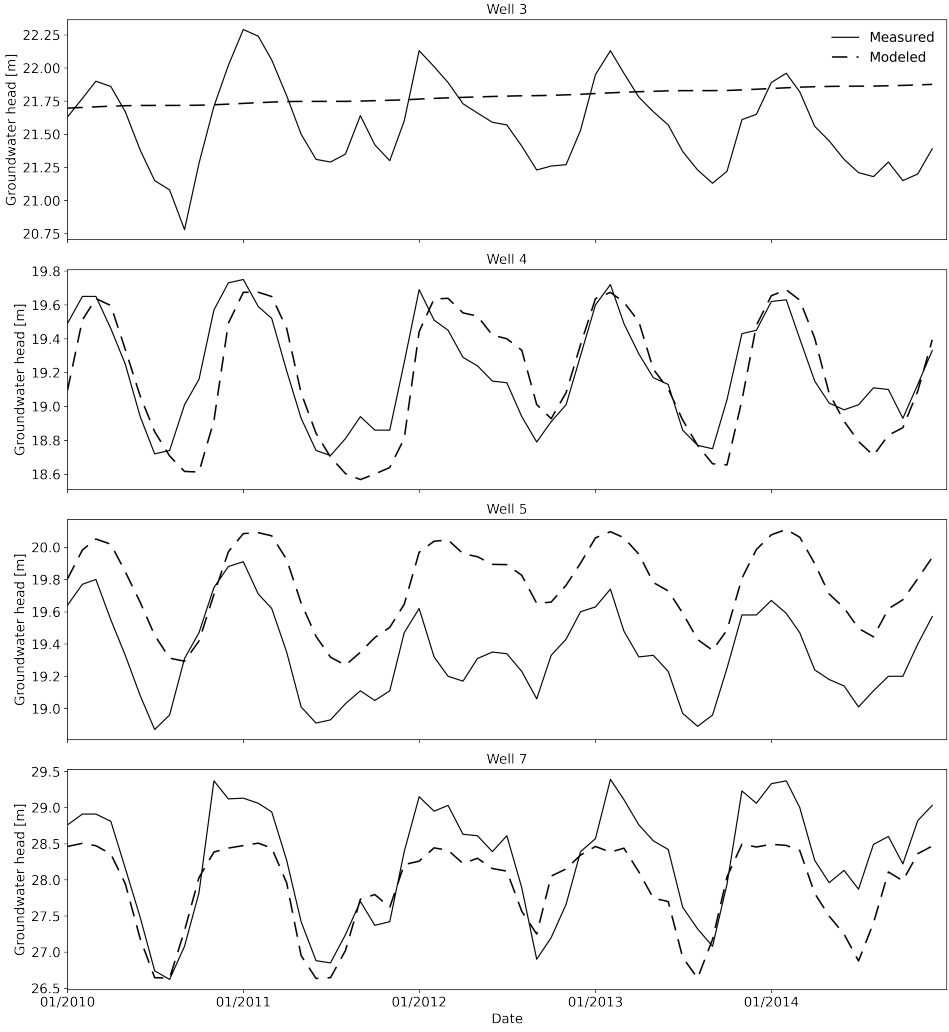


Figure 4.15: Timeseries plot for the modeled and measured groundwater head for calibration strategy 2 (using both streamflow and groundwater head). The plot is for well locations 3 , 4 , 5 , and 7 (from top to bottom).

The stream discharge calibrated model is tested for its ability to predict the catchment groundwater head at 7 locations without calibrating its groundwater levels (Tab. 4.4). Even though the modeled groundwater values are relatively close to the observed ones in some locations, the seasonal variability in the model-generated groundwater levels is not captured. While in locations 5 and 6, a slight seasonal variability is seen in the model groundwater

heads, the model values are constant during the simulation period for all the other locations (Fig. 4.14).

The timeseries plot also has indicated a strong bias in most of the wells with no seasonality in well 3 (Fig. 4.15). In well 3, the model is able to capture the average groundwater head. There is also over and underestimations in the different wells. Hence, this initiated the idea of calibrating the model using streamflow and groundwater heads, and the results are discussed in the next section.

The statistical comparison between the observed and the model–generated groundwater heads is shown in (Tab. 4.4). The RMSE and MAE values are high for all the locations during the calibration period except for locations 1 and 6, which have low RMSE and MAE values. Besides, by comparing the values of RMSE and MAE for wells other than 1 and 6, a slight difference between them indicates a small variance in the individual errors (high precision).

Result of the SWAT+gwflow model by including ditch (calibration using streamflow and groundwater head data)

This section represents the results of calibrating the model by including ditches using both mean monthly streamflow at the catchment outlet and mean monthly groundwater heads at 7 locations.

- Model parameter comparison

The model parameters for the first case (calibrated for streamflow) overestimate the hydraulic conductivity (K) values compared to the measurement data stated in Dams et al. (2009). On the other hand, the model calibration using streamflow and hydraulic head managed to get K values in a range suggested by Dams et al. (2009). For instance, the first approach overestimates K values for zones 6, 10, 11, and 13 (Fig. 4.16). This overestimation led to the inappropriately increasing ditch flow (increased by five folds compared to the second approach).

A difference in model parameters is also observed on the soil hydraulic conductivity (SOL_K), which is shown to increase lateral soil flow and saturated excess flows, decreasing the surface runoff and ditch flow for the second approach. This is plausible as the more permeable the soil is, the ease to allow more lateral soil and saturated excess flows. Contrarily, higher SOL_K initiates more water entering the soil, decreasing the surface runoff. These combined create lower water removal via the ditches. The higher value of the SOL_K parameter is plausible for two reasons, one is due to the prevalence of sandy soil, and the second is due to the water balance components (mainly subsurface processes) that are better represented due to the accurate estimation of the groundwater head values.

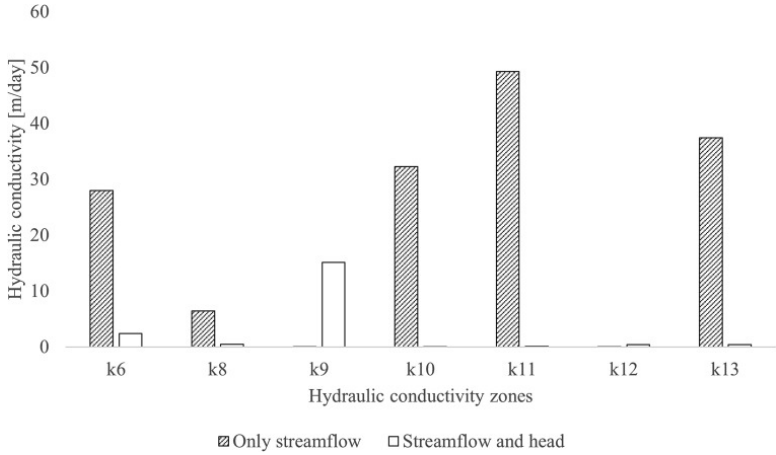


Figure 4.16: The calibrated hydraulic conductivity values based on two calibration strategies (based on streamflow – SWAT+gwflow 1 and based on streamflow and hydraulic head – SWAT+gwflow 2). For zone numbers, refer to Fig. 4.11

The CAN_MX is expected to be higher due to the existence of pine trees, which are increasing the interception loss. As for channel manning coefficient (CH_N) and hydraulic conductivity (CH_K), when CH_N increases, velocity decreases, leading to more channel flow, and this is also indicated in the CH_K where the channel bed conductivity has reduced, resulting in more channel flow. However, the CH_K parameter difference is not substantial based on the two approaches, and the CH_N value attained by the second approach is closer to the value attained by Nossent (2012) for the Kleine Nete watershed but using the old SWAT model. Note that the sensitivity of these two parameters is very low compared to the other parameters. The most sensitive parameters are those related to subsurface processes (e.g., K, Sy and drain depth).

- Streamflow simulation result

The model performed very well in representing the streamflow and attaining seasonal variability (Fig. 4.17). There is a underestimation of the peak flows during the wet years. Besides, the low flows are relatively well represented, with slight underestimation (Tab. 4.2). During the validation period, the models' performance is satisfactory, with NSE of 0.61 (Moriasi et al., 2015). Even though the model depicts the seasonal variability of the discharge well, it underestimated the peak flows during all the years except during the normal year of 2020. Moreover, there is a strong underestimation during the wet years 2016 and 2021. Also, the model slightly underestimated the low flows, particularly during the dry years 2017, 2018, and 2020. The two calibration strategies comparison on simulating the streamflow at the catchment outlet shows similar under- and overestimations during the calibration period.

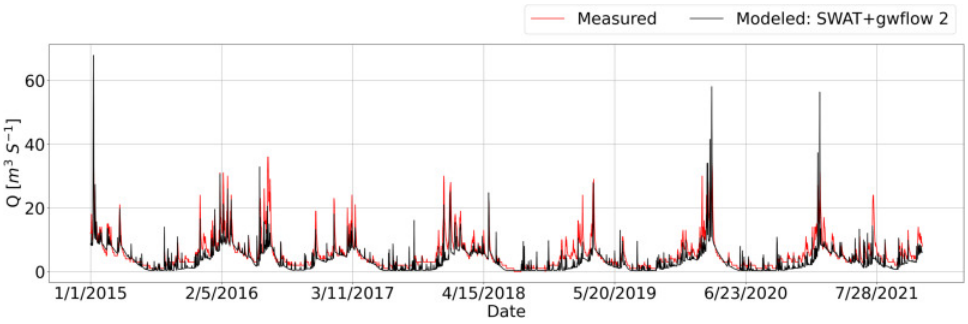


Figure 4.17: Daily simulated and observed streamflow values according to SWAT+gwflow 2 modeling approach.

Table 4.2: Model performance for calibration and validation periods

Model setup	**Calibration**		**Validation**	
	NSE [-]	PBIAS [%]	NSE [-]	PBIAS [%]
Standalone SWAT	0.18	−15.4	0.37	−5.15
SWAT+gwflow 1	0.91	−2.1	0.72	19.70
SWAT+gwflow 2	0.86	9.91	0.61	31.83

- Water balance

The water balance assessment has indicated that the calibration strategy can also significantly affect the water balance components. Mainly, groundwater boundary inflow, surface runoff, lateral soil flow, and ditch flow show a considerable difference between the two calibration approaches (Fig. 4.18).

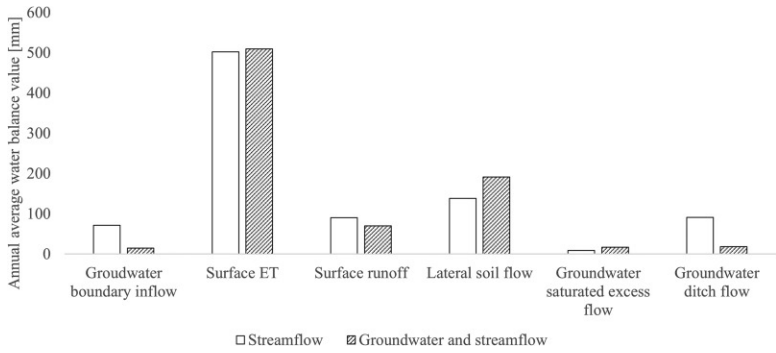


Figure 4.18: Water balance value differences due to the two calibration strategies we followed

On average, during the simulation years, the difference between the scenario with and without a ditch network is seen mainly in the groundwater ditch flow, groundwater evapotranspiration (ET), saturation excess flow, and stream seepage to groundwater (Tab. 4.3). The decrease in saturation excess flow is expected due to the removal of excess water from the groundwater by the ditches (corresponds to around a 50% reduction in drain flow: from 33.04 mm to 16.59 mm). Moreover, the groundwater ET decreases when ditches are implemented, indicating that the groundwater removal by the drainage units lowers the water table, ultimately decreasing the ET from the groundwater system. In addition, the baseflow fraction of the total precipitation decreases when ditches are removed from the system. This is explained by the routing of more groundwater to the rivers via the drainage systems. Note that water leaving the groundwater system and entering streams via the drainage system, saturated excess flow, etc., are accounted as baseflow. Since ET and stream seepage are very small, and what is excess is taken by the ditches, hence, no water enters the streams via surface runoff and/or lateral flow from the groundwater system. This indicates that groundwater processes are more critical in the modeling scheme, mainly for groundwater-dominated watersheds.

Table 4.3: Inputs and Outputs to the watershed (mm)

	Without drain	With drain
Inputs to the watershed (mm)		
Precipitation	826.01	826.01
Boundary inflow	13.91	14.35
Outputs from the watershed (mm)		
Surface ET	509.52	509.52
Surface runoff	70.27	70.27
Soil lateral flow	191.29	191.29
Stream seepage to groundwater	−1.35	−1.88
Saturation excess flow	33.04	16.59
Groundwater ET	0.35	0.29
Groundwater ditch flow	0.00	18.38

We have boundary inflows to account for any groundwater that is coming from neighboring aquifers. This is determined by the hydraulic head difference, where the water balance is estimated for each grid in the boundary, and the only unknown is boundary inflow, which will be assigned as the remaining. This boundary inflow, thus, varies according to the water table. Since the condition with and without ditches made the hydraulic head to be different, the boundary inflow has changed. This is indicated in Bailey et al., 2020, Bailey et al., 2022.

Groundwater system

The model calibration for the streamflow and groundwater head resulted in a better representation of both the streamflow and groundwater head. Especially for the groundwater head, RMSE and MAE have decreased considerably (refer to Fig. 2.4), with all values except one well location having values less than 0.5 m (Tab. 4.4). This indicates the usefulness of the calibration strategy followed for this research.

Table 4.4: The root mean square error (RMSE) and mean absolute error (MAE) for the calibration period based on SWAT+gwflow 1 (top) and SWAT+gwflow 2 (bottom) calibration strategies.

Indices	L1	L2	L3	L4	L5	L6	L7
RMSE	0.17	1.31	1.47	0.85	1.59	0.44	1.75
MAE	0.14	1.25	1.43	0.80	1.58	0.36	1.57
RMSE	0.16	0.36	0.41	0.23	0.46	0.43	0.55
MAE	0.13	0.30	0.34	0.18	0.43	0.35	0.48

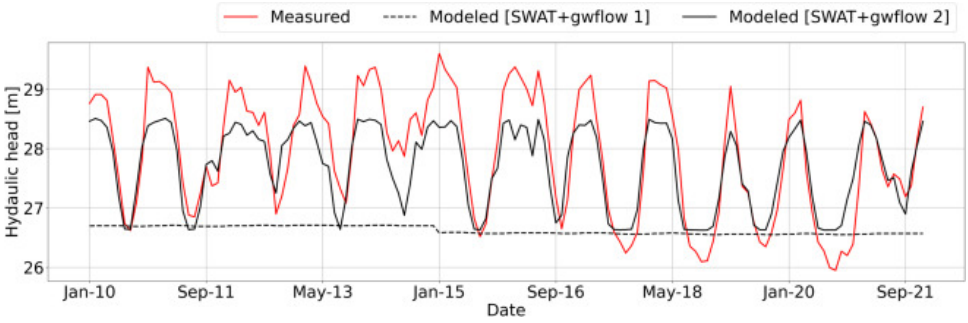


Figure 4.19: The simulated and observed hydraulic head values at L7 (refer to Fig. 1 for well name) for the calibration and validation period. The plot is for the two calibration strategies; calibrating the coupled model for only streamflow and calibrating the coupled model for both streamflow and groundwater head.

As described in the previous section, the groundwater head seasonality was not captured, while the model was calibrated for only streamflow. On the other hand, while using both streamflow and hydraulic head, it is possible to get the seasonality that supports the choice of the calibration strategy (Fig. 2.4). Understanding the seasonality of groundwater head is important for managing and protecting groundwater resources (e.g., during dry periods – drought, groundwater pollution - concentration), and for ensuring the sustainability of water supplies and ecosystems that depend on groundwater. I.e., the seasonal patterns of groundwater recharge (affecting the hydraulic head) can help water managers to better predict water availability and plan for future water needs. Also, the periodic changes

in groundwater levels can affect groundwater quality due to the concentration of existing pollutants during low recharge (low water level) moments.

The calibration strategy also showed a significant difference in representing the seasonal variation, timing, and values of groundwater table depth (Fig. 4.20). The groundwater depth simulation shows the watershed has very shallow groundwater with depths varying from a meter to 1.2 m (according to calibration strategy 2). The result can be misleading unless an appropriate calibration strategy is followed, as shown by calibration strategy 1, indicating a declining water table depth trend.

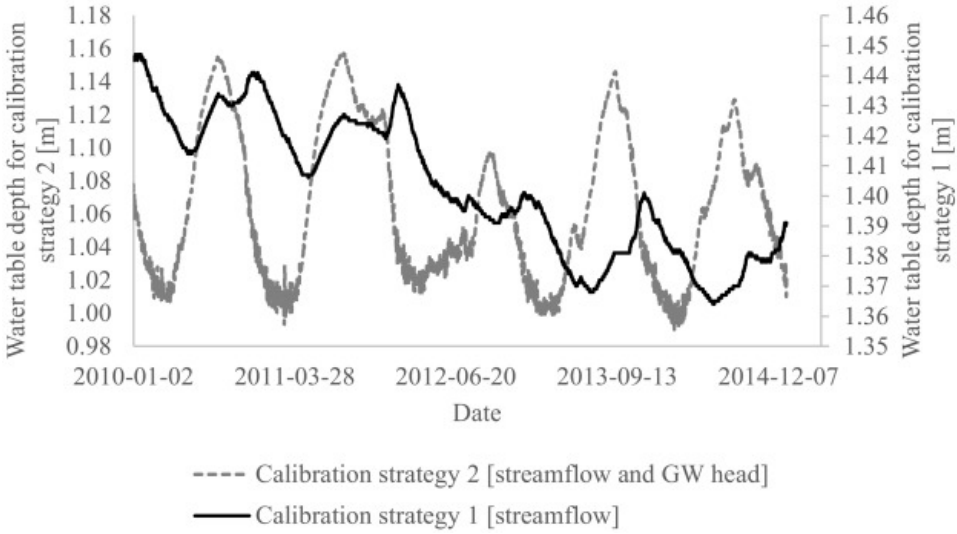


Figure 4.20: The variation of water table depth according to calibration strategy 1 (SWAT+gwflow 1) and strategy 2 (SWAT+gwflow 2)

The effect on the water table depth is observed when drainage units are included in the modeling scheme, where a maximum basin daily average of 0.12 m decrease in water table depth is seen (Fig. 4.21). This drop in water level is consistent but lack of drainage water measurement makes the validation of this result difficult. This decrease in water level corresponds to a considerable volume of water being lost from the groundwater system due to the application of these features, as shown in Fig. 4.21. This can lead to vulnerability during dry spells where groundwater drought prevails. Therefore, to mitigate the impact, an approach to water management known as “adaptive drainage” is modifying drainage systems in response to environmental changes, such as shifting weather patterns or other elements that affect water flow (Van Der Zee et al., 2017).

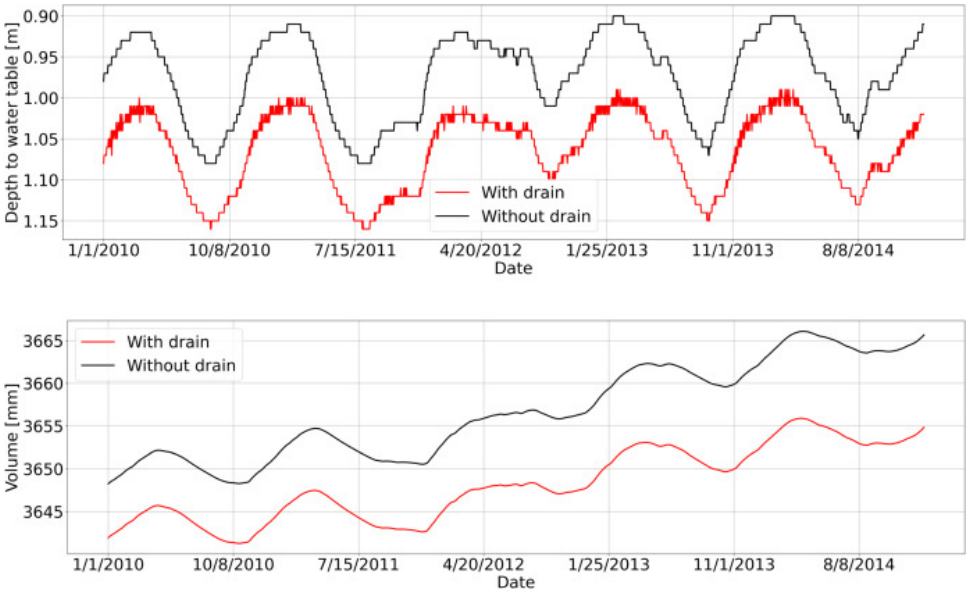


Figure 4.21: The average water table depth and volume of groundwater before and after the application of the drainage unit in the modeling scheme

4.2.6 Discussion

When Bailey et al. (2020) developed the gwflow module, the GIS preprocessing to prepare the inputs of gwflow was made manually using QGIS or ArcGIS. However, a Python script is developed for this research that relatively makes the model development easy. The coupled model (SWAT+gwflow) can run in a few minutes for the Kleine Nete watershed, but the computational requirement increases during model calibration which is mainly due to the high number of parameters related to different hydraulic conductivity zones. Nevertheless, we opt to remove some zones that are small in areal coverage, hence, the computation time has been reduced. Note that the calibration is done using PEST, a local optimization tool that can create an issue if a local optimum value is found. For our case study, the calibration was successful where the simulated and observed streamflow and hydraulic head values were in good agreement, hence, PEST worked very well in finding optimum parameter values. However, in the future, a global optimization tool has to be integrated to lower the uncertainty of the parameter estimation.

The comparison between the standalone SWAT+ model and SWAT+gwflow indicated the drawbacks of the conceptual representation of the groundwater component by the standalone SWAT+ model setup. This limitation has been described earlier in literature (Deb et al., 2019; Gassman et al., 2007; Peterson and Hamlett, 1998; Spruill et al., 2000; Srivastava et al., 2006). Also, our SWAT+ application for the groundwater-dominated Kleine

Nete watershed showed that a simplified representation of the groundwater system by the standalone model hinders geohydrological simulations. On the other hand, we were able to show that SWAT+gwflow is appropriate for simulating geohydrological processes at the watershed. This is in line with the suggestion of (Schilling et al., 2019), who indicated that the appropriate representation of the groundwater system could affect the performance of geohydrological models.

The Kleine Nete watershed is groundwater-driven, where the groundwater system is more dominant than the surface processes due to the shallow groundwater nature. Thus, model parameters related to the subsurface process are vital, and the calibration result on hydraulic conductivity and specific yield indicated that the values are in the range suggested by Dams et al. (2009). The parameters are also found to vary according to the two approaches we followed (calibration of the model for only streamflow (SWAT+gwflow 1) and for both streamflow and groundwater head (SWAT+gwflow 2)). For instance, The SWAT+gwflow 1 calibration strategy leads to the inappropriate overestimation of hydraulic conductivity values, which ultimately increases the ditch flow by five folds. Mainly, the two calibration approaches show considerable differences in groundwater boundary inflow, surface runoff, lateral soil flow, and ditch flow.

The results of the calibration strategy have revealed the usefulness of including both streamflow and groundwater head in the calibration procedure. This can be considered from two perspectives. One is that if the model is calibrated for only streamflow, it's less probable that the groundwater head will be captured. This includes simulating both seasonality and hydraulic head values. Second, if the intention is only to focus on the streamflow, it's not necessary to calibrate the model for both groundwater head and streamflow. However, the general water balance will be affected, and reliance on the model water balance values is incorrect. Oppositely if the intention is only on groundwater head, calibration for only hydraulic head can be sufficient. Nevertheless, calibrating for groundwater head and streamflow can be insufficient in some cases, for e.g., as shown by Voeckler et al. (2014) using the MIKE SHE model. This case study has indicated the need to include other hydrological components in the calibration strategy to improve model simulations. The unsatisfactory groundwater head simulations indicates the need to include more wells in the calibration strategy. Additionally, closer look into the initial conditions is needed to find the cause for wells to show no seasonality.

Finally, the impact of agricultural water drainage has caused a substantial decrement (50% compared to the case where drainage systems are not included in the modeling scheme) in the saturated excess flow, as drains take the water once it's above a certain level (waterlogging the root zone). Water drainage has also lowered the groundwater table, decreasing groundwater volume. The consistent drop in water level is due to the shallow nature of the aquifer where mostly drainage units are placed at a depth between 0.5 to 1.5 meters and the depth to the water table in the Kleine Nete watershed is consistently in that range, hence, the model will assume any water in that depth will be drained and sent to the nearest

stream. The model setup makes the ditch/tile drains act like a head-triggered, quasi-steady sink: they remove water whenever the water table rises above the drain elevation.

The lowering of groundwater via drainage ditches has critical implications for water quality downstream of the catchment as pollutants, nutrients, pesticides, etc., can travel towards the streams via the drained water (Gärdenäs et al., 2006; Kiesel et al., 2010; Rozemeijer et al., 2010; Warsta et al., 2013). Several researchers have calculated the amount of water drained from agricultural land using SWAT (Bauwe et al., 2016; Guo et al., 2018; Koch et al., 2013; Moriasi et al., 2013, 2015; Schilling et al., 2019). Due to a lack of measurements on drained water for the Kleine Nete catchment, it is difficult to rely entirely on the model simulation. In future research, it is recommended to measure drain water and calibrate geohydrological models for streamflow, groundwater head, and drain flow. This can reduce the uncertainty in estimating drain water and other water balance components. Assessing the amount of drained water can be vital for investigating the environmental impact it can cause and act accordingly to reduce the effect.

4.2.7 Conclusion

Agricultural drainage units are used to remove excess water from groundwater and allow the root zones of crops to have sufficient oxygen. However, drainage systems have environmental and hydrological impacts where the groundwater volume will decrease, and pollutants can be transported faster downstream. Hence, investigating the impact of these features on hydrology is crucial, which is lacking in the dense ditch-dominated Kleine Nete watershed. For this study, we compared three approaches. In the first one, we modeled the Kleine Nete catchment using the standalone Soil Water Assessment Tool (SWAT+). Secondly, we used the newly developed groundwater module (gwflow) inside the SWAT+ model. Finally, we compared calibration strategies where the coupled model is first calibrated for only streamflow, and then calibration is done using both streamflow and hydraulic head observation data. Analysis with and without the inclusion of drainage systems is presented at the end.

The standalone modeling result indicated the model's poor performance (NSE of 0.18 and 0.37 during calibration and validation periods, respectively). Hence, we opt for using the coupled model with the first calibration strategy where the streamflow was captured but with the limitation of attaining a good match between observed and simulated hydraulic head values. Furthermore, the seasonality was not captured well with this approach. Therefore, this led to using streamflow and groundwater heads to calibrate the coupled model. This resulted in depicting the hydraulic head well with a root mean square error of less than 0.5 m, while it was above 1 m for the previous approach. Hence, calibrating the model using the latter approach is superior. Moreover, the calibration strategies showed considerable differences in water balance values, hence, to attain appropriate water balance values, it is recommended to calibrate models for multiple aspects (streamflow, groundwater head, ET, soil moisture, etc.). The inclusion of drainage units in the watershed model indicated a substantial decrease in saturated excess flow (up to 50%: from 33.04 mm to 16.59 mm),

and around 18.4 mm of drainage water is removed. Moreover, the basin's average water table depth is reduced by a maximum of 0.12 m. Therefore, investigating and applying necessary measures to minimize the impact of drainage systems is crucial for sustainable management of the Kleine Nete watershed. This has an implication for the general hydrological modeling community to pay close attention to drained water as it affects the different water balance components and the environment.

4.3 Regional evaluation of groundwater-surface water interaction in the Scheldt basin using SWAT+gwflow

4.3.1 Summary

A proper representation of groundwater–surface water interactions with (geo)hydrological models is possible via a coupled model. However, such models have disadvantages, such as complex code modifications and new tunings, and are computationally expensive. Therefore, their application on large spatial scales is limited. A newly developed model, SWAT +gwflow integrates the Soil Water Assessment Tool (SWAT+) with the groundwater module gwflow and has the potential to overcome these limitations. However, this coupled model has not yet been evaluated at a regional scale; hence, we present the evaluation of this model for regional studies using a global aquifer data over the seven watersheds in the Scheldt basin. Furthermore, we have investigated and quantified water balance components within the basin, with a focus on groundwater-surface water exchange.

From the results (Nash-Sutcliffe efficiency (NSE) of 0.8–0.9 for all catchments based on monthly average streamflow during calibration and validation periods), we consider the model to be a good simulator of hydrology in the basin. In addition, the simulated groundwater head shows good agreement with observed well data (with a mean absolute error of less than 0.42 m). Also, the rivers in five of the seven watersheds are found to be strongly dependent on groundwater discharge to the streams. We conclude that (1) the SWAT+gwflow model is capable of accurately modeling hydrological processes and state variables in the seven watersheds using global aquifer data and limited computational time, (2) the climate-gridded dataset can successfully be used for (geo)hydrological studies, and (3) the groundwater-surface water interaction increases over the years (from 1975 to 2021) with a strong increment found in the Grote Nete (3.7 fold) and upper Scheldt (2.3 fold) watersheds. These results are, moreover, promising for data-scarce regions where geohydrological modeling relies on the use of global datasets, but the mere success of this modeling application does not guarantee the accuracy of the dataset for other locations, hence, further verification is required. Furthermore, although in this study, the gwflow module is integrated into the SWAT+ model, it could also be integrated into other surface water models for other studies.

This section is published as: **Yimer, E. A.**, Bailey, R. T., Van Schaeybroeck, B., Van De Vyver, H., Villani, L., Nossent, J., & van Griensven, A. (2023). Regional evaluation of groundwater-surfacewater interactions using a coupled geohydrological model (SWAT+gwflow). Journal of Hydrology: Regional Studies, 50, 101532. https://doi.org/10.1016/j.ejrh.2023.101532

4.3.2 Introduction

The SWAT+ model is a watershed modeling that simulates the storage and movement of water, sediment, and nutrient mass within an integrated watershed system on a daily time step. The model often is used to assess hydrological processes and water supply, subject to changes in climate and land use and land cover management scenarios. The main computational unit is the hydrologic response unit (HRU), a unique spatial unit with a combination of land use, soil, and slope classification (Arnold et al., 1998). All processes start from the HRU level and are combined into landscape units (LSUs), then routed to the sub-basin level and ultimately aggregated to obtain the streamflow at the catchment outlet (Neitsch et al., 2011).

Since the groundwater component of the SWAT+ model is based on the simplified concept of a linear reservoir, the model's capability to represent groundwater hydrology is questionable.This led to the creation of the gwflow module. This module uses a grid–based approach to solve for groundwater storage, groundwater head, and groundwater sources and sinks for individual grid cells throughout the watershed system. The objective of this study is to evaluate SWAT+gwflow at a regional scale which has not yet been performed. The regional application consists of seven connected watersheds. The model setup uses a global aquifer property dataset for model development. For our regional study, a gridded climate dataset for Belgium with a 5 km resolution is used. The gridded dataset was evaluated based on meteorological data from gauging stations, but the effect of using this dataset for hydrological analysis has not been explored to date. Therefore, in addition to evaluating the coupled model, this research aims to assess if the Belgian gridded data can effectively be used in hydrological modeling. Next, different water balance components are investigated and compared, focusing on groundwater–surface water interactions for the seven watersheds inside the Scheldt basin. The lack of study on groundwater–surface water interactions for the whole Scheldt basin adds novelty to our study.

4.3.3 Study area and data

The study area mainly covers the northern part of Belgium (Fig. 4.22), with two catchments having part of their watershed inside France (the Leie and upper Scheldt River catchments). Belgium has a mild cold season during winter (from November to March) and temperate summers (from June to September). According to the Royal Meteorological Institute of Belgium, the mean annual precipitation is around 848 mm, which shows a steady increase in annual precipitation (Brouwers et al., 2015). The topography is mainly flat, with lower elevations in the northern end and higher altitudes in the southern part of the country (Yimer et al., 2023b). The study area has very shallow groundwater, mostly in the northern part of Flanders. The northern part of Belgium (Flanders) is mostly inside the regional Scheldt River basin. The Scheldt River has a mean, maximum, and minimum streamflow of 108, 832, and 17 m^3/s, respectively. The research conducts (geo)hydrological modeling of catchments with areas varying from 510 to 5,817 km^2.

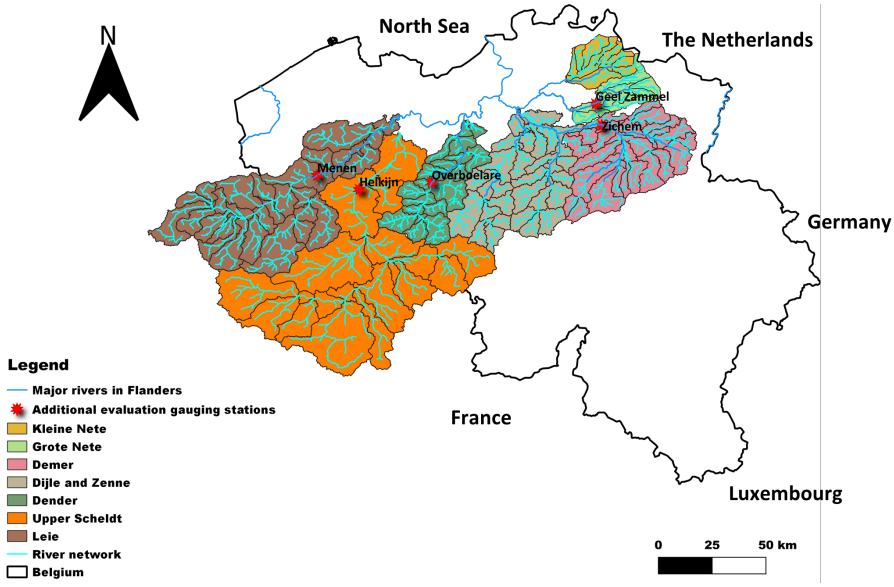


Figure 4.22: The seven catchments, their boundaries, their respective river network, and validation gauging stations used for model evaluation (they are not used to calibrate the coupled model)

The daily average weather data necessary to force the model (P, Tmin, Tmax, RH, W, SLR) was obtained from the Royal Meteorological Institute of Belgium (RMI) for the period 1970–2021. Furthermore, the streamflow data is downloaded from Waterinfo (https://www.waterinfo.be/, last accessed 21 February 2022). The input data for the SWAT+gwflow model setup are outlined in Tab. 4.5.

A common problem when applying geohydrological models is the lack of reliable, spatially and temporally extended climate data. Geohydrological models mainly require meteorological data, and as a first alternative, data from gauging stations are preferably used. In some regions, gauging stations are more sparsely distributed and scarce, hence, alternative means of obtaining meteorological forcing data are required. One alternative is to combine gauging station data with remote sensing via interpolation, producing a gridded dataset (Coustau et al., 2015; Essou et al., 2016; Funk et al., 2015; Habets et al., 2008; Jones et al., 2016; Quintana-Segui et al., 2008; Raimonet et al., 2017; You et al., 2015). For example, the Copernicus program assembles meteorological data worldwide (Cornes et al., 2018), and a similar regional effort exists, for instance, for Asia (Yatagai et al., 2009). Other widely used datasets are the Climate Hazards Group InfraRed Precipitation with Station data (CHIRPS) (Yimer et al., 2022), covering most of the world with a focus on Africa (Funk et al., 2015), and the Climate Research Unit (CRU) dataset for the globe (Harris et al., 2020). The resolution of these gridded datasets ranges from 5 to 50 km, and they are subject to uncertainty due to the scarcity of gauging stations involved in data aggrega-

tion (Bastola and Misra, 2014; Piani et al., 2010; Tarek et al., 2021). Furthermore, the low spatial resolution, weather model bias, and inaccurate orographic specifications intensify the uncertainty in the meteorological data (Raimonet et al., 2017). Moreover, the observed solar radiation, wind speed, and relative humidity are not as commonly available as temperature and precipitation but may nevertheless be important for hydrological studies. Hence, observational gridded datasets are the major contributors to fulfilling the data demand for such variables. Therefore, we used the observational gridded dataset of RMI for forcing the geohydrological models.

Table 4.5: The list of model inputs required to set up the SWAT+ and the coupled SWAT+gwflow model

Data	Source	Resolution
For SWAT+model setup		
DEM	Accessed: 1 Feb 2022, https://viewer.nationalmap.gov/, USGS National Elevation Data	30m
Land use	Accessed: 1 Feb 2022, https://remotesensing.vito.be/, VITO	10m
Soil map	Accessed: 1 Feb 2022, https://www.fao.org/land-water/en/	Vector polygon
For SWAT+gwflow model setup		
Aquifer thickness (cm)	Accessed: 10 Mar 2022, https://soilgrids.org/ (global dataset)	250m
Permeability zones (m/day)	Accessed: 10 Mar 2022, https://dataverse.scholarsportal.info/dataset.xhtml?persistentId=doi:10.5683/SP2/TTJNIU (global dataset)	Vector polygon

4.3.4 Methodology

The SWAT+gwflow model setup for individual case studies begins with catchment delineation, and then based on unique land use, soil, and slope classifications, HRUs are created. Henceforth, weather inputs are generated for the respective catchment from the observational gridded dataset. The calibration and validation periods are chosen depending on the availability of streamflow data in the catchment (Tab. 4.6). Only catchments within the Scheldt basin that are not or only mildly affected by the tidal effect are considered, as this effect is not represented in the SWAT+gwflow model.

The delineated catchments (see Fig. 4.22) have a different number of streams, sub-basins, and HRUs. Each has its defining character, where Leie and Demer feature the highest

number of streams. This shows that the number of streams contributing to the main rivers, Leie and Demer, is higher than the other catchments.

After the SWAT+ model was set up for all the catchments, the gwflow inputs were prepared using a Python script (the manual and the Python script can be found on the official website of the SWAT model: https://swat.tamu.edu/. This starts with discretizing the catchments into square-sized grid cells. The cell size used for each catchment is listed in (Tab. 4.6). The larger a given catchment, the larger the grid size to ensure a reasonable computation time. The homogeneous hydraulic conductivity and specific yield zones are outlined based on the global database, GLobal HYdrogeology MaPS 2.0 (GLHYMPS 2.0) (Huscroft et al., 2018). Since computation time and overfitting can be an issue, limiting the number of zones for the catchment to be calibrated is vital. There are instances where the number of unique zones with different aquifer properties reaches 165 (for the Upper Scheldt catchment). Hence, we only took major zones for each catchment, as stated in (Tab. 4.6). Additional input required by the groundwater module is the depth to the impermeable layer, provided by the global dataset of Shangguan et al. (2017). With this, we aim to evaluate to what extent the global aquifer depth dataset is able to reproduce reasonable water balance components, streamflow and groundwater head (in seven watersheds inside the Scheldt basin with the focus on capturing groundwater dynamics only in the Kleine Nete).

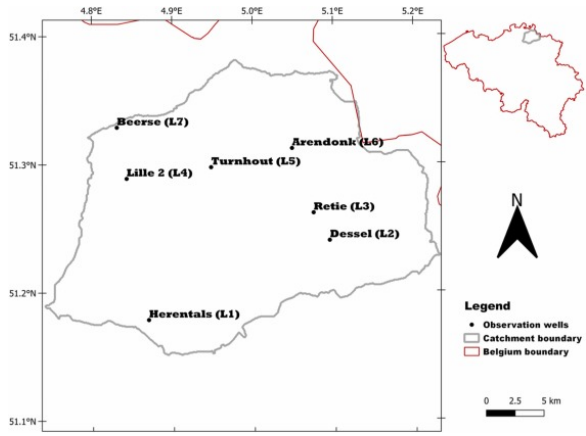


Figure 4.23: The locations of observation wells inside the Kleine Nete watershed that are used for calibration and validation

After the model setup, parameters are calibrated until the statistics between measured and simulated streamflow no longer improve with continued calibration. The calibration for all the model setups constitutes the following parameter groups; hydrology.hyd (Soil evaporation compensation factor: esco, Plant uptake compensation factor: epco, Percolation coefficient: perco), river channel parameters (manning coefficient and conductivity), soil parameters (available water content: awc and soil hydraulic conductivity) and gwflow parameters

Table 4.6: The number of sub-basins, HRUs, channels, calibration and validation periods, area, groundwater discretization, number of homogeneous hydraulic conductivity zones, and dominant zones used for calibrating the model (e.g. 10 zones are used instead of 165 zones for calibrating the upper Scheldt basin)

Catchment name	**Number of sub-basins**	**Number of HRUs**	**Number of streams**	**Calibration period**	**Validation period**
Kleine Nete	15	1345	99	2010-2014	2015-2021
Grote Nete	11	326	89	2000-2004	2008-2021
Dijle and Zenne	41	6086	293	2005-2009	2015-2021
Demer	37	5257	305	2005-2009	2013-2021
Dender	21	4083	243	2005-2009	2015-2021
Upper Scheldt (USC)	17	1570	197	2013-2017	2018-2021
Leie	33	2445	347	2006-2010	2016-2021

Catchment name	**Area (km^2)**	**Grid size (m)**	**Number of zones**	**Number of major zones**
Kleine Nete	551.6	200	15	7
Grote Nete	509.5	200	11	5
Dijle and Zenne	2428.2	300	49	8
Demer	2204.0	200	31	6
Dender	1352.1	300	27	4
Upper Scheldt	5816.6	500	165	10
Leie	3793.7	500	107	13

(hydraulic conductivity, specific yield, river bed hydraulic conductivity). The final calibrated values, along with their initial and boundary values, are included in the supplementary material - https://www.sciencedirect.com/science/article/pii/S2214581823002197.

The model evaluation is done on streamflow data gauging stations different from those used for calibration. For example, for the Upper Scheldt catchment, a gauging station near Helkijn is used to evaluate the model simulation for the calibration and validation period. Similarly, for the Grote Nete catchment, a gauging station near Geel-Zammel is used. As for Dender, Leie, and Demer, streamflow at Overboelare, Menen, and Zichem is used to further investigate the optimized model parameters (see Fig. 4.22). The presence of water infrastructures (e.g., sluices, canals, etc.) influences the Dijle-Zenne catchment strongly (Yimer et al., 2023a), hence biasing the simulated discharge. Therefore, this catchment is validated for a different time window at the catchment outlet but is not validated using other gauging stations (validation gauging stations) data. The use of streamflow at validation gauging stations to test the results obtained from the models provides a more critical assessment of the observational gridded dataset. Finally, the Kleine Nete watershed model setup is calibrated for both streamflow and groundwater head to show the capability of

the coupled model to simulate groundwater head at different points in the watershed (Fig. 4.23). To investigate the groundwater-surface water interaction (GW–SW), the flow to and from aquifers and streams is estimated by comparing the hydraulic head and river stage. If a river stage is higher than the hydraulic head in the aquifer, water flows from the streams to the aquifers. On the other hand, if the groundwater head is higher than the stream water level, water flows from the aquifer to the rivers.

The model is calibrated using the parameter estimation tool (PEST) for mean monthly streamflow values. The model evaluation is done using the Nash-Sutcliffe efficiency (NSE) (Nash and Sutcliffe, 1970). The classification made by Moriasi et al. (2015) is used to evaluate model simulations at monthly and daily time scales. The soil water balance at the watershed and groundwater system level (GW balance) is calculated using Eq. 4.10, 4.11 where P is precipitation, gwsoil is the groundwater transferred to the soil profile, Surq is surface runoff, Latq is lateral flow, Pr is percolation (equivalent to recharge), and ET is evapotranspiration; for Eq. 4.11, gwet is ET from groundwater, swgw is the amount of water leaving the streams to the groundwater, gwsw is discharge of groundwater to streams, satex is saturation excess flow, pump is municipal pumping, and bound is the amount of water coming from aquifers outside of the watershed, through the boundaries of the watershed.

$$\text{Water balance}_{\text{SWAT+gwflow}} = P + \text{gwsoil} - \text{Surq} - \text{Latq} - \text{Pr} - \text{ET} \tag{4.10}$$

$$\text{GW balance} = \text{rech} - \text{gwet} - \text{gwsw} + \text{swgw} - \text{satex} - \text{gwsoil} - \text{pump} + \text{bound} \tag{4.11}$$

The percentage of error at the watershed level is estimated by dividing the water balance by the total input (P+gwsoil), while for the groundwater system, the error is the difference between what is coming in and taken out of groundwater (Yimer et al., 2023a).

4.3.5 Results

Calibration and validation

The parameter that adjusts soil moisture for percolation to occur (perco) is mostly around 1.0 (Demer, Dijle and Zenne, upper Scheldt (USC) and Leie), which indicates that most of the water percolates to groundwater (Fig. 4.24). This mostly occurs when the soil is very permeable. A significant difference is seen mainly between Grote Nete and Kleine Nete watersheds, neighboring catchments with nearly similar characteristics (weather, soil type, land use). This can be due to the clay deposit in the Kleine Nete (Dams et al., 2009) that can hinder water movement in the soil, reducing the value of perco. The soil type in the northern part of Belgium is mostly sandy, hence, a perco value near 1.0 is reasonable. Soil available water capacity (awc) is lower wherever the water percolates towards the groundwater, leaving the soil (awc is less than perco) and vice versa. Except for the Grote Nete watershed, perco is higher than awc.

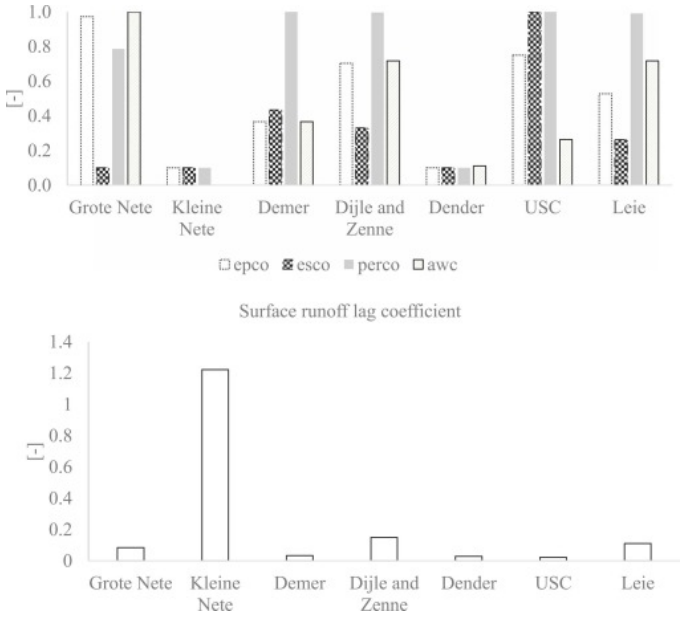


Figure 4.24: The parameter that adjusts soil moisture for percolation to occur (perco), soil evaporation compensation factor (esco), plant uptake compensation factor (epco), and Soil available water capacity (awc) (top) and surface runoff lag coefficient (sur_lag) (bottom) calibrated parameters

The near-one value for the Grote Nete watershed is an artifact of the calibration procedure. But, note that the awc parameter is not sensitive for this watershed, hence, the value did not affect the streamflow simulation but can affect other water balance components.

The plant uptake compensation factor (epco) shows a similar trend/values as awc except at USC and the Leie watersheds, where epco increases as awc decreases. The inverse relation between awc and epco is reasonable as whenever there is little available water, epco increases, which initiates the uptake of plant water demand from lower layers and vice versa. The soil evaporation compensation factor (esco) is mostly low, indicating that the evaporative demand is met from the lower layers of the soil. Next, the surface runoff lag coefficient (sur_lag) is investigated, representing the fraction of water allowed to enter a stream, hence, lagging surface runoff. The lower the value of sur_lag, the more water is stored before releasing it to the nearest stream reach. The Kleine Nete catchment has a relatively higher sur_lag coefficient compared to the other six watersheds, signifying the release of water (runoff) towards the rivers more quickly than the others.

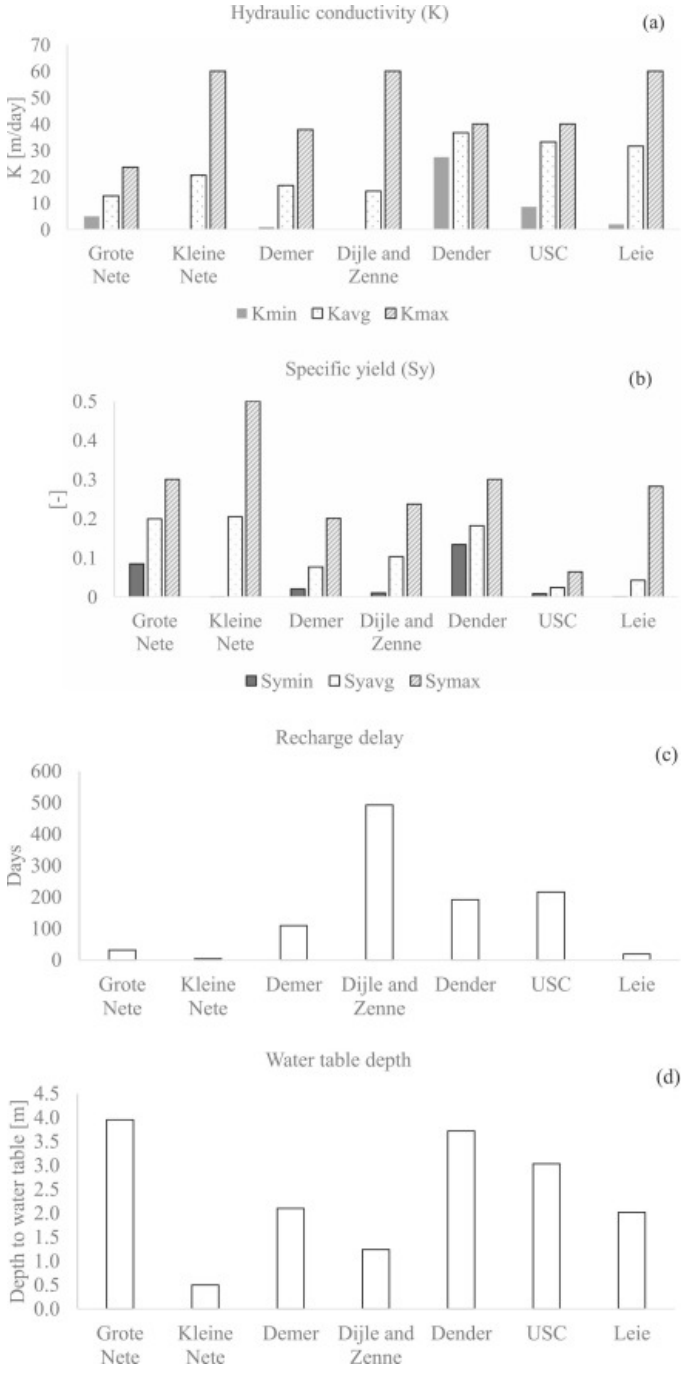


Figure 4.25: The minimum, average, and maximum hydraulic conductivity (a) and specific yield (b), recharge delay (c), and water table depth (d)

The calibrated hydraulic conductivity (K) values for the Dijle-Zenne watershed are approximately similar to the study made by Wossenyeleh et al. (2021) for the Doode Bemde wetland area inside the Dijle watershed, where the dominant aquifer is the "Brussels Sand". Similarly, the K value is similar compared to a study made by Dams et al. (2009) for the Kleine Nete catchment. According to the calibrated values, the variation of hydraulic conductivity values in the Dender watershed is low (difference between minimum (K_min) and maximum (K_max) hydraulic conductivity values). However, for the other watersheds, the difference between K_min and K_max is high (Fig. 4.25). In the Dender watershed, the lowest K is more than or nearly equal to the average K value of the other basins. Therefore, the relatively high K values are because of the very conductive nature of the aquifer material.

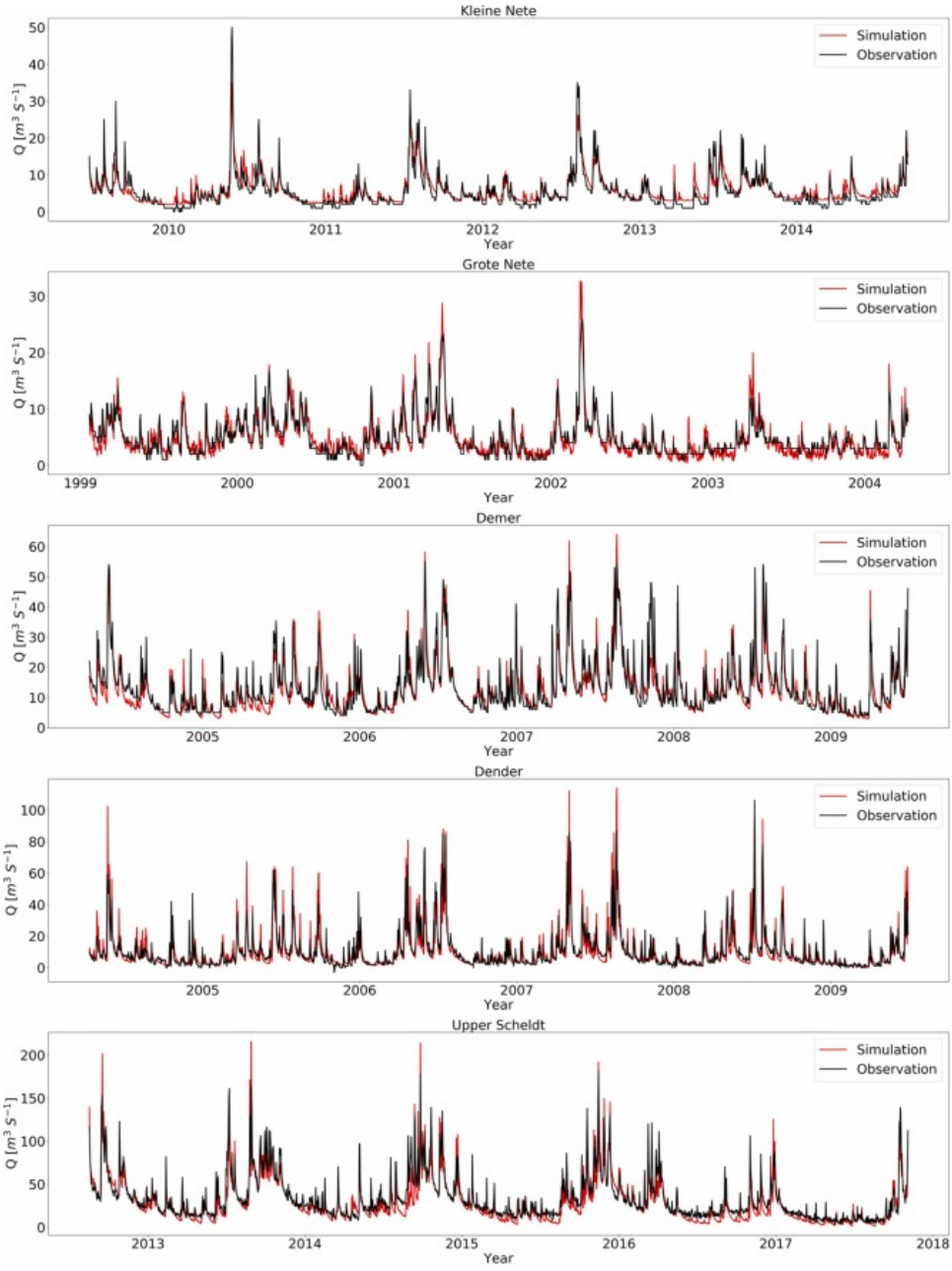
The Dender catchment's minimum Sy values (after calibration) are higher or approximately similar to the rest of the catchments average Sy values. The higher the Sy values, the higher the proportion of groundwater volume removed for a given change in groundwater head. When it comes to the number of days it takes for water to reach the water table, the Dijle–Zenne watershed requires, on average, the most extended number of days to recharge the aquifer (493 days), which can be attributed to the mass extent of urbanization (e.g., Brussel, Leuven, Mechelen, etc.). Impermeable surfaces (e.g., pavements in urban areas) lead to more surface runoff, hence, less groundwater recharge (Foster et al., 1994; Minnig et al., 2018; Tam and Nga, 2018). On the other hand, the Grote Nete, Kleine Nete, and Leie have the shortest recharge delay (ranging between 4 and 31 days).

Tab. 4.7 shows the NSE values for all calibration and validation periods for monthly and daily streamflow values. All values range between 0.6 and 0.8, and according to Moriasi et al. (2015), the models have satisfactory to very good results. The analysis for the daily streamflow indicates successful modeling of the high and low flows, signifying the appropriateness of the model and the data used to set up the model (Fig. 4.26). Here, a well–performing model is one of the indications of accurate weather inputs; hence, the gridded dataset is instrumental. Moreover, the model simulations at gauging stations different from those used for calibration were also checked, and the results indicated good similarity between measured and simulated streamflow (NSE above 0.46).

As shown in Fig. 4.26, there is a bit of noise in representing the baseflow for the Grote Nete watershed, mainly during the validation period, a slight overestimation of baseflow for the Kleine Nete and a small underestimation for the Demer catchments by the model is seen. In the rest of the cases, the baseflow is well simulated. Baseflow is a dominant feature in the rivers across Flanders (Van Camp et al., 2010), so capturing baseflow by our model is vital.

Table 4.7: The Nash-Sutcliffe efficiency (NSE) for the analyzed catchments for the calibration and validation periods (at daily and monthly streamflow values). This result is based on the gauging station near the catchment outlet (top) and other internal stations (bottom). The asterisk (*) indicates that validation gauging stations are unavailable or not used. Refer to Fig. 4.22 for the locations of the validation gauging stations.

Catchment name	Nash-Sutcliffe efficiency			
	Calibration period		Validation period	
	Monthly	Daily	Monthly	Daily
Kleine Nete	0.87	0.81	0.79	0.74
Grote Nete	0.92	0.82	0.84	0.74
Dijle and Zenne	0.80	0.70	0.80	0.70
Demer	0.87	0.82	0.78	0.76
Dender	0.94	0.56	0.88	0.66
Upper Scheldt	0.86	0.83	0.89	0.84
Leie	0.94	0.87	0.93	0.88
Based on validation gauging station				
Catchment name	Calibration period		Validation period	
	Monthly	Daily	Monthly	Daily
Kleine Nete	*	*	*	*
Grote Nete	0.47	0.46	0.80	0.70
Dijle and Zenne	*	*	*	*
Demer	0.85	0.80	0.86	0.80
Dender	0.70	0.54	0.89	0.75
Upper Scheldt	0.70	0.63	0.80	0.56
Leie	0.94	0.82	0.91	0.84


Kleine Nete
Simulation
Observation
Q [m³ S⁻¹]
Year
Grote Nete
Demer
Dender
Upper Scheldt

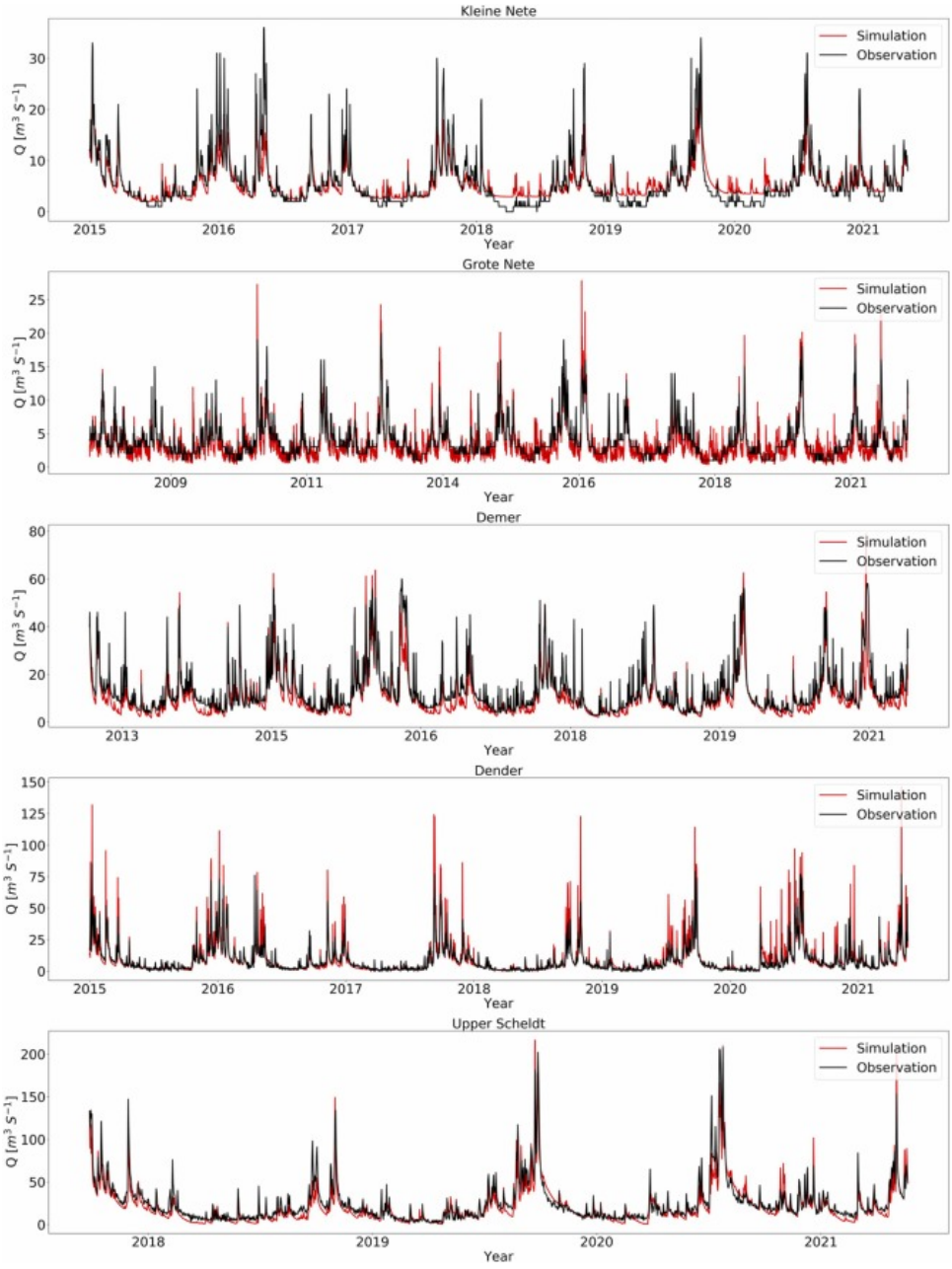


Figure 4.26: Comparison between streamflow model output and measured values for calibration and validation periods for the Kleine Nete, Grote Nete, Demer, Dender, and upper Scheldt catchments

Water balance

The water balance closure is an essential criterion for assessing the quality of the model simulations. The soil water balance here closes for all the models with less than 0.4% based on the analysis at the watershed level. The groundwater error is very low (compared to a study made by Bailey et al., 2020), with a maximum difference of 5.8 mm for the Dijle and Zenne catchment (Tab. 4.8). The reason for such discrepancy can be uncertainty on inter-aquifer boundary inflow, model parameter estimation, inputs, numerical solver, rounding off, the exclusion of pumping, etc. The ability of the model to reasonably close the soil water balance and capture the streamflow makes the model setup useful for understanding basin average water balance components and long–term streamflow conditions. However, to fully capture the geohydrology in the Scheldt basin, other aspects, such as simulated soil moisture, deep percolation, and other water balance components, need to be verified. In addition, assessing water balance at groundwater and watershed levels strengthens the evaluation of the coupled model.

Table 4.8: Watershed Soil Water Balance and Groundwater Balance Error

Catchment name	Watershed soil water balance				Groundwater balance error	
	Calibration		Validation		Calibration	Validation
	%	mm	%	mm	%	%
Kleine Nete	-0.17	1.57	0.00	-2.15	-0.13	-0.30
Grote Nete	0.30	3.26	0.15	1.41	-0.43	-0.16
Dijle and Zenne	0.33	3.40	0.36	3.60	5.31	5.78
Demer	0.09	2.97	-0.04	-1.23	0.79	-0.09
Dender	0.11	1.04	0.10	0.85	0.44	-1.27
Upper Scheldt	-0.49	-5.59	0.39	3.91	-0.82	0.77
Leie	0.23	-3.24	0.29	3.69	0.21	0.23

The basin average water balance components indicated that the average precipitation ranges between 773 and 844 mm across the seven watersheds with an average of 810 mm. Part of this goes to surface runoff (ranging between 124 and 225 mm), evapotranspiration (519 –695 mm), and lateral flow, which accounts for a small portion of the total water budget (ranging between 0.01 and 5.6 mm). Saturated excess flow is also dominant in all the watersheds, with an average value of 90 mm (Fig. 4.27).

The ET is highest in the Dijle-Zenne and lowest in the Dender watersheds but maintains nearly similar values in the rest of the watersheds, hence, ET does not vary significantly across the different watersheds. The difference in ET between the Dijle-Zenne and Dender can be due to the difference in the land use type, where urban areas and forests are more dominant in the Dijle-Zenne than in the Dender. Agricultural/forestry in the Dijle–Zenne and Dender accounts for 66% and 40.7% of the total area, respectively, hence, the ET is expected to be higher for the Dijle-Zenne than the Dender watershed. The basin average surface runoff also does not vary considerably across the catchments, but the highest runoffs

are observed in the Dender, Grote Nete, and Kleine Nete. As for the saturated excess flow, when groundwater is above the ground surface, it is routed to the nearest stream, which is prevalent in the Kleine Nete and Grote Nete watersheds, which can be due to the shallow nature of groundwater in those catchments.

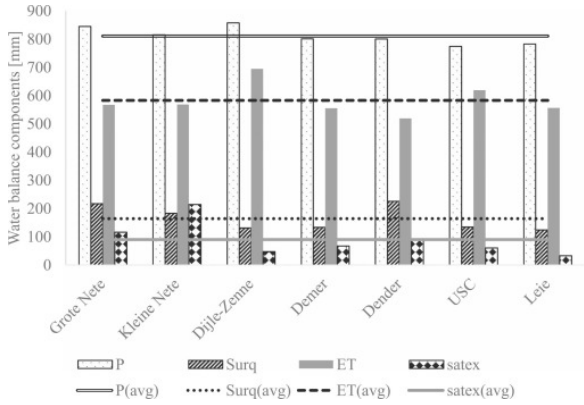


Figure 4.27: The basin average water balance components, precipitation (P), surface runoff (Surq), evapotranspiration (ET), saturated excess flow (satex), and the average of the seven watersheds (in mm)

The groundwater flow into the system from the adjacent catchment is found to be dominant for the Kleine Nete, Leie, and Dijle-Zenne watersheds (Fig. 4.28). The aquifer in the Dender catchment receives only a small portion of groundwater from adjoining watersheds. The neighboring watersheds, Grote Nete and Demer have nearly similar boundary inflows into their aquifer and yearly variations. In most of the catchments, it is seen that there are annual variations that indicate the dependence of boundary flow in the groundwater flow/hydraulic head variability from the feeding aquifer. Since the amount of boundary flow is significant, any form of eco-geohydrological impact on one watershed (e.g., pumping, drought, deforestation, etc.) can affect others within the Scheldt basin. Note that calibrating the model for both streamflow and groundwater head can result in groundwater head values being different from those attained while calibrating the model for only streamflow, affecting boundary flow and, in general, the groundwater fluxes. Note that the model setup is only validated for streamflow, hence, to ensure appropriate water balance components are attained, a multi–variable model verification/calibration protocol is needed. Also, the gwflow module should allow users to specify a mix of boundary conditions (currently supports either constant head or no flow boundary), which can ultimately affect boundary flux and other water balance components.

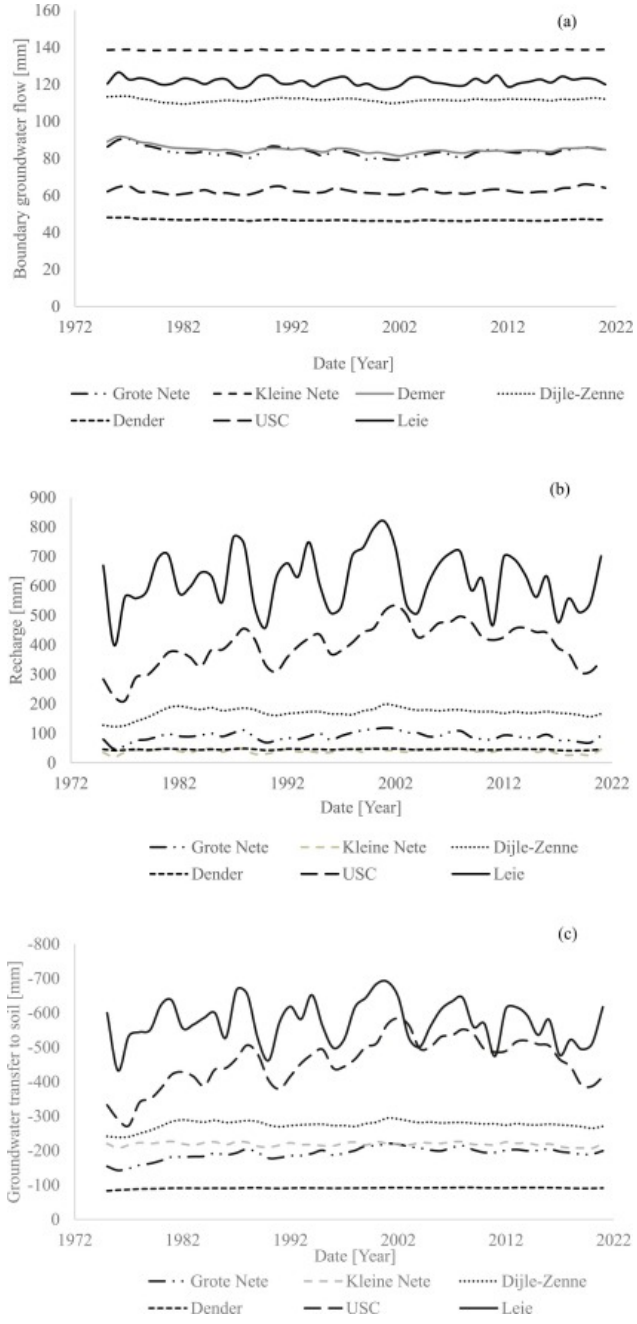


Figure 4.28: The boundary groundwater flow at catchment boundary (a) and recharge (b) and groundwater transferred to the soil profile (c) given in mm

Recharge shows considerable temporal and spatial variations among the seven watersheds. The highest recharge value is seen in the Demer watershed, but since it is high compared to other watersheds (average value of 3172 mm), we exclude it from the plot as it distorts the view for the other catchments. The Demer watershed needs to be calibrated for multiple aspects (e.g., groundwater head, soil moisture), which can ultimately lead to plausible recharge values. However, it is important to note that the water that reaches the water table can also be taken back by the groundwater soil interaction (gwsoil), hence, the net recharge is the difference between recharge and gwsoil. Recharge and gwsoil show a similar trend; if one increases, the other decreases, and vice versa. This is plausible as the rise of the groundwater table due to recharge leads to groundwater transfer to the soil profile if the aquifer is too shallow.

GW-SW interaction has a higher magnitude for the Grote Nete, Kleine Nete, Demer, USC, and the Leie, while it's insignificant for the Dijle-Zenne and Dender watersheds. The groundwater discharge into those rivers is low, which can be due to the lower conductivity of the streambed, blocking water inflow to the streams. The interaction is seen to increase over time for all the watersheds, indicating the increasing influence of the groundwater system in feeding the streams in the Scheldt river basin (Fig. 4.29).

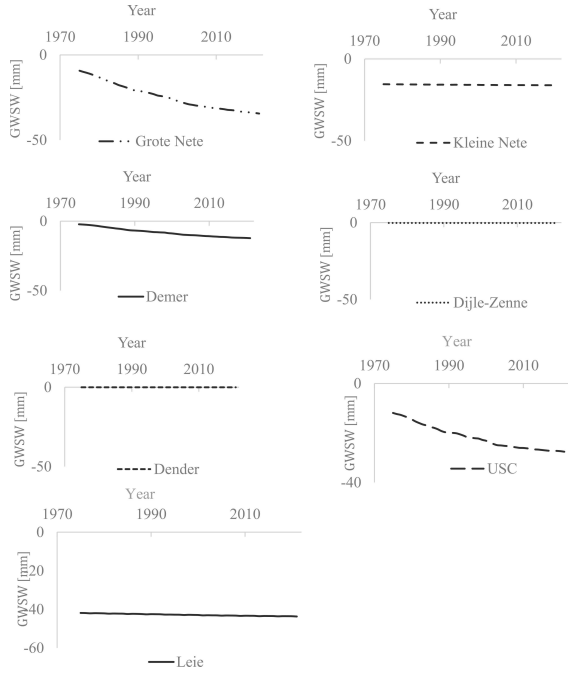
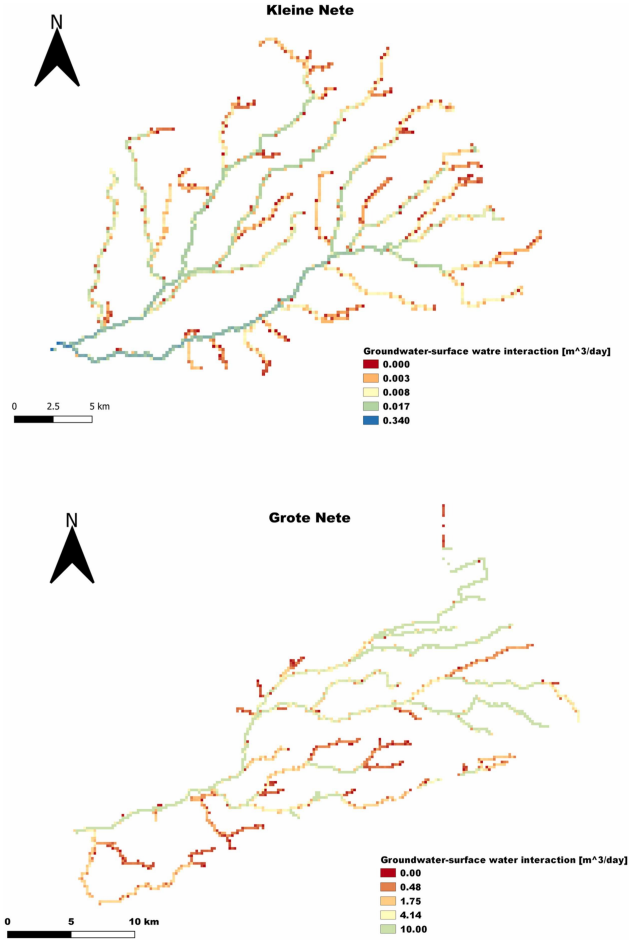
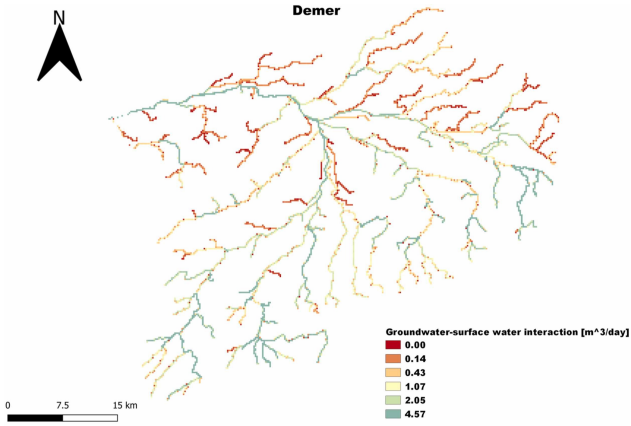
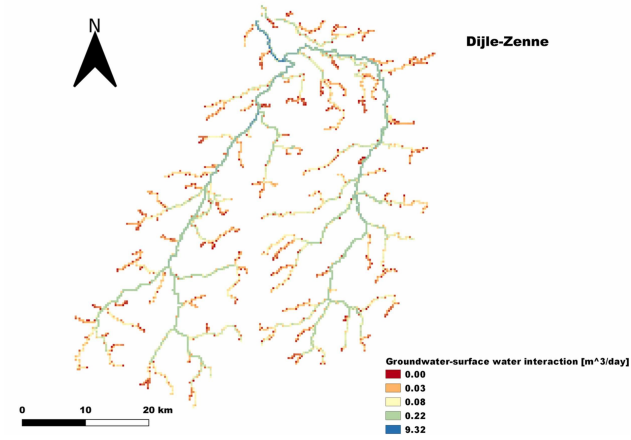


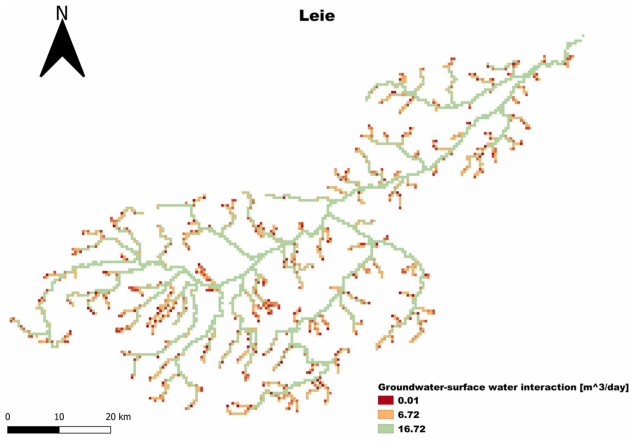
Figure 4.29: Groundwater-surface water interaction (GW-SW) in the seven watersheds from 1975 to 2021. The values are negative as they are sinks (taken out of the groundwater) and given in mm's

The GW–SW interaction plays a vital role during extremely low streamflow moments (e.g., during drought), which leads to rivers being fed with groundwater discharge (Fig. 4.30). This is the reason for selecting a day during the summer month to show GW-SW interaction in Fig. 4.30. Note that GW-SW interaction and saturated excess flow form the total baseflow. As seen in Fig. 4.30, major interaction is seen on the main river reaches of the watersheds as compared to the tributaries. Also, the USC and Leie are shown to be dominated by a large flux of groundwater into their respective rivers. On this specific date (during summer), the flow in all seven watersheds is from groundwater to the streams. The reason is because of groundwater influence (shallow water table), hence, baseflow dominates.




Demer
N
Groundwater-surface water interaction [m^3/day]
0.00
0.14
0.43
1.07
2.05
4.57
0
7.5
15 km


Dijle-Zenne
N
Groundwater-surface water interaction [m^3/day]
0.00
0.03
0.08
0.22
9.32
0
10
20 km


Leie
N
Groundwater-surface water interaction [m^3/day]
0.01
6.72
16.72
0
10
20 km

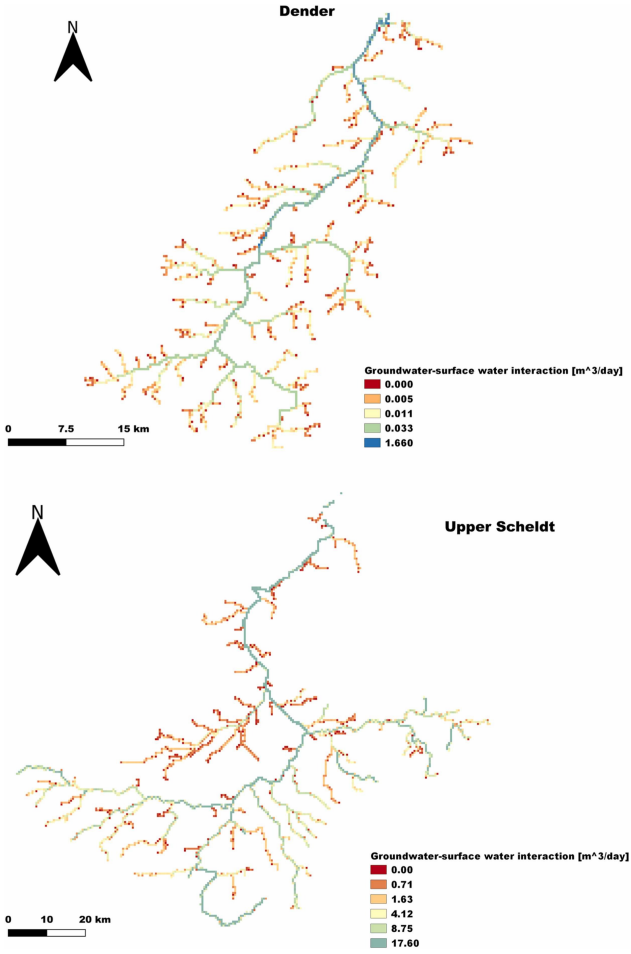


Figure 4.30: Groundwater-surface water interaction in the seven watersheds during summer time (1st August 2007). The numbers stand for minimum, quartiles (three or four quartiles), and maximum values of GW-SW interactions. As for the Leie, the third quartile and maximum values are the same. As indicated in the previous figure, the USC and Leie watersheds constitute significant baseflow

Discussion

The SWAT+gwflow coupled model produced results within reasonable computation time, where running the models took minutes on a personal computer. The only issue working with this model is the extended time needed to calibrate the model with PEST, which is attributed mainly to the existence of different hydraulic conductivity zones that make the number of parameters to be calibrated high. However, due to our approach of reducing the

number of zones based on areal coverage (small zones are removed from the calibration), the calibration time has decreased. Small-scale applications of coupled models (Galbiati et al., 2006; Guzman et al., 2015; Kim et al., 2008; Luo and Sophocleous, 2011; Menking et al., 2003; Sophocleous et al., 1999) neglect basin-wide interactions, hence, the regional application as done on the Scheldt basin by accounting this interaction helps to simulate and understand the regional scale geohydrology.

The model parameters have physical meaning, hence, it was easy to fix their minimum and maximum value and assess the final calibrated parameter values. For example, the hydraulic conductivity and specific yield are within the range suggested in Dams et al. (2009) for the Kleine Nete watershed. The calibrated model parameter values for the Dijle–Zenne watershed are similar to those obtained by Wossenyeleh et al. (2021). The parameters can indicate the geohydrological variability among the seven watersheds which is shown with distinct surface and groundwater-related parameters.

Using the coupled model, we can better understand hydrologic fluxes, particularly GW–SW interaction, in the study basin. Since such interactions have not been measured in the field, this study needs to be verified using measurement data. There are several methods to measure such interactions, for example, using tracer test (Harvey and Bencala, 1993), permeameter, and seepage meter (Avery, 1994), based on streambed temperature (Conant Jr, 2004; Devito et al., 1996; Fryar et al., 2000; Keery et al., 2007; Silliman and Booth, 1993), electrical resistivity Nyquist et al. (2008) and measuring streamflow at baseflow condition. The increasing trend in the amount of water being discharged from the aquifer into the rivers inside the Scheldt basin indicates the need to assess this interaction which can affect water quality (Lamontagne et al., 2005), wetland processes (Jolly et al., 2008) and in general the ecological function of the various water systems (Hayashi and Rosenberry, 2001; Ludwig et al., 2005; Van der Kamp and Hayashi, 2009).

The study made by Zomlot et al. (2015a) for the whole of Flanders using the surface water model WetSpass indicated the prevalence of baseflow across the rivers. This is also confirmed in the study of Van Camp et al. (2010) using the MODFLOW model, where they estimated the baseflow to vary between 69% and 87% of streamflow. Therefore, baseflow is a crucial component to investigate inside the Scheldt basin closely, and from the streamflow simulation, it is seen that our model captures the baseflow. The variation of GW–SW interaction (which shows an increasing trend in the Scheldt basin) is vital to assess its impact on water quality and the ecological functioning of the rivers. The increasing trend can be due to the decrease in streamflow due to climate change (Guevara Ochoa et al., 2020), drought in streams (Ying et al., 2025), urbanization and land use change (Barron et al., 2013), etc., hence, increasing groundwater discharge to the rivers. The model setup we developed can also help to investigate how GW–SW interaction will evolve in a changing climate, as done by Waibel et al. (2013), which will be helpful for policymakers to act on the impact accordingly.

In addition, the annual average recharge estimated by the SWAT+gwflow model setup indicated approximately similar values as estimated by Zomlot et al. (2015) and Van Camp et al. (2010) for most of the watersheds. An additional groundwater model output is boundary inflow that shows the interaction with adjoining watersheds. This model output is essential as the impact on one watershed can affect the water–receiving aquifer, hence, integrated water resource management at a basin level is required, and this inter-basin interaction can be obtained from the coupled model (SWAT+gwflow). It is vital to calibrate the regional scale model for streamflow and groundwater head, as done for the Kleine Nete watershed, to capture the water balance components more accurately.

4.3.6 Conclusion

Large–scale studies using coupled groundwater–surface water models are rare due to complex coupling and computation issues. In this work, we evaluated a distributed (geo) hydrological model at a regional scale using global aquifer datasets and a gridded meteorological observational dataset of Belgium within seven watersheds inside the Scheldt basin (France and Belgium). We focused on groundwater-surface water interactions in the basin, as these have yet to be studied in the Scheldt basin spatially and temporally.

The streamflow in all the catchments was simulated very well, with NSE values above 0.6 for both calibration and validation using daily and monthly streamflow values. In addition, the model output evaluation is performed using additional independent gauging stations (validation gauging stations). The result suggests a good agreement between measured and modeled streamflow with NSE values above 0.46, signifying that the SWAT+gwflow model represents well streamflow in a large part of the Scheldt basin. Moreover, the gridded dataset gave satisfactory results while forcing the (geo)hydrological model, implying its usefulness for such regional studies. Next, the groundwater-surface water interaction is found to be increasing over the years (from 1975 to 2021), with a strong increment found in the Grote Nete (3.7 fold) and upper Scheldt (2.3 fold) watersheds. Finally, the fact that using the global dataset (available for any location) for model development resulted in well-simulated streamflow and hydraulic head indicates the opportunity to apply this coupled model in data-scarce regions (lacking geological survey and aquifer property information). Nevertheless, the success of this modeling application does not guarantee the accuracy of the dataset for other locations, hence, further verification is required.

Chapter 5

Drought assessment in the Scheldt basin

In this chapter there are three major parts where the first part deals with assessing historical meteorological, agricultural and hydrological drought in the Schedlt basin. The second part evaluates the impact of climate change on streamflow in seven watersheds inside the Scheldt basin. Finally, similar assessment is done on groundwater hydrology of the Kleine Nete catchment.

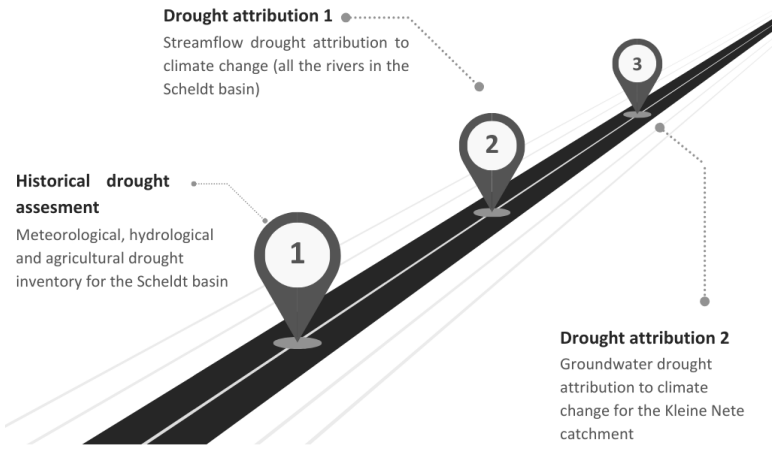


Figure 5.1: Major parts of Chapter 5 which focuses on drought assessment

5.1 A coupled SWAT+gwflow model application for comprehensive drought analysis in the Scheldt Basin

5.1.1 Summary

Drought affected millions of people across the globe, yet, it remains underexplored. Although the geohydrological functioning of watersheds is studied well using models, less has been done to develop comprehensive methodology for an easy understanding of drought using the outputs of these models. Thus, three major tasks were performed: 1) Assess the three types of droughts, namely, meteorological, hydrological, and agricultural droughts for seven watersheds inside the Scheldt River basin using the Standardized Index-Based (SIB) and Threshold-Based (TB) methods. Henceforth, these two methods are compared to identifying historical periods. 2) Develop a simplified algorithm to conduct Goodness of Fit (GoF) tests at different locations within all watersheds to determine the optimal statistical distribution for drought analysis using the SIB method. 3) Perform drought propagation analysis focusing on the-time lag between meteorological and hydrological droughts.

Both SIB and TB methods have their respective advantages and disadvantages; therefore, a combination of these methods shall be used for future studies. For the SIB method, higher variability in statistical distributions selection is seen for streamflow droughts than meteorological droughts across all watersheds. A longer accumulation period in streamflow drought favored the gamma distribution, while meteorological drought predominantly followed the Generalized Extreme value distribution. Moreover, the necessity of conducting GoF tests on distributions was evident. This was because soil moisture and groundwater heads for agricultural and hydrological drought showed high rejection frequencies for which the SIB was not used to assess these drought types. The identified droughts by either SIB or TB methods showed reasonable alignment with reported historical drought events, validating its potential for application in real time. The drought propagation analysis revealed that the lag times of streamflow and groundwater were found to be relatively close in magnitude, indicating the impact meteorological drought can cause to both streams and aquifers nearly at the same time. This offers valuable insights for drought management policies in the Scheldt basin.

This section is under draft stage: **Yimer, E. A.**, Alula, K., T., Nossent, J., & van Griensven, A. (2025). Comparing drought analysis methodologies for accurately capturing historical meteorological, agricultural and hydrological droughts.

5.1.2 Introduction

The final choice of statistical distribution function in previous drought studies (Stagge et al., 2015; Yimer et al., 2022; Vicente-Serrano et al., 2010; Mishra et al., 2010; Dayal et al., 2018) after a GoF test recommends one distribution function overlooking the variability of statistical distributions spatially and at different temporal scales. Furthermore, since the calculation procedure of the hydrological and agricultural drought indices is similar to that of SPEI and/or SPI, as observed in Bhuiyan (2004) and Hao et al. (2014), it is also important to look at the distribution variability of other indices. In addition, the use and comparison of different drought analysis methods, notably the SIB and TB approaches in evaluating historical drought events is also an important insight that will be raised. Finally, drought propagation from meteorological to hydrological will be investigated. Through these rigorous analyses, drought assessment methodologies will be enhanced to increase their accuracy and reliability, thereby facilitating the development of more robust water resource management strategies.

5.1.3 Study area and Data

The research region shown in Fig. 4.22 primarily includes the seven watersheds in the northern portion of Belgium and the eastern part of France, including the Demer, Dender, Grote Nete, Dijle & Zenne, Kleine Nete, Leie, and Upper Scheldt. Henceforth, for convenience, Dijle and Zenne will be referred to as Dijle throughout this study. The data used for this analysis comes from the model outputs of the coupled regional model in Chapter 4. The meteorological and agricultural droughts are assessed at the HRU level, while the hydrological drought is investigated at each river stretch and observation well for streamflow and groundwater drought assessment, respectively.

5.1.4 Methodology

For the Meteorological drought index using standardized index-based method (SIB), candidate probability distributions typically call for a location parameter because the climatic water balance is not constrained by zero and can have negative values if PET exceeds Precipitation (Stagge et al., 2015). The Generalized Logistic, Generalized Extreme Value (GEV), and Pearson Type III distributions are among the distributions compared for SPEI as done in Stagge et al. (2015). For detailed description of SIB method, the reader is advised to refer to Chapter 2.

Two-parameter distributions were taken for use with non-negative hydrometeorological variables like recharge, soil moisture, streamflow, and groundwater. These include the following: Gamma, Logistic, Log-Logistic, Lognormal, Weibull minimum, Weibull maximum, and Normal.

Since evaluating the associated statistical distribution function is vital, the Shapiro–Wilk test (S–W), was used. This test is comparable to the traditional GoF tests and evaluates a

given dataset's normality (Stagge et al., 2015). In other words, normality was tested when transforming the cumulative distribution functions to the standardized normal distribution when estimating drought indices.

The following hypothesis-based test was put forth by Shapiro and Wilk (1965) to test the composite hypothesis of normality using a univariate random sample of size $n, X_1, X_2, \ldots, X_n$:

$$W = \frac{\sum_{i=1}^{n} a_i X_i}{\sum_{i=1}^{n} (X_i - \text{mean}(X))} \tag{5.1}$$

where $\bar{X}$ denotes the mean of the univariate random sample. Considering a typical normal random sample of size n, the a_i values represent elements of a vector that is a function of the expected values and the covariance matrix of the order statistics vector.

The 3-month accumulation period is used to study short-term meteorological drought, labeled as 'short-term meteorological drought'. Henceforth, the long-term meteorological drought was examined using the 6-month accumulation period for SPEI and was termed 'long-term meteorological drought'.

Using the TB method, a drought occurs when the variable of interest (P-PET, streamflow, soil moisture, or groundwater head) falls below a predetermined threshold (Yevjevich, 1967). This method deals with deficits of water and thus has a significant benefit in managing water resources (Van Loon, 2015). A variable threshold was used to account for the seasonal variation of variables, which is depicted in Fig. 2.2. Drought events begin when the variable falls below the threshold level and lasts for at least two months until the threshold was again exceeded.

The 80^{th} percentile variable threshold was used to examine meteorological drought using the climatic water balance. It should be noted that these percentiles refer to exceedance probabilities; therefore, $80th$ percentile thresholds refer to values for which 80% of the data are above and 20% of the data are below.

When considering flux variables such as precipitation and streamflow, the deficit volume was the most frequently used proxy of severity. It was estimated by summing up the respective values under the threshold (Hisdal et al., 2024). For state hydrometeorological variables (soil moisture and groundwater head), the maximum value was taken instead of the sum from the given drought event because taking the sum (volume) of state variables is physically senseless (Tallaksen et al., 2009). Hence, the term 'Deficit' was used when analyzing 'flux variables, and the term 'Deviation' was used when analyzing state variables.

For the analysis of drought propagation, the threshold-based method outlined above was used. The Kleine Nete watershed is used to analyze drought propagation as it was calibrated and validated for streamflow and groundwater head as outlined in Yimer et al. (2023b).

5.1.5 Results

Distribution function selection

After running the simplified algorithm for statistical distributions, the overall rejection frequency was plotted after aggregating it for each of the seven catchments. It is observed that for meteorological drought analysis using the SIB method, the statistical distributions have been fully accepted (rejection frequency of 0%) for at least one distribution for all catchments, as shown in Fig. 8.1.

It is observed that generalized extreme distribution spatially dominates for both long–term (6-month accumulation period) and short-term (3-month accumulation period) droughts for all 7 catchments. Catchments such as the Dijle and Leie had occurrences where the Pearson type III and generalized logistic distributions were used for the short-term drought, as shown in Fig. 5.2. Additionally, catchments such as the Keine Nete, Grote Nete, and Dijle had occurrences of the generalized logistic distribution for long term drought. The rejection frequency value attained for generalized extreme distribution at those particular subbasins is on average 17%.

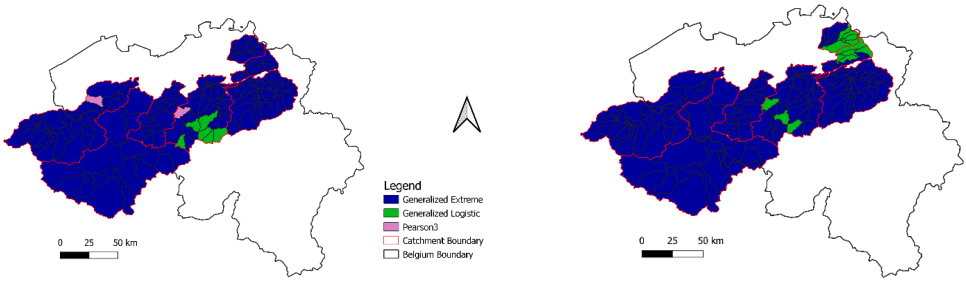


Figure 5.2: Spatial plots of distribution functions for shortterm (left) and longterm (right) meteorological droughts respectively

For agricultural drought, the overall rejection plot aggregated over each catchment shows a relatively high rejection frequency as compared to meteorological drought. The Kleine Nete catchment stands out the most, with both the short-term and long-term drought events having rejection frequencies greater than 80%, as shown in Fig. 8.2. Moreover, the Demer catchment shows rejection frequencies above 25% except for the 12-month accumulation period. Hence, for agricultural drought, rejection frequencies above the 25% limit would lead to uncertainties when estimating drought events. Due to that reason, only the threshold-based method is used to analyze agricultural drought.

For streamflow, rejection frequencies less than 10% are observed for at least one of the distributions for all catchments except the Grote Nete (Fig. 8.3). The normal and Weibull max distributions are observed to have rejection frequencies higher than 25%. It is also

shown in the spatial plots of Fig. 5.3, distributions are more evenly distributed spatially for short-term droughts as compared to long-term droughts. In addition, for long-term droughts, the Gamma distribution is spatially dominant for all seven catchments.

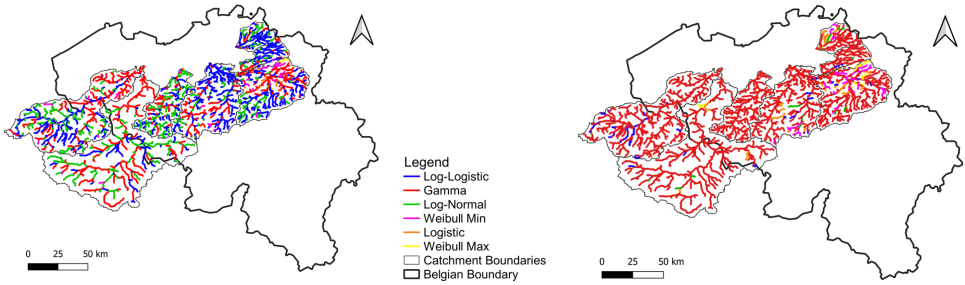


Figure 5.3: Spatial plots of distribution functions for shortterm (left) and longterm (right) streamflow droughts respectively

When looking at groundwater heads at different sites within the Kleine Nete watershed, the rejection frequencies are relatively high, surpassing the threshold of 25% as shown in Fig. 5.4. There was an instance where, for the third accumulation period for the Weibull max distribution, it was observed that the rejection frequency was just below 25%. However, all other distributions and accumulation periods show that the SIB method for groundwater will not give reliable results similar to that of soil moisture. Hence, the TB method is employed for the analysis of groundwater drought.

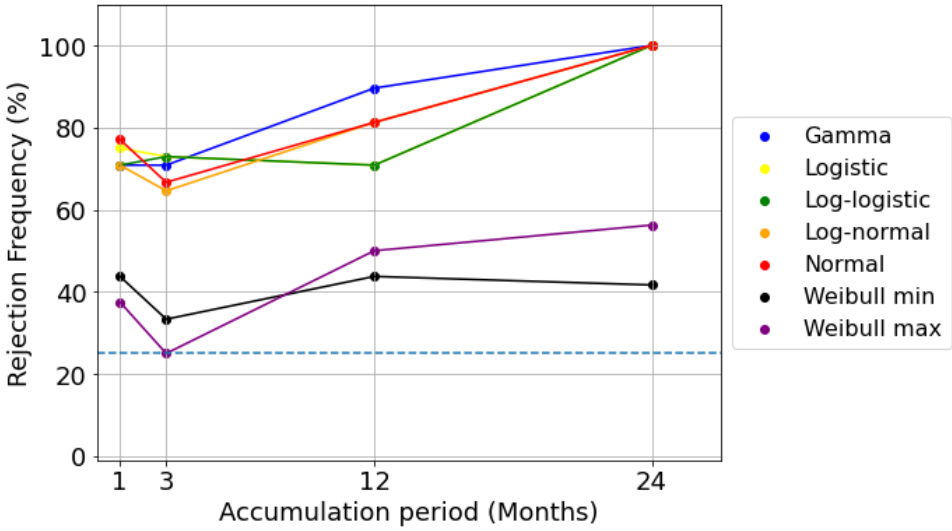


Figure 5.4: Overall rejection frequency plots using groundwater head for Kleine Nete, 25% represents limit of rejection frequency

Historical drought assessment

A. Meteorological drought

Standardized index based assessment

The correlation analysis in Fig. 8.4 shows that the highest median Pearson correlation coefficient (R-value) when comparing SSI-1 with SPEI-1, SPEI-2, SPEI-3, SPEI-6, SPEI-9, SPEI-12, and SPEI-24 is attained at SPEI-3. Catchments such as the Leie, Kleine Nete, Dender, USC, and Demer exhibited the highest R-value at SPEI 3. In contrast, Grote Nete and Dijle exhibited the highest Pearson correlation coefficient at SPEI-1.

Although the R-value for the 3-month accumulation period is higher, the 6-month accumulation period still shows R-values greater than 0.48 across all watersheds, indicating a 'Moderate' to 'Strong' correlation according to Schober et al. (2018). Additionally, the 3- month accumulation period was already used to study short-term meteorological drought due to the operational use of this accumulation period by the Flemish Environmental Agency (VMM) and to be consistent and keep the comparability of our result with the historical drought periods recorded by documents basing this accumulation period to assess short-term drought events. Henceforth, the long-term meteorological drought was examined using the 6-month accumulation period for SPEI and was termed 'long-term meteorological drought'. Moreover, it was also observed that the 1 and 3-month accumulation periods have Pearson correlation coefficients greater than 0.5 for all watersheds. Neverthe-

less, Pearson correlation coefficients decrease for all watersheds as the accumulation period increases.

All the major drought events that occurred in Belgium in 1976, 1995, and from 2017 to 2020 are identified by the analysis we made. In Fig. 5.5 and Fig. 8.5, the x-axis refer to the starting dates of droughts for all the seven catchments. Additionally, the longest short-term drought in the summer of 1976 lasted nine months and occurred in all catchments except the Upper Scheldt Catchment (USC). The most severe short-term drought, with a severity score above 10, also commenced in 1976 in the Leie catchment. The historical period's most intense short-term drought events had onsets between 2017 and 2021. The 2011 drought began in March and April across all seven watersheds, while the 2017 drought started in May and June for the Dender, Dijle, Leie, and Upper-Scheldt catchments.

Moreover, drought events decrease in frequency when transitioning from short-term to long-term droughts. The drought events that began in 1976 and 2018, evident in all catchments, are also visible in long-term analyses (Fig. 8.5), indicating their serious impact on streamflow, reservoir levels, and/or groundwater heads. However, this needs to be further verified by conducting analyses on streamflow and groundwater droughts.

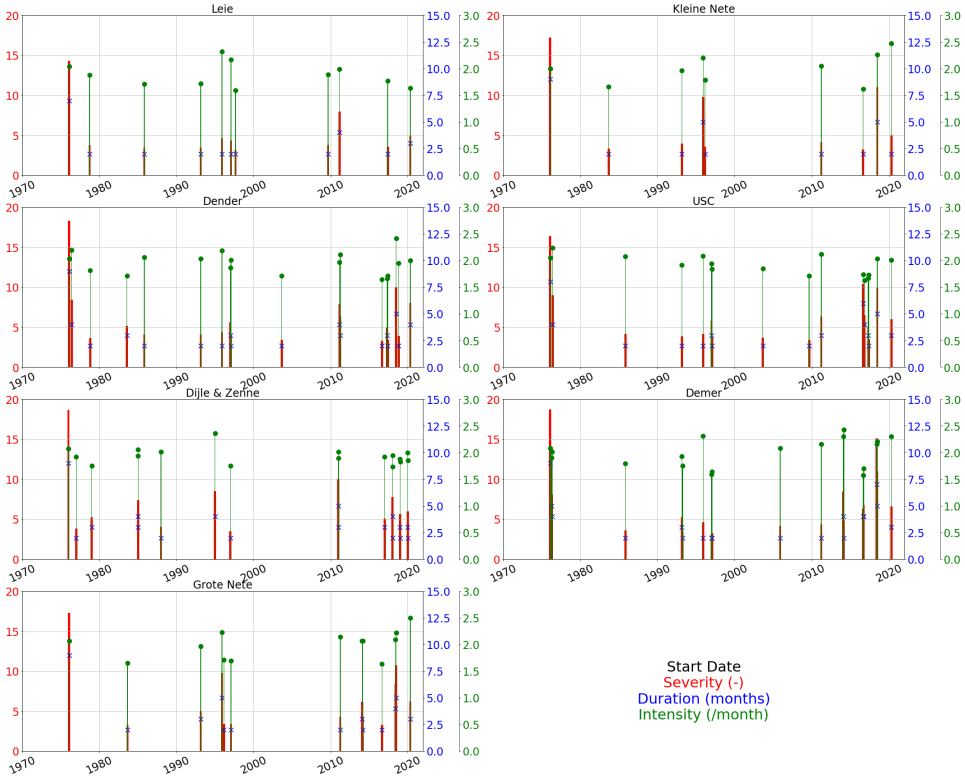


Figure 5.5: Summary of short-term meteorological drought events for all catchments (obtained at SPEI < -1.5)

Threshold Based Method

Based on the TB method, the 1976 drought event exhibited deficits greater than 150 mm for all seven catchments, supporting the significant 1976 short-term meteorological drought estimated using the SIB method, as shown in Fig. 5.6. Furthermore, the drought events that occurred in the summer of 1995 had deficits above 45 mm across all seven watersheds. In May 2017, the Leie, Kleine Nete, Dender, and Upper Scheldt catchments experienced deficits greater than 50 mm, while the other watersheds had deficits between 30 and 40 mm. The spring 2018 drought events resulted in deficits greater than 100 mm in the Leie, Upper Scheldt, and Dender catchments, with the rest of the catchments experiencing deficits greater than 150 mm for that year.



Figure 5.6: Summary of meteorological drought events for all catchments using Threshold based method

B. Agricultural drought

Threshold Based Method

Based on the TB method, agricultural drought events were observed in the spring of 2011 in the Leie, Grote Nete, Kleine Nete, Dender, and Upper Scheldt Catchment, with deviation ranging from approximately 0.6 to 2 mm. From April to May 2017, soil moisture deviations ranging from 0.6 to 1.5 mm were observed in the Leie, Kleine Nete, Dender, and USC watersheds, as shown in Fig. 5.7. In the summer of 2018, deviations ranging from 0.8 to 1.2 mm were recorded in the Kleine Nete, USC, Dender, and Grote Nete catchments. The relatively high deficit in 2018 was surpassed by drought periods in the summer of 1975 in the Grote Nete catchment with a deficit of 2 mm. In the summer of 2019, deviations less than 0.5 mm were observed in the Leie and USC.

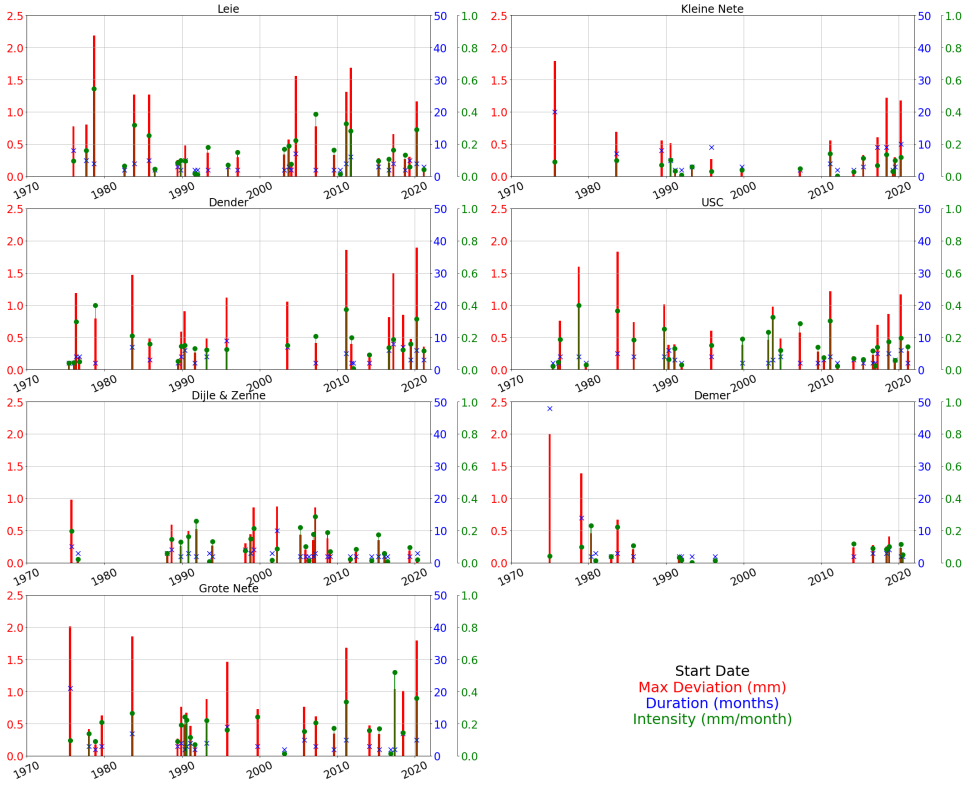


Figure 5.7: Summary of agricultural drought events for all catchments using Threshold based method

C. Hydrological drought

Standardized Index-Based Method

The major streamflow drought event of 1976 is evident in all catchments, supporting findings from long-term meteorological drought studies. This year also experienced the most severe drought across all catchments, as shown in Fig. 5.8 and Fig. 8.6. Drought events from the summer of 2018 were observed in the Kleine Nete and Upper Scheldt for short-term durations and in the Kleine Nete, Upper Scheldt, Demer, Dender, and Grote Nete for long-term durations. The longest short-term drought event occurred in the Upper Scheldt and Demer catchments, lasting eight months. The 1995-96 (late 1995 and early 1996) drought events affected all catchments in the short term, except for the Demer and Dijle, with a maximum severity score of 7. These events also impacted all catchments in the long term, with a maximum severity score of approximately 20.

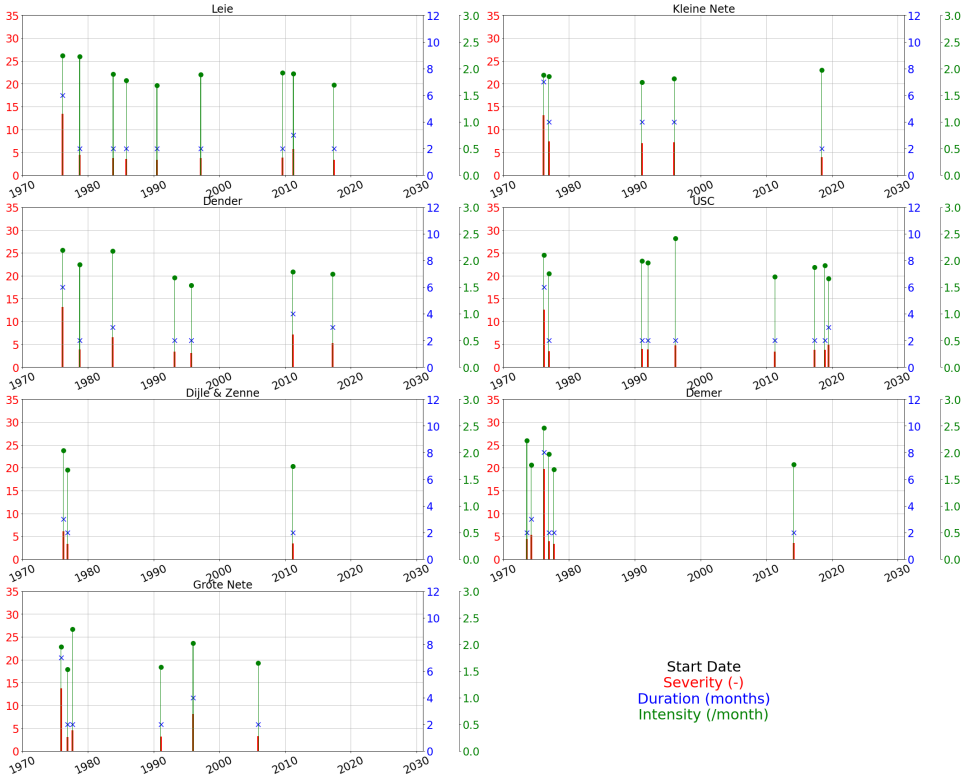


Figure 5.8: Summary of short-term streamflow drought events for all catchments (SSI < -1.5, 1-month accumulation period)

Threshold Based Method (Streamflow)

The 1976 drought was clearly observed using the TB method, which was applied to streamflow, as shown in Fig. 5.9. Particularly, the Leie catchment experienced a monthly streamflow deficit of approximately 32 m³/s during this event, and lasted about 6 months. The Upper-Scheldt and the Demer followed, with monthly streamflow deficits of 27 m³/s and 22 m³/s and durations of 6 and 9 months, respectively, in the same year. The rest of the watersheds experienced monthly streamflow deficits of less than 10 m³/s in 1976. In late 1995 and early 1996, all watersheds exhibited comparable intensities to the 1976 drought events, with deficits ranging from 0.7 to 11 m³/s. These hydrological drought events can be attributed to the meteorological drought events that occurred in 1995 and 1996. Hydrological drought events observed using the SIB method in the summer of 2018 in the Kleine Nete, Demer, Dender, and Upper Scheldt were also observed using the TB method, with intensities ranging from approximately 0.3 to 13 m³/s.

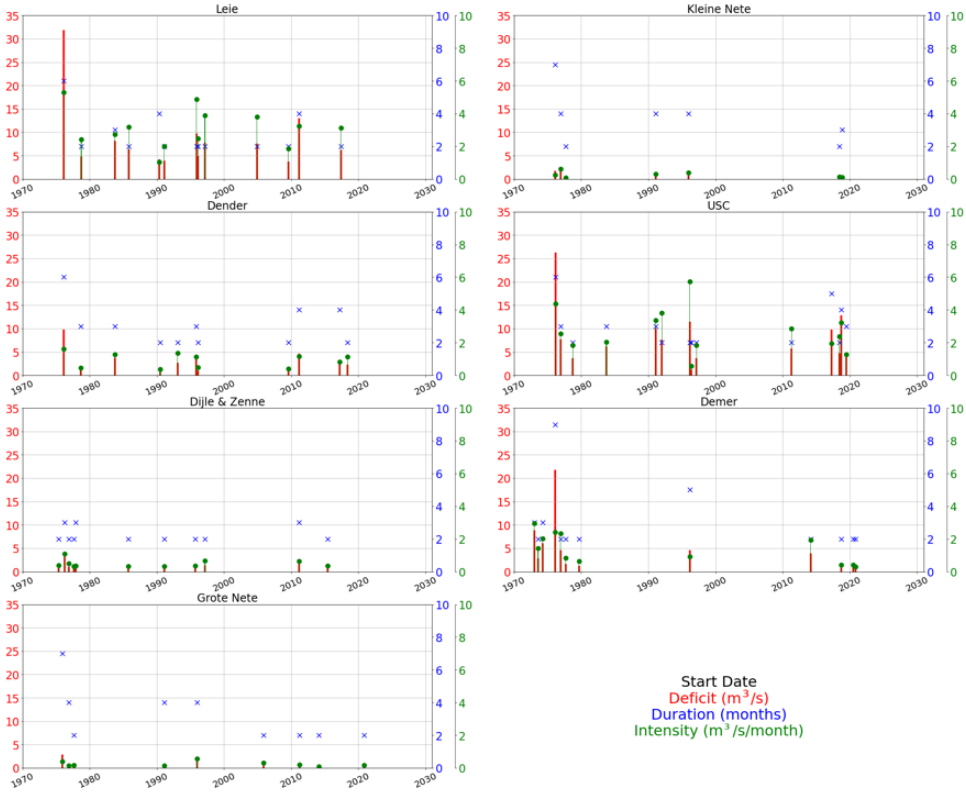


Figure 5.9: Summary of streamflow droughts using the TB method for all catchments

Threshold Based Method (Groundwater Head)

Four well locations within the Kleine Nete were used to assess drought over the catchment, as shown in Fig. 5.10. These are Lille 2, Turnhout, Arendonk, and Beerse. When analyzing the groundwater head at these locations using the TB method, several major drought events were identified, notably in 1976, 1995-96, 2011, and 2017-2020. The drought event in early 1976 was particularly severe, with a deviation of 4.3 meters and a duration of up to 15 months, making it the most extreme event recorded. In comparison, the drought in the fall of 2018 exhibited a deviation of approximately 3.5 meters, with a duration ranging from 5 to 10 months across different sites within the watershed.

Overall, the years 1976 and 2018 experienced the highest deviations in groundwater heads across all sites in the Kleine Nete. Additionally, drought events were noted in June and July of 2017 and August of 2019, though these were of smaller magnitudes. The 2017 drought lasted between 3 and 6 months, while the 2019 drought lasted about 2 months.

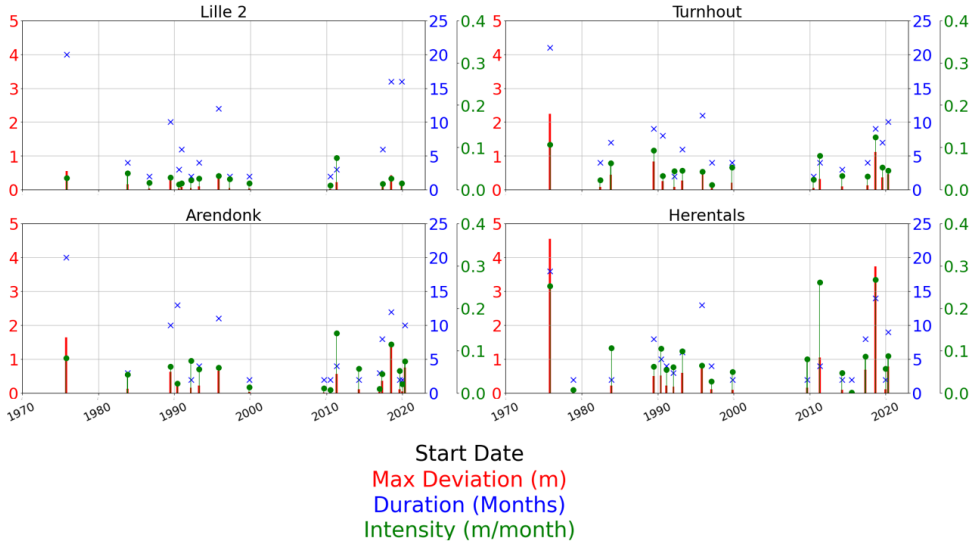


Figure 5.10: Summary of groundwater droughts using TB method for different sites within Kleine Nete

5.1.6 Discussion

Optimization of distributions

From the results, it was observed that SPEI distributions exhibit lower rejection rates, indicating that the cumulative climatic water balance is more easily fitted with the available parametric distributions. This is partly owing to the additional location parameter but more likely due to the unbounded nature of climatic water balance, which eliminates the need to fit a piecewise distribution with a limit of zero (Stagge et al., 2015). The results where the majority of the statistical distribution function used was found to be Generalized Extreme distribution for the climatic water balance are concurrent with the findings of Stagge et al. (2015) for both long-term and short-term meteorological droughts. However, there was an instance where the distribution chosen was the generalized logistic and Pearson type III for particular subbasins. In these subbasins, the rejection frequency value attained for generalized extreme distribution was on average 17%. Although this is an acceptable value according to Stagge et al. (2015), the algorithm we developed still chose the distributions with less rejection frequencies at the particular subbasins.

Regarding streamflow drought, a higher spatial variability of statistical distributions is observed for short and long-term droughts. In addition, the study of Vicente-Serrano et al. (2012), found that no single probability distribution for all the series was appropriate for obtaining a robust standardized streamflow series. This is also seen in the results as the spatial variation of the candidate distributions for streamflow was more prominent than that of

climatic water balance for all seven catchments and for both short and longterm droughts.

When looking at soil moisture data and groundwater heads simulated by SWAT+gwflow, the majority of the distributions showed relatively high rejection frequencies. The implication is that, for example, if the rejection frequency is 25%, it means that 25% of the 12 months from the whole time series rejects the null hypothesis. In other words, there is not enough evidence to indicate that the standardized index time series values come from a normal distribution. A rejection frequency of 0% is what is highly preferred because it will indicate that the null hypothesis is accepted for all months over the whole length of the time series as per the SW test. This will indicate that the process of converting the fitted datasets to a standard normal distribution went correctly, indirectly implying that the data fitting is acceptable. However, high rejection frequencies imply that conducting drought analysis by directly using soil moisture and groundwater head data using the SIB method can be challenging in this particular case. Furthermore, it was also seen in the study of Ahmad et al. (2010) where soil moisture data was found to be challenging to fit into a statistical distribution since it is spatially erratic and is impacted by factors such as vegetation cover and soil characteristics. In addition, geographic variations in the relative intensities of components such as seasonality, evaporation, runoff, and land-atmosphere interaction make it challenging to fit soil moisture data into statistical distributions (Koster and Suarez, 2001). Similarly, Smith and Freeze (1979) highlighted that groundwater head data is difficult to fit into a statistical distribution because of regional trends in hydraulic conductivity and the requirement to take the flow system and conductivity within the flow domain into account. In addition, Freeze (1975) mentioned that it is challenging to fit groundwater head data into a statistical distribution because the degree of uncertainty rises with the porous medium's degree of nonuniformity.

Short-term meteorological and soil moisture drought events

The major drought events that occurred in Belgium were further verified by the Royal Meteorological Institute (RMI), in which the years 1995-1996, 1975-1976, and 2016-2017 were found to be the lowest rainfall totals for a period of 12 months from measurements taken at Brussels–Uccle where measurements were taken starting from 1833 (KMI, 2017). The drought period that started in early 1976 and ended in August of 1976 was also observed in Kleine Nete and Grote Nete and was also reported in KMI (2017). Furthermore, the high heat and drought event in 1976 caused a number of forest fires, particularly in Antwerp and Limburg Kempen (KMI, 2017). Moreover, due to the 1976 event, the government had to put severe limitations on potable water usage to counteract more significant impacts.

In addition, the short-term meteorological drought event of 2018 (events estimated using SPEI < -1.5) was reported in CIW (2018). This report also outlined that in 2018 the basins of the Upper Scheldt, Dender, and Demer were affected concurrent. Moreover, all basins had abnormally dry conditions from the end of September to the end of October 2018 which shows the immediate response of the short-term drought in the basins (CIW, 2018). Furthermore, April through June of 2017 was an abnormally dry month, particularly in the

west of Flanders (CIW, 2017). This was in line with what was observed for the Leie, in which June and July were under drought. A drought event starting in September was also reported in CIW (2019) which was observed in the Dijle watershed.

The agricultural drought inferred from the short-term meteorological drought was also validated by VMM (2021) using the recognized agricultural disasters where data is available as of 2011. Based on that, the 2011 drought that had an onset in March and April for all seven watersheds was distinctly observed from the outputs of the analysis. This period coincides with the agricultural disaster of 2011 for flax and spinach that occurred throughout Flanders (VMM, 2021). Moreover, one of the agricultural drought events using the TB method coincides with the 2011 agricultural disaster in Flanders. In addition, drought events starting within 2017 also led to financial damage of 98 Million euros; particularly in the regions of West and East Flanders (VMM, 2021). These drought events were also quantified using the TB method and were found to have deficits in the spring of 2017, which was also the time of the disaster. Moreover, the 2018 agricultural disaster also had a significant impact (VMM, 2021). It was reported to be worse than the one from 2017 affecting the Flemish area with an estimated financial damage amounting to 457 Million Euros. These events were also shown in the summer of 2018, enabling the approximate quantification of the water deficit the crops were experiencing. Drought events from September 2019 also affected specific crop types in the western part of Flanders. However, using SPEI at the 3–month scale only shows this event in the Dijle watershed requiring the analysis of soil moisture drought. So, estimating the soil moisture drought events using the TB method showed that in the catchments located in the western part of Flanders (Leie and Upper-Scheldt), soil moisture deficits were observed in the summer of 2019. These deficits coincided with the drought disaster in 2019, as reported in VMM (2021). This validation, based on officially recognized agricultural disasters and documented losses across the seven watersheds, is useful for operational drought early warning management in the larger Scheldt basin by applying an appropriate method and accumulation period.

Hydrological and long-term meteorological drought

The 3–month Accumulation period showing the highest correlation for five out of seven watersheds indicates a strong positive relationship between SPEI and SSI. It can be inferred that streamflow drought at 1 month accumulation period strongly follows meteorological drought at the 3–month accumulation period. Hence, SPEI at the 3–month scale can be used to investigate streamflow drought.

Additionally, it was mentioned in Mishra et al. (2010) that streamflow drought is generally characterized by longer accumulation periods (12, 24, etc.) of SPEI showing the 1 and 3-month are relatively low accumulation periods for which high correlations were attained. On the contrary, Baez-Villanueva et al. (2024) outlined that there is not a given accumulation period that best characterizes streamflow drought. The determination of the proper temporal scale depends on the catchment memory of each watershed. For instance, the Kleine Nete watershed is characterized by a quick response time due to its hydrological

features such as an extensive ditch network that facilitates the drainage of excess water (Yimer et al., 2023b). Hence the high R-values attained might be attributed to the river networks in the watersheds responding quickly to meteorological drought events at 3–month accumulation periods.

Hydrological drought events happening in the short and long-term are designated as droughts that last long and significantly impact the ecological flow. Meteorological drought events that occur in the long-term are designated as being streamflow droughts. This is in line with the arguments made by Sur et al. (2020) and Zhu et al. (2016) that long–term meteorological droughts can be used to characterize hydrological droughts. Also, VMM uses SPEI-3 for short-term drought assessment and the Pearson correlation coefficient difference between 3-month and 6-month are in the range of 0.1. Hence, after comparing the Pearson correlation coefficients for SSI–1 and different SPEI accumulation periods, the 6–month SPEI best characterizes long-term streamflow droughts.

Accordingly, the 2018 summer drought events observed in all catchments except the Leie and Dijle are in line with the findings of VMM (2021). It was mentioned in this report that, beginning from spring of 2018, discharges along the non–navigable streams also decreased gradually, reaching the lowest flow values. Moreover, the fall of 2018 in the Kleine Nete for the longterm meteorological drought showed that there were 'Severely Dry' events. Similarly, 2nd highest groundwater deviations in the Kleine Nete are observed in the fall of 2018. This indicates how strong of an indicator the high accumulation period meteorological drought can be for long-term droughts. The groundwater drought events that were observed in 2018 and these were also reported by VMM (2021). It was outlined that in the periods from the second half of June to the beginning of July 2017 and from the second half of July 2018 to December 2018 (for absolute groundwater levels), 50% or more of the available groundwater measuring locations in Flanders have a very low status.

The 1976 drought events, where the end dates were in the summer of the year, were found to be even more severe than that of 2018. Moreover, the 1976 events, observed as both short-term and long-term streamflow droughts, are also visibly seen in the long-term meteorological drought. This indicates that while looking at the 6-month accumulation period of meteorological droughts, the 1976 drought is partly transitioning to streamflow deficits. The long-term meteorological drought events are also visible in the Kleine Nete in early 1976, which agrees with what is seen in the groundwater deviations in early 1976. In addition, the hydrological drought events in 1976 persisted both in the short and long term when looking at streamflow for all catchments, exemplifying the significant impact it had on streamflow. From this, it can be inferred that the drought event in 1976 had a significant impact on all three types of drought considered in this study. Also, the 2018 short- and long-term hydrological droughts persisted in Kleine Nete. Moreover, the 2018 long-term meteorological drought persisted for the Upper-Scheldt.

The drought events observed in late 1995 and late 1996 in the groundwater sites of the

Kleine Nete further show the propagation of drought meteorological to groundwater drought. These events from the mid–90s are also seen in the streamflow drought for all catchments. This further shows how the long-term meteorological drought is propagating toward hydrological drought. In other words, these hydrological drought events are attributed to the response to multiple meteorological droughts that occurred in 1995 and 1996. Note that the maximum deficit observed on the 1976 groundwater drought needs careful assessment as deficit values on the range of 3 to 4 meters are unrealistic.

From the end of June to the end of September 2019, there were only a few episodes of consistent precipitation. In several places in Flanders, this resulted in record low water levels and flows in non-navigable watercourses or the drying up of watercourses that depend on a source flow where no drying ordinarily happens (VMM, 2021). This assessment was in line with the Upper-Scheldt catchment where both short and long term hydrological drought was observed in the summer of 2019.

5.1.7 Conclusion

This study developed methodology and open source scripts to analyze model outputs from SWAT+gwflow and/or SWAT+ for a comprehensive drought assessment. The tool evaluates three types of droughts: Meteorological, Agricultural, and Hydrological. These evaluations are conducted using two primary methods: the Threshold-Based method and the Standardized Index–Based (SIB) method. Appropriate distribution selection for estimating each drought type is conducted for the SIB method. Further analysis, such as drought propagation, was performed to provide valuable insights.

Using the SIB method, higher spatial variability of statistical distributions for streamflow droughts compared to meteorological droughts was observed across all studied watersheds. Moreover, longer time scales of streamflow droughts tended towards a more uniform choice of statistical distributions, predominantly the Gamma distributions. For meteorological droughts, the generalized extreme value distribution emerged as dominant both spatially and across various time scales for the seven studied watersheds. Consequently, the necessity of conducting Goodness–of–Fit (GoF) tests on statistical distributions when applying the SIB method of drought analysis was established, as distributions can vary spatially and over different accumulation periods. Moreover, the comprehensive assessment was applied to seven watersheds in Belgium and parts of France, and the outputs aligned well with drought events reported by VMM (2021), CIW (2017), CIW (2018), and CIW (2019). This concurrence suggests that the tool can be effectively used in real-time to analyze droughts in other watersheds by taking the outputs of the SWAT+gwflow and/or SWAT+ model.

Finally, the analysis of drought propagation revealed that streamflow and groundwater droughts respond similarly in terms of lag time to meteorological drought events. These response times were quantified and approximated on average as 12 and 14 months. This is a valuable information to assist in formulating effective drought mitigation policies.

5.2 Attributing climate change impact on streamflow decrease at regional scale using coupled surface – groundwater model

5.2.1 Summary

Drought is global disaster influenced by either climate change or unsustainable human activities that seriously impact the economy, environment and people. Yet, catchment scale attribution studies that separate natural climate variability from anthropogenic human impacts are still limited. The present study employed both factual (with climate change) and counterfactual (without climate change) climate datasets from the Inter-Sectoral Impact Model Intercomparison Project (ISIMIP3a) impact attribution setup to solely quantify the role of climate change in seven watersheds inside the Scheldt river basin, Belgium. Both datasets were forced into a fully distributed and physically based model where water balance components and their uncertainty and trends, streamflow, drought deficit and duration were investigated.

Results showed non-significant decrease in annual precipitation while evapotranspiration (ET) increased significantly. Runoff, percolation and soil moisture showed significant decrease except in the Kleine Nete and Grote Nete catchments. Seasonal analysis revealed large decreases in winter and spring precipitation, winter and autumn runoff, and spring ET. Notably, streamflow indicated a significant decrease attributed to climate change in all the watersheds. The low flows decreased between 3.5 and 14%. The cumulative drought deficit showed the highest impact on the Upper Scheldt catchment. Furthermore, the Upper Scheldt and Leie basins experienced an average increase in streamflow deficit of about 10 m3/s. Similarly, drought duration increased due to climate change. Uncertainty analysis indicated a decrease in precipitation, runoff, percolation and soil moisture depth with an increase in ET leading to increased drought deficit and duration. Therefore, in the Scheldt river basin, the impact of climate change is evident and policy makers and water managers should consider appropriate measures based on the drought deficit that is estimated by prioritizing watersheds according to the severity of the impact.

This section is to be submitted as: **Yimer, E. A.**, Lien, D.T, Erasto, B.M, Elsaidy, A.,, Nossent, J., & van Griensven, A. (2025). Attributing climate change impact on streamflow decrease at regional scale using coupled surface – groundwater model.

5.2.2 Introduction

Climate variability, land cover changes, and catchment characteristics changes hydrological processes in river basins (Ahmed et al., 2022; De Niel and Willems, 2019). Detection and attribution of changes in natural systems offer a robust tool for understanding the complex causes of climate change, enabling the development of more effective mitigation and adaptation strategies (Didovets et al., 2024; Mondal and Mujumdar, 2012). The detection of changes examines the system change without identifying the reasons for that change, whereas attribution assesses the relative contributions of the causal factors to that change (Ahn et al., 2016; Mondal and Mujumdar, 2012). The used methods can be divided into data–based and simulation-based approaches (Gelfan et al., 2023). This can involve comparing observed discharge with detrended climate data, without climate change, or by excluding human influence in anthropogenic affected systems (Didovets et al., 2024). Studying detection is complicated by challenges such as high runoff variability, urbanization, deforestation, interactions among drivers, and short streamflow records (De Niel and Willems, 2019; Gelfan et al., 2023)

For all these analyses, a tool to simulate the geohydrological components is required. This is where geohydrological models play a role. Simulated streamflow, groundwater head, runoff, evapotranspiration (ET), percolation, and soil moisture are primarily used to perform spatiotemporal analysis of drought in watersheds (Guevara Ochoa et al., 2020). In drought attribution studies, the use of models is essential if the objective is to investigate hydrological and agricultural drought (Ding et al., 2021; Sun et al., 2023; Wang et al., 2023).

By using this new coupled surface-groundwater model, attribution work can be improved (Yimer et al., 2023c). Thus, by using well-calibrated and validated models for watersheds within the Scheldt River basin, hydrological drought is investigated. There is a clear lack of catchment-scale assessments regarding the attribution of climate change on drought, which serves as the main driver for conceiving this research article. Furthermore, uncertainty analysis arising from models has not yet been explored using catchment-scale models. Recent major drought events across Belgium have affected the entire Scheldt basin (Wossenyeleh et al., 2021). Thus, policymakers are keen to know whether climate change is a major cause and, if so, to what extent.

The major objectives of this research are as follows:

- Evaluate the differences in water balance components using factual and counterfactual data.
- Investigate whether historical hydrological drought events can be attributed to climate change.
- Determine the temporal deficit and duration of hydrological droughts.

- Assess the uncertainty of different climate detrending methods in drought characterization.

5.2.3 Study area and data

The InterSectoral Impact Model Intercomparison Project (ISIMIP) 3a is used to force the already calibrated and validated coupled SWAT+gwflow model for the Kleine Nete, Grote Nete, Demer, Dijle with Zenne, Dender, upper Scheldt and the Leie catchments. There are four different detrending methods, hence, to analyze the uncertainty, all the four dataset are used for the drought attribution.

5.2.4 Methodology

The SWAT+gwflow model

The present study utilized the current restructured version of the Soil and Water Assessment Tool (SWAT+) (Bieger et al., 2017) coupled with the gwflow module (Bailey et al., 2020a) which is a physical and semi–distributed model capable of simulating both surface and subsurface hydrological processes. It was used as the primary model to simulate discharge generation mechanisms and assess water balance components using both factual and counterfactual climate forcings of the seven watersheds in the Scheldt basin. For more details about the model, please refer to Yimer et al. (2023c).

Datasets and model setup

We used open and freely available global datasets to setup the coupled SWAT+gwflow model. Four climatic datasets, (both factual and counterfactual) were sourced from the Inter-Sectoral Impact Model Intercomparison Project (ISIMIP3a) impact attribution setup from 1901 to 2015 (https://data.isimip.org, last accessed on 05.09.2024). The factual data represented data with anthropogenic climate change while the counterfactual (detrended) data represented data without anthropogenic climate change (Mengel et al., 2021). The four datasets included the GSWP3-W5E5, 20CRv3-W5E5, 20CRv3-ERA5, and 20CRv3. The detrended versions of these datasets were derived using the ATTRICI (ATTRIbuting Climate Impacts) method, that attempts to preserve the internal variations within the observations while identifying the long–term shifts in daily climate variables that correlate with changes of global average temperature. GSWP3-W5E5 blends GSWP3 for 1901–1978 with W5E5 for 1979–2019, bias-adjusted to W5E5 for a smooth handover; 20CRv3-W5E5 does the same but uses the newer 20CRv3 reanalysis pre-1979; 20CRv3-ERA5 anchors 20CRv3 to ERA5 instead of W5E5 for 1979–2021; and 20CRv3 is unadjusted 20CRv3 (control). Further details describing each individual dataset and the detrending method can be found at Mengel et al. (2021) and https://data.isimip.org/10.48364/ISIMIP.982724.1, last accessed on 05.09.2024).

Other data for setup such as the Digital Elevation Model (DEM), soil and Land use were

also used with further details in Yimer et al. (2023c). Initially, the model was setup using observed climate variables in a QGIS interface. The model was calibrated and validated using observed discharge data for the seven watersheds. Then, the parameter structure and settings of the calibrated model were held constant while forcing the model with the four datasets from ISIMIP3a each comprising of both factual and counterfactual data. In total, eight model simulations were conducted. We utilized all the four datasets in order to account for climate input data uncertainty in our simulations.

Climate attribution of water balance components

Both the factual and counterfactual simulations at the annual and seasonal timescales for different water balance components (e.g., precipitation, runoff, evapotranspiration (ET), lateral flow, percolation and average soil water depth) were compared. This involved calculating the difference between the two simulations considering the counterfactual as the baseline. The four seasons used include the Winter (December to February), Spring (March to May), Summer (June to August) and Autumn (September to November). These were summed for each year and compared for factual and counterfactual scenarios.

Further analysis involved the utilization of the classical non–parametric Mann–Kendall (MK) approach Kendall (1948); Mann (1945) to detect trends in the timeseries of various water balance components and their significance. One indication that a change in a system is attributed to climate change is when we observe statistically significant trends in model simulations using factual data, but non–significant trends in model simulations using counterfactual data Nkwasa et al. (2024). The MK test is based on the statistic S computed using Eq. 5.2.

$$S = \sum_{i=1}^{n} \sum_{j=i+1}^{n} \operatorname{sgn}(X_j - X_i) \tag{5.2}$$

where X_j and X_i are sequential data values, n is the length of the time series, and

$$\operatorname{sgn}(X_j - X_i) = \begin{cases} 1, & \text{if } X_j > X_i \\ 0, & \text{if } X_j = X_i \\ -1, & \text{if } X_j < X_i \end{cases} \tag{5.3}$$

By considering that the observations are independent and randomly ordered, under the null hypothesis of 'no trend', the variance of the statistic S may be calculated as:

$$\operatorname{Var}(S) = \frac{n(n-1)(2n+5) - \sum_{i=1}^{M} U_i(i)(i-1)(2i+5)}{18} \tag{5.4}$$

where M is the number of tied groups and U_i denotes the size of the i^{th} group. Note that the summation term is only applicable if the data series contains tied values. For large n, the statistic S approximates a normal distribution. The standardized test statistic Z is computed using Eq. 5.5.

$$Z = \begin{cases} \frac{S-1}{\sqrt{\mathrm{Var}(S)}}, & \text{if } S > 0 \\ 0, & \text{if } S = 0 \\ \frac{S+1}{\sqrt{\mathrm{Var}(S)}}, & \text{if } S < 0 \end{cases} \tag{5.5}$$

The Z statistic indicates both increasing (positive) and decreasing (negative) trends in a time series at the selected significance level α. If $|Z| \geq Z_{1-\alpha/2}$, the null hypothesis H_0 is rejected. $Z_{1-\alpha/2}$ is obtained from standard normal cumulative distribution tables. In this study, a 5% significance level was adopted to quantify the significance of trends.

Climate attribution of streamflow changes

To quantify the contribution of climate change in river discharge variations, the long-term mean difference (deficit) between model simulations forced by factual and counterfactual climate data were compared for all the watersheds. Additionally, the uncertainty among the datasets was quantified by considering the maximum and minimum values for the simulated values.

The Flow Duration Curve (FDC) was used to assess the low, medium and high flow changes and quantify their deficit. Exceedance probabilities at 20%, 50% and 99% were used to characterize low, medium and high flows respectively. The deficit was calculated by taking the difference between factual and counterfactual quantiles at these probabilities and expressing it in percentage. This proportional difference adds value by providing a clear, interpretable, and relative measure of change, helping to compare impacts across different watershed sizes and flow conditions.

Drought characterization

Drought events using discharge data were identified by considering the 80th percentile as the threshold. This approach has been widely used and recommended for investigating low flow events (Van Loon et al., 2012). Drought duration was estimated using the run theory approach (Yevjevich, 1967) where drought events with duration above 1–month were considered. The drought deficit was calculated as the difference between factual and counter factual discharge within a drought event. Furthermore, threshold based method was used to quantify by how much is a given drought creating a deficiency in streamflow, which is quite important for policy makers in the efforts to apply necessary measures to mitigate the impact of extreme low events.

5.2.5 Results

A. Climate attribution of annual average water balance

The annual average water balance between factual and counterfactual model simulations showed varying trends across different watersheds in the Scheldt basin, as shown in the

boxplots in Fig. 5.11. Negative values indicated a decrease in the respective water balance component due to climate change, while positive values indicated an increase. Fig. 5.12, Fig. 5.13 and Fig. 5.14 display the trends of annual average precipitation, evapotranspiration, and soil moisture over 1970-2020 and whether these trends are significant under climate change across various Scheldt basin's watersheds.

In the upper-left plot of Fig. 5.11, notable variations in annual precipitation were observed across the watersheds and climate attribution models. While some watersheds, such as the Grote Nete and Demer, exhibited consistent precipitation differences, substantial variation was evident in the Leie watershed. Overall, the median annual precipitation had a negative value, suggesting a decrease due to climate change. However, some simulations also showed positive values (Fig. 5.11). Statistically, no p-value met the 5% significance threshold, indicating that these changes were considered non-significant across all watersheds (Fig. 5.12). The most pronounced decreases in precipitation were observed in the Dender and Leie watersheds, while the smallest decreases occurred in the Demer and Grote Nete watersheds (Fig. 5.11).

For the annual average evapotranspiration component, shown in the upper-right plot of Fig. 5.11, a more evident trend emerged. The median value for each watershed was positive, indicating an increase in evapotranspiration under climate change conditions (Fig. 5.11). Not only was this trend visually evident, with the factual evapotranspiration time series consistently staying above the counterfactual time series, but all p-values were also below the 5% significance level. This indicated a significant increasing trend across all watersheds (Fig. 5.13). The increase was most notable in the Upper Scheldt (USC), with smaller increases observed in the Demer and Grote Nete watersheds (Fig. 5.13).

In contrast, the average annual lateral flow difference, shown in the middle-left plot of Fig. 5.11, was close to zero, indicating negligible changes across most watersheds. Minor variations were observed, such as a decrease of 27 cm in the Kleine Nete (Fig. 5.11). Consequently, lateral flow was not statistically evaluated for trend significance, and no apparent increase or decrease in lateral flow due to climate change was identified.

The lower half of Fig. 5.11 highlights three additional average annual components—surface runoff, percolation, and soil moisture—all generally showing negative median values across most watersheds, indicating decreasing trends due to climate change. Surface runoff displayed a decrease (Fig. 5.11), with p-values indicating significance across all watersheds except the Kleine and Grote Nete watersheds. The most substantial decline occurred in the Dender watershed, reflecting reduced surface water availability (Fig. 5.11).

Percolation showed declines (Fig. 5.11), with smaller, non-significant declines in the Dender, Grote Nete, and Kleine Nete, where percolation remained near zero. The Upper Scheldt (USC) watershed exhibited the most substantial reduction in percolation, suggesting decreased groundwater recharge (Fig. 5.11). Soil moisture decreased across all water-

sheds, with the most significant reductions in the Dijle-Zenne (D and Z) and USC and a lesser decline in Demer, indicating overall drier soil conditions due to climate change (Fig. 5.11). However, the Grote and Kleine Nete watersheds showed no significant trends in soil moisture, similar to their trends in percolation.

Watersheds with substantial precipitation declines, such as the Dender and Leie watersheds, also showed notable reductions in surface runoff and, in some cases, soil moisture. Additionally, watersheds with pronounced precipitation decreases, like USC and Leie, exhibited compensatory increases in evapotranspiration, suggesting that evapotranspiration rose as rainfall declined.

Together, these observations point to a general trend of reduced precipitation, surface runoff, percolation, and soil moisture, accompanied by a rise in evapotranspiration across most watersheds. Reductions in surface runoff correlated closely with decreased precipitation, particularly in the Dender, which experienced the most significant precipitation decline (Fig. 5.11). The considerable percolation reduction in USC (-38 mm) also aligned with its significant precipitation decrease, indicating reduced water penetration into deeper soils or groundwater layers (Fig. 5.11). Overall, higher precipitation reductions were associated with more substantial declines in surface runoff, soil moisture, and, occasionally, percolation.

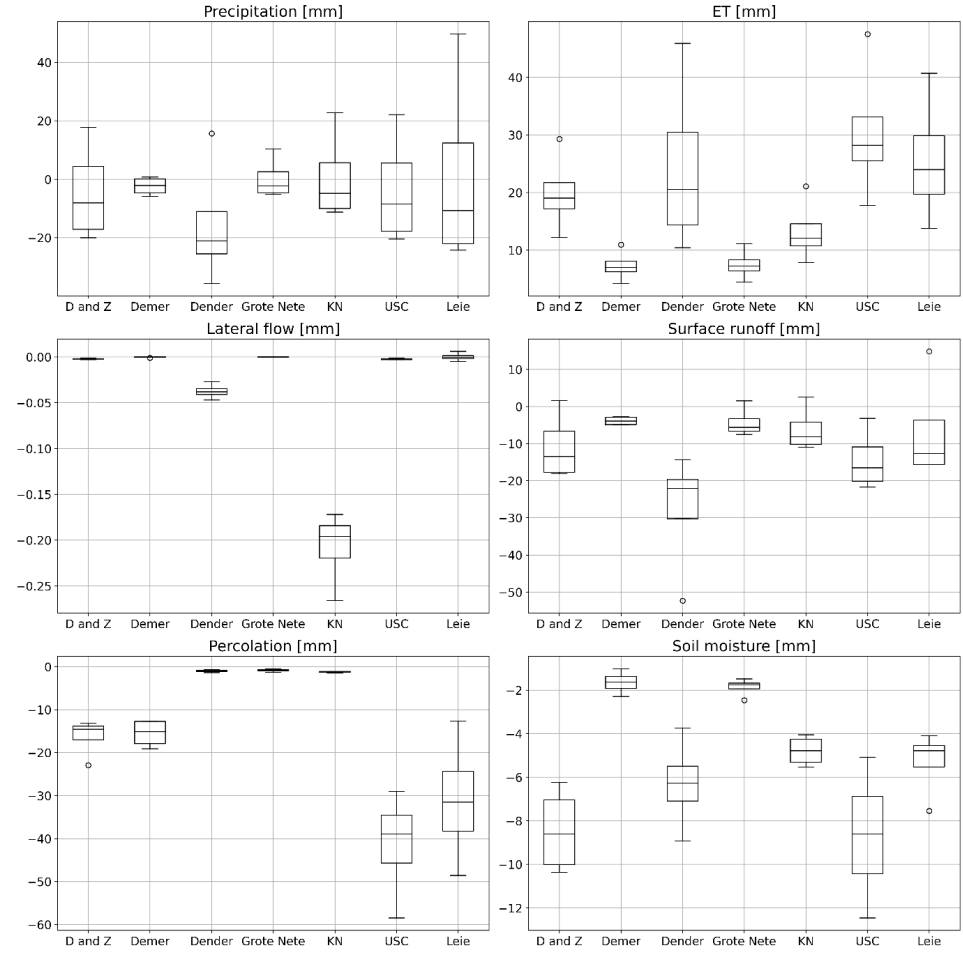


Figure 5.11: Differences in water balance components (precipitation, evapotranspiration, lateral flow, surface runoff, percolation, and soil moisture) between factual and counterfactual scenarios across watersheds in the Scheldt basin. Results are presented for three climate attribution models

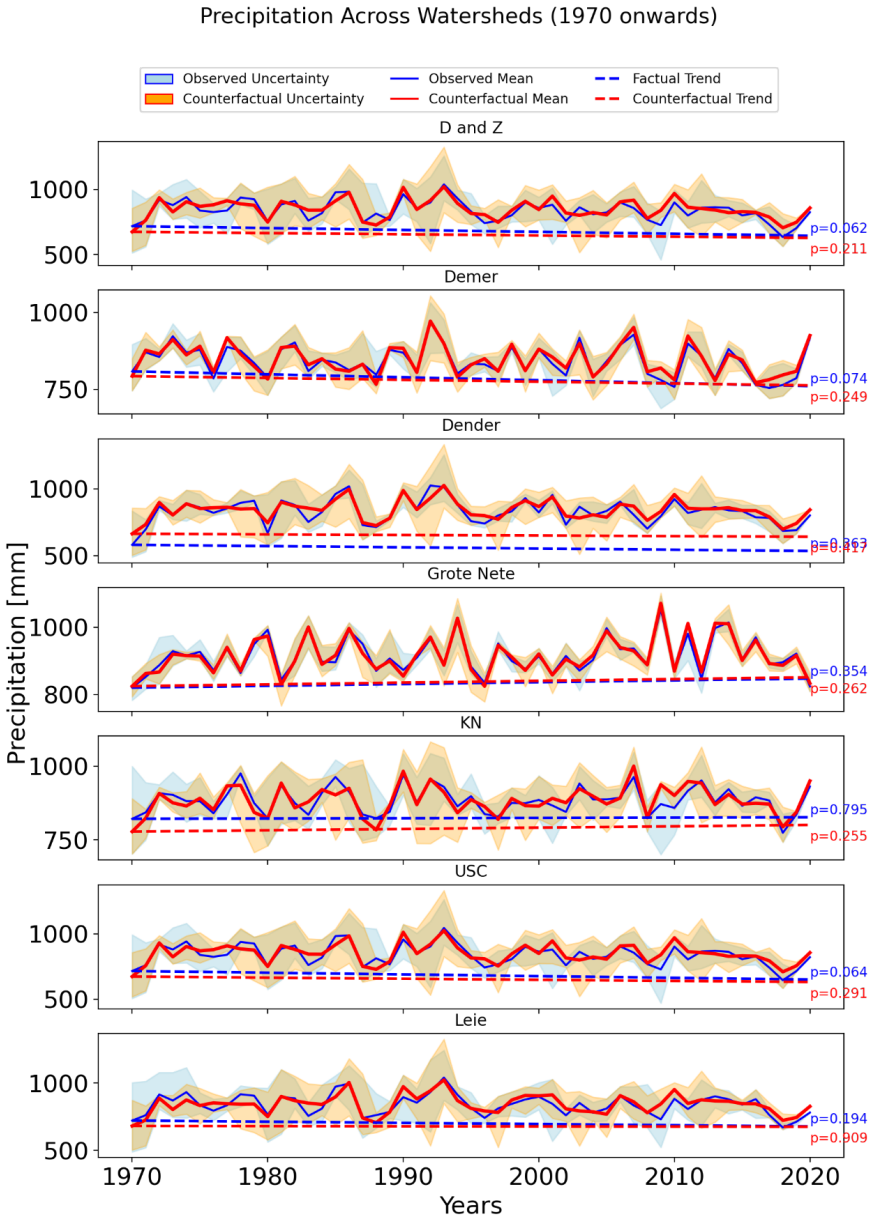


Figure 5.12: Differences between observed and counterfactual mean precipitation (mm), averaged across three climate attribution datasets, for various watersheds in the Scheldt basin. Shaded areas represent associated uncertainty ranges, while solid lines indicate mean values. Dashed lines show the observed (blue) and counterfactual (red) trends. P-values indicate the statistical significance of these trends, with values below 0.05 considered significant

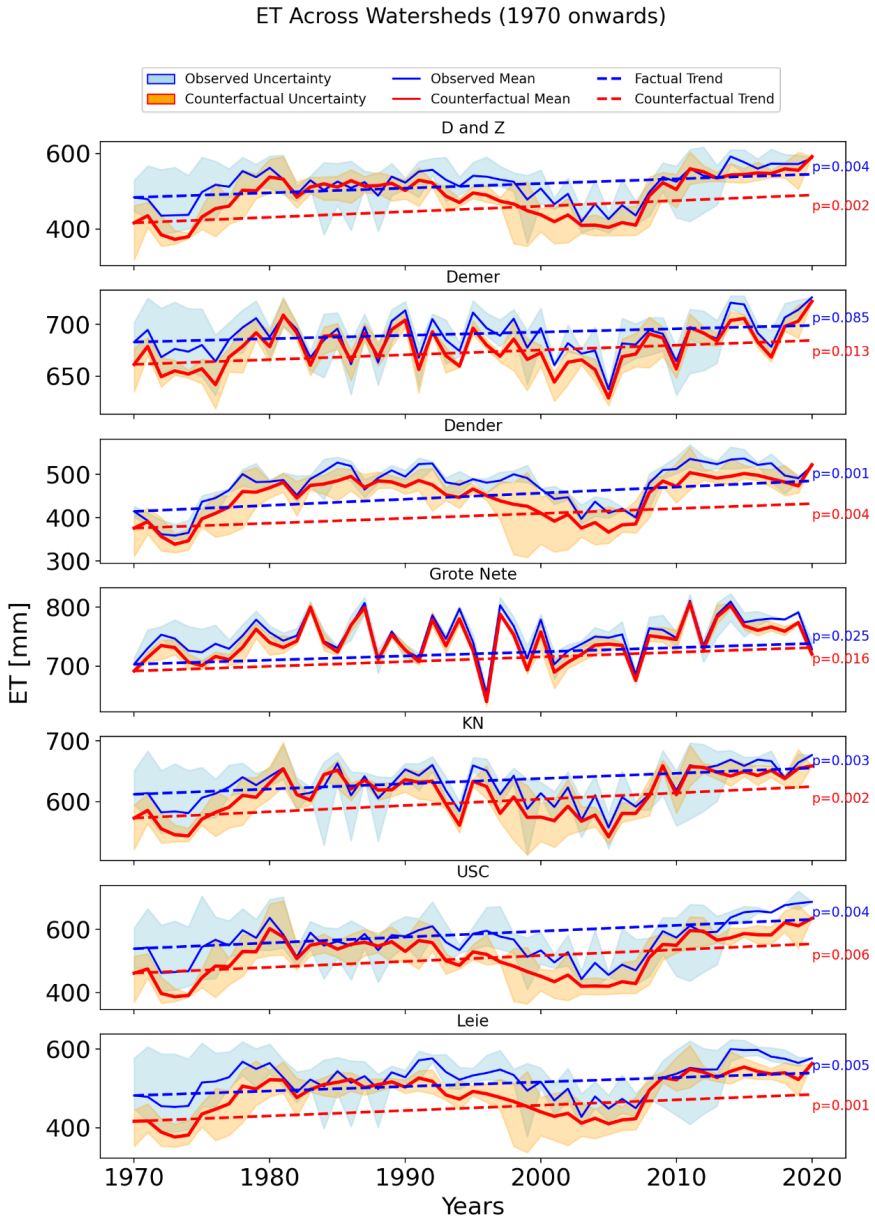


Figure 5.13: Differences between observed and counterfactual mean evapotranspiration (mm), averaged across three climate attribution datasets for various watersheds in the Scheldt basin. Shaded areas represent associated uncertainty ranges, while solid lines indicate mean values. Dashed lines show the observed (blue) and counterfactual (red) trends. P-values indicate the statistical significance of these trends, with values below 0.05 considered significant

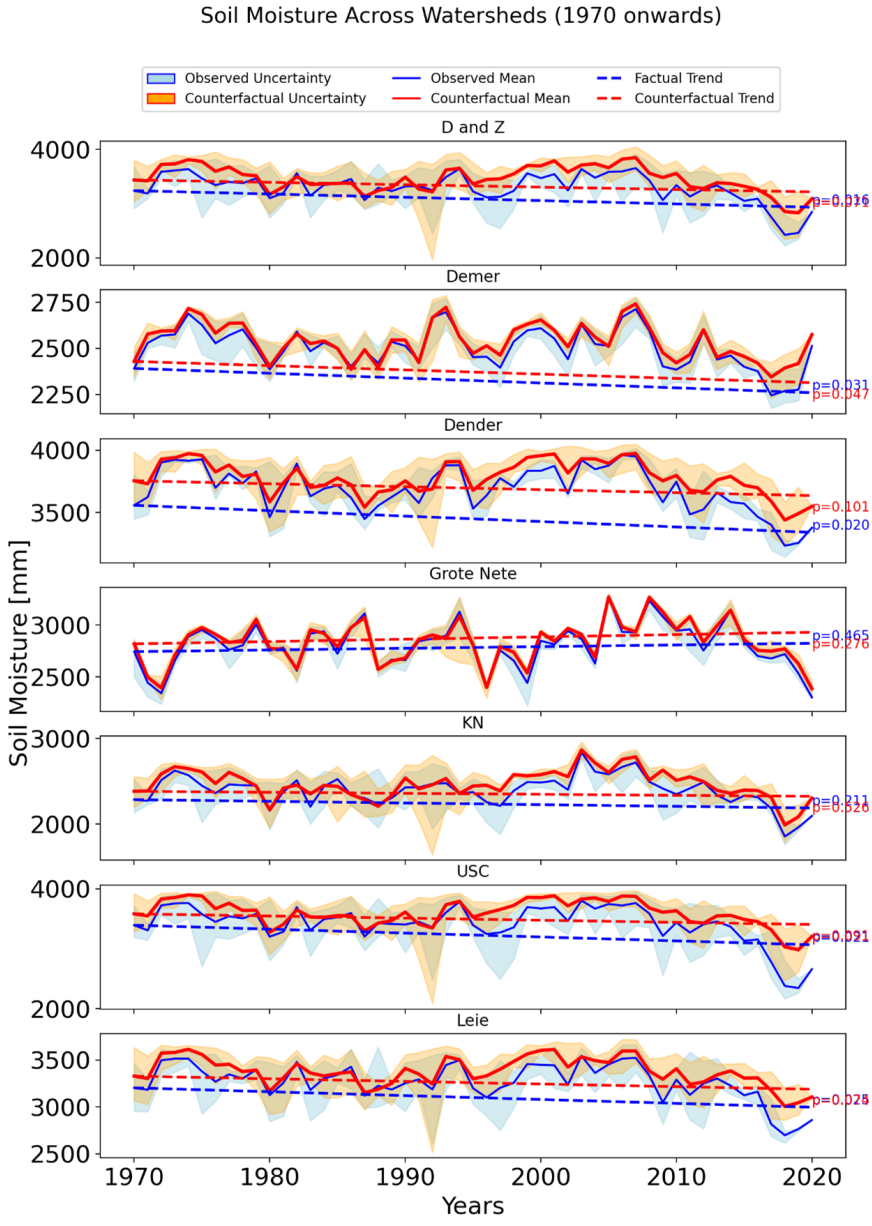


Figure 5.14: Differences between observed and counterfactual mean soil moisture (mm), averaged across three climate attribution datasets, for various watersheds in the Scheldt basin. Shaded areas represent associated uncertainty ranges, while solid lines indicate mean values. Dashed lines show the observed (blue) and counterfactual (red) trends. P-values indicate the statistical significance of these trends, with values below 0.05 considered significant

B. Climate Attribution of Seasonal Annual Water Balance

The seasonal trends in water balance for all watersheds are presented in Fig. 5.15, Fig. 5.16, and Fig. 5.17 for precipitation, evapotranspiration, and surface runoff, respectively. Similar seasonal variations in trends were observed across different watersheds. For precipitation, there was an overall increase in the difference due to climate change across all seasons, with the smallest changes observed in the Demer and Grote Nete watersheds, and the largest in the Dender, Leie, and USC watersheds (Fig. 5.15). Inter–seasonally, the most substantial differences were found in winter and spring, reaching nearly -10 mm, while differences in autumn were smaller, and summer had the smallest changes, barely reaching -3 mm (Fig. 5.15). The largest decreases align with the months that currently experience the highest rainfall, specifically the winter and spring months (NWS, 2022).

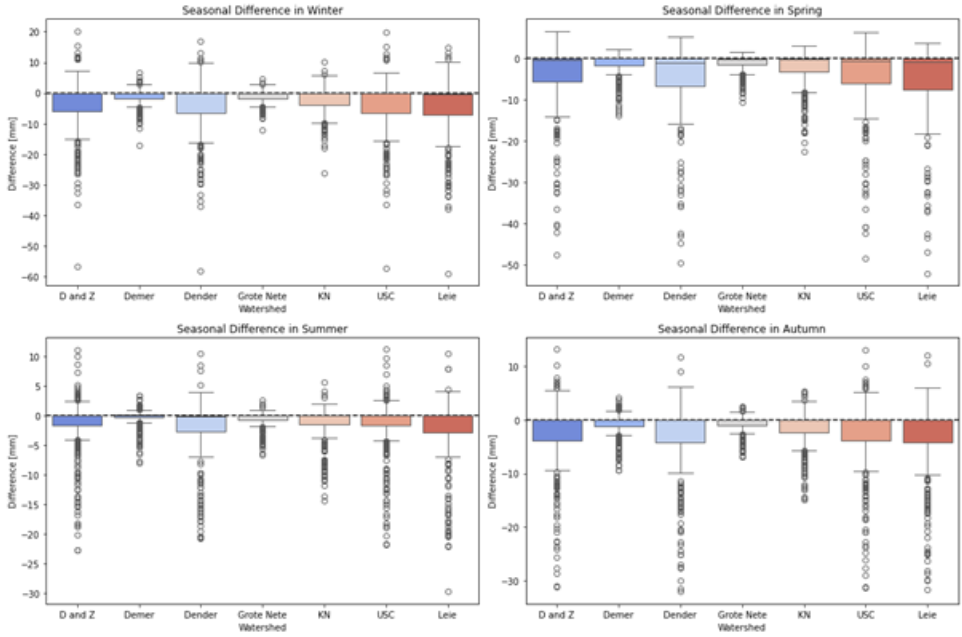


Figure 5.15: Seasonal differences in precipitation (mm), summed for each season across the years 1970–2020, between factual and counterfactual simulations for three individual climate attribution datasets. Seasons are defined as follows: Winter (December–February), Spring (March–May), Summer (June–August), and Autumn (September–November)

The seasonal differences in evapotranspiration showed similar patterns across watersheds. The greatest evapotranspiration differences were found in the Dijle-Zenne (D and Z), USC, and Leie watersheds, while smaller differences were observed in the Demer, Grote Nete, and Kleine Nete watersheds (Fig. 5.16). Across seasons, the largest differences occurred

in spring, with increases exceeding 10 mm for many watersheds under climate change conditions. This was followed by summer, while winter and autumn showed the smallest changes (Fig. 5.16). This seasonal variation is logical, as lower temperatures in winter and autumn are generally associated with reduced evapotranspiration compared to warmer spring and summer months.

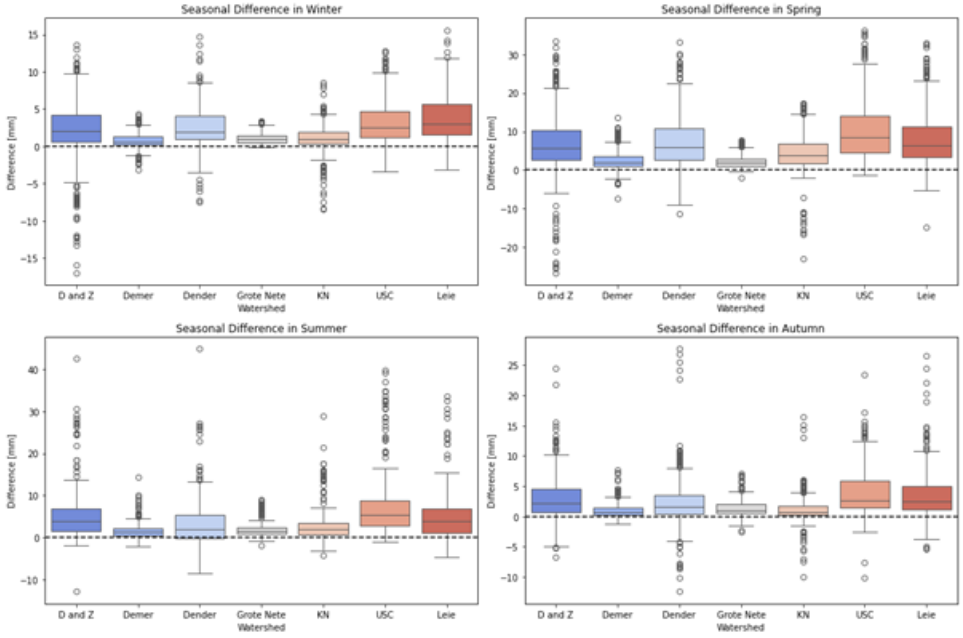


Figure 5.16: Seasonal differences in evapotranspiration (mm), summed for each season across the years 1970–2020, between factual and counterfactual simulations for three individual climate attribution datasets. Seasons are defined as follows: Winter (December–February), Spring (March–May), Summer (June–August), and Autumn (September–November)

For surface runoff (Fig. 5.17), seasonal differences showed trends similar in magnitude to those observed in precipitation. Consistent patterns were found again across watersheds, with the smallest seasonal differences seen in the Demer, Grote Nete, and Kleine Nete watersheds. Inter–seasonally, a more substantial decrease in runoff is seen in winter and autumn under climate change conditions, while spring and summer show smaller decreases. In conclusion, the seasonal analysis revealed substantial decreases in winter and spring precipitation, winter and autumn runoff, and increases in spring evapotranspiration across watersheds in the Scheldt basin.

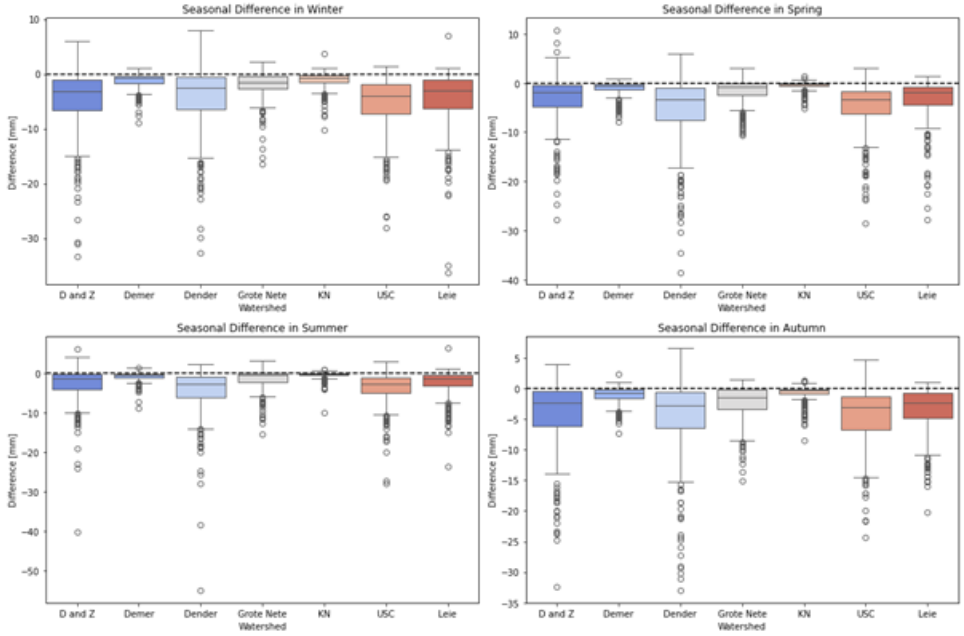


Figure 5.17: Seasonal differences in runoff (mm), summed for each season across the years 1970–2020, between factual and counterfactual simulations for three individual climate attribution datasets. Seasons are defined as follows: Winter (December–February), Spring (March–May), Summer (June–August), and Autumn (September–November)

C. Climate Attribution of streamflow

The factual mean streamflow was compared with the observed streamflow for each watershed, as shown in Fig. 8.11. This comparison evaluated whether the model accurately represented observed trends and determined its suitability for further climate attribution analysis. In most watersheds, the factual mean streamflow aligned well with the observed streamflow, indicating model reliability. However, in the Grote Nete watershed, the model did not accurately capture observed streamflow, suggesting it is not reliable for further evaluation. Additionally, in some watersheds, such as the Demer and Kleine Nete, peak flows were not well captured (Fig. 8.11).

Since this research focused primarily on drought, with low flows being of primary importance, and as the model represented low flows accurately, most results were considered reliable for the intended drought analysis. All watersheds showed a reduction in average low streamflow, reflecting the baseflow under climate change conditions, with this reduction being especially noticeable in the Kleine Nete and Leie watersheds (Fig. 5.18). Further analysis, represented in Fig. 5.18, shows the difference between the factual and counterfactual model simulations over the historical time series. For most of the period, negative

values were obtained, suggesting a decrease in average river flow across all watersheds. This decrease was most pronounced in the USC and Leie watersheds, while the smallest reductions were observed in the Kleine Nete and Demer watersheds.

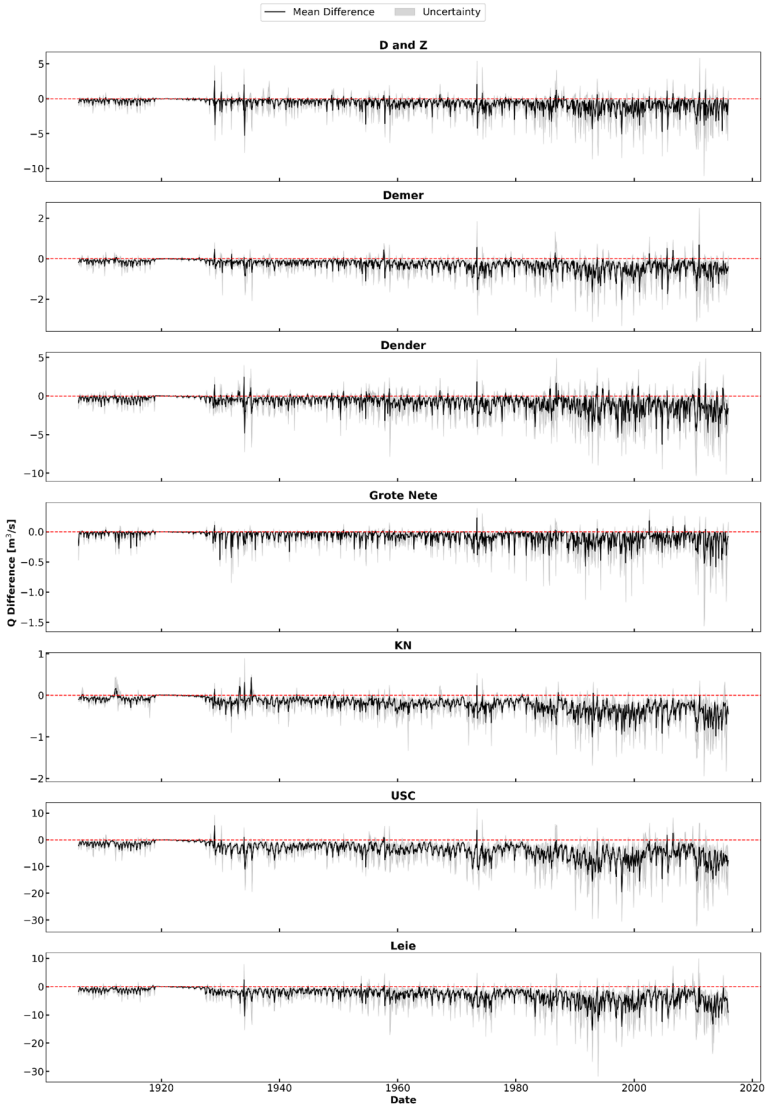


Figure 5.18: Long-term mean difference (deficit) in streamflow from model simulations using factual and counterfactual climate data, averaged across three climate attribution models. Shaded areas represent uncertainty ranges, and the dashed red line indicates no difference

Fig. 5.19 compares the difference between factual and counterfactual quantiles across different flow regimes and climate attribution models for all watersheds. For most watersheds, this difference was relatively small. However, in the Upper Scheldt (USC) watershed, the differences were highest among the three models and flow regimes. For example, for high flows with a 99% exceedance probability, a decrease of approximately 3.38% to 5.91% was observed in this watershed. For medium flows with a 50% exceedance probability, a decrease between 9.21% and 14.83% was noted. For low flows with a 20% exceedance probability, the reduction ranged from 12.11% to 13.99% (Fig. 5.19).

All the negative percentages in the labels indicated a decrease in flow in the factual scenario compared to the counterfactual scenario, suggesting that climate change has reduced flow under climate conditions. Across the study area, low flows decreased by 1.89% to 13.99% depending on the climate attribution model and watershed (Fig. 5.19). The fact that reductions were observed across multiple exceedance levels and climate attribution models suggests that climate change has had a consistent impact on reducing water availability, potentially affecting both flood peaks and baseflow levels.

Fig. 5.19 illustrates the relative difference between factual and counterfactual quantiles, expressed as a proportion of the factual quantiles, for three climate models across all watersheds in the Scheldt basin. This difference highlighted the significant impacts of climate change in larger watersheds, such as the Upper Scheldt (USC), where the relative flow rate difference for an exceedance probability of 20% reached nearly 5 m^3/s. In contrast, smaller catchments like the Kleine Nete showed differences below 0.5 m^3/s, reflecting a smaller relative impact (Fig. 5.19). The consistent positive values across models and watersheds confirm the substantial reduction in streamflow due to climate change, with variability in the magnitude of this reduction depending on the climate model and flow exceedance probability.

Fig. 5.19 also indicated that climate change disproportionately affects lower flows in most of the watersheds, as seen with the higher reductions at the 20% exceedance probability level. This suggests that baseflows, which are critical for maintaining ecological stability and water availability during dry periods, are particularly sensitive to climate change impacts. Meanwhile, flows with a higher exceedance probability, such as extreme high flows, were relatively less impacted but still showed reductions, underscoring climate change's consistent effect across flow regimes.

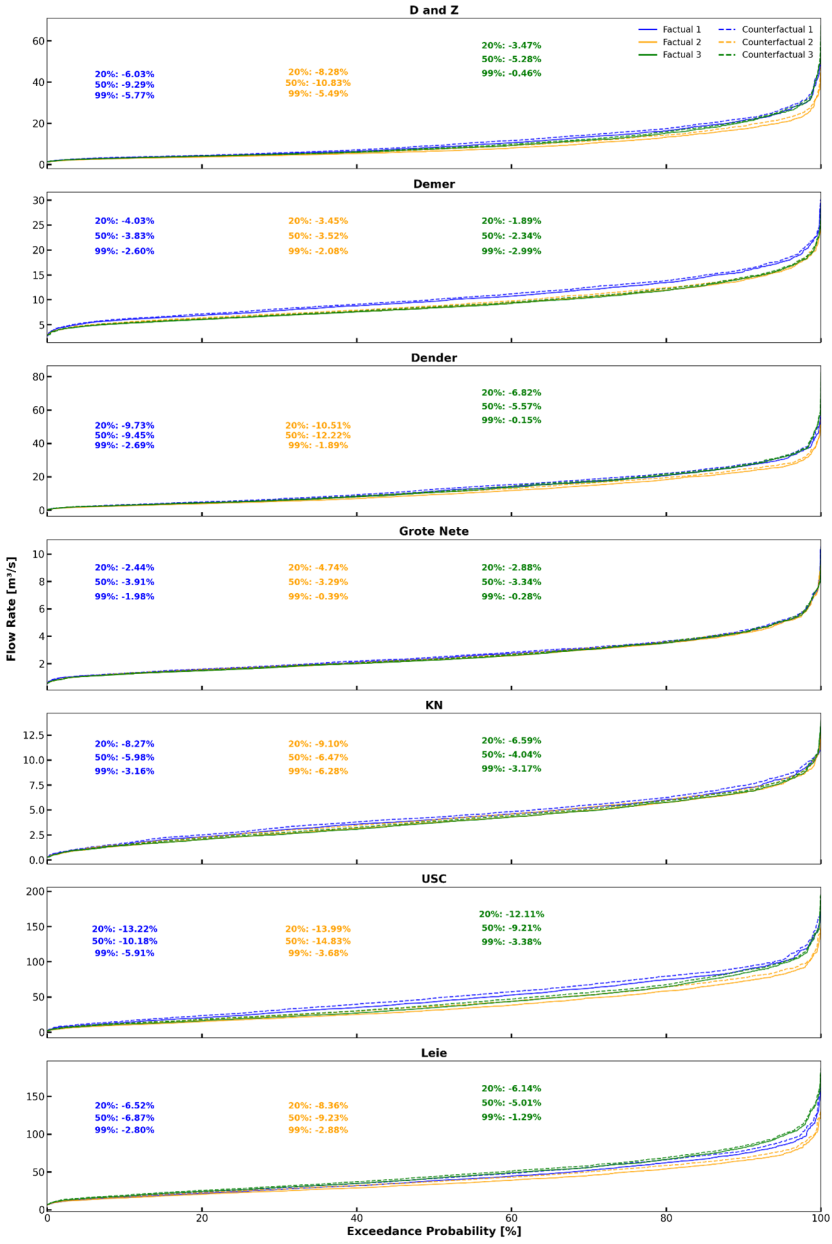


Figure 5.19: Flow Duration Curves comparing factual and counterfactual quantiles across different flow regimes and climate attribution models. Exceedance probabilities of 20%, 50%, and 99% represent low, medium, and high flows, respectively, highlighting changes in flow under climate change scenarios

D. Drought analysis

Fig. 5.20 illustrates the cumulative drought deficit over time, comparing factual and counterfactual streamflow deficits across various watersheds and climate models. Across all watersheds and models, the cumulative factual deficit was consistently higher than the counterfactual deficit, indicating an increasing streamflow deficit under current climate conditions due to climate change. The cumulative deficit also steadily increased over the analysed period, demonstrating a compounding effect of climate change on drought severity (Fig. 5.20). Watersheds with higher flow rates, such as the Upper Scheldt (USC) and Leie, exhibited steeper cumulative deficits, highlighting a greater sensitivity to drought impacts under current climate conditions. For instance, the USC showed a cumulative deficit reaching between 1375 and almost 2000 m³/s over time. In smaller watersheds with lower flow rates, such as the Kleine Nete, the cumulative deficit was also substantial, reaching around 130 m³/s (Fig. 5.20).

The results indicated that factual deficits were consistently higher than counterfactual deficits across drought events, suggesting a reduction in water availability under current climate conditions due to climate change (Fig. 5.22). Additionally, certain watersheds, such as the Leie, USC and Dender watersheds, exhibited significant peaks in drought deficits between 1960 and 1980, particularly around 1976, indicating a period of pronounced streamflow deficits within the study area. Differences between factual and counterfactual values also varied by watershed, with larger deficits observed in the larger watersheds. For many drought events in the USC watershed, an increased streamflow deficit of around 10 m³/s was observed (Fig. 5.22).

Fig. 5.21 presents drought durations (in months) for factual and counterfactual scenarios across various watersheds in the Scheldt basin and multiple climate models. The results showed variability in drought durations across watersheds and events, with factual drought events generally lasting longer than counterfactual events (Fig. 5.21). This finding suggests that climate change has extended the duration of drought events, particularly in watersheds such as the Dender, USC, and Leie. As also visible in the individual and cumulative deficit plots, there was variability in model results, indicating potential areas of uncertainty across different climate models.

Fig. 5.22 displays the difference between the factual and counterfactual discharge deficits within each drought event across all watersheds and three climate models. The results showed that differences between factual and counterfactual values varied by watershed, with larger differences observed in the larger watersheds (Fig. 5.22). As illustrated in Figure 15 and further confirmed, the Scheldt and Leie watersheds experienced the highest impacts, with an increased streamflow deficit of around 10 m³/s, except for some outliers. In contrast, other watersheds, such as the Dijle and Zenne, Demer, and Dender, showed a more modest increase in streamflow deficit, averaging around 1 m³/s per drought event under climate change.

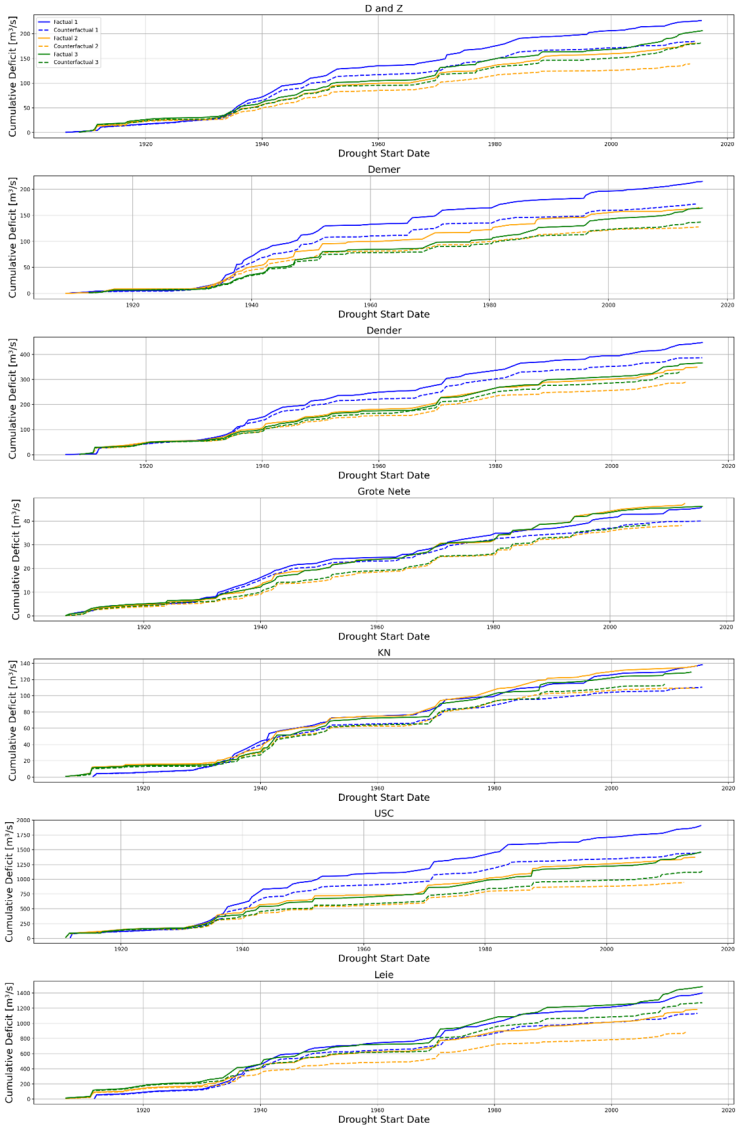


Figure 5.20: Cumulative streamflow deficit (m³/s) of factual and counterfactual discharges, summed for each drought event across various watersheds in the Scheldt basin and analyzed using three climate attribution models

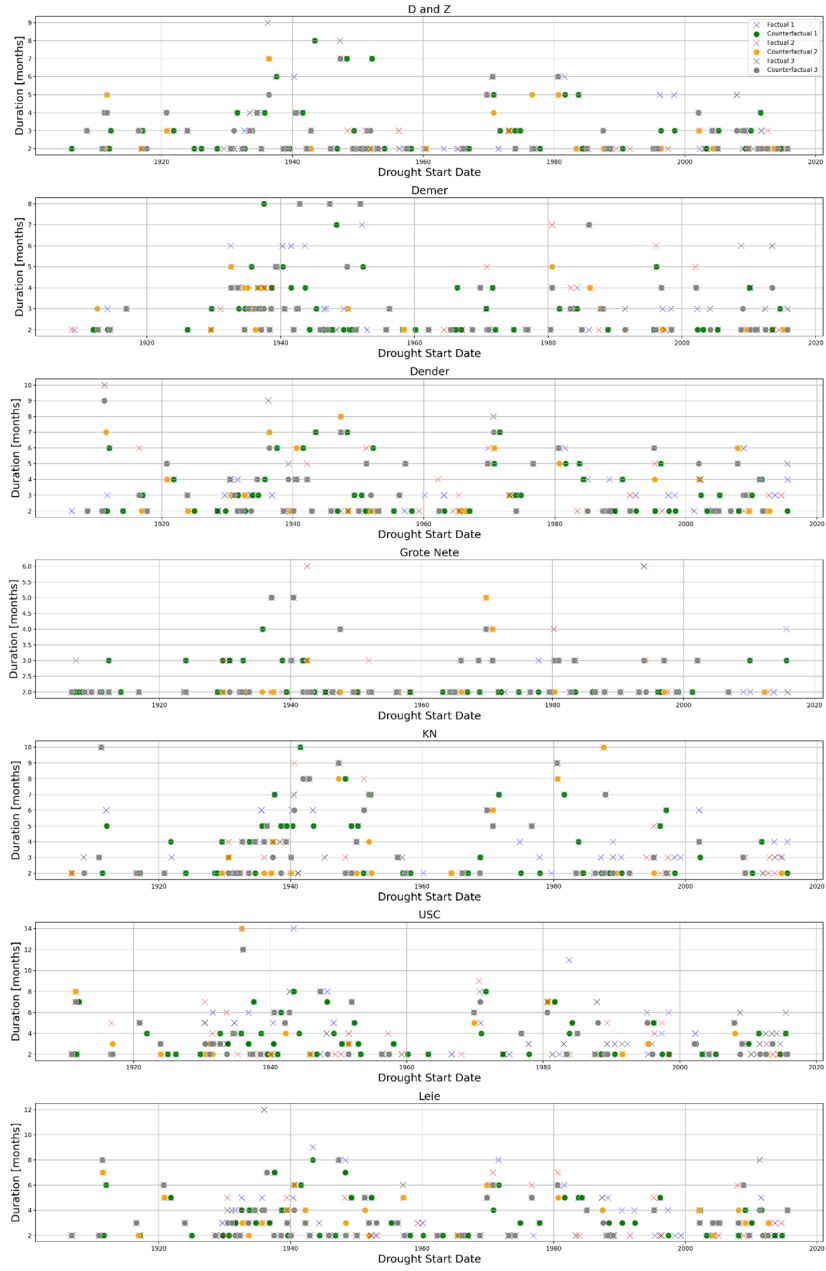


Figure 5.21: Drought duration (in months) of factual and counterfactual drought events across various watersheds in the Scheldt basin and analyzed using three climate attribution models

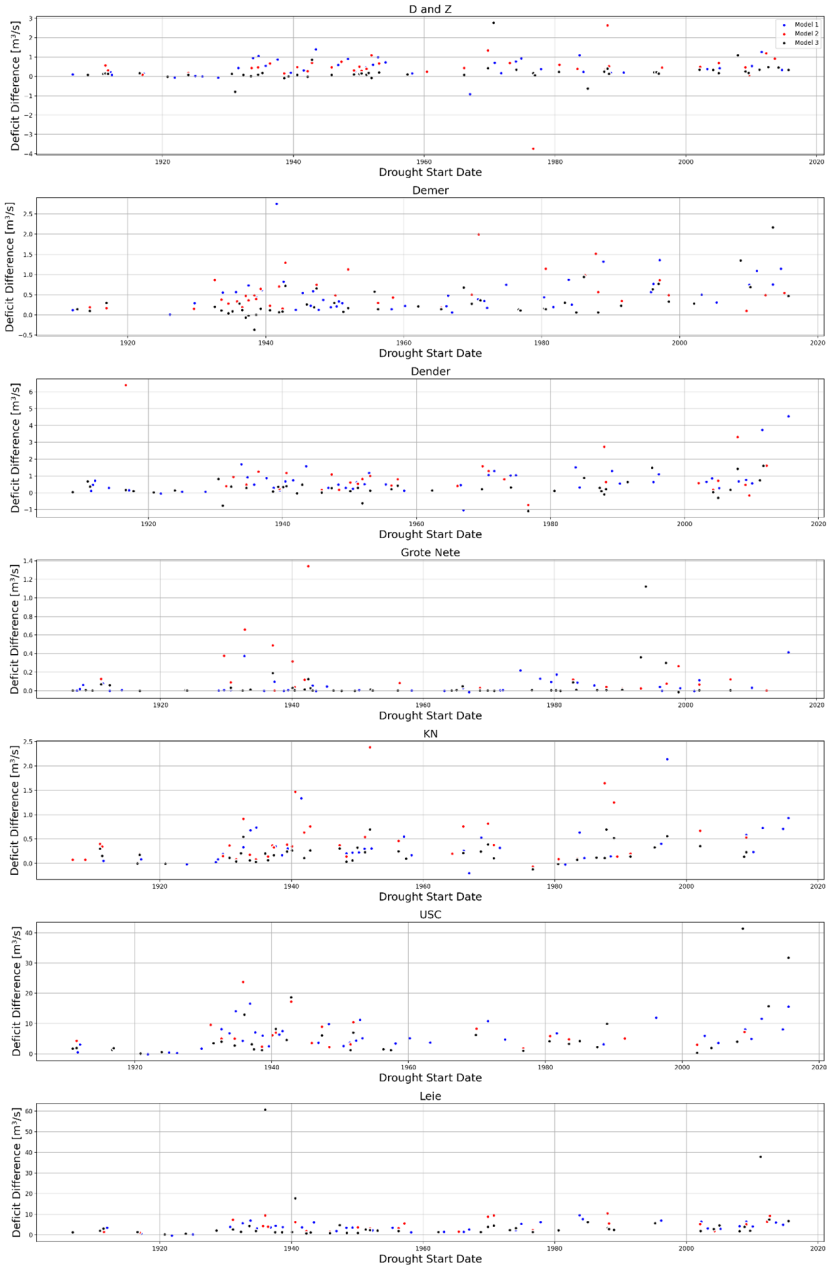


Figure 5.22: Streamflow deficit difference (m³/s) of factual and counterfactual discharges for each drought event, across various watersheds in the Scheldt basin and analyzed using three climate attribution models

5.2.6 Discussion

A. Climate attribution of annual and seasonal water balance

The results of this study indicate significant changes in various components of the water balance across the Scheldt basin watersheds due to climate change, with pronounced seasonal differences. Our climate attribution analysis found a non–significant decrease in mean precipitation, as well as in winter and spring precipitation across the watersheds. Large uncertainties in the impact of climate change on precipitation trends, both annually and seasonally, made it challenging to identify clear trends. This aligns with findings in the literature, which highlight substantial uncertainty over precipitation changes, particularly during summer months, further complicating the detection of significant trends (Commission, 2010).

No historical attribution studies were found specifically for this region. However, findings from climate projection studies provide contrasting results. For example, Ntegeka et al. (2010) reported that climate change in the Scheldt basin is expected to lead to wetter winters and drier summers. Tabari et al. (2015) similarly observed a slight decrease in summer precipitation and an increase in winter precipitation in Belgium over the past century. These seasonal patterns align with broader projections for Western Europe, as Jacob et al. (2014) also predict drier summers and wetter winters in many European regions. In this study, the increased evapotranspiration aligns with Spinoni et al. (2018), who projected heightened drought risks across Europe due to rising temperatures and evapotranspiration rates. Tabari et al. (2015) further supported these findings by reporting increased evapotranspiration during both winter and summer in Belgium.

B. Climate attribution of streamflow

The study identified a consistent reduction in streamflow across all watersheds, with variations in magnitude depending on watershed and flow regime. This result aligns with Vansteenkiste et al. (2014), who analysed different hydrological models and calibration methods to assess climate change projection impacts on the Grote Nete watershed, revealing a persistent drying trend and up to 60% reduction in low flows under the driest scenario. In our study, the Grote Nete watershed results were not considered due to the unreliability of the climate models for this watershed. The study also noted that uncertainties in climate projections and model structures significantly influence hydrological predictions, particularly for low flows, underscoring the need for model selection and calibration precision. The variability observed in our results due to differences in climate attribution models further supports this finding, emphasizing the role of model-specific differences in introducing uncertainty in drought impact projections.

A climate projection study by Ntegeka et al. (2010) investigates the potential impacts of climate projections on hydrological extremes (floods and low flows) in the Scheldt River

basin using multiple regional climate models. It reports comparable findings, showing that low flows decrease significantly in all cases studied, indicating a widespread and consistent impact of climate change on streamflow, particularly in low-flow conditions. The study also finds that factors like physical-morphological characteristics (such as land shape, soil type, and riverbed structure), historical climate patterns, and hydrological features (like groundwater connectivity or vegetation) have only a minor influence on the differences in how climate change affects low flows across locations. This suggests that, despite these local variations, low flow reductions due to climate change are generally similar. Consequently, drought adaptation strategies for mitigating low flow reductions may be broadly applicable across regions.

C. Drought analysis

The increase in streamflow deficit and the extended duration of drought events observed in this study align with projections by Greve et al. (2018), who anticipate longer and more intense droughts across Europe due to climate change. The variability in drought duration across models highlights the influence of model structure on drought predictions, with some models indicating a higher vulnerability to prolonged droughts than others. This underscores the importance of using multiple models to capture a range of potential outcomes and emphasizes the need for adaptive management strategies to address this uncertainty.

The increasing cumulative drought deficit over time reflects broader European trends. Stagge et al. (2017) reported a rise in drought frequency and severity across various European regions, attributing this trend to climate change. The substantial cumulative increase in drought deficit observed in this study suggests a compounding effect, particularly in sensitive watersheds such as the Upper Scheldt and Leie. This differential impact cannot be attributed solely to watershed area, as evidenced by the significantly higher reductions in low flows. When considering relative differences, the variation appears more influenced by factors such as river dimensions and streamflow rates. For example, the USC watershed can reach peak streamflow values of up to 150 m^3/s, leading to streamflow deficits up to ten times greater than in watersheds with smaller streamflow rates. Additionally, findings from a study conducted with the Belgian government (Commission, 2010) suggest that southern basins are more vulnerable to heat and drought, which may explain the heightened sensitivity of these basins.

The high peaks in streamflow deficit and drought duration observed across many watersheds between 1960 and 1980 correspond to the severe drought event of 1976, which affected large parts of Western Europe. The year 1976 was marked as one of the driest in Flanders' history, with prolonged periods of low rainfall and extreme temperatures (NWS, 2017). This meteorological drought had significant impacts on agriculture, water resources, and the natural environment (Drought 1976, n.d.), serving as a benchmark for understanding the potential severity of prolonged dry periods in Flanders.

D. Implications for drought management in Flanders

The consistent reduction in streamflow and increased drought duration under climate change across most watersheds underscore the need for enhanced drought management strategies, including Nature-Based Solutions, to mitigate impacts on water resources (Yimer et al., 2024a,b). Reflecting this priority, the Flemish government has invested around 500 million euro through the Blue Deal and of which 10 million euros are invested over the past two years in sustainable water-saving measures across various industries (VITO, 2022).

Additionally, the potential socio–economic implications of these findings cannot be overlooked. Reduced water availability in rivers may stress supplies for industry and agriculture, potentially leading to economic strain in sectors reliant on dependable water access. Water-intensive sectors already account for 33.7% of the gross added value of the Flemish economy, equating to 80 billion euros (VITO, 2022).

Effective drought management in the Scheldt basin is therefore essential, underscoring the need for strategic, prioritized action from policymakers and water managers to target the most climate–impacted areas. Our quantitative assessments of drought deficits can help guide policy and management strategies that address the most pressing climate impacts efficiently.

5.2.7 Conclusion

The prevailing impact of climate change has been explored in this research by looking into the yearly, seasonal water balance components and hydrological drought. To attribute impact of climate change on streamflow, geohydrological simulations with factual and counterfactual dataset is done for seven watersheds inside the Scheldt basin. The results indicate that climate change has significantly reduced the yearly runoff, percolation and increased evapotranspiration (ET) at 95% confidence interval in most of the watersheds. Seasonal analysis revealed large decreases in winter and spring precipitation, winter and autumn runoff, and spring ET. Notably, streamflow indicated a significant decrease attributed to climate change in all the watersheds. The low flows decreased between 3.5 and 14%. The cumulative drought deficit showed the highest impact on the Upper Scheldt catchment. Furthermore, the Upper Scheldt and Leie basins experienced an average increase in streamflow deficit of about 10 m^3/s. Similarly, drought duration increased due to climate change. This finding provides vital information for water managers to consider applying appropriate measures (e.g. nature–based solutions) to mitigate the drought deficit that is amplified by climate change.

5.3 Is climate change aggravating groundwater drought? A case study in a groundwater dominated watershed

5.3.1 Summary

Groundwater, often regarded as a hidden gem among water resources, is mostly considered unaffected by hydroclimatic extremes. However, recent studies have highlighted the severe impact that drought and water scarcity can have on groundwater reserves. This impact can result from factors such as climate change, inefficient irrigation practices, and overexploitation of water sources (e.g., pumping). To attribute specific causes to these effects, a critical examination of scenarios with and without each cause is necessary. Recently, the Inter-Sectoral Impact Model Intercomparison Project (ISIMIP) has produced four datasets containing factual (with climate change) and counterfactual (without climate change) data. These datasets are primarily used to study variations in meteorological forcing, such as precipitation and/or evapotranspiration. However, there is a lack of geohydrological attribution studies focused on groundwater. Therefore, this research conducted geohydrological simulations of groundwater heads using both factual and counterfactual data as forcing units to perform a groundwater drought analysis. The study area is the Kleine Nete in Belgium, which has a shallow aquifer potentially vulnerable to extreme events.

The factual dataset simulations, which closely matched the measured groundwater head data, revealed a consistent and significant decrease in groundwater head across all five analysed wells when compared to the counterfactual simulations. Notably, recent years (from 2010 onwards) have shown a considerable decrease. Overall, from 1970 onwards, there is an average decline of 10 cm in groundwater head, with some locations experiencing a maximum decline ranging between 0.1 and 1.5 meters, illustrating the spread of uncertainty. The drought assessment indicated an increase in maximum drought deficit and duration due to climate change. The deficit is particularly high for short-term (1 to 3 months) and yearly impacts but recovers on a 24-month timescale. This is attributed to the shallow nature of the aquifer water table, which declines over shorter timescales and recovers over longer ones. These findings underscore the potential risks of not implementing mitigation or adaptation measures to reduce the impact of climate change on the Kleine Nete and, in general, on unconfined groundwater reserves.

This section is to be submitted as: **Yimer, E. A.**, Lien, D.T, Erasto, B.M, Elsaidy, A.,, Nossent, J., & van Griensven, A. (2025). Is climate change aggravating groundwater drought? A case study in a groundwater dominated watershed.

5.3.2 Introduction

Climate change is observed to exacerbate drought events worldwide, while also increasing the frequency of extreme wet periods (Christidis and Stott, 2021; Zaitchik et al., 2023). These impacts are seen not only on the surface but also on groundwater systems (Secci et al., 2021). Since groundwater is considered the hidden gem, it is thought to be less affected due to the overlying ground, which has led to it being less studied Al Atawneh et al. (2021). However, unconfined aquifers with shallow water tables are seen to be affected (Richardson et al., 2024). To the best of our knowledge, hypothetical climate change scenarios have been explored, but further research is needed on attribution studies using detailed geohydrological models.

To evaluate the impact of climate change on groundwater reserves, it is crucial to understand the cascading effects of drought (Van Loon, 2015; Zhaoqiang et al., 2024). Drought is primarily defined as an abnormal deviation in precipitation or meteorological factors, such as precipitation and evapotranspiration (ET), from typical conditions. This is commonly referred to as meteorological drought (Van Loon, 2015). This deviation will likely result in less water available in the soil for roots to absorb, leading to agricultural drought (Zhaoqiang et al., 2024). These two combined drought types will ultimately impact groundwater, rivers, reservoirs, and other water bodies, leading to significant deviations in these components, which in turn contributes to hydrological drought (Van Loon, 2015). These cascading effects illustrate how deviations in meteorological forcing from normal conditions can lead to drought in groundwater reserves, indicating that climate change has the potential to impact groundwater (Van Loon, 2015; Zhaoqiang et al., 2024).

The three main types of droughts can be caused by climate change (Bouabdelli et al., 2022; Gudmundsson and Seneviratne, 2016; Secci et al., 2021). The causal effect analysis is gaining more attention from policymakers to support their actions regarding hydroclimatic extremes. Thus, attribution studies based on scenarios with and without climate change are being conducted (Gelfan et al., 2023; Lloyd and Shepherd, 2020). Out of the three types of drought, hydrological drought, which primarily affects groundwater, is considered to be less studied due to the difficulty in modeling aquifers (Peters et al., 2005). The issue is particularly common in developing countries that lack the data needed to build geohydrological model setups. The situation is even more challenging for attribution studies related to climate change and its impact on groundwater (Dragoni and Sukhija, 2008; Taylor et al., 2013). Hidalgo et al. (2009), Wang et al. (2023), and Yuan et al. (2018) examined the impacts of climate change on streamflow, while Fu et al. (2019), Wu et al. (2023), and Wunsch et al. (2022) focused on its effects on groundwater storage.

To better understand and estimate the extent to which climate change can affect groundwater, geohydrological and numerical models are crucial. Extended periods of low groundwater levels, directly impacted by climate change, were demonstrated in Germany using convolutional neural network modeling (Wunsch et al., 2022). Fu et al. (2019) identified both climatic and non–climatic stressors in Australia for studying the impact of climate

change on groundwater recharge, utilizing a regression model. Furthermore, seven aquifers were examined using a fully coupled model to investigate future changes in groundwater storage by comparing climate-driven and anthropogenic impacts (Wu et al., 2020). One of the widely used models is the Soil and Water Assessment Tool (SWAT), which has a restructured version called SWAT+ (Bieger et al., 2017), featuring an advanced representation of upland and lowland areas and discretizing processes in greater detail (Yimer et al., 2023b,a,c).

Although this latest version includes improvements, the groundwater representation remains conceptual, which limits its ability to accurately capture the geohydrology. Therefore, the conceptual groundwater representation has recently been replaced by a fully distributed and physically based groundwater module called gwflow. As a result, the coupled model is now referred to as SWAT+gwflow (Bailey et al., 2020a). Several recent applications of the model demonstrate its potential for modeling both surface and groundwater systems (Bailey et al., 2023, 2022; Yimer et al., 2023b,a,c). Specifically, the model was successfully employed to investigate agricultural drainage in the Kleine Nete watershed in Belgium (Yimer et al., 2023b).

Models alone cannot fully evaluate attribution studies. Therefore, different scenario datasets are needed to simulate factual (with climate change) and counterfactual (without climate change) conditions. The Inter-Sectoral Impact Model Intercomparison Project (ISIMIP) provides four detrended datasets to help understand and disentangle the effects of climate change and natural variability (Mengel et al., 2021). Each method comes with its own associated uncertainty, so it is crucial to show this uncertainty to policymakers when discussing potential declines in groundwater head (Nkwasa et al., 2024). For this reason, four detrended datasets are used to drive the SWAT+gwflow model setup for the Kleine Nete watershed, allowing for an assessment of the impact of climate change on drought.

Since geohydrological models are challenging to build, calibrate, and obtain reliable results from, attribution studies focusing primarily on groundwater are limited. Furthermore, most drought attribution studies are regional (Bindoff et al., 2014; Lane et al., 2023; Stott et al., 2010), with few conducted at the catchment scale. In this article, we investigate the geohydrological impact of climate change on groundwater drought. The major objectives of this study are as follows: First, to evaluate whether the factual dataset produces groundwater head values similar to the observed measurements. Next, to compare model runs using both factual and counterfactual datasets to quantify the extent to which groundwater head decline can be attributed to climate change. Finally, we conduct a hydrological drought assessment using a threshold-based method to determine if historical drought events in the watershed can be attributed to climate change.

5.3.3 Study area

Kleine Nete watershed located in Belgium is used to evaluate the impact of climate change on the aquifer. The catchment is known to have a shallow unconfined aquifer, making it vulnerable to the impact of climate change on the groundwater reserve.

5.3.4 Methodology

The methodology follows similar approach as in the first and second sections of Chapter 5. Additionally, in Chapter 2, definition and description of the drought analysis methods is elaborated. The contribution of climate change on groundwater head variability was quantified by taking the difference between model simulations forced by factual and counterfactual climate data (groundwater head deficit) at annual and seasonal timescales using Eq. 5.6.

$$CC = C_F - C_C \tag{5.6}$$

where CC is the climate change impact, C_F is the long-term annual (or seasonal) groundwater head under factual climate, and C_C is the long-term annual (or seasonal) groundwater head under counterfactual climate.

Additionally, the long-term trends in groundwater head were investigated using the non-parametric Mann-Kendall (MK) test (Kendall, 1948; Mann, 1945). A statistically significant trend with factual simulations indicated the influence of climate change on the groundwater head changes (Nkwasa et al., 2024).

5.3.5 Results

A. Climate Attribution of Groundwater Heads

Fig. 5.23 presents five scatter plots comparing measured and simulated factual groundwater head data at five wells (L1 to L5) across various climate datasets. The Root Mean Square Error (RMSE) and Mean Absolute Error (MAE) values are shown for each dataset to indicate the accuracy of the factual simulations relative to the measured data. Visually, most measurements are centred around the centroid, indicating generally good predictive performance. However, the measured values for wells L1 and L2 are consistently greater than the simulated factual values, suggesting a model bias toward underestimation. In contrast, for well L4, the scatter points are primarily positioned below the 1:1 bisector line, indicating a model bias toward overestimating the measured groundwater head values.

Based on the goodnessoffit statistics, wells L1 and L3 show the best fit between measured and simulated factual groundwater data, with the lowest RMSE and MAE values. Well L2, on the other hand, has the highest RMSE and MAE values, indicating the least accurate simulation, especially when compared to L1. Wells L4 and L5 show moderate fits with intermediate RMSE and MAE values. This variability in model performance across

wells suggests that site-specific conditions may influence the accuracy of groundwater head simulations. Overall, the RMSE values for most wells, except for well L2, remain below 1 meter, with values below 0.5 meters for wells L1 and L3, which is typically considered good for groundwater level predictions. This indicates that the factual simulations using different climate datasets are reliable for predicting the impact of climate change on groundwater heads.

Fig. 5.24 shows the annual average mean factual and counterfactual groundwater head values across the entire time series for each well (L1 to L5), with the uncertainty bands indicating variability across different climate models. Groundwater heads fluctuate within small to moderate ranges, as indicated by the y–axis values. For instance, well L2 exhibits minor fluctuations (15–16 meters), while well L5 shows a more extensive range of variation (25–29 meters). The plot reveals that factual groundwater heads are consistently lower across all five wells, suggesting a systematic decrease in groundwater heads under climate change. The uncertainty bands reflect apparent variability across different climate models, with generally less uncertainty in higher groundwater head values and more pronounced uncertainty in the lower values, as indicated by the broader bands at lower levels.

This declining trend is further confirmed in Fig. 5.26, which shows negative values across all wells (L1 to L5) in the anomalies between factual and counterfactual groundwater head values. Based on the p-value of zero for each well, the decrease in groundwater head is not only consistent across all five wells but also statistically significant. Additionally, the groundwater head decrease has intensified over time, with a notable decline observed from 2010 onwards. The magnitude of this decline varies across wells. The decrease is relatively modest for wells with smaller fluctuations, such as L1 and L2, ranging from 0.1 to 0.2 meters in extreme cases. In contrast, for well L5, which exhibits more fluctuation, decreases of over 1 meter are modelled. Overall, since the beginning of the period in 1970, there has been an average decrease of 10 cm in groundwater head, with maximum declines ranging between 0.1 and 1.5 meters in specific locations. This variation again highlights the uncertainty associated with different climate models.

Another way to represent the significant decrease in groundwater head is through scatter plots of the factual and counterfactual simulations, as shown in Fig. 5.27. These plots show that, for all wells, most points are positioned above the 1:1 line, indicating that factual groundwater head values are generally lower than counterfactual values, confirming this decrease associated with climate change. However, the spread of points away from this line increases for certain wells, particularly those with higher fluctuations in groundwater head values, such as well L5, indicating more significant differences between factual and counterfactual simulations. This spread likely reflects the impact of climate change on groundwater levels, with variability observed across different wells. As can be seen in the Fig. 5.25, the first two wells have shifted groundwater simulations compared to factual data. The rest of the three wells have reasonable result with a bit of bias and shift.

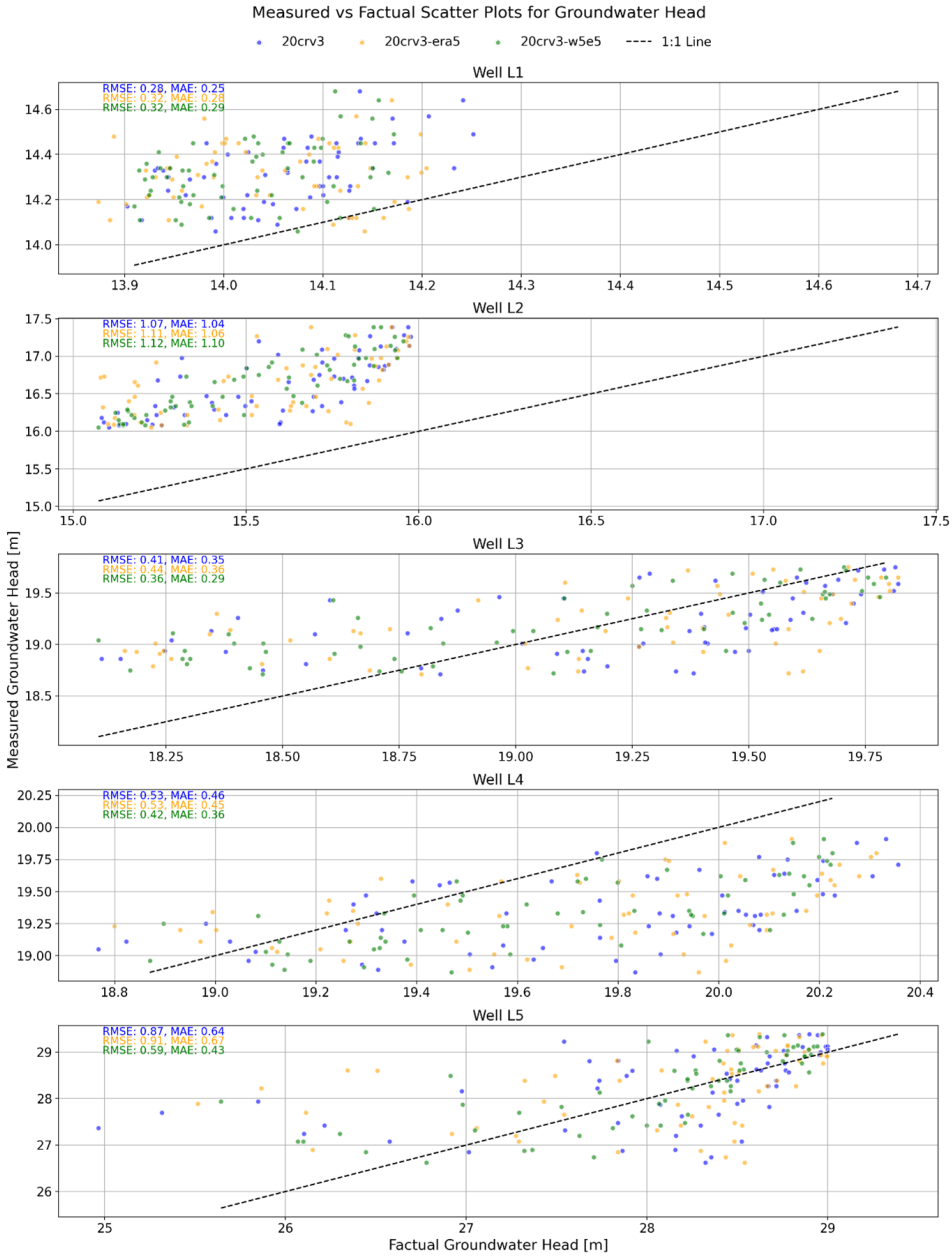


Figure 5.23: Comparison of measured and (factual) simulated groundwater head data (m) at five wells (L1 to L5). Each subplot represents one well, with coloured dots indicating the different climate attribution models. The 1:1 dashed line represents perfect agreement, highlighting deviations between measured and simulated factual values

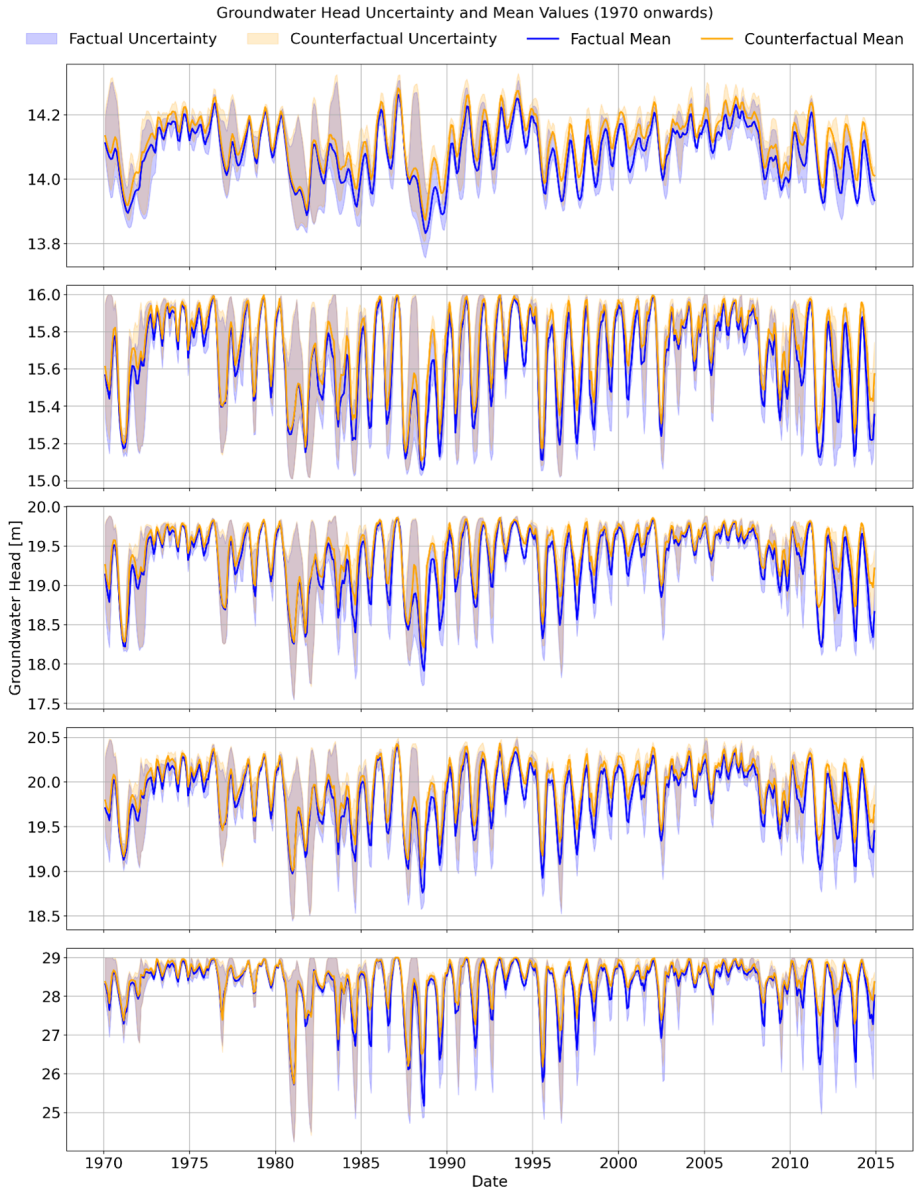


Figure 5.24: Comparison of annual average mean factual and counterfactual groundwater heads (m) from 1970 to 2015, averaged for three climate attribution models. Each subplot represents a different well, showing both factual (blue line) and counterfactual (orange line) simulations. Shaded bands around each line indicate the range of uncertainty in the simulations

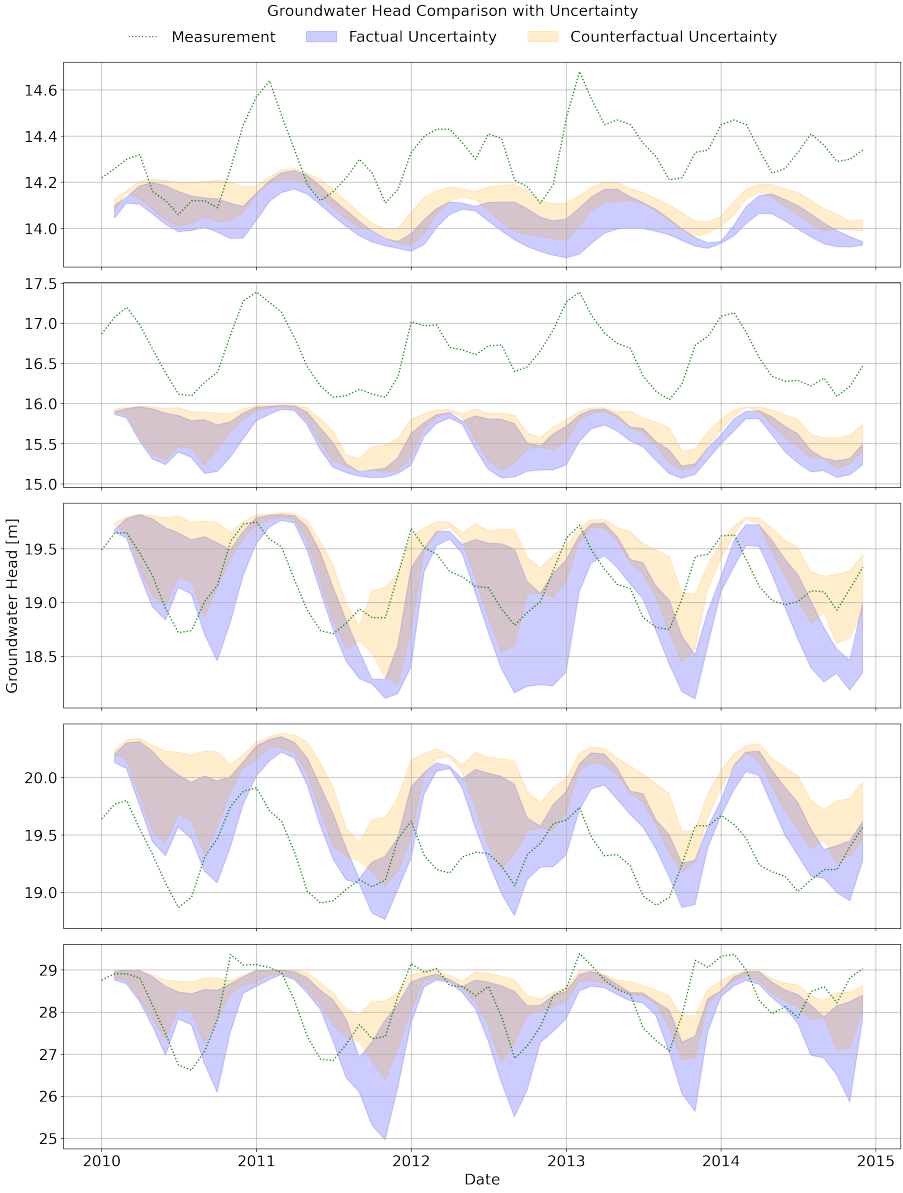


Figure 5.25: Comparison of measured, factual and counterfactual groundwater heads (m), with their uncertainty range. Each subplot represents a different well, showing both factual (purple) and counterfactual (light orange) simulations. Shaded bands indicate the range of uncertainty in the simulations

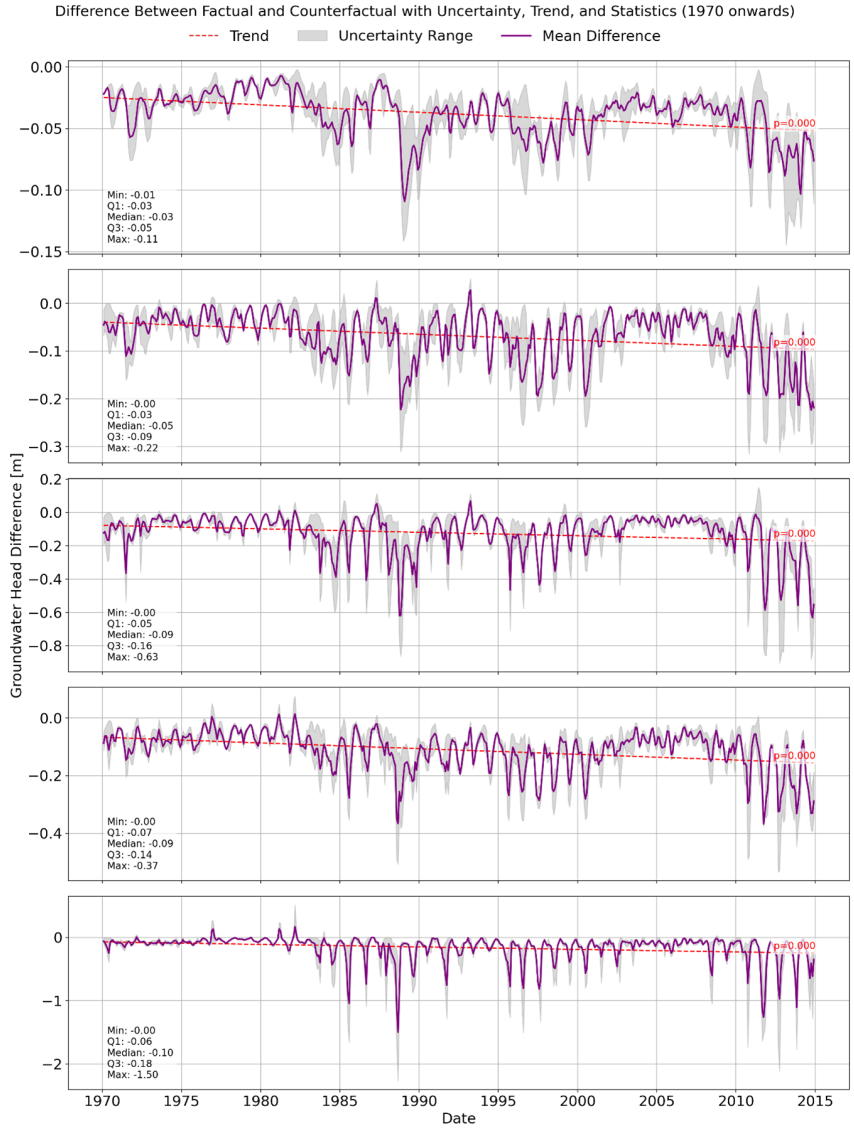


Figure 5.26: Differences between annual average mean factual and counterfactual groundwater head values (m) from 1970 to 2015 for wells L1 to L5. Each subplot represents a different well, with the purple line indicating the anomaly (factual minus counterfactual values) and the grey shading representing the uncertainty band across different climate datasets. The red dashed line denotes the trend in anomaly values, and the p-value indicates the statistical significance of the trend over time

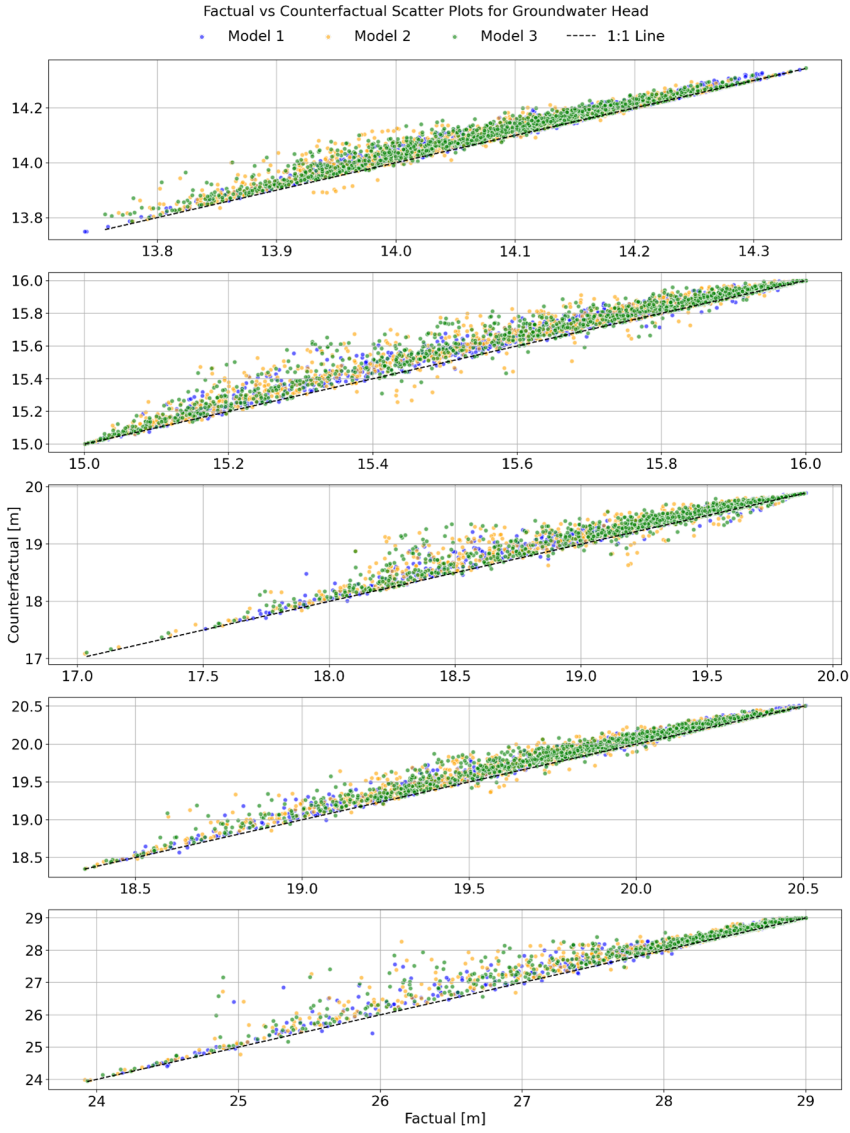


Figure 5.27: Scatter plots comparing factual and counterfactual groundwater head values (m) for five wells (L1 to L5), illustrating the alignment between simulated groundwater heads under factual and counterfactual scenarios. Each subplot represents one well, with coloured dots representing different climate datasets. The dashed 1:1 bisector line indicates perfect agreement between factual and counterfactual values

B. Seasonal Climate Attribution of Groundwater Heads

Fig. 5.28 shows the yearly seasonal differences between factual and counterfactual groundwater heads from 1970 to 2015 for different climate models. Although all wells showed an overall decrease in groundwater heads under climate change, as confirmed in Fig. 5.27, the seasonal analysis revealed differences among the wells. Well L1, which demonstrated the best agreement between factual simulations and measurements (Fig. 5.23), showed the most minor decrease every season, with low variability throughout the year (Fig. 5.28). This aligns with the tiny fluctuations in groundwater head and the minimal differences between factual and counterfactual simulations observed in Fig. 5.24 and Fig. 5.26. In contrast, higher reductions were observed each season for wells with highly fluctuating groundwater heads, such as L4 and L5. Well L3 also exhibited large seasonal fluctuations in decrease, especially pronounced in summer and autumn (Fig. 5.28). This may not have been due solely to significant variations in groundwater head but could be linked to the lower performance of the factual model simulations, as indicated in Fig. 5.23.

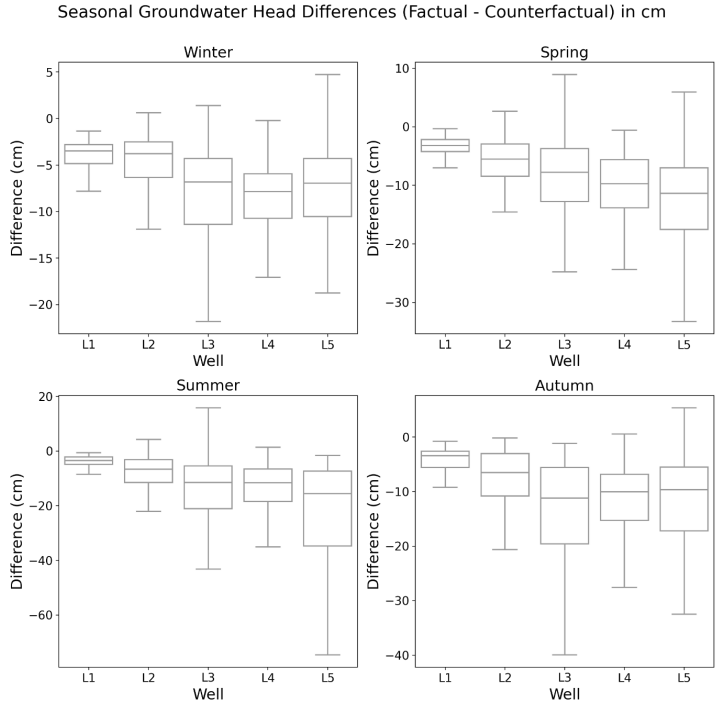


Figure 5.28: Annual average seasonal differences (cm) between factual and counterfactual groundwater head simulations for 1970-2015 for the three climate attribution dataset and displayed for each well (L1 to L5). Each panel represents one season (winter, spring, summer, and autumn)

Inter-seasonal changes were also evident in Fig. 5.28. The most significant decreases occurred in the summer and autumn seasons. For well L3, the decrease exceeded 40 cm in both seasons. While the decline was still substantial in winter and spring, it was limited to approximately 20 cm in these seasons. Notably, the highest decrease was recorded in summer for well L5, where a more than 60 cm reduction was observed (Fig. 5.28). The more substantial groundwater head decreases observed in summer and autumn may be exacerbated by reduced recharge rates during these seasons and increased abstraction for agricultural irrigation. The seasonal comparison highlights how the impact of climate change on groundwater levels varies throughout the year, with certain seasons showing greater median differences and wider variability across different climate models. This seasonal variation may reflect different recharge and depletion dynamics influenced by seasonal climate conditions.

C. Drought Analysis

Fig. 5.29 showed the yearly maximum drought deficit calculated using thresdhold-based method across three climate attribution datasets and various drought accumulation periods ranging from 1 month to 24 months for both factual (red) and counterfactual (black) scenarios. The range of maximum deficit varied between the different wells (L1 to L5), with smaller deficits for wells L1 and L2 (Fig. 5.29). This corresponded well with the smaller differences between factual and counterfactual groundwater head values observed in Fig. 5.26.

For most wells, the boxplots corresponding to the factual scenarios consistently showed higher deficits than the counterfactual scenarios for shorter accumulation periods (1, 3, and 6 months), indicating an increase in maximum drought deficit due to climate change over these periods. Around the 9-month accumulation period and especially at the 12–month period—the opposite trend was observed, with the mean maximum deficit becoming equal to or lower for the factual scenarios, suggesting a lower maximum drought deficit under climate change for these periods. At the 24–month accumulation period, the trend switched again, showing a higher maximum deficit under climate change conditions (Fig. 5.29).

For well L1, the pattern was slightly different. The mean maximum deficit under the counterfactual scenario was higher or equal to the deficit under the factual scenario for shorter accumulation periods up to 6 months, indicating a decrease in deficit under climate change. However, for longer accumulation periods, the trend reversed, with an increase in maximum drought deficit under climate change (Fig. 5.29). This pattern suggests that the groundwater system may have initially stabilized but experienced increased stress as drought conditions persisted over a year or more. Fig. 5.29 also showed different responses to the maximum drought deficit across accumulation periods, with a decreasing mean maximum deficit as drought accumulation periods increased for most wells (except for well L1), suggesting that deficits were higher for short-term drought events (1-6 months) and generally smaller for long-term drought events (9-24 months) (Fig. 5.29). This pattern implies that short-term droughts resulted in more substantial groundwater deficits, while longer–term

droughts resulted in smaller but more consistent deficits.

As the accumulation period increased, the variability in the yearly maximum deficit tended to decrease in most scenarios, as shown by the shorter whiskers in the boxplots, particularly in the factual scenario (Fig. 5.29). This reduction in variability with longer accumulation periods suggests that prolonged drought conditions led to more consistent groundwater deficits, resulting in less fluctuation in yearly maximum deficit values. In contrast, shorter accumulation periods captured more variable, shorter–term drought events, leading to greater fluctuations in groundwater deficit.

Additionally, the wells showed differences in their response to drought accumulation periods (Fig. 5.29). For instance, wells L4 and L5 displayed a wider range of deficit values (longer whiskers and more outliers), indicating greater variability in deficit linked to fluctuations in groundwater heads and sensitivity to prolonged drought events. This might suggest that these wells were located in areas more affected by climate variability or had characteristics that made them more vulnerable to drought.

Fig. 5.30 show the yearly drought duration differences between factual and counterfactual scenarios for three drought event accumulation periods (1-month, 12-month, and 24-month), illustrating how drought durations evolve under climate change conditions. Positive values represent an increase in drought duration under the factual scenario, indicating the intensification of droughts due to climate change.

1-Month Accumulation Period

Well L1 exhibited a significant intensification of drought duration under the factual scenario on a 1–month accumulation scale, as shown by frequent orange and red zones throughout the years (Fig. 5.30). In contrast, wells L4 and L5 displayed predominantly dark blue zones, where the differences were mostly zero, indicating little to no change in drought duration under factual conditions. Only a few scattered red zones were observed for these wells, representing occasional increases in drought duration. For wells L2 and L3, blue zones dominated, indicating also small drought duration increases under the factual scenario and suggesting a smaller impact of climate change on drought duration for these locations. A distinct pattern was observed across most wells (L1 to L4) in the year 1987, with an exceptional increase of 10–13 months in drought duration under climate change conditions for that year. For the 1–month accumulation period, the three climate attribution models exhibited consistent patterns across most wells, particularly for wells L4 and L5 (Fig. 5.30).

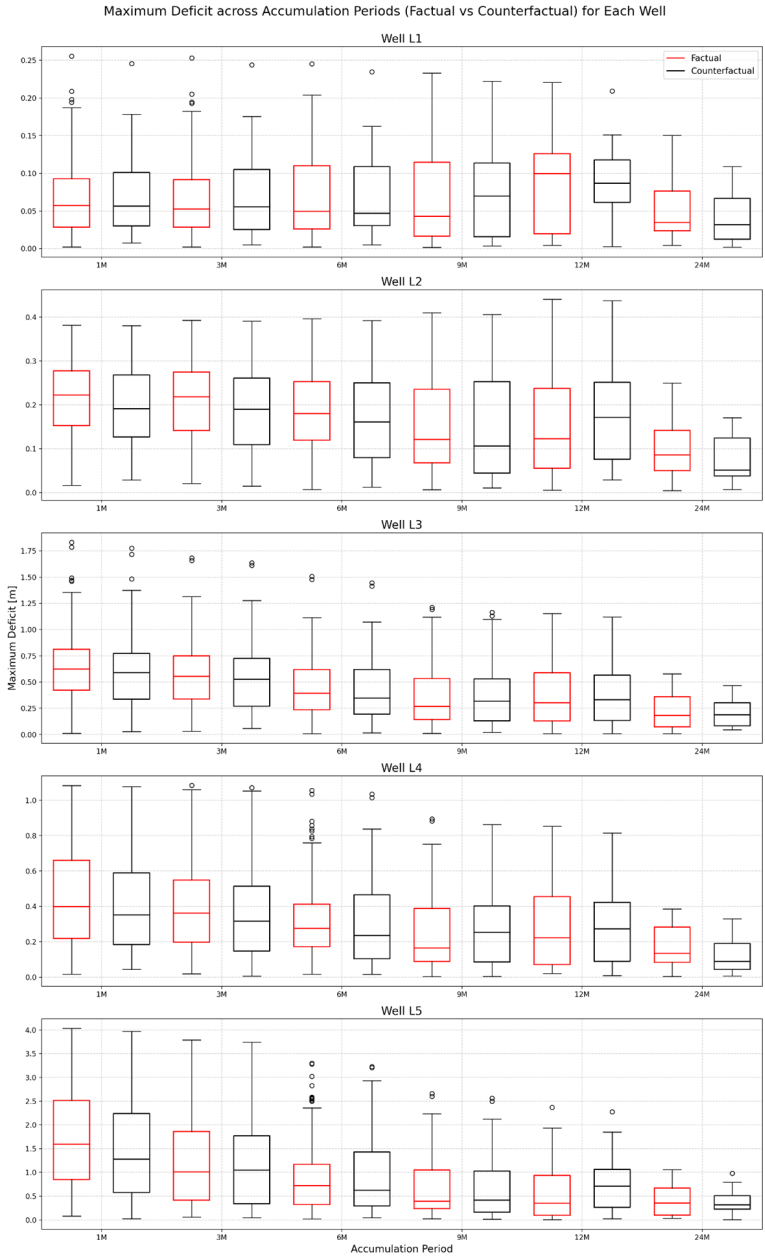


Figure 5.29: Boxplots of maximum deficit (m) for factual (red) and counterfactual (black) scenarios, for the three climate attribution datasets and displayed for various drought accumulation periods (1M = 1 month, 24M = 24 months, etc.).

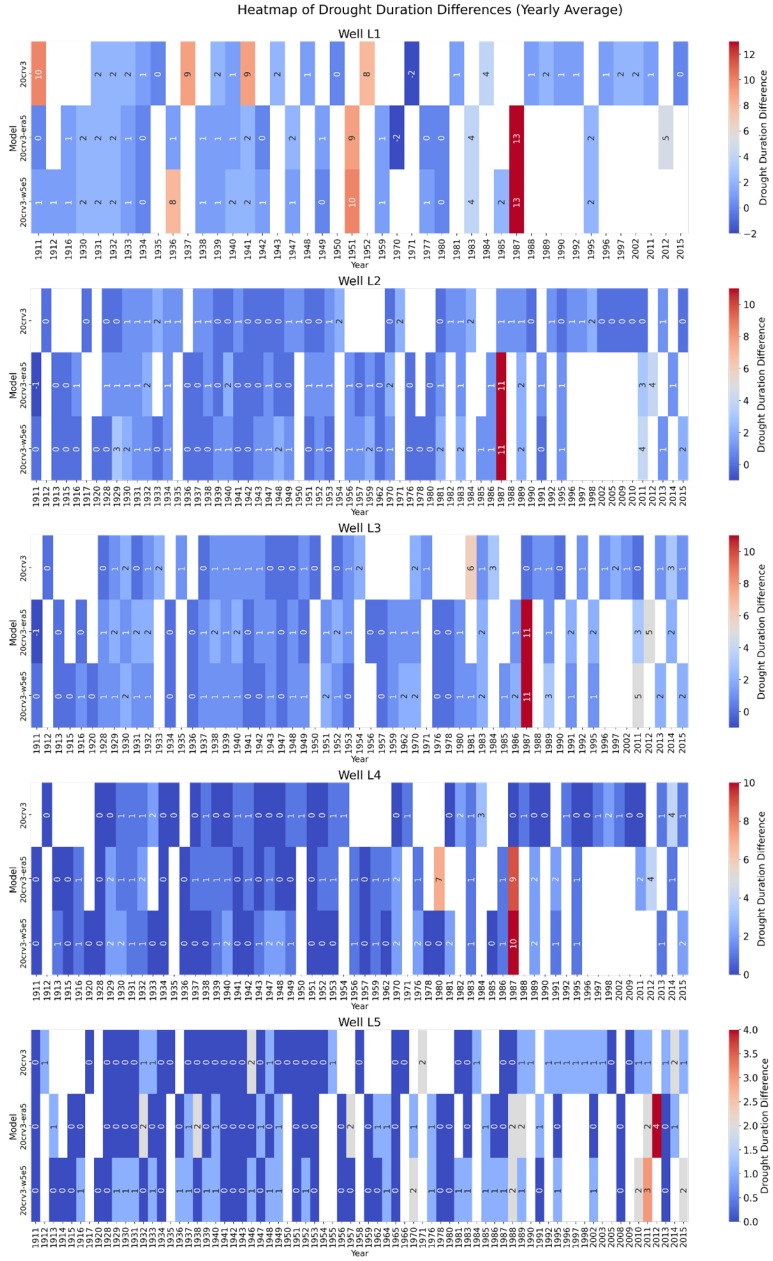


Figure 5.30: Heatmaps showing the yearly drought duration differences (in months) between factual and counterfactual scenarios for drought events at a 1-month accumulation period across three climate attribution models and five wells (L1 to L5).

12-Month Accumulation Period

Positive values continued to dominate over a 12–month accumulation period, confirming the consistent increase in drought duration under the factual scenario. Compared to the 1–month accumulation scale, logically, a higher magnitude of drought duration differences was observed across all wells, indicating prolonged drought events under climate change conditions. Unlike the 1–month scale, less distinction was observed between the wells, as they all exhibited similar behaviour. Between 1936 and 1937, a significant increase in drought duration was observed across all wells, with differences ranging from 11 to 80 months depending on the climate attribution model. Additionally, the year 1987 stood out again as an exceptional year, with all wells, except well L5, exhibiting a consistent increase of approximately 12 months in drought duration under the factual scenario, mirroring the pattern seen in Fig. 5.30. Well L5 continued to display minimal differences, often showing 0–month differences, suggesting localized resilience or differing responses to climate-induced drought conditions.

24-Month Accumulation Period

Like the 12–month accumulation plots, similarities were observed between the wells when accumulating the duration for a 24–month period. Unlike the 1–month accumulation period, where well L1 showed the most positive differences, this pattern expanded. Wells L2 and L3 also displayed high differences throughout the simulation period, indicating more prolonged drought durations under the factual scenario. The period around 1936–1937 again exhibited significantly higher differences compared to the rest of the timeframe, suggesting a longer, more intense drought event under climate change conditions. During this period, drought durations increased by 29–75 months, varying across wells and climate attribution models. Additionally, the period around 1987–1988 showed notable differences, with increases of around 9–10 months observed across most wells, although this was less distinctive compared to the earlier period. Another noteworthy observation was again for well L5. While previously showing minimal differences, well L5 now indicated higher differences under the factual scenario, with drought durations increasing by 1–5 months.

5.3.6 Discussion

1. Yearly and Seasonal Climate Attribution on Groundwater Heads

No previous climate attribution studies on groundwater heads were identified. However, comparisons can be drawn with climate projection studies. The results of this study align closely with observations reported for Flanders. Based on future climate data used in the IMPACT tool, which projects the effects of climate change for future periods, decreases in the lowest groundwater levels due to climate change are estimated to range, on average, between 10 and 25 cm for the short-term period (2050) (Milieumaatschappij, 2021). This estimate aligns well with the observed average decrease of approximately 10 cm in ground-

water heads across most wells under the factual scenario in this study (Fig. 5.26). Additionally, although specific drought duration maps were not generated using the IMPACT tool, the portal indicates an increase in the number of drought days per year, consistent with the observed extended drought durations under the factual scenario for all drought accumulation periods (Milieumaatschappij, 2021).

Another climate projection study by Vansteenkiste et al. (2014) evaluated the impact of wet, medium, and dry scenarios on groundwater levels in the Grote Nete watershed. They reported significant decreases during summer and autumn under dry scenarios, with variations in magnitude across aquifers and locations. Declines in groundwater head levels ranged from 0.1 to 1.2 meters, depending on aquifer properties and topographical factors. Similar seasonal trends and ranges were observed in this study, where an average decrease of 10 cm in groundwater heads was recorded, with maximum declines ranging from 0.1 to 1.5 meters in certain locations within the Kleine Nete watershed. The most pronounced decreases in groundwater heads were observed during the summer and autumn seasons.

Outside the Flemish region, Fallahi et al. (2023) examined the effects of climate change on groundwater level variations in the Razan Plain. They reported different seasonal patterns, with the largest declines occurring in spring and summer due to rising temperatures and reduced precipitation. They also attributed more than 60% of groundwater depletion to human activities, such as over-extraction, identifying climate change as a secondary driver. Similarly, Kidmose et al. (2013) examined extreme groundwater levels and observed modest decreases, consistent with this study, with changes generally within tens of centimetres (Fig. 5.26).

Although most studies indicate a decreasing trend in groundwater levels under climate change, the impacts can vary significantly depending on local conditions, aquifer characteristics, and human activities (Davamani et al., 2024). Some regions may experience increased recharge due to more intense precipitation events (Stoll et al., 2011), while others may face significant declines in groundwater levels, as repeatedly demonstrated in our study, driven by reduced recharge and heightened evapotranspiration (Davamani et al., 2024).

2. Drought analysis

Wells L4 and L5 exhibited highly fluctuating groundwater heads but smaller differences in drought duration between the factual and counterfactual scenarios. This counterintuitive pattern, despite higher groundwater deficits predicted for these wells, may be explained by their hydrogeological characteristics. Well, L4 and especially L5 are located in zones with a high hydraulic conductivity (Yimer et al., 2023c). The rapid recharge potential, enables quick recovery from groundwater deficits, thereby buffering prolonged drought durations. Conversely, wells with more stable groundwater heads tended to show greater differences in drought duration, likely due to slower recharge dynamics and greater sensitivity to cumulative climatic stress.

The stabilization of maximum deficits around the 9– to 12–month accumulation period under climate change conditions, particularly evident in most of the wells L2, L4, and L5, could be linked to the characteristics of shallow aquifers prevalent in Flanders (Adriaens, 2021). These aquifers are known to respond rapidly to recharge events, with seasonal and interannual precipitation contributing significantly to their recovery. The quick recharge dynamics and hydraulic connectivity typical of shallow aquifers may mitigate prolonged deficits caused by shorter drought events, leading to stabilization over longer accumulation periods. Additionally, studies on shallow aquifers in nature reserves in Flanders (e.g., the Doode Bemde) have demonstrated how these systems buffer drought impacts through efficient recharge and shorter retention times, allowing for equilibrium under prolonged stress (Wossenyeleh et al., 2021).

The significant increases in drought duration observed in 1936–1937 and 1987 under climate change conditions warrant further attention, as these years did not correspond to known severe droughts in Flanders. For example, while 1976 is recognized as a severe drought year in this region (NWS, 2017), it did not show an increase in drought deficit and duration in this study. The drought period of 1987, captured in the simulations, was not highlighted in local records but is notable in this study for showing the lowest groundwater head values across all wells and the largest groundwater deficits, reaching even up to 1.5 meters in well L5. The 1976 drought, by contrast, appears to have been purely meteorological, with no significant impact on groundwater levels. While Fig. 5.12 confirms a period of low rainfall in 1976, it did not result in prolonged groundwater deficits.

A possible explanation for these findings may lie in the global scope of the climate attribution datasets used in this study. For instance, 1936–1937 was characterized by extreme drought conditions in the United States and Canada (Hoyt, 1938), while 1987 was also a globally significant dry year, with severe droughts reported in regions such as India (Krishnamurti et al., 1989) and California, USA (Center, 2016). This suggests that the observed signals may also reflect global or regional drought patterns rather than localized conditions in Flanders. These discrepancies highlight the complexity of interpreting drought impacts using global datasets and underscore the importance of integrating localized data to capture region–specific climate impacts more accurately.

5.3.7 Conclusion

Groundwater is usually considered as not to be affected by climate change as its below the ground surface. In this research, shallow aquifer of the Kleine Nete watershed in Belgium is investigated to evaluate the extent of climate change's impact on hydrological drought. Notably, recent years (from 2010 onwards) have shown a considerable decrease in groundwater head. Overall, from 1970 onwards, there is an average a significant decline of 10 cm in groundwater head, with some locations experiencing a maximum decline ranging between 0.1 and 1.5 meters, illustrating the spread of uncertainty. The drought assessment indicated an increase in maximum drought deficit and duration due to climate change. The deficit is particularly high for short-term (1 to 3 months) and yearly impacts but recovers on

a 24-month timescale. The results highlighted the need to apply necessary mitigation measures to counteract the impact of climate change on Kleine Nete watershed and in general to unconfined aquifers.

Chapter 6

Nature-based solutions for drought mitigation

This chapter has two major parts where in the first part, a detailed literature review has been made to find the extent of NbS application to mitigate the impact of drought on water resources. In the second part, emphasis is given on finding suitable locations of detention basins and managed aquifer recharge areas across a given landscape.

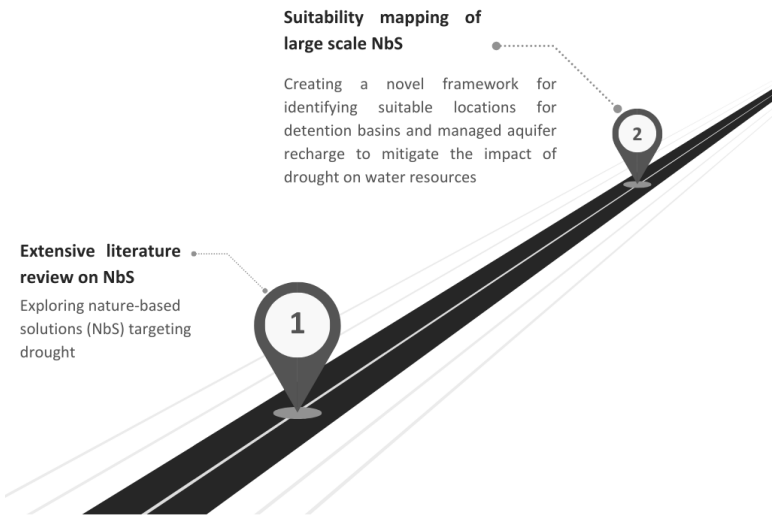


Figure 6.1: Major parts of Chapter 6 which focuses on drought mitigation/adaptation measures via nature-based solutions

6.1 The underexposed nature-based solutions: a critical state-of-art review on drought mitigation

6.1.1 Summary

Droughts are the most expensive climate disasters as they leave long-term and chronic impacts on the ecosystem, agriculture, and human society. The intensity, frequency, and duration of drought events have increased over the years and are expected to worsen in the future on a regional and planetary/global scale. Nature-based solutions (NBS) such as wetland and floodplain restorations, green infrastructures, rainwater harvesting, etc., are highlighted as effective solutions to cope with the future impacts of these events. While the role of NBS in coping with the impacts of other disasters, such as floods, has been extensively studied, there has been a lack of comprehensive review of NBS targeting drought. The following paper provides a unique critical state-of-the-art literature review of individual drought-related NBS around the world, in Europe, and particularly in Belgium, and assesses the critical differences between the NBS applied globally and in Flanders. An extensive literature review was conducted to systematically analyze NBS, listing the type, the location, the status of the implementation, and the possible recommendations proposed to optimize future NBS applications. Finally, a comparison is made between small- and large-scale applications of NBS. By analyzing all these aspects, especially the level of effectiveness and recommendations, insight was gained into the future potential of NBS and possible improvements.

The research indicated a lack of scientific publications, especially in Belgium. Hence, grey literature was also included in the literature review. Only four papers included a quantitative assessment regarding the effectiveness of drought on a global level, all stating a positive impact on groundwater recharge. In contrast, at regional and country levels, the performance of NBS was not quantified. The number of large-scale implementations is low, where landscape- or watershed-scale holistic approaches to drought mitigation are still scarce. Some successfully implemented projects are only very local and have a long realization time, two aspects that limit achieving visible impact at a larger scale. Among the many NBS, wetlands are recognized as highly effective in coping with drought but are still degraded or lost despite their significant restoration potential. A common effectiveness evaluation framework shall be followed, which gives policymakers a clear view of the different NBS investment options. Furthermore, a more collaborative approach is recommended globally, including different stakeholder groups, with specific attention to the local communities. To conclude, future research should increase the evidence base and implementation of drought-mitigating NBS.

This section is published as: **Yimer, E. A.**, De Trift, L., Lobkowicz, I., Villani, L., Nossent, J., van Griensven, A., 2024. The underexposed nature-based solutions: A critical state-of-art review on drought mitigation. Journal of Environmental Management 352, 119903. https://doi.org/10.1016/j.jenvman.2023.119903

6.1.2 Introduction

Despite being popularized only recently (Nesshöver et al., 2017), NbS received high interest from the research community, proved by the high number of related publications. Several literature reviews have already been conducted, focusing, for example, on hydro–meteorological risk reduction (Ruangpan et al., 2020), water management in European cities (Oral et al., 2020), stakeholders' engagement in NbS planning (Ferreira et al., 2022), health benefits (Kabisch et al., 2017; Van Der Zee et al., 2017), and nature-based infrastructures to improve coastal resilience. Nevertheless, the lack of a comprehensive review of NbS targeting drought led to this review paper's conception.

Hence, the central part of this study aims to review the current state-of-the-art NbS measures targeted at mitigating drought at global (worldwide), regional (Europe), and country (Belgium) levels. Belgium is chosen due to the wide range of NbS applications and their potential benefit in drought mitigation. Indeed, Northern European countries such as Belgium urge to find readily–applicable solutions to cope with drought, as this phenomenon was extremely rare in the past, and water managers lack experience and solutions to tackle it effectively. The literature review focuses on the measures maximizing the total water storage capacities in the landscape and retaining the water in the aquifers and soils. More specifically, NbS designed to mitigate droughts, their effectiveness, and future recommendations are investigated. On top of that, these NbS are compared across different countries, focusing on the critical differences between NbS applied in Belgium and worldwide. Next, the most effective future drought interventions are discussed in the face of a changing climate. Finally, small-scale and large-scale NbS applications targeting drought are assessed and compared.

Since NbS is an emerging concept, having a critical review of the current state–of–the–art with detailed and comprehensive information about the effectiveness and lessons learned from pilot projects is needed. In this regard, key objectives were formulated as follows:

- Critically assess the current state-of-the-art drought-mitigating nature-based solutions (NbS) in literature at global (worldwide), regional (Europe), and country levels (Belgium).
- Critically compare NbS targeting drought across different scales, and examine what Belgium (Flanders) can learn from existing NbS applications in other parts of the world and vice versa.
- Examine and compare drought-mitigating NbS applied at small and large scales.

6.1.3 Methodology

The methodology consisted of different steps. After the conceptualization of the research and the definition of the two main topics covered, namely NbS and drought, the literature

string search and the criteria for inclusion or exclusion were defined. Then, different individual drought-related NbS were critically assessed at the global, regional, and country levels. Moreover, a comparison was made to examine what Belgium can learn from other parts of the world and vice versa. Finally, small- and large-scale NbS applications are analyzed. In this paper, we refer to the term "level" when considering the geographical application of the NbS, while we use "scale" to compare the application scale of the NbS.

Search strategy and geographical location

The analysis uses online information sources published in English journals, Dutch reports, and websites. Since the concept of NbS is recently introduced (Nesshöver et al., 2017), not only scientific journal articles were reviewed but also reports and non-scientific articles. As the research focuses on NbS specifically designed to cope with droughts, only those increasing the water storage in the landscape were included. Nevertheless, some NbSs reducing the flood risk were also considered when they were also judged efficient for drought mitigation.

The critical assessment was done for different locations, where we started by investigating applications at a global level except Europe, then Europe corresponding to the regional level, and Belgium as the country level. The literature review searched for relevant publications on the Scopus database using defined search terms. The search strategy for this literature review was adapted from a review on hydro-meteorological risk and NbS (Ruangpan et al., 2020). The string used to perform the literature search summarized the two main concepts, NbS, and drought, with the synonyms, and it is reported below:

("Nature–based solutions" OR "Low impact development" OR "Sustainable Urban Drainage Systems" OR "Water Sensitive Urban Design" OR "Best Management Practices" OR "Green infrastructure" OR "Green blue infrastructure" OR "Ecosystem-based adaptation" OR "Ecosystem–based disaster risk reduction" OR "Green and grey infrastructure" OR "Landscape approach" OR "Landscape ecology" OR "Agroecology") AND ("Drought" OR "Hydro–meteorological" OR "Streamflow deficit" OR "Hydrological drought" OR "Meteorological drought" OR "Low flow" OR "Disaster")

The search terms were all combined into one search on the Scopus database. A few publications were taken out due to being duplicates of the same study or not being recognized as valid reviewed papers. These results were then filtered by reading titles and abstracts for publications of NbS related to drought. Papers were classified as relevant if they included the term drought or synonyms and if the paper mentioned NbS or techniques that can be classified as such.

Large and small–scale application comparison

A table was constructed for all levels (global, regional, and country) to compare the measures across different scales. Different aspects were delineated, including NbS type, lo-

cation, begin (& end) year of implementation, status by now, level of effectiveness, and possible recommendations set by the researcher to improve future implementation. By analyzing all these aspects, especially the level of effectiveness and recommendations, insight was gained into the potential future NbS measures and improvements.

As a final step, the relevant papers were scanned for the different types of scales for NbS regarding drought that were applied. A distinction was made between large- and small-scale NbS. Where the type of scale could not be concluded from the abstract, the whole paper was reviewed. Within this process, some papers were again excluded from the selection as, although drought was mentioned in the abstract, the case studies mentioned in the paper did not specifically addressed drought.

A classification of what is counted as small-scale and large-scale is reported in Tab. 6.1. For example, if a publication discussed the so-called sponge cities, this was classified as a large-scale application of NbS since it has a city-wide approach. Also, if many small-scale applications were being used simultaneously within the same region or watershed, they were classified as large-scale applications of NbS.

Table 6.1: Small-scale and Large-scale Solutions

Small-scale solutions	**Large scale solutions**
1. Singular projects on a single plot of land	1. City-wide approach
2. Small experiments	2. Landscape approach
3. Singular NbS in one location within a city or landscape	3. Watershed approach
4. Modelling of a single NbS	4. Multiple projects (large-scale application of small-scale solutions)
	5. Modelling on a landscape or city-wide scale
	6. Country-wide approach

6.1.4 Result

The literature search in the Scopus database yielded 1322 results within a period from 1988 until the end of 2022. After the screening process, 134 articles were finally selected for this study. The topic of NbS for drought is very underrepresented in comparison to floods as a hydrometeorological hazard, as also highlighted by Ruangpan et al. (2020). This emerged clearly from the literature review (Fig. 6.2), as many articles include drought as an add–on to flood mitigation or as another problem in the hydrometeorological risk list. This underrepresentation is also the result of the wide range of vocabulary with which the authors define and conceptualize these topics. Also, drought might not have been the

main topic of some research and was excluded from the title or the abstract, even if, when reading the paper, drought was mentioned and assessed as part of a broader spectrum of hydro-climatic risks. Out of the 134 selected papers, 95 publications specifically mention drought in their title or abstract. However, only 24 also mention NbS in connection with drought. It can therefore be assumed that the research on NbS and drought is still very limited and underrepresented in the scientific community and requires further research into how NbS at different scales would be successful in mitigating the effects of drought.

Globally, incentives have created resilience against water scarcity using nature and ecosystem services. Table in the appendix (https://www.sciencedirect.com/science/article/pii/S0301479723026919 summarizes a literature review of current nature-based projects at a global level to increase water availability, including the NbS type, year of implementation, status, level of effectiveness, and possible recommendations set by the researcher to improve the application in the future. The location of the NbS varied greatly, with a few countries showing a lot of research regarding drought and NbS (Fig. 6.3). Among the leading countries in this literature review were China, the USA, and South Africa. Within Europe, there was a wide range of countries with different climates that also contributed to the research, such as Italy and Spain, Germany, and the Czech Republic. What is visible from the range of countries is the fact that drought is becoming a widespread phenomenon and that mitigation strategies for different climates and landscape types need to be found. Furthermore, the highest drought impacts typically occur in Sub-Saharan Africa, but most applications are spread across Europe and north America. The past decade experienced increased applications of NbS targeting drought, with Europe leading the way. The number of projects in the world, Europe, and Belgium is reported in Tab. 6.2 and 6.3, ordered by decade and implementation status, respectively.

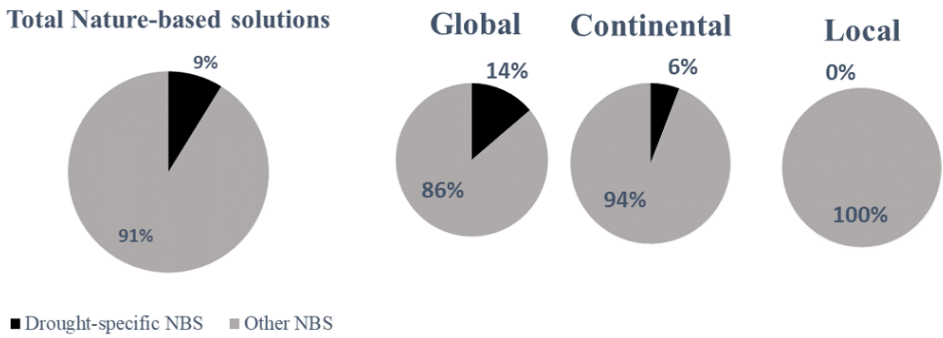


Figure 6.2: The percentage of NbS applications targeting drought or other hydroclimatic extremes at global, regional (Europe), and local levels (Belgium)

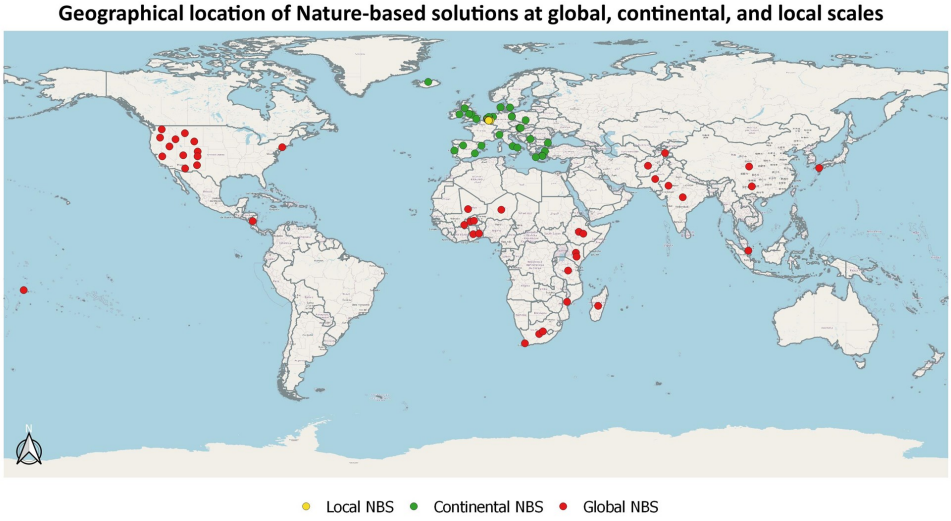


Figure 6.3: The number of nature-based solutions targeting drought at different scales and their spatial distribution

Table 6.2: The number of projects that are implemented and ongoing for the different decades

Decades	Number of projects		
	Globally	Europe	Belgium
1990 to 2000	0	2	1
2000 to 2010	2	8	1
2010 to 2020	18	19	6
2020 onwards	6	8	1

Table 6.3: The number of projects which are successfully implemented, ongoing, or with no status information

Implementation status	Globally	Europe	Belgium
Successfully implemented	20	20	2
On going	7	14	4
Not stated	2	1	0

NbS to mitigate drought and water scarcity in the world

Most of the existing global NbS are successfully implemented or still in the active stage (pilot project stage). A major pilot project is the implementation of sponge cities in China. Although the main reason for this project is to cope with the effect of rapid urban development on the natural environment and its water-related problems, such as urban flooding, it will also be efficient in coping with droughts by improving the urban water logging (Liu et al., 2017; Nguyen et al., 2019). The implemented NbS (such as green infrastructure and infiltration ponds) infiltrate and store the excess rainwater, which can be used for future water use (Liu et al., 2017). However, this solution's effectiveness is not yet quantified; there are still many technical, physical, financial, legal, and regulatory challenges to overcome before successful implementation can be achieved (Nguyen et al., 2019).

Similar to the sponge cities in China, many other papers do not evaluate the effectiveness of NbS for drought. Some examples are the river restoration and riparian wetland restoration projects in Colorado (Cohen-Shacham et al., 2016), the beaver restoration projects in the Western USA (Pilliod et al., 2018), the green infrastructure projects in New York City (Kalantari et al., 2018), (rain)water harvesting in Tucson (Radonic, 2019) and the Sub-Saharan countries (Critchley and Di Prima, 2012), and the implementation of greenways in Burkina Faso (Sy et al., 2014). As the dynamics and impacts of drought are difficult to be fully understood, Cohen-Shacham et al. (2016) recommend examining further the lower-flow scenarios related to drought, while Pilliod et al. (2018) state the requirement of more quantitative data on the NbS performance. A critical recommendation set by Kalantari et al. (2018) is the exigency of good stakeholder involvement to fully understand the potential impacts. Critchley and Di Prima (2012) offer a more holistic and integrated approach for improving the implementation while also gaining insight into the farmer's knowledge about the NbS technologies integrated into their practices on the field.



Figure 6.4: The widely applied nature based solutions (NbS) at a global scale (except in Europe). The bigger the text's size, the wider the NbS application.

Other papers evaluate drought-related benefits and co-benefits without quantitative assessment and evaluation of the effectiveness. Cui et al. (2021) explored the implementation of green infrastructure (urban park) in combination with the river restoration in the Bishan AMK Park in Singapore. An increase in the water supply and many other co-benefits are expected, such as the increase in water and food supply, recreation, and tourism. Although the benefits are recognized, a quantitative understanding of the effectiveness and other benefits of the project (such as mental health benefits and access to green space) is still lacking. WWAP (United Nations World Water Assessment Programme) and UN-Water (2018) also provide some examples of drought-mitigating NbS, such as many reforestation and sustainable management projects in African countries (Ghana, Mali, Madagascar, Togo, Ethiopia, Burkina Faso, Niger, Kenya, Mozambique, and Nicaragua) and landscape restoration, sustainable management, and green solution projects in Asian regions (India, Pakistan, Afghanistan, Tajikistan). The recognized benefits are increased groundwater recharge, including water table stabilization, and improved water retaining capacity of the soil, which reduces the risk in periods of droughts (WWAP (United Nations World Water Assessment Programme) and UN-Water, 2018). The widely applied NbS are afforestation, wetland, and rainwater harvesting (Fig. 6.4). Note that some studies, such as Koiv-Vainik et al. (2022), although they have investigated and has significant implication on stormwater retention across different climates to cope with hydroclimatic extremes, it was excluded from the analysis as drought is not mentioned inside the abstract. Similarly, Mabon et al. (2022) were excluded for the same reason, though has a unique perspective where mere stakeholder participation is inadequate; rather, a diverse stakeholder group/knowledge is required to enforce NbS. Thus, future work shall account for multiple research arenas by widening the search strategy.

Four papers obtained a quantitative model result regarding the effect of specific NbS on drought. Holden et al. (2022) assessed the impact of catchment restoration, specifically invasive tree species clearing, on streamflow drought. The modeling improved the low flows caused by climate change by 3-16%. Therefore, removing alien tree species is an important technique to reduce the climate drought risk. However, combining with other adaptation techniques must be considered to reduce climate change acceleration. A second study by Amano and Iwasaki (2022) estimated the groundwater recharge due to artificial groundwater recharge in abandoned paddy rice fields using Geographic Information Systems (GIS) and found a substantial increase in recharge. Most of the total recharge (33.61%) is the groundwater recharge from paddy fields. Another paper by Gathagu et al. (2018) modeled the impacts of structural conservation measures (e.g., terraces and grassed waterways) on the sediment and water yield in the Thika-Chania catchment in Kenya. The presence of terraces showed a substantial increase of 8.38% in the baseflow component due to infiltration, while a general increase in recharge was found in the shallow groundwater aquifers by 5.08%. However, the effectiveness can still be improved by combining this implementation with other NbS types. Lastly, Welderufael et al. (2013) simulated the effect of rainwater harvesting on groundwater recharge in South Africa using the Soil Water Assessment Tool (SWAT). The modeling resulted in improved water infiltration in the case of in-field rainwater harvesting and a general increase in groundwater recharge (40 mm/year) compared

to the reference consisting mainly of pasture (32 mm/year). Solely there are still many uncertainties in the model results, which could affect the water yield components, such as the lateral and groundwater flow components.

NbS to mitigate drought and water scarcity in Europe

In recent decades, meteorological droughts occurred more frequently in the European region (Kumar et al., 2020). For example, during the summer months of 2018 - 2020, Europe had to cope with droughts due to a combination of heatwaves and limited precipitation (Trémolet et al., 2019). In addition, there are increased human-caused pressures, such as (over)-abstraction for agricultural (Yimer et al., 2023b), domestic, and industrial water use and degradation or loss of aquatic ecosystems, on the ecosystems triggering water scarcity and droughts (Trémolet et al., 2019). The widely applied NbS in Europe is wetland restoration, rainwater harvesting, and green roofs. Contrarily, less afforestation is applied (Fig. 6.5). The number of successfully implemented and ongoing projects is higher in Europe compared to other continents.

Since 2013, the European Commission has shown increased attention to NbS: the concept of NbS is made more concrete, and its relation is defined to the other ecosystem–based approaches. The following year, the European Commission put together an expert group for further analysis and to increase awareness of the use of NbS in European cities. In 2015, a survey on the public perceptions of nature in cities was conducted for developing future projects (Faivre et al., 2017). The Horizon 2020 program, a funding program for research and innovation (2014-2020), provided nearly 80 billion of funding to create opportunities for new ideas and remove barriers to innovation in Europe. Some subprojects of the program, such as CONNECTING, URBAN GreenUP, GROW GREEN, and UNALAB, have implemented NbS to improve climate resilience and water security (Faivre et al., 2017).

Following the successful Horizon 2020 funding program for research and innovation, the current Horizon Europe program until 2027 provides a budget of 95.5 billion euros to tackle climate change impacts and achieve the Sustainable Development Goals (SDGs) (European Comission, n.d.; Ricciardiello et al., 2021). The program is comparable to the previous one and consists of three general objectives and newly introduced separate missions. In general, they aim to strengthen collaboration between different sectors and emphasize the power of research and innovation in the development and growth of cities. It also supports science and knowledge and boosts the EU's competitiveness.

Several NbS for water security have been proposed and implemented in Europe to face the increasing drought and its impacts. However, the extent to which European countries have implemented NbS is challenging to assess as the available information is limited and fragmented (Trémolet et al., 2019). Table inside the appendix shows a literature review of the current nature-based projects in Europe (https://www.sciencedirect.com/science/article/pii/S0301479723026919).



Figure 6.5: The widely applied nature based solutions (NbS) at European scale (except in Belgium). The bigger the size of the text, the more widely the NbS application.

In line with NbS in the world, most existing regional projects are also successfully implemented. An example of an ongoing project is given in an assessment by the (Davies et al., 2021). From 2009-2019, the first multi-functional wetland restoration and remeandering project (Tulltorpsån 1.0) was carried out in the rural areas of Sweden. As the 1.0 project gained success, the 2.0 project was arranged in 2019 to enlarge the agricultural resilience against floods and droughts. It is crucial to notice that this experiment was initially set up by a few local landowners, covering almost 100 NbS projects within a decade along 30 km of the river course. Another important aspect of this project is the created evidence base by the project itself and the extensive fair stakeholder involvement. The lessons learned from the past projects convinced current project holders in other areas to participate in the project. Also, more than ninety farmers, four hundred villagers, and local people are considered in the economic environment to discuss future projects and problems.

The latter aspect is also recommended in other reviewed papers. Ricart and Rico-amoros (2021) suggest a total involvement of the primary water consumers (in this case: farmers) in the process as they possess potential information about when and how constructed wetlands are efficient solutions to drought, water scarcity, and water pollution challenges. New forms of collaboration between and among different stakeholder groups might help face water scarcity and reduce water conflicts. Frantzeskaki et al. (2020) also affirms the need for a collaborative governance approach to successfully implement and operate NbS (a collaboration between urban planners and urban officers, citizens, NGOs, social innovation networks, and experts). In addition, different fora for the co-creation and co-design of NbS are required using urban social innovation as an essential instrument. A case study by (NAIAD, n.d.) opts for clear communication with water users about the situation to reach a successful solution. Based on a summary of existing NbS by Davies et al. (2021), bottom-up projects from citizens have an essential role in realizing green spaces. As they influence and change public policies, it is recommended to integrate these projects into the policies. Finally, the total involvement of different stakeholder groups and a collaborative approach are thus considered essential elements in climate change adaptation.

Based on a critical review by Oral et al. (2020) on NbS for urban water management in the Mediterranean region, the most frequently mentioned NbS are constructed wetlands. They are designed for water storage and infiltration, which are important functions to mitigate drought and remove nutrients and emerging micropollutants while providing additional co-benefits. Solely limited data is available about the implementation of treated wetlands in cities. Davies et al. (2021) also state that the limitation of space is a remaining challenge for successful implementation since it is difficult to create new green spaces due to the fast-growing and densely-populated cities. To realize the full range of potential benefits, urban planning, and architecture must be combined to accommodate NbS more efficiently (Oral et al., 2020). Other challenges to the success of NbS in cities are related to private ownership (de Boer and Bressers, 2011), climate change, economy, expertise and knowledge, quality of life, and water-related hazards (Davies et al., 2021).

Many studies also show the benefits of each NbS and whether they can cope with droughts or other societal challenges (Frantzeskaki, 2019; Trémolet et al., 2019). Frantzeskaki (2019) evaluate NbS in different European cities and mention for each implementation the benefits, including increased water retention, flood protection, food production, habitat restoration, and recreation. Trémolet et al. (2019) also offer both environmental and social benefits for natural wetland restoration and construction of wetlands in Spain. In Castilla y Leon, water availability and water security improvements are recognized. Equivalently, in the North Metropolitan Area of Barcelona, improved water quality and biodiversity, adaptation to floods and droughts, and more recreational opportunities are offered potential benefits. The riparian forest restoration and riverbank protection in Greece, also propose many benefits, including an increased resilience against climate change impacts, improved infiltration and water storage, reduction of drought risk, and additional benefits for the biodiversity and quantity and quality of the green (& blue) infrastructure. Hein et al. (2016) state the need for quantitative and comparable data to control the success of NbS restoration projects. However, in contrast to the NbS projects in the world, a quantitative assessment of the effectiveness of regional NbS for drought is lacking for each paper. Although the benefits and co-benefits are often mentioned and recognized, there are no evidences or modeling results available to demonstrate the usefulness of each implemented NbS type for drought mitigation.

NbS to mitigate drought and water scarcity in Belgium

Belgium is one of the hotspots for water shortage and scarcity (De Ridder et al., 2020). Apart from the southeast region of England, Belgium has been registered as the most drought-hit region of Europe for some time (Trémolet et al., 2019). Current data indicates an increasing trend in more frequent and prolonged occurrences of low or very low groundwater levels in the past few years (2017-2022), particularly during the summer months when drought conditions are prevalent (VMM, 2021). Belgium is characterized by a dense population, mainly in Flanders and Brussels, which consumes an intensive amount of water (e.g., households and industry) and leads to a high vulnerability to drought and water stress (De Ridder et al., 2020). Also, an overall decrease in extreme high and low flows is ex-

pected in the future climate. However, the direction and magnitude of change remain highly uncertain, and these uncertainties must be considered in future climate change adaptation measures (Leta and Bauwens, 2018).

Sigmaplan Flanders is an initiative to cope with the impact of climate change. It is not only designed for flood protection in the Scheldt and its tributaries, but it also offers solutions and measures in periods of extreme drought. They aim to catch and retain the rain and surface water to increase groundwater levels and storage ("Flemish Waterway"). Remeandering as a NbS plays a crucial role as it creates a longer trajectory and reduces the natural drainage of water, resulting in higher water availability. Secondly, the construction of wetlands and flood control areas contributes to a decrease in floods and droughts due to its "sponge function". They soak up the excess water in wet periods and slowly release it in periods of drought ("Flemish Waterway").

The Flemish "Blue Deal" (2019-2024) plays an essential role in the fight against drought and water scarcity. This prime initiative, deployed by the Flemish government, focuses on using specific structural instruments while involving important stakeholders such as industry and farmers. One of the six aims of the blue deal is to consider nature and the environment as part of the solution against climate change and, in turn, drought. It intends to restore specific ecosystems, such as forests, grasslands, meandering rivers, and wetlands. Therefore, the Blue Deal is in line with the concept of implementing NbS as a drought mitigation measure. Additionally, it not only focuses on staking NbS but also emphasizes saving water, efficient water use, circular use of water, use of alternative water sources, etc. ("Blue deal").

Many small projects have already been planned or carried out to secure water in the future. Table in the appendix (https://www.sciencedirect.com/science/article/pii/S0301479723026919) shows a literature review of the existing and ongoing NbS projects, including the NbS type, year of implementation, status, level of effectiveness, and possible recommendations set by the researcher to improve the results in the future. The number of projects aiming at restoring rivers and wetlands comprises the highest number (Fig. 6.6).



Figure 6.6: The widely applied nature based solutions (NBS) in Belgium. The bigger the size of the text, the more widely the NBS application.

Although there is a recent upswing of small NbS-related projects in Belgium, only two scientific papers regarding regional NbS for drought mitigation were included in the review (Frantzeskaki, 2019; Gorissen et al., 2018). Frantzeskaki (2019) analyzes existing NbS projects in different cities, including "The Green Corridor" in Antwerp. This current project aims to connect people with nature and their sense of place in the city of Sint-Andries. Equivalent to the wetland restoration and remeandering project in Sweden (Tulltorpsån 1.0), an important aspect is the involvement of different stakeholder groups with divergent backgrounds and knowledge while creating the space. Although this linear park was initially constructed for flood protection, it also brings other benefits related to water retention, recreation, and biodiversity (Frantzeskaki, 2019). The second drought-coping group of NbS in Belgium is the (Food) & Nature conservation and restoration projects (including blue-green infrastructure) in Genk, namely the Green Corridor (Stiemerbeek Valley), Bee Plan, Heempark, and Organic allotment gardens projects (Gorissen et al., 2018; Kabisch et al., 2017). Although these projects increase resilience against climate change, there are also many other co–benefits, such as increased sustainable urbanization, restoration of the ecosystems and their functions, and increased education about NbS ("Genk").

The Sigmaproject comprises different nature-based projects in Flanders, for example, the Project Bovendijle and Dijlemonding, located in the Dijle-Zenne basin. The Sigmaproject Bovendijle also has different subprojects, such as the construction of wetlands and flood control areas in Rijmenam, Pikhaken, and Hollaken-Hoogdonk ("Sigma project"). The Sigmaproject handles a different approach to coping with rivers' embankments. High dikes were built on both sides of the riverbed in the past, so the river only overflowed its banks during very extreme events. During the floods of 1953 and 1976, this method proved to be insufficient. The Sigmaproject opted for a different approach: lowering and reinforcing the existing dikes and constructing a higher ring dike further away, creating a flood control area between the two dikes. This approach allows the river to overflow regularly in the flood control area, removing large volumes of water from the bed and reducing the flood risk in the more downstream urban areas. Next to flood protection, the ecology is also allowed to develop in and around the flood control area. The subproject in Rijmenam and Hollaken-Hoogdonk, respectively covering an area of 60 and 70 ha, will be fully established as a flood control area ("Sigma plan").

In the subproject of Pikhaken, a wetland of 30 ha is constructed instead of a flood control area. The reason can be explained by the tides and the flow of the water. The controlled flooding can be most easily provoked in the other two areas. Those areas are located where the rising of the tides collides with the water from the upper reaches at elevated water levels due to, for example, abundant precipitation. Additionally, Pikhaken is established as a habitat directive area. So, the aim is to invest in fully reconstructing the natural ecological state. In the case of a flood control area, the pollution with Dijle water could harm the area's natural value. Therefore, constructing a wetland is a better option in the area around Pikhaken. The implementation of wet grasslands can bring back some rare species that used to be abundant in the valleys of the tidal rivers.

The Sigmaproject Dijlemonding is divided into subprojects: Grote Vijver, Tien Vierendelen, and Zennegat. At the Dijle's mouth, the Zenne, Nete, and the Canal of Leuven–Dijle converge with an additional influence of the tides. This place is a very important water junction, which creates the opportunity to implement different nature–based projects to reduce climate change risks and increase nature's value (Coordinatiecommissie Integraal Waterbeleid, 2021). Both projects include the implementation of a flood control area. In the Zennegat (65 ha) and the Grote Vijver (100 ha), the flood control areas have reduced tides that mimic a tidal river's natural processes. Via combined inlet and outlet sluices, a small amount of water can flow into the flood control area during flow tides; in ebb tides, the water flows back to the river. Thence, the sporadic tidal nature of mudflats and salt marshes is recovered (Coordinatiecommissie Integraal Waterbeleid, 2021). However, in line with the existing NbS in Flanders, the information is collected from non–scientific literature (e.g., publications from Sigmaplan or website articles).

Comparison of NbS across the different scales

As shown in Fig. 6.7, small– and large-scale NbS are equally represented in the analyzed literature. For 21% of the publications, the scale could not be clearly defined, while both scales can be assigned to 8% of the papers. The full table summarizing small- and large-scale applications is available in the appendix (https://www.sciencedirect.com/science/article/pii/S0301479723026919). From the literature review, 44 publications assessed the effect of small-scale solutions. These differed from common methods such as rain gardens, bio-swales, and retention ponds (Chalid and Prasetya, 2020; Gülbaz and Kazezyilmaz-Alhan, 2017; Hankins et al., 2008) to lesser-known techniques such as a wicking tank, which supplies trees with water through synthetic wicks from a storage tank underneath (Nichols and Lucke, 2015). Additionally, some indigenous techniques that have been used for centuries, such as "Careo" channels and "amunas", that supply water through channels that are constructed in the mountains, which hold and infiltrate water (Jódar et al., 2022), were also mentioned within the literature. There is a vast range of small-scale methods at hand that are already being implemented, as can be seen from the 28 applied small–scale projects that this literature review was able to identify. The application ranges in variety, from multiple methods being used within one location, as was done in a retrofitting project of an Avenue in Los Angeles (Belden and Steele, 2011), or a single method, such as a retention basin in Germany (Fröhle et al., 2022). Also included in this category were experiments, which included ten examples. The experiments include innovative ideas such as Microbially induced Calcite Precipitation (MICP), which is a method applied at the soil level (Liu et al., 2021).

Furthermore, 43 of the publications mentioned large-scale projects such as sponge cities or water–sensitive urban design strategies, green infrastructure, or agroecology. Among these large–scale NbS were also efforts to apply small-scale solutions in a broader way, such as in a city–wide implementation of green infrastructure (Jokar et al., 2021; Zhang et al., 2022). Some of the studies included in this category also tried to model the large–scale effects of NbS on drought or the potential for such solutions, such as Jakubínský et al. (2022), where

the suitability of different areas for infiltration was assessed. For the large-scale application of NbS, it became visible from the literature that watershed or even country-wide policies are not yet being implemented in many places. For the large-scale implementation of NbS for drought, only 19 applied projects could be found. These included approaches such as the monitoring of the adoption of drought-proof landscaping (Lassiter, 2022) or forests (McCauley et al., 2022; Wang et al., 2019) and wetlands (Belle et al., 2018; Nolan et al., 2018). The concept of a sponge city was also mentioned several times. The scale of the projects often depended on the location but not on the methods themselves, meaning that small-scale solutions were applied on a bigger scale. An exception to this is agricultural and farmland practices that could be adopted on a large scale, such as the use of drought-adapted crops (Hussain et al., 2020) or rangeland resting (Ouled Belgacem et al., 2019).

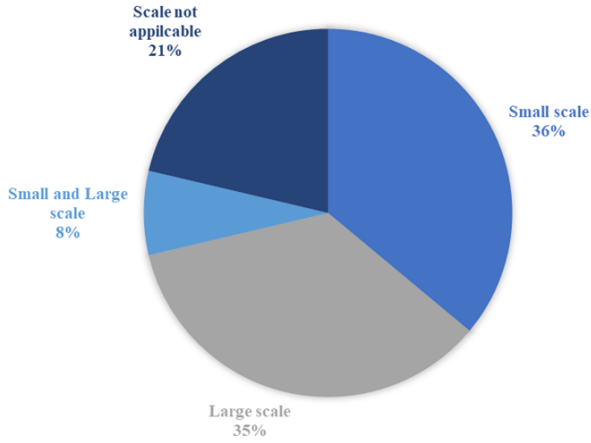


Figure 6.7: The number of literature that corresponds to small scale, large scale, and without scale mentioned

Nine of the publications had to be classified for both categories, as they mentioned small-scale and large-scale applications within the same study, even if in different projects. An example of this is the publication by Rogé et al. (2014), which discusses different methods used by farmers in Mexico, which are small-scale solutions but used within a whole region, therefore possibly having a large-scale impact. Twenty-six of the articles were relevant to the topic of NbS and drought but did not have a project that could be classified to a certain scale (Fig. 5.17). An example of this would be the Framework Hydro–meteorological risk assessment methods and management by nature-based solutions by Sahani et al. (2019).

When assessing the scale of the projects, no distinction was made between theoretical and practical approaches. Therefore modeling of the effects of NbS for drought was considered in their scale in the same way as practical examples of implemented projects. This is why the number of large-scale implementations might seem high, although the implementation

of landscape- or watershed-scale holistic approaches to drought mitigation is still scarce. Another study by Koiv-Vainik et al. (2022) examines the stormwater retention capacity of NbS at different climatic conditions. Although this study focused on mitigating the flooding risks as a response to climate change and was left out of the review, they suggest performing more large-scale case studies to fill missing data gaps, resulting in reduced or eliminated barriers of NbS implementation."

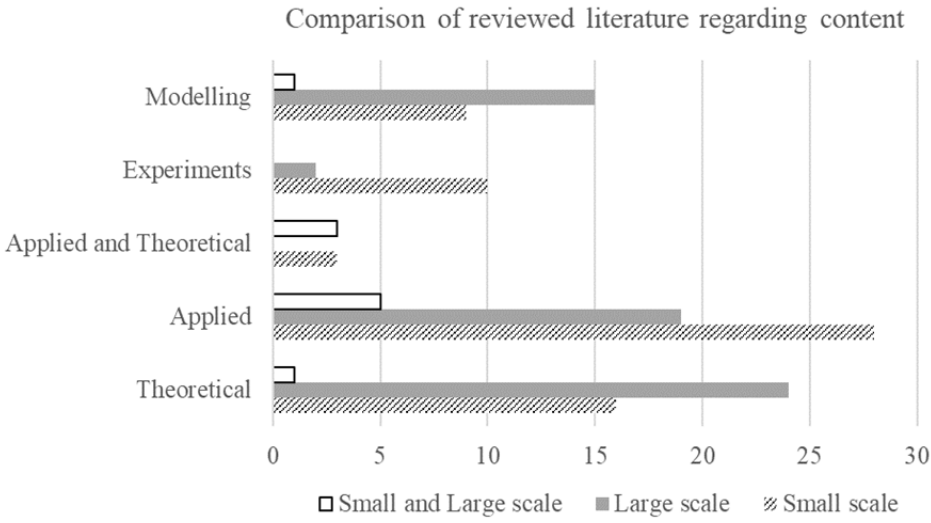


Figure 6.8: Comparison of reviewed literature regarding content - Applied or Theoretical, Methods (Focus on Experiments and Modelling)

Lessons learned from different projects

Diverse NbS types are implemented globally, at regional and country levels. Typical examples are landscape (catchment) restoration, remeandering, flood control areas, green infrastructure, forest and river restoration, and restoration and construction of wetlands. The latter is mentioned in most research and appears to be a frequently-mentioned NbS type in Belgium and the Dijle-Zenne catchment (Oral et al., 2020; Ricart and Rico-amoros, 2021; Frantzeskaki, 2019; Trémolet et al., 2019; Cohen-Shacham et al., 2016).

In contrast to the global and regional NbS, only a couple of projects in Belgium have reached the prosperous implementation state: the Food & Nature conservation and restoration projects in Genk (Gorissen et al., 2018) and the river restoration and remeandering pilot project along the Demer in Rotselaar ("Aarschot"). Similar to the regional NbS and unlike the global NbS, a quantitative understanding of the effectiveness of drought–specific NbS is absent. Moreover, there are no evidences or modeling results to validate the effectiveness of each implemented NbS type. Although the NbS in the Dijle–Zenne catchment

are effective and build resilience against floods and droughts, no research is available to recognize the (co)–benefits and the performance against drought. Quantitative validation of the effectiveness of each implemented NbS type for drought mitigation is also missing.

Flanders can still learn from other parts of the world. Although the Blue Deal provides 343 million euros to subsidize nature-based projects to cope with drought and water scarcity, there are still many limitations. First, because there is no sense of urgency and insufficient funding, projects are only implemented locally. Only a few pilot projects have been realized at a small scale in Flanders yet. There is thus still room to scale up these initiatives all over the country or region, like some global initiatives such as the "Sponge Cities in China" (Liu et al., 2017; Nguyen et al., 2019), the beaver restoration projects in the Western USA (Pilliod et al., 2018), or the rainwater harvesting technologies in Southwestern USA (Radonic, 2019). Although pilot projects are primarily voluntary, implementing stricter legislation might motivate people to carry out projects.

A second lesson might be to shorten the time between planning and realizing projects in the fields of Flanders. In the world, pilot projects are realized in less than one year (Sy et al., 2014). Many extensive worldwide projects also have a short implementation time. Peculiar examples are the WHaTeR project in Sub–Saharan–Africa (Critchley and Di Prima, 2012) and the HYDROUSA projects in the Mediterranean region (Oral et al., 2020), which are both implemented in four years. Another successful example is Sweden's multifunctional wetland restoration and remeandering project, implemented in only a decade. In Belgium, the lack of cooperation of local authorities slows down some potential projects, such as the restoration of wetlands in the 'Valei van de Zwarte Beek' due to permission declines. Not only the local authorities must be blamed, as the Flemish policy might also contribute more to achieving the goals of the Blue Deal.

The primary obstacles are the regulatory and institutional barriers, along with financial constraints (Coördinatiecommissie Integraal Waterbeleid, 2020). Legislative regulations and policies might not fully support NbS projects for drought mitigation, and some policies can even hinder their adoption. Implementing these projects requires collaboration between agencies, private organizations, and local authorities. The complex governance structure and institutional barriers might slow the decision-making process and stakeholder coordination. Additionally, the lack of budgets, such as the Blue Deal, may limit the available funding for these projects, making it challenging to scale up beyond pilot projects (Coördinatiecommissie Integraal Waterbeleid, 2020). Secondly, the lack of social engagement plays a role. The success rate of NbS relies on the active engagement of local communities and stakeholders. If communities are not adequately involved in the decision-making process or do not perceive direct benefits, resistance or opposition to these projects may arise. As demonstrated in the case of Genk, one of the challenges is the knowledge gap on how to insert an effective collaborative governance to implement and maintain NbS (Frantzeskaki et al., 2020). Furthermore, Flanders, being a heavily urbanized region in Belgium, faces a scarcity of land suitable for NbS implementation. This is mainly because rapid urbanization

has resulted in the disappearance of natural landscapes. Compared to other densely populated European regions, Flanders has the highest proportion of urban and built-up areas and the lowest proportion of natural ecosystems (Bastiaensen et al., 2023). As the population continues to grow and urban areas expand, the loss of natural ecosystems persists, leading to a potential further reduction in suitable space for NbS. This presents a significant challenge for implementing NbS effectively in the region.

On the contrary, worldwide projects can also learn from the European and Flanders projects. Many European publications mention the importance of collaboration and stakeholder involvement (Frantzeskaki, 2019). They are essential in bringing together different kinds of expertise. Especially by involving local communities and farmers in the decision–making process, the region's knowledge is transferred, ensuring all aspects are considered and increasing the successful implementation of NbS. Moreover, involving stakeholders from the early stages of a project helps build trust, a sense of ownership and enhances acceptance and stakeholder awareness. Individuals who are included in decision-making tend to be more supportive and actively engaged in NbS. Involving not only bottom-up projects from locals and citizens but also policymakers and government agencies early in the process helps align NbS with existing policies and regulations, creating opportunities for new water management policies that ensure sustainable water and other natural resources use. Additionally, the learning process is significant. Stakeholders can learn from what has worked or not worked in the past on similar projects. By sharing their successes and failures, they can develop better ways to manage the project over time and improve its outcomes (Davies et al., 2021; Frantzeskaki et al., 2020; Ricart and Rico-amoros, 2021). Although Flanders still has much to learn, the Blue Deal stresses this aspect. Everyone must contribute, including the citizens, government, farmers, scientists, companies, and other associations, to be able to roll out positive results and battle drought in the future. Two important existing examples are the food & nature conservation and restoration projects and the multifunctional wetland restoration and remeandering in Genk (Flanders) and Sweden (Europe), respectively. Notably, the local communities initiated those NbS projects (Gorissen et al., 2018).

Different aspects related to stakeholder participation, including fair public participation, recognition of diverse expertise and the importance of balancing diverse knowledge perspectives, can influence the extent to which stakeholder involvement contributes to the effectiveness of environmental management policy responses in urban planning (Mabon et al., 2022). Sustainable urban planning often relies on active community engagement, as it can lead to policies and initiatives that are more aligned with the needs of local communities. Effective public participation can contribute to sustainability by fostering a sense of ownership and cooperation among stakeholders. However, Mabon et al. (2022) argue that mere participation will not significantly influence the policy responses in cases where insights and expertise of residents cannot change the direction in which the city plans the adaptation strategies. Recognition and valuing diverse forms of expertise is essential for sustainable environmental management policies. Different experts can provide insights into various aspects of sustainability, such as ecological resilience, social equity, and economic

viability. Knowledge in the context of urban NbS may lead to policies focused solely on measurable targets, as depicted by Mabon et al. (2022). This suggests a more balanced approach, which considers a diversity of knowledge perspectives, to contribute to the development of more sustainable environmental management policies. These elements contribute to the development of holistic, equitable policies which are capable of addressing the complex challenges of urban sustainability.

The occurrence of wetlands in many studies is not random, as they have a great potential to mitigate slow-onset drought events in the future (Endter-wada et al., 2020). Wetlands are not only indispensable for humans' survival but also belong to one of the world's most productive ecosystems. Apart from drought mitigation, wetlands contribute to other ecosystem services such as flood, stormwater, and coastal protection, regulating regional climate and soil moisture, improving water quality and biodiversity, increasing water efficiencies, carbon sequestration, and groundwater regeneration (Alikhani et al., 2021). Many studies prove the disappearance of wetlands due to major trends such as climate change, land use change for intensive agriculture, domestic and industrial infrastructure, and overexploitation of freshwater and wetland resources to sustain a growing population. Additionally, quantitative research has stated the fast global loss of wetlands in the near past. 64-71% of the wetland area has been degraded or lost during the 20th and early 21st centuries (Davidson, 2014).

In Flanders, the same trend is observable. A study by Decleer et al. (2016) claims that about 75% of the total wetland ecosystems have been lost in the last 50-60 years due to rapid urbanization, intensification of agriculture, and increased forest area. Although only 5% of the total area of Flanders remains (68.000 ha), there is still a great potential for restoration. Calculations show the possibility of creating or restoring more or less the appropriate biophysical and ecological conditions of 147.000 ha of wetlands (Decleer et al., 2016). Although the Flemish Blue Deal has already funded the restoration of 1.600 ha of wetland area, it is not enough to mitigate droughts and only a minor fraction (less than one percent) of the covered area in mid 20th century. Wetlands are highly valuable ecosystems that offer a multitude of benefits, especially in the context of drought mitigation in Flanders. According to a study conducted by Decleer et al. (2016), wetlands provide essential ecosystem services that play crucial roles in sustaining the environment and supporting human well–being.

One of the key ecosystem services of wetlands is drought regulation. During periods of drought, wetlands act as natural buffers by storing water accumulated during wet spells and gradually releasing it during dry periods. This function helps to maintain water levels in surrounding areas and recharge groundwater reserves. Through their porous soil and vegetation, they allow water to percolate into the ground, recharging aquifers and providing a sustainable and natural water supply that is vital in mitigating the impacts of droughts. Furthermore, wetlands serve as natural filters, effectively removing pollutants and excess nutrients from water before it enters streams, rivers, and groundwater. This purification pro-

cess enhances water quality, reducing the risk of contamination and benefiting both human populations and aquatic life. In addition to their role in drought and water quality regulations, wetlands act as effective flood control measures. They can absorb and store excess water during heavy rainfall or flooding events, thereby reducing the risk of downstream flooding and protecting communities and infrastructure. Moreover, wetlands are rich and diverse ecosystems that offer habitat and breeding grounds for a wide range of plant and animal species. They contribute significantly to biodiversity conservation in Flanders, supporting various rare flora and fauna. Beyond their ecological significance, wetlands hold cultural and recreational value for local communities. They offer recreational opportunities such as birdwatching, hiking, and nature appreciation while also serving as places of traditional practices and cultural heritage.

Wetlands in Flanders have faced the impact of both global trends and local factors, resulting in significant loss during the 20th century. Among the local factors contributing to this loss, intensive agricultural practices and land use changes have been particularly detrimental (Schoukens, 2022). Presently, about 45% of the region is devoted to intensive agriculture, which involves heavy fertilization, drainage, and irrigation, leading to wetland conversion for farming purposes (Meyer et al., 2011). This transformation has significantly diminished natural wetland habitats, sacrificing them for agricultural expansion. Urbanization has also taken a toll on wetlands, with approximately 13% of the region's soil now paved and 26% urbanized (Meyer et al., 2011). As human settlements and infrastructure expanded, they encroached upon wetland areas, further contributing to their decline. The remaining wetlands, covering only a small portion of the region, face additional threats like eutrophication and pollution due to disrupted hydrological regimes (Decleer et al., 2016). Local pollution sources, including industrial discharges, urban runoff, and agricultural runoff, continue to contaminate wetlands, negatively impacting water quality and harming flora and fauna.

While the above-mentioned local factors are primary drivers, climate change acts as a global aggravator, compounding the challenges faced by these vulnerable ecosystems. Climate–induced changes, such as reduced summer precipitation, higher temperatures, and increased evaporation, lead to drier soil conditions. This poses a threat to habitats and species adapted to moist climates, including wetland ecosystems, which face increased vulnerability as extreme droughts become more frequent. The intensified frequency of extreme droughts may even lead to the reduction or complete elimination of these ecosystems (INBO, n.d.).

Future research and initiatives focusing on wetland restoration as a NbS for drought mitigation can significantly enhance ecosystem resilience and sustainability. To achieve this, several key recommendations have been proposed. Firstly, conducting more hydrological studies related to low-flow conditions during droughts will help understand the role of wetlands in water storage and groundwater recharge (Cohen-Shacham et al., 2016; Moeskops, 2018). Secondly, raising awareness through education and training is crucial in changing perceptions about the importance of wetland restoration for drought mitigation among the

public, decision-makers, and stakeholders (Nguyen et al., 2019). Thirdly, long-term monitoring of wetland restoration projects will provide valuable insights and support future efforts. Once the effectiveness of a project is assessed in mitigating drought, other projects will more likely be setup, and other local people will be convinced to participate in the project (European Topic Centre on Climate Change impacts, Vulnerability, and Adaptation, 2021). Integrating these measures into climate change projections and models is also essential to ensure that restored wetlands can withstand future climate challenges and garner support from local authorities and citizens (Moeskops, 2018). Collaboration between researchers, local communities, and policymakers is recommended for a holistic approach (Frantzeskaki, 2019; Ricart and Rico-amoros, 2021). Community engagement is particularly vital, as local knowledge can determine when and how wetlands effectively address water scarcity and pollution challenges, leading to successful implementations (Ricart and Rico-amoros, 2021). Lastly, while wetland restoration is valuable, additional measures such as wetland recovery or carbon sequestration may be necessary to further mitigate water availability issues (Trémolet et al., 2019).

6.1.5 Discussion and Conclusion

The paper presents a critical state-of-the-art literature review on NbS for climate change mitigation at different levels, including the global (worldwide), regional (Europe), and country (Belgium) levels. Focusing on NbS specifically targeting drought, this paper is unique as the effectiveness of drought mitigating NbS is scarcely studied. Moreover, the major obstacle is the assumption of flooding-based NbS applications as a direct measure of drought. Due to this, less attention is given to drought-mitigating NbS, and appropriate measures should be adopted targeting specifically drought. The review procedure started by constructing a table for all levels. Different aspects were delineated, and then a comparison was made between small- and large-scale applications, which can indicate the degree of mitigation.

As few scientific publications evaluate existing drought-relevant NbS, the information is collected from various sources. Scientific reports are included, and non-scientific papers and website articles to incorporate as much local knowledge as possible. Especially regarding the NbS in Belgium, for which only two scientific publications are found, non-scientific articles and grey literature (books and reports) were considered. To ensure publications are not excluded, articles focusing on floods are also included if they are recognized as beneficial in increasing water storage and infiltration.

Most existing NbS projects have reached the requested implementation state worldwide, and in Europe, while in Flanders (Belgium), most projects linger in the pilot project stage. Despite the launch of the Flemish “Blue Deal,” there is still a lack of funding and a sense of urgency, which hinders the successful implementation. A second remark concerns the longer time between the planning and implementation stages in Flanders. Possible solutions might be providing financial incentives, implementing stricter legislation motivating stakeholders to carry out projects, and strengthening cooperation among local authorities.

There are two major benefits of fiscal incentives; 1) suggesting fiscal incentives instead of implementing stricter legislation can be a viable approach to encourage the development of innovative technologies by providing financial rewards for those who invest in green solutions (Köhler and Kaiser, 2021). 2) by introducing financial incentives, policymakers can create a system where compliance with certain policies or regulations becomes more attractive due to the potential economic benefits or advantages associated with it, encouraging implementation or maintenance of NbS by the public. However, while valuable, fiscal incentives might not be fully effective on their own and should be integrated into a comprehensive approach that includes strict regulations, education, and public awareness campaigns. As concluded by Mendonça et al. (2021), different policy instruments are needed to encourage the implementation of NbS. Stricter legislation becomes essential in situations where voluntary measures fall short or when the severity of drought impacts poses significant risks to human and environmental health. By combining fiscal incentives with robust regulations, we can tackle the challenges of drought and promote sustainable water management practices.

Specifically for Flanders, a comprehensive and integrated approach is required to promote collaboration among policymakers, scientists, local communities, and relevant stakeholders. Aligning policies, limiting institutional barriers, and providing adequate financial support are essential steps to pave the way for the successful implementation of NbS projects for drought mitigation in Flanders, Belgium.

However, the world can also learn something from Belgium: participation of different stakeholder groups played an important role in the realization of different projects by including diverse voices, ideas, and values. Although the Blue Deal is not fully realized yet, it embraces this concept and pleads for a collaborative approach between the citizens, government, farmers, scientists, companies, and other associations. In particular, the involvement of the local communities is essential. Considering the local knowledge of residents contributes to a better project design and might even improve the implementation.

Furthermore, (co–)benefits are stated, and the effectiveness is mentioned globally and regionally. However, for Europe, it is only stated whether they are effective against droughts or not without any quantitative evidence or model validation results to control the success of restoration/construction projects. On the contrary, a quantitative assessment of the effectiveness of drought is given in a few publications in the world, which proved to have a positive impact on groundwater recharge. As most information is taken out of grey literature for Flanders, no information on the benefits and no quantitative model validation on the effectiveness of drought is given. Consequently, a common effectiveness evaluation framework shall be followed, which gives policymakers a clear view of the different NbS investment options. Finally, the comparison between small– and large-scale applications indicated the lack of implemented projects at a larger scale. Moreover, the assessment of NbS for drought mitigation is still at the modeling stage, indicating less attention is given to drought regarding NbS applications.

Among the various drought–mitigating NbS, wetlands are recognized to have significant restoration potential from worldwide to Belgium. Despite its potential for future drought mitigation and the additional help of the Flemish Blue Deal, few initiatives were taken to improve the conditions of wetlands in Flanders. Future research is recommended to investigate the effectiveness of wetland restoration and implementation at a larger scale. Once the evidence base is enlarged and the sense of urgency is spread, more initiatives will be taken to mitigate droughts. A good and effective stakeholder engagement approach, including residents, will also make room for collaboration and help convince people that NbS are creating a better future. In future research, geohydrological modeling will be the key to assessing and quantifying drought's future impacts before and after wetland restoration.

Geohydrological modeling might play a crucial role in assessing the impact of NbS on drought. It involves integrating geological and hydrological data to simulate and understand the behavior of water in the Earth's subsurface. A previous study by (Ejaz et al., 2022) predicts long-term changes in groundwater storage and depletion by considering not only the rainfall-runoff processes but also the groundwater stores and exchange fluxes together with streamflow throughout the whole geohydrological modeling process. It is possible to simulate water movement in the subsurface, including flow through aquifers and the interactions between surface water and groundwater. Understanding these dynamics is essential for evaluating how NbS may influence water flow and availability during drought periods, as we need to get more insight into how groundwater storage is changed after the implementation.

It is to be noted that due to the search string, some NbS projects/papers are not included in our analysis. The study made by Mabon et al. (2022), Koiv-Vainik et al. (2022), and Meilinger and Monstadt (2022) are few examples of such studies which are excluded from our review. The latter has a unique point from a sustainability standpoint, where communities can lessen their reliance on centralized stormwater methods and increase their resistance to climate change and other environmental concerns by supporting the use of decentralized and green infrastructures. Cities may share the costs and benefits of public infrastructure development and encourage more equitable and sustainable methods of stormwater governance by modifying legislation and finance tools to support green infrastructure. Additionally, communities may improve their ability to manage stormwater effectively and encourage more integrated and sustainable land use by enhancing the synergies between stormwater and land use regulation.

Droughts' frequency, duration, and intensity have increased in the last few years. This trend is also expected to continue in some parts of the world. Therefore, staking NbS as the solution is put in the spotlight instead of a technical solution because they create multiple benefits, not only for droughts but also for climate change and other essential ecosystem services needed to sustain human life. With this review, we exposed the urgency of exploring the potential of drought-mitigating NbS and producing more quantitative evidence

of their effectiveness. More research is certainly needed at the global level, but even more in those regions of the world, such as Sub-Saharan Africa, that are currently facing strong negative impacts caused by drought.

6.2 Framework for mapping large–scale Nature-Based Solutions for drought mitigation: regional application in Flanders

6.2.1 Summary

Droughts are classified as the most expensive climate disasters as they leave long-term and chronic impacts on the ecosystem, agriculture, and human society. The intensity, frequency, and duration of drought events have increased in the past and are expected to continue rising at global, continental, and regional scales. Nature-based solutions (NBS) are highlighted as effective solutions to cope with the future impacts of these events. Despite this, there has been limited comprehensive research on the effectiveness of NBS for drought mitigation, and existing suitability mapping frameworks often overlook drought-specific criteria. To address this gap, a new framework is proposed to identify areas suitable for two drought-coping NBS types at a regional scale: detention basins and managed aquifer recharge. Two multi-criteria decision-making techniques (MCDM), i.e. Boolean logic and Analytic-Hierarchy Process (AHP), were used to map suitable large-scale NBS.

The new framework accounts for unique criteria to specifically address drought conditions. By incorporating climate change scenarios for both surface and groundwater, recharge, and different groundwater characteristics, it identifies suitable and sustainable locations capable of managing extreme drought events. Executed through Boolean logic at a regional scale in Flanders (Belgium), the framework's strict approach yields significant potential areas for detention basins (298.7 km²) and managed aquifer recharge (867.5 km²). Incorporating AHP with the same criteria introduces a higher degree of flexibility for decision-makers. This approach shows a notable expansion across Flanders, varying with the level of suitability. The results underscore the highly suitable potential for detention basins (2552.2 km²) and managed aquifer recharge (2538.7 km²), emphasizing the adaptability and scalability of the framework for addressing drought in the region. The comparison between potential recharge volume due to detention basin and groundwater use in the region indicated that the detention basins could partially compensate for the high water demand. Therefore, creating a framework targeting drought is vital for the sustainable management of water scarcity scenarios.

This section is published as: Yimer, E.A., De Trift, L., Dondeyne, S., Speijer, L., Huysmans, M., Cools, J., Nossent, J., van Griensven, A., 2024a. Framework for mapping large-scale nature-based solutions for drought mitigation: Regional application in Flanders. Water Research 261, 122003. https://doi.org/10.1016/j.watres.2024.122003

6.2.2 Introduction

As underscored in the literature, there is a scarcity of studies focusing on drought-mitigating NbS (Yimer et al., 2024b). Moreover, studies addressing suitability mapping of these NbS are limited in number. Consequently, there is a pressing need to not only quantitatively assess the effectiveness of drought-mitigating NbS but also to develop a new suitability mapping framework tailored specifically for effective drought management, including drought-specific criteria. Since many current methods rely on GIS techniques, our research builds on this foundation to attain innovative insights for drought management.
The key objectives of the study are as follows:

1. Develop a suitability mapping framework for identifying the suitable locations for two types of widely applicable drought-mitigating nature-based solutions (NbS), namely, detention basins (DB) and managed aquifer recharge (MAR).
2. Apply this framework to a regional scale, the region of Flanders in Belgium.
3. Assess the impact of including or excluding criteria on the suitability of DB and MAR.
4. Identify primary criteria influencing the spatial allocation of DB and MAR sites.
5. Compare multiple multi-criteria decision-making techniques to locate suitable areas for DB and MAR.
6. Determine if the suitable locations for DB and MAR align with regions projected to have a high impact on groundwater levels in the future.
7. Evaluate whether the additional recharge from DB is sufficient to meet high groundwater demand and mitigate future climate change impacts.

6.2.3 Study area

The Flemish region, situated in northern Belgium, boasts a diverse environment characterized by various land uses and soils. While the topography remains relatively flat in the northern part, with a significant portion of Flanders comprising low-lying terrain just above or below sea level, the southern part is slightly hilly (Fig. 6.9). The northern part of Flanders is predominantly characterized by sand and loamy sand, whereas silty loam and sandy loam dominate the southern part. The coastal region stands out for its presence of clay and heavy clay (Zomlot et al., 2015b).

In Flanders, land use exhibits a diverse mix of urbanized, agricultural, and (semi)-natural areas (Fig. 6.9). Urban and industrial zones, along with infrastructure, cover approximately 30% of the region, reflecting its high population density, averaging 488 inhabitants per km², notably concentrated in urban centers like Brussels, Antwerp, Ghent, and Leuven (Poelmans and Van Rompaey, 2009). Agriculture is prominent, occupying 51% of the area, with meadows and fields supporting various crops such as cereals, vegetables, and

fruit orchards. Despite urban and agricultural dominance, natural vegetation covers 16% of the region, including woodlands, semi-natural grasslands, and heathlands (Maes et al., 2016; Vriens et al., 2006).

Water bodies occupy the remaining 2% of the study area (Maes et al., 2016; Vriens et al., 2006). The topography is dominantly influenced by alluvial river valleys, which may be slightly lower in height than nearby uplands but often higher than the alluvial plains they cross, where backswamps occur. A small fraction (less than 1%) comprises dunes, beaches, and coastal marshes along the North Sea coast in the northwest of the region (Maes et al., 2016; Vriens et al., 2006).

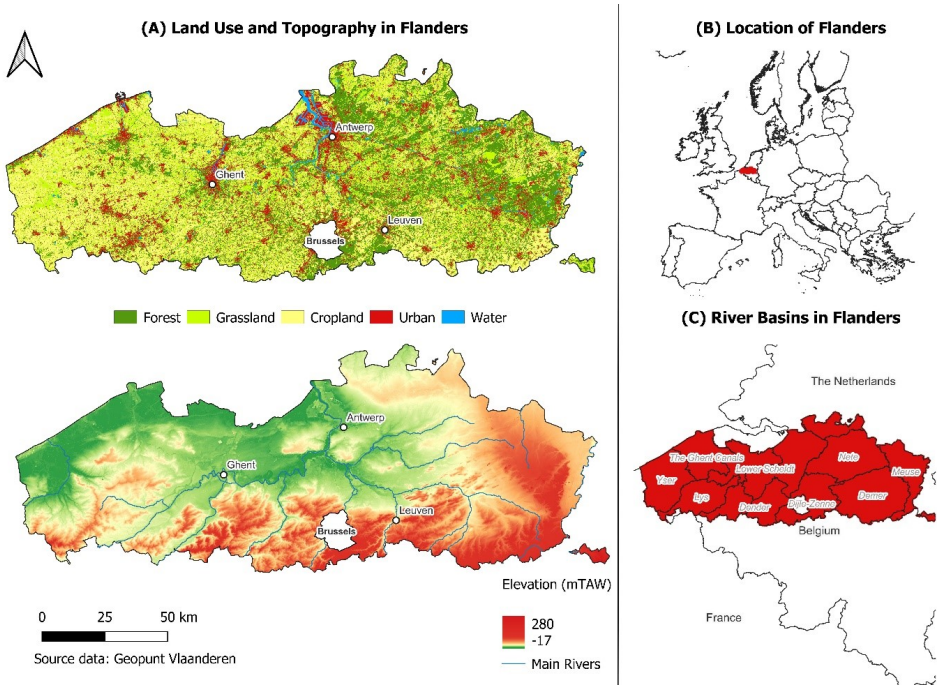


Figure 6.9: (A) Land cover, topography and river network of the Flemish region, (B) Location of Flanders in Europe, (C) River basins in Flanders

6.2.4 Methodology

To locate suitable areas for drought mitigation, a new methodology was created, focusing on detention basins (DB) and managed aquifer recharge (MAR) which includes: (1) identifying criteria specific to drought; (2) creating a new framework that combines drought-criteria and commonly used GIS multi-criteria decision-making (MCDM) methods; (3) applying this framework to a study area where suitability mapping has not been applied

to in detail. Afterwards, additional analysis was done by comparing the outlined suitable locations with (4) future scenarios showing climate change impacts on drought and (5) the estimated potential recharge in DB.

Definitions

Within the scope of this paper, detention basins (DB) are categorized as a spreading method, involving the infiltration of water from the ground surface through permeable materials to recharge unconfined aquifers (Zhang et al., 2020). Specifically, detention basins manifest as infiltration ponds, describing a process wherein surface water is captured by off-stream basins and naturally infiltrates through an unsaturated zone into the underlying unconfined aquifer (Dillon et al., 2009). Furthermore, it is posited that infiltration basins can function as rainwater harvesting systems, utilizing runoff from neighboring impermeable surfaces as an additional source for infiltration.

In contrast, managed aquifer recharge (MAR) is characterized as soil aquifer treatment (SAT), involving the infiltration of treated wastewater effluent through the unsaturated zone to facilitate the removal of contaminants (Dillon et al., 2009). Notably, our research assumes direct injection of water into the top of the unsaturated zone instead of passive infiltration from the surface. This paper also considers the use of stormwater and river water (surface water) as a potential source for managed aquifer recharge, broadening the spectrum of water sources under consideration.

The fundamental distinction between MAR and DB, as elucidated in the initial section, lies in the depth of water infiltration. In detention basins, water is passively infiltrated from the surface, whereas in managed aquifer recharge, water is initially injected into the soil, allowing time for subsequent passive infiltration. Consequently, detention basins and managed aquifer recharge can be categorized as shallow and slightly deeper managed aquifer recharge techniques, respectively.

Selection criteria

Given that many NbS designed to mitigate flood risks have also proven effective in addressing droughts, the technical criteria for locating detention basins were adopted from flood-focused literature, as further detailed in the introduction. Commonly used criteria for detention basins include slope, soil type/texture, land use/land cover classification, distance buffers from infrastructure (roads and buildings) and rivers and other water supply sources (lakes, reservoirs).

In addition to these, other criteria were added to outline the locations. Firstly, possible hazardous locations (landfill sites) were included in this framework as management criteria. It is evident to avoid these locations and prevent eventual water contamination in the detention basins. Secondly, hydrometeorological criteria such as, groundwater recharge was

included to ensure detention basins are implemented in regions with a high actual groundwater recharge (Zomlot et al., 2015a). In other studies (Rejani et al., 2017; Sayl et al., 2020; Soliman et al., 2022), a runoff (depth) layer was included as a proxy for recharge (Sallwey et al., 2018). Finally, to consider the future climate change impacts on precipitation, a single European climate model output quantifying the change in precipitation by 2041 – 2070 for the moderate climate scenario RCP 4.5 was used in the analysis. To address uncertainties in suitability mapping regarding future conditions and variability in climate scenarios, the framework was applied taking into account multiple climate simulation outputs and multiple future Representative Concentration Pathways (RCPs).

For MAR, criteria selection was based on a literature review evaluating 63 different suitability mapping studies by (Sallwey et al., 2018). In line with detention basins, slope, land use, geology, and soil characteristics remain the most important criteria, while subsurface or aquifer characteristics are not always included in the mapping process. This is explained by the worldwide availability and larger resolution of surface characteristics. The precise characteristics of the subsurface and aquifer are not always available through GIS data sets, especially in high resolution and quality that aligns with the scale of the NbS measure (Sallwey et al., 2018). This analysis included the available groundwater depth and aquifer phreatic type datasets.

Highlighting the distinction between two concepts, the groundwater characteristics play a crucial role in both detention basins and managed aquifer recharge. Specifically, for detention basins, it is essential that the groundwater is shallow to facilitate rapid recharge. In contrast, for managed aquifer recharge, this requirement is not necessary, as the groundwater must be sufficiently deep to allow for effective purification and to create space for significant increases in groundwater levels. In addition, the possible hazardous locations, recharge, and climate change impact criteria were also considered for MAR.

To give structure to the selected criteria, they were grouped into four general broad categories (Fig. 6.10): (1) Surface criteria (including natural characteristics of the landscape); (2) Management criteria (a wide range of parameters covering the economic aspects of MAR site selection); (3) Aquifer characteristics (including groundwater depth and aquifer type); and (4) Hydrometeorological criteria (including precipitation/evapotranspiration and recharge maps)

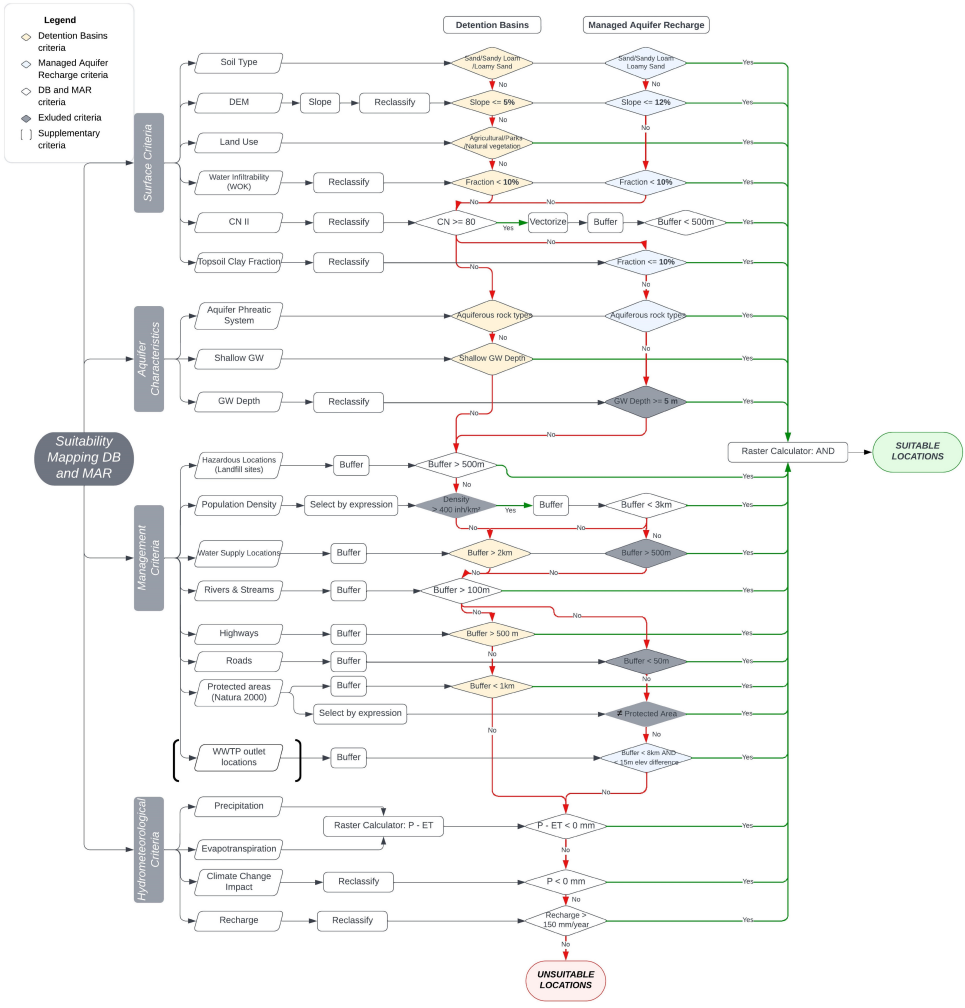


Figure 6.10: : Flowchart for identifying suitable locations for DB and MAR.

Conceptual Framework using Boolean logic

Using the specific criteria outlined, a new framework was developed explaining the input and processes required for generating a suitability map for detention basins and MAR as the output (Fig. 6.10). The analysis was conducted using QGIS v. 3.22.6 and QGIS v.3.30.2. The chosen approach for the conceptual framework includes a strict Boolean constraint mapping where no weighing was employed. The data layers were first converted from raw data into base maps, essential for later-stage Boolean map generation. In this step, the

slope was derived from a digital elevation model (DEM) using the 'Slope' Tool. The evapotranspiration map was subtracted from the precipitation map in the 'Raster Calculator' to get the effective precipitation raster layer. The population density layer was constructed by linking the municipalities vector layer with the population numbers per municipality from 2022 and dividing these numbers by the total area of each municipality. Ending, vector and raster base maps were clipped to the Flanders study area to minimize computation time in further steps.

Secondly, vector input data was also prepared for raster conversion and reclassified into a Boolean scale by assigning '0' and '1' in the attribute table of the vector layer. For soil, the different textures were classified to distinguish between the favorable (sand, loamy sand, sandy loam, silt, silt-loam) and not favorable soils (clayey and anthropogenic soil textures). The Corine land use map was divided into agricultural land, parks, natural vegetation, and industrial and urban land cover. The phreatic aquifer dataset, showing whether a region is having phreatic aquifers or not, was also assigned a value of '1' and '0', respectively. To fulfill the population density criteria, first, all municipalities with a density of 400 inhabitants/km² were selected using the 'Select by Expression' Tool, hereafter, a buffer was constructed to include only the areas in proximity to high population density areas.

The shallow groundwater depth dataset provides 'YES' or 'NO' polygons, which were converted to '1' and '0' Boolean values respectively. For the protected areas layer, it is important to notice that a different approach was followed for detention basins and MAR. For the latter, all protected areas were given a value of '0' to exclude them entirely. Detention basins keep protected areas in proximity by creating a buffer and assigning a value of '1' to areas inside this buffer. For the other vector layers, possible hazardous locations, water protection zones, rivers and streams, highways, roads, and wastewater treatment plant (WWTP) outlet locations, buffers were constructed according to the conditions specified in Table 1 before reclassifying to a Boolean scale. The 'Rasterize' Tool facilitated the smooth translation of these vector layers to 50m x 50m raster output maps, and 'No Data' values were set to '-1' for each generated map.

Thirdly, the base maps, provided in raster format, were standardized to a uniform resolution of 50m using the nearest neighbor resampling method. Though detailed assessments are needed for local challenges, they often require a lot of computing power and face data limitations. Since drought is a regional phenomenon and much data is unavailable in high resolution, our approach focuses on providing larger-scale insights into drought mitigation strategies. According to the criteria in Table 1, the slope, water infiltrability, runoff curve number, topsoil clay fraction, groundwater depth, precipitation, evapotranspiration, climate change impact, and recharge maps were all transformed into Boolean maps using the 'Reclassify by Table' Tool. Areas meeting the criteria conditions specified in Table 1 were assigned a value of '1', and those not a value of '0'. Using the Boolean scale allowed the combination of multiple layers through straightforward logical operations, as all resulting maps shared a consistent and simplified scale (Mubeen et al., 2021).

Subsequently, each individual map was combined to generate a suitability map, delineating areas where all conditions were met. This was done using the 'AND' operator in the 'Raster Calculator'. The result of the analysis comprised two suitability vector layers, each consisting of polygons, for both detention basins and MAR.

Principal Component Analysis (PCA): reduction of redundant criteria

The suitability mapping framework includes 15 criteria for each NbS type. This can lead to potential redundancy, where some variables may duplicate information found in others. To address this issue, Principal Component Analysis (PCA) proves to be a valuable tool for multiple applications, as demonstrated by various authors (Iqbal et al., 2021; Mallik et al., 2021).

PCA is a mathematical technique used to reduce the dimensionality of multivariate data with a large sample size. Its goal is to find a few uncorrelated synthetic variables that retain the most valuable information. By doing so, PCA simplifies decision-making processes, especially when dealing with numerous variables. It identifies and excludes redundant (closely related) variables, creating as few new variables as possible while preserving the original information. This helps to minimize complexity and enhance data understanding (Zhang et al., 2019). The analysis was conducted using RStudio version 2023.03.1 Build 446 "Cherry Blossom" Release separately for detention basins and managed aquifer recharge (MAR) using the PCA package. Initially, QGIS v3.30.2 was employed to uniformly distribute 100 observation points across Flanders using a grid, ensuring a representative dataset that prevents disproportionate influence from specific regions and captures the overall variance. All non-numeric factors, such as soil texture, land use, phreatic aquifer type, shallow groundwater, and WWTP location and elevation difference, were excluded from the analysis as PCA is designed for numerical data. Numeric values for each observation point were obtained using various QGIS tools. For raster datasets, the 'Sample Raster Values' tool extracted pixel values directly at specified observation point locations, while the 'Shortest lines between features' tool calculated the shortest distance to hazardous locations, rivers and streams, roads, protected areas, and water protection zones datasets for vector datasets. Subsequently, the extracted values were organized into a spreadsheet with observation points in rows and criteria in columns, then loaded into RStudio. Secondly, the data was normalized to prevent criteria with larger values from dominating those with smaller values.

After normalization, the correlation matrices were computed for detention basins and MAR. The correlation index values range from 1, with stronger correlations indicating a stronger relationship between variables. A positive value signifies a direct relationship, while a negative value suggests an inverse relationship between two variables (Mukaka, 2012). Next, PCA was executed and different visualization techniques were used to identify the significance of criteria. Scree plots provide information about the variance distribution and the explained percentage of variance associated with each principal component (Gour et al., 2017). These plots were used to determine the number of principal components retained

in the dataset. To assess the significance of each variable concerning the principal components, square cosine (Cos2) plots were generated for detention basins and MAR. The Cos2 values serve as indicators of the variable's representation on the principal components. A higher Cos2 value suggests that the variable is well represented by the principal components, while a lower value indicates poor representation (Naffees Gowsar et al., 2019).

Multi-criteria decision making using Analytical Hierarchy Process (AHP)

As the Boolean constraint mapping approach is highly strict, non-compliance with a single criterion results in the classification of areas as unsuitable for implementing detention basins (DB) and managed aquifer recharge (MAR). To address this limitation, a multi-criteria decision-making analysis incorporating weighted factors was employed to comprehensively assess the degree of suitability of both types of nature-based solutions (NbS).

In this study, the Analytical Hierarchy Process (AHP) was selected to establish criteria priorities, given its recent utilization in land suitability mapping studies (Hani et al., 2023; Morales and de Vries, 2021; Topuz and Deniz, 2023) and the availability of the EasyAHP plugin in QGIS for automated calculations (Mohd Zaini et al., 2021).

A. Selection of criteria and score assignment

To enable a comparison with results obtained through the Boolean overlay, identical criteria outlined in the established framework were applied, utilizing the corresponding dataset. The phreatic aquifer type dataset, being Boolean, was excluded from the multi-criteria decision-making process. To simplify, only the distance aspect of wastewater treatment outlet locations was considered for managed aquifer recharge (MAR), excluding elevation differences. Roads were also omitted for MAR due to computational complexity.

Each layer underwent conversion to raster format and reclassification to ensure consistent scoring between 1 and 5 for all criteria. Vector input layers, such as soil texture, land use, and phreatic aquifer type, had the values assigned in the attribute table and were rasterized using QGIS's 'Rasterize' function. For raster input layers (slope, water infiltrability, clay fraction, climate change impact on drought, and recharge), the 'Reclassify by table' tool was used to directly assign scores. To score distances from vector attributes like rivers, streams, highways, and wastewater treatment outlets, the 'Multi-Distance Buffer Plugin' was employed.

The supplementary material in https://www.sciencedirect.com/science/article/pii/S0043135424009035 provide a comprehensive overview of scores assigned to each criterion, along with its suitability classification for detention basins and managed aquifer recharge. After generating factor maps with consistent scores for each criterion, these layers were selected as input layers in the initial step of the EasyAHP plugin, chosen from the available raster layers.

It's important to note that the following criteria: possible hazardous locations and water protection zones were retained as constraint maps with a Boolean scale (0-1) for the analysis of detention basins. In the case of managed aquifer recharge, protected areas were additionally considered as constraints. These maps will not be utilized in the computation of the suitability map using AHP but will be employed in a later stage to exclude potential areas. This extra layer of filtering is done as its not possible to touch these areas due to their vital use as water supply and the water companies are not willing for any form of nature-restoration around their vicinity.

B. Construction of pairwise comparison matrix

In order to compare criteria, it is essential to establish scores based on preferences. The comparisons between criteria were conducted using a numerical scale developed for this purpose, as outlined in Tab. 6.4, adapted from Saaty (1980). The scale ranges from 1 to 9, where "1" signifies that the criteria are equally important, and "9" indicates that one criterion is significantly more important than another (Ward et al., 2021).

Overall, higher preferences were accorded to drought-specific criteria in accordance with the established framework and to frequently mentioned criteria in literature. For detention basins, these encompassed soil texture, slope, land use, curve number, climate change impact, and recharge. For managed aquifer recharge, greater importance was assigned to soil, slope, clay fraction, and aquifer type. The pairwise comparison matrix for detention basins and managed aquifer recharge was completed during the second step of the EasyAHP plugin.

Typically, preferences are formed through input from various stakeholders (Ahmadisharaf et al., 2016; Romano et al., 2015; Ward et al., 2021). However, in our approach, we departed from this conventional practice, opting instead to assign preferences based on our own judgment and expertise. We recognize the importance of stakeholder involvement and intend to incorporate their input in future research.

Table 6.4: Fundamental scale for comparing criteria relative to each other, adapted from Saaty (1980)

Intensity of importance	Definition
1	Equal importance
3	Moderate importance
5	Strong importance
7	Very strong importance
9	Extreme importance
2, 4, 6, 8	Intermediate values
1/3, 1/5, 1/7...	Values for inverse comparison

C. Consistency check

In the context of comparing 15 criteria among each other, potential inconsistencies may arise linked to errors in judgment during the pairwise comparison process. While AHP can manage a certain level of inconsistencies, it does have its limitations (Morales and de Vries, 2021). To evaluate consistency, the EasyAHP plugin computes automatically the Consistency Index (CI) and the Consistency Ratio (CR) in the second step (Mohd Zaini et al., 2021). It's important to emphasize that a CR within the acceptable range should be below 10%. An exceeding CR suggests inconsistencies in the pairwise comparisons, compromising the accuracy and reliability of the results (Morales and de Vries, 2021). In such situations, adjustments to the assigned preferences in the pairwise comparison matrix become necessary. However, in our case, the criteria were met during the initial assignment of preferences, and no adjustments were made.

D. Calculation of weights and weighted linear combination

The calculation of criteria weights was automated following the construction of the pairwise comparison matrix in the third step of the EasyAHP plugin. Utilizing these weights, a weighted linear combination process was executed, wherein all 12 factor maps for detention basins and 11 factor maps for managed aquifer recharge were merged and overlaid to generate the suitability map.

This process was conducted outside the plugin using the 'Raster calculator,' where each factor map was multiplied by its corresponding weight and then summed. The resulting map included values from a continuous scale ranging between 1 and 5. These values were further classified into four suitability classes:

- 1–2: Not suitable
- 2–3: Less suitable
- 3–4: Suitable
- 4–5: Highly suitable

Once the suitability maps were constructed, they were further processed by overlaying current land use maps. This step involved eliminating all suitable areas that overlapped with existing water bodies, wetlands, and urban land uses to address potential conflicts.

Climate Change Impact on Average Lowest Groundwater Levels and Its Relation to the Suitability Mapping

To assess the significance of integrating recharge criteria into the identification process of suitable locations, the results are overlayed with data from relevant literature. The analysis incorporates the influence of climate change on drought, superimposed onto the previously

derived outcomes indicating appropriate sites for detention basins and managed aquifer recharge, both for the short-term future (2050) and the long-term future (2100). This data originated from a comprehensive study conducted by VMM and Sumaqua, which examined the impact of climate change on phreatic aquifer levels (VMM, 2021). The study encompassed several locations across Flanders and utilized advanced spatial interpolation techniques and models to extend the findings to the regional scale (Franken and Wolfs, 2022).

Estimating Potential Recharge from Detention Basins

In order to showcase the value of the detention basins for increasing the groundwater volume, additional recharge coming from the detention basins was estimated. The additional recharge is calculated using the assumption that the difference between precipitation (P) and evapotranspiration (ET) and runoff (Q) yields percolating water into the groundwater system.

$$\text{Recharge} = P - ET - Q \quad \text{(Before the implementation of detention basins)} \tag{6.1}$$

$$\text{Recharge}_{\text{after}} = P - ET - Q + (\%\text{Q}) \quad \text{(After the implementation of detention basins)} \tag{6.2}$$

The %Q is the percentage of runoff that will be held by the detention basins. Annual average runoff data was obtained from Zomlot et al. (2015a) and the numbers can be confirmed by water balance calculations in Yimer et al. (2023a,c). The difference between Recharge and $\text{Recharge}_{\text{after}}$ is the additional recharge which is expected due to the implementation of detention basins.

The additional recharge is then approximated as (%Q), hence, three scenarios are considered. The scenarios account for 50%, 30% and 15% of the runoff as additional recharge. These numbers were chosen to account for minimum environmental flow in streams, hence, a significant amount of the runoff cannot be considered as recharge.

Comparative Analysis: Water Use, Recharge, and Climate Impact on Phreatic Aquifer Levels

In order to gain a deeper understanding of the significance of drought-specific criteria, the total annual groundwater use for the year 2020 was compared with the previously mentioned volumes per basin, encompassing both recharge and the impact of climate change on phreatic aquifer levels. This analysis aimed to assess whether the potential recharge is substantial enough to offset the adverse effects of climate change and meet the increasing groundwater demand.

The data for total yearly water use was sourced from Vlaams Kenniscentrum Water and was presented in tabular format, with water usage values specified in cubic meters per

subsector and province. Utilizing these numbers and the total number of establishment units per municipality, we made an estimate of the overall water usage per municipality, assuming a linear correlation between water use and the number of establishment units. Establishment units are enterprises such as shops, companies, hotels, hospitals, universities, etc. which contributes to the total groundwater water use. The estimated total water use per municipality is illustrated in https://www.sciencedirect.com/science/article/pii/S00431 35424009035.

Utilizing these numerical values, we conducted an estimation of the overall groundwater usage per basin by aggregating these values within each basin. Simultaneously, the total potential recharge per basin was calculated by aggregating the potential recharge within the detention basins grouped per basin. To gauge the comprehensive impact of climate change, we estimated the total decrease in the lowest groundwater level by averaging the decrease across each basin.

For a more comprehensive understanding of our methodology, including details on how to estimate the total groundwater use per municipality and basin, as well as the calculation of potential additional recharge and decrease in the average lowest groundwater level per basin, please refer to Section 3 of the Supplementary Material (https://www.sciencedirect. com/science/article/pii/S0043135424009035).

6.2.5 Result

Suitable detention basin (DB) and managed aquifer recharge (MAR) locations in Flanders using Boolean logic

Fig. 6.11 and 6.12 represent the initial suitable locations for DB and MAR. The annex in https://www.sciencedirect.com/science/article/pii/S0043135424009035 provides the total suitable areas in km² for DB and MAR before and after PCA. Before the removal of criteria through PCA, MAR exhibited more suitable areas than DB, with respective areas of 382.6 km² and 196.4 km². Additionally, a relatively small area is found suitable for both types, primarily located in the northeastern section of the study area.

Fewer locations are suitable for both NbS types in the western part of the Flemish region, particularly along the coastal region and Scheldt polders, which can be attributed to lower recharge rates and heavy clay presence. However, specific spots along the coastal region with a lower clay fraction (<10%) are identified as suitable for MAR. Proximity to protected areas poses a contradiction in identifying suitable sites for DB and MAR, with DB strategically located near these zones while MAR tends to avoid them. Several nature reserves lost suitability due to their proximity to significant water production centers (WPCs). Both DB and MAR sites are positioned near areas with high runoff potential, with a concentration of MAR sites in regions with high population densities in western Flanders.

Another trend observed is the scarcity of DB and the absence of suitable MAR locations in the southern part of the Flemish region. The limited presence of DB is primarily due to slope restrictions and non-shallow groundwater depth. Concerning MAR, all potential implementation areas are excluded due to high topsoil clay fractions in the southern part of Flanders. While detention basin sites are present in various small regions within Flanders, MAR locations exhibit clustering, concentrated in zones with low clay fractions, close to urban centers, and within a distance from wastewater treatment plants (WWTP) facilities. Similar to other findings, MAR sites are situated near locations with high runoff potential, ensuring a distinct separation of adjacent MAR sites.

Principal Component Analysis (PCA) reveals significant correlations and patterns in the data. Figures A2 and A3 in the annex (https://www.sciencedirect.com/science/article/pii/S0043135424009035) display the correlation matrices for detention basins (DB) and managed aquifer recharge (MAR). Negative correlations are observed between recharge and permeability for DB and between topsoil clay fraction and recharge for MAR. Positive correlations are found between population density and distance from rivers and streams. Scree plots and statistics reveal that the first four principal components explain 79.6% of the total variances for detention basins and 76.2% for MAR, indicating their significance in representing underlying patterns. Cos2 plots show the limited impact of population density within the detention basins dataset. At the same time, variables like distance to protected areas, water protection zones, and roads have minimal influence on the principal components in the MAR dataset.

Eliminating redundant criteria considerably expands the suitability maps for both NbS types (Fig. 6.11 and 6.12). The total suitable area for DB increases to 298.710 km², with rural areas around Antwerp and the eastern part of the Flemish region prominently featured. For MAR, the total suitable area more than doubled to 867.495 km², with subtle visual differences, primarily in filling gaps between closely located suitability areas. Exceptions include the northwest region of Ghent and a significant expansion in eastern Flanders.

The exclusion of the water protection zones criteria reveals a significantly suitable area near Ghent's large surface water. Additionally, newly identified suitable sites in the eastern part of Flanders align with major nature reserves. In practical terms, however, implementation within drinking water protection zones is restricted due to stringent regulations aiming to safeguard both ecological integrity and public water supplies. Additionally, including the distance from roads criterion helps fill gaps within suitable polygons without significant expansions across Flanders. Shared suitable locations for both detention basins and managed aquifer recharge span across the Flemish region, concentrated within buffer zones surrounding nature areas, excluding nature areas themselves but in close proximity.

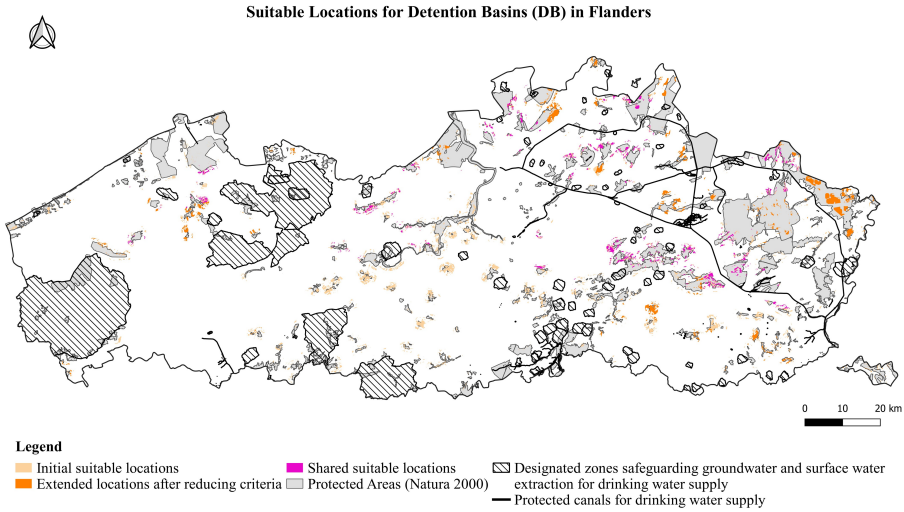


Figure 6.11: :Suitable areas for detention basins (DB) in the Flemish region, initially identified with Boolean constraint mapping based on 15 criteria and refined through PCA by reducing the criteria to 14

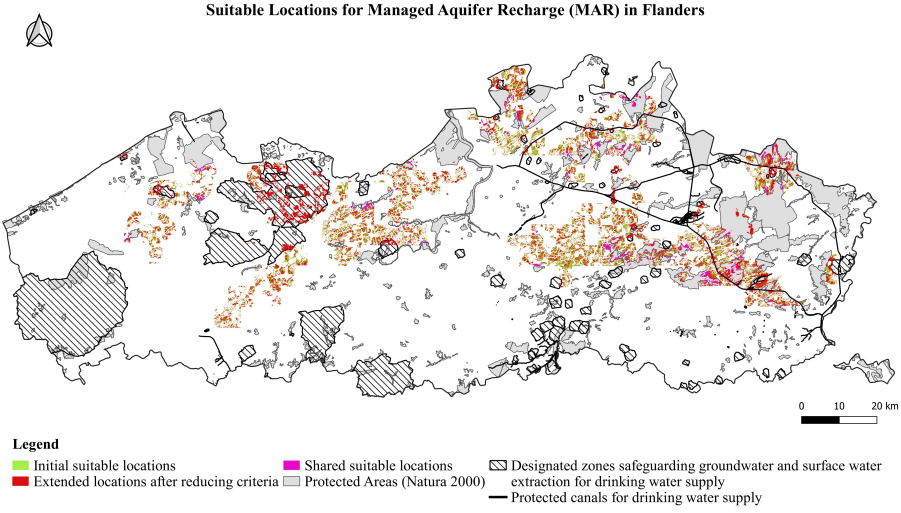


Figure 6.12: :Suitable areas for managed aquifer recharge (MAR) in the Flemish region, initially identified with Boolean constraint mapping based on 15 criteria and refined through PCA by reducing the criteria to 12

Suitable detention basin (DB) and managed aquifer recharge (MAR) locations in Flanders according to multi-criteria analysis using Analytical Hierarchy Process (AHP)

The application of a more flexible multi-criteria approach significantly increases the suitable areas for both nature-based solution (NbS) types (Fig. 6.13 and 6.14). DB areas increase nearly tenfold to around 2500 km², while MAR expands from 886 km² to 2538.7 km², exclusively compromising the most optimal locations falling within the highest suitability class. Considering the broader context of the "suitable" class, this expansion spreads across the entire Flemish region.

Examining DB implementation areas reveals trends that align with the stricter Boolean approach, with more highly suitable regions in the northern and eastern parts of Flanders (Fig. 6.11). Favourable soil textures, high recharge rates, and anticipated negative climate change impact on future precipitation drive suitability in these areas. Conversely, the southern region exhibits scarcity in highly suitable DB areas due to lower recharge rates and less favourable soil textures, as well as slope constraints. An exception to this trend in the south is the identification of a highly suitable spot near Brussels, corresponding to a large forest area. Unlike the Boolean approach, the shallow groundwater does not explain this, as this Boolean dataset was removed from the analysis.

The western part, marked by extensive protection zones for drinking water supply, faces constraints, rendering much of the coastal area unsuitable for DB implementation. Similar constraints apply compared to the Boolean approach, with low recharge rates and unsuitable soil textures posing challenges in coastal regions with dunes and polders. The combination of these unfavourable circumstances classifies almost the entire coastal area as unsuitable for detention basin implementation.

Despite the presence of suitable conditions in soil texture, land use, slope, and recharge rate, certain areas near Antwerp are classified as less suitable for NbS implementation due to the substantial positive impact of climate change on precipitation. Notably, there is a shift from the Boolean approach, where proximity to protected areas was a dominant factor in explaining the location. Now, highly suitable and suitable areas extend beyond these zones, indicating a change in the criteria influencing site selection. The most influential criteria in determining suitability include soil texture, slope, land use, recharge, and climate change impacts on precipitation, collectively accounting for nearly 80% of the total weights in the final suitability map.

The comparison between the AHP and Boolean constraint mapping approach for managed aquifer recharge (MAR) reveals similar patterns (Fig. 6.12). Highly suitable locations predominantly cluster in the northern and eastern parts of the study area. Analogous to DB, the determination of highly suitable areas and unsuitable regions is influenced by factors such as soil textures, slopes, recharge rates, and anticipated climate change impacts, particularly in the eastern areas showing a significantly negative impact.

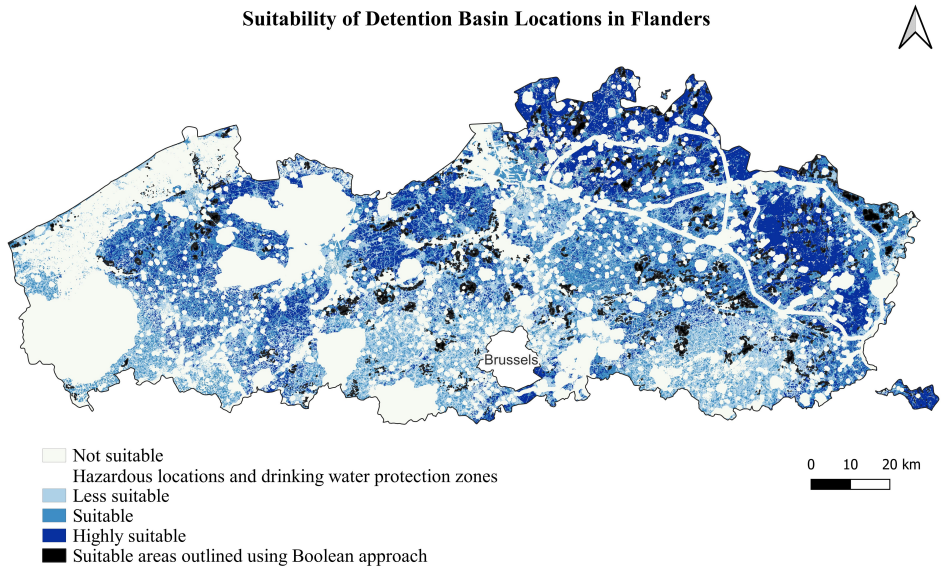


Figure 6.13: :Comparison of suitable areas for detention basins (DB) in the Flemish Region: multi-criteria decision-making (approach 2) vs. Boolean constraint mapping (approach 1)

Suitable areas for MAR are more restricted compared to DB due to the nature protection areas constraint, in addition to the hazardous locations and drinking water protection zones. Many previously identified suitable locations for MAR overlap with these protection zones, as these criteria were omitted post-principal component analysis.

Using the Boolean approach, high clay fractions restricted the suitability in the southern part of the Flemish region. In the suitability map using AHP, the entire region also has clay fractions exceeding the threshold for suitability, often surpassing 15%. However, these areas were not classified as unsuitable due to the dominance of other criteria, such as soil texture, as well as highly suitable and suitable recharge rates and slopes.

Despite some isolated spots along the west coast classified as "unsuitable", the region is generally labeled as "less suitable" for MAR application. This classification is attributed to dominant criteria like slope, climate change impact on meteorological drought, and aquifer type, which have high individual scores and contribute to the final suitability score.

Soil texture, slope, climate change impacts on meteorological drought, and recharge rates are still key factors in selecting suitable locations, with clay fraction and aquifer type also playing significant roles. However, aquifer type does not significantly impact results, as most aquifers are classified as highly or moderately productive. These dominant criteria

collectively account for almost 80% of the final suitability map (Tables A2 and A3)

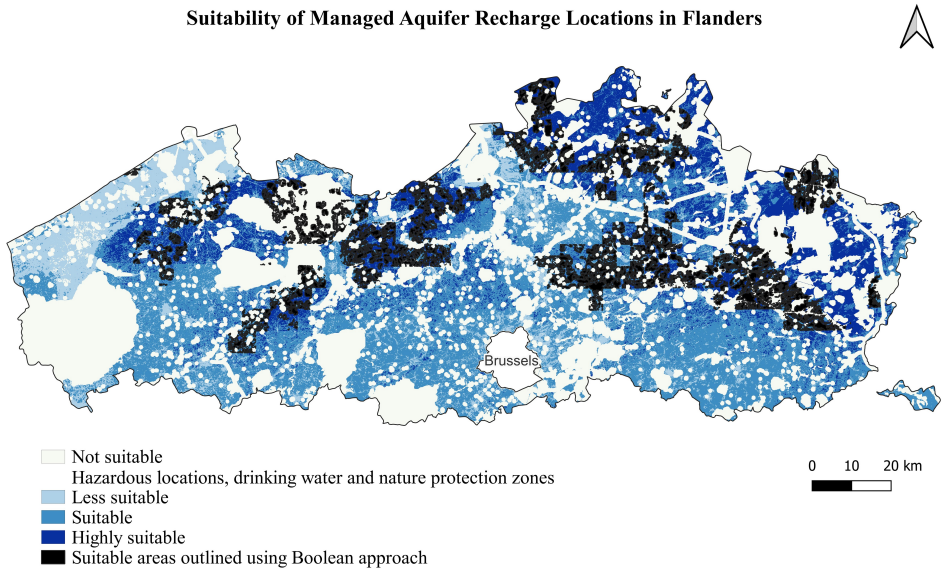


Figure 6.14: :Comparison of suitable areas for managed aquifer recharge (MAR) in the Flemish Region: multi-criteria decision-making (approach 2) vs. Boolean constraint mapping (approach 1)

Climate Change impact on average lowest groundwater levels and its relation to suitability mapping

This research incorporated unique drought-criteria, as specified in Table 1, to identify suitable DB and MAR locations. To stress the importance of these criteria for drought mitigation, a further comprehensive analysis was conducted, comparing the suitability maps with projected climate scenarios from the Flemish Environmental Society ("VMM"). (Fig. 6.15 and 6.16) show a comparison between the identified suitable locations for detention basins and managed aquifer recharge and the projected impacts of climate change on groundwater levels for one future scenario: the short-term future (2050). The comparison of the suitability maps with the long-term future (2100), showing a high decrease in groundwater levels for almost the entire Flemish region. According to the Boolean approach, both types of NbS align with regions expecting the highest decrease in average lowest groundwater levels. The suitable areas overlaying with the areas corresponding to increases in groundwater levels are negligible. However, using AHP, suitable areas will also arise in locations expecting a low decrease or even increase in the average lowest groundwater level due to the dominance of other criteria, such as recharge, land use and soil, in the selection process.

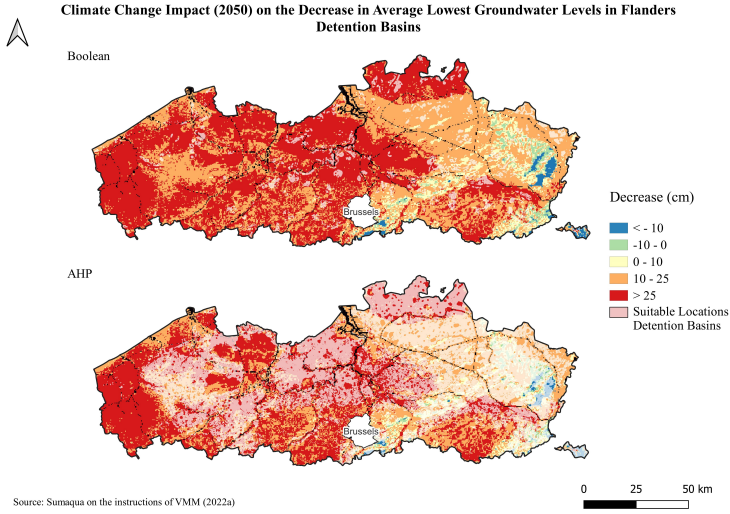


Figure 6.15: Climate change impact on the decrease in average lowest groundwater levels in Flanders (VMM and Sumaqua) for 2050, with suitable detention basin locations outlined using two methods (Boolean constraint mapping and AHP)

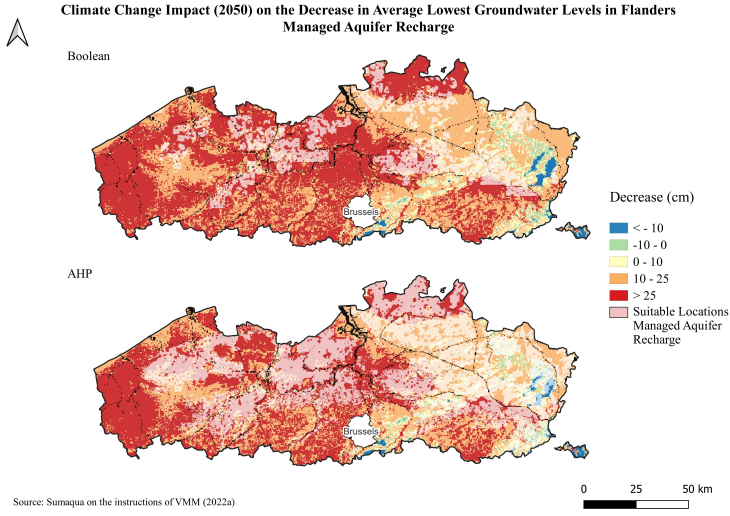


Figure 6.16: Climate change impact on the decrease in average lowest groundwater levels in Flanders (VMM and Sumaqua) for 2050, with suitable locations for managed aquifer recharge outlined using two methods (Boolean constraint mapping and AHP)

Comparative analysis: water use, recharge, and climate impact on phreatic aquifer levels

Fig. 6.17 compares the estimated yearly groundwater use and annual potential recharge for three scenarios (in m³/year). Considerable discrepancies arise among basins concerning yearly groundwater use, notably with the Lower Scheldt basin having nearly 20 million m³/year. In contrast, the Yser, Ghent-canals, Upper Scheldt, and Dender basins all fall below 5 million m³/year.

Table A9 in the annex (https://www.sciencedirect.com/science/article/pii/S0043135424009035) offers a detailed breakdown of water use, yearly potential recharge, and groundwater level reduction values for each basin. The yearly potential recharge volumes are not able to offset the substantial water use rates in each basin and exhibit significant variations across all basins (Fig. 6.17). The annual average estimated recharge is generally low in the suitable locations of detention basins. The yearly potential recharge is lower in the western part of Flanders, specifically in the Yser, Lys, Bruges Polders, and Ghent canals basins, mainly attributed to a scarcity of suitable locations compared to other regions in Flanders. Similarly, the Upper Scheldt, Dender, and Dijle-Zenne basins record comparatively lower values, coinciding with the basins that register the lowest recharge values and even negative summer recharge values. Conversely, the northern regions of Antwerp and the eastern portion of Limburg, encompassing the Lower Scheldt, Nete, Meuse, and Demer basins, exhibit the highest yearly, summer, and winter recharges.

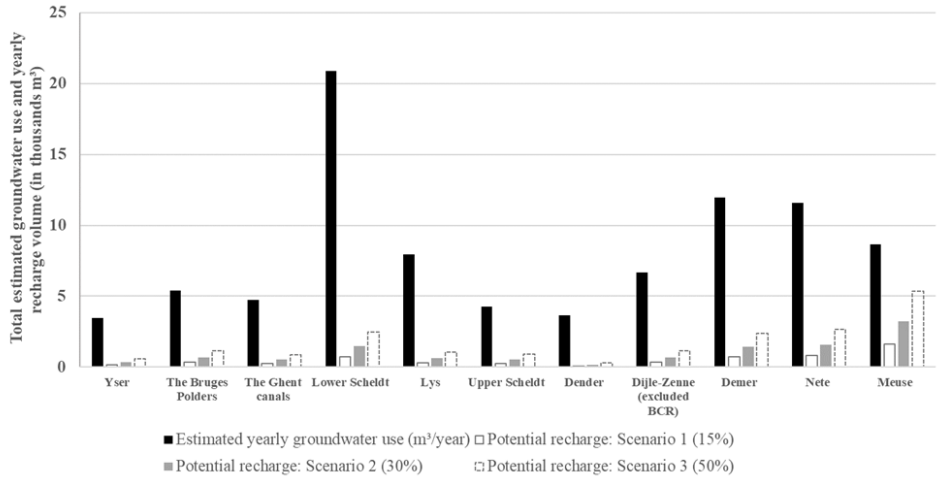


Figure 6.17: Comparison between estimated yearly groundwater use and potential yearly recharge due to detention basins with three different scenarios for 2050 and 2100 per basin

The findings are concerning in the analysis of the anticipated average decrease in phreatic

aquifer levels for 2050 and 2100 per basin, as shown in Fig. 6.18. Calculations suggest a decrease of approximately 636 m³ in 2050, more than doubling to 1471 m³ in 2100. In the southern basins, which experience low or negative recharge rates during the summer, the decrease in groundwater volume is projected to be even more pronounced due to the impacts of climate change. However, in other basins, where intermediate or high recharge volumes, particularly during the winter months, predominate, this effect of climate change is less pronounced.

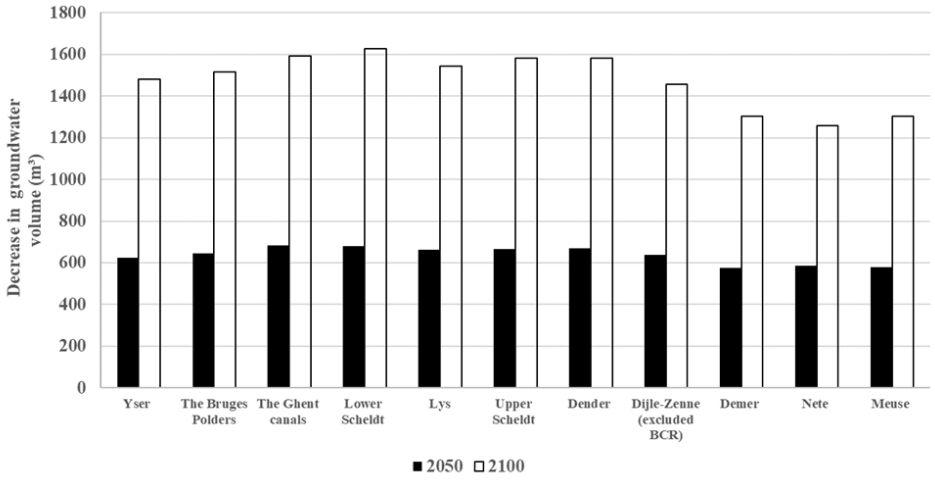


Figure 6.18: Estimated decrease in groundwater volume (m³) due to climate change for 2050 and 2100 per basin

6.2.6 Discussion

Impact of Inclusion/Exclusion of Criteria on NbS Suitability

Analyzing criteria's impact on suitability provides valuable insights, facilitating NbS site identification for drought mitigation. After PCA, less significant factors like population density and road accessibility were excluded, alongside criteria such as proximity to nature reserves and protected zones for drinking water abstraction. Additional locations were incorporated into the detention basin (DB) suitability map without conflicting with the protected zones. However, in managed aquifer recharge (MAR), the exclusion of three criteria raised validity concerns for certain identified locations. Thus, careful consideration during PCA is essential to avoid targeting infrastructure and protect habitats, ensuring effective and sustainable NbS deployment while mitigating adverse environmental and health impacts.

Comparative Analysis of Influential Factors for DB and MAR Site Selection

The study reveals varying factors influencing the location of DB and MAR sites across different regions in Flanders, providing insights into their suitability for large-scale drought mitigation. Recharge, given the highest weight in the suitability analysis, is one of the most influential criteria for identifying areas crucial for effectively mitigating droughts. By considering not only average yearly recharge but also seasonal variations, we gain valuable insights into the suitability of different locations based on their varying recharge capacities spatially and seasonally.

The application of criteria exhibits subjectivity, introducing variability across studies. While recurrently cited factors such as land use constraints and hydrogeological limitations have surfaced in the literature (Sallwey et al., 2018), the influential factors explaining DB and MAR selection will change in the local context. Thus, while implementing these solutions in reality, it is important to recognize that the selection of precise sites for DB and MAR depends on specific geographical characteristics and the intended purpose of utilizing (reclaimed) water.

A limitation that influences the selection of suitable locations is the availability of input data, i.e., groundwater characteristics, recharge data, and especially climate change impact on precipitation. For the latter, the difference in spatial distribution and total suitability area is reflected across different climate change scenarios (refer to supplementary material: https://www.sciencedirect.com/science/article/pii/S0043135424009035), reflecting the uncertainties in predicting future environmental conditions.

Advantages of Analytical Hierarchy Process (AHP) compared to Boolean Constraint Mapping

Comparing the Boolean approach to the more adaptable multi-criteria decision-making method, the Analytic Hierarchy Process (AHP), highlights significant differences in identifying suitable areas for DB and MAR in Flanders. While the Boolean approach delineates suitable areas for DB in small, discrete strips, AHP notably expands coverage for DB, similarly, for MAR, almost the entire study area, except the coastal region and around Antwerp, is considered suitable or highly suitable.

The key advantage of AHP lies in its flexibility. It enables decision-makers to weigh multiple criteria simultaneously based on their preferences, resulting in a nuanced and adaptable evaluation. This means that, in the presence of numerous criteria, an area may still be considered suitable even if one criterion scores less favourably. In contrast, the Boolean approach relies on binary criteria and classifies an area as unsuitable if any criterion is not met. Transitioning from the Boolean approach to AHP not only broadens spatial suitability but also emphasizes the importance of adopting a flexible and holistic methodology in complex decision-making contexts.

Considerations about Groundwater for NbS Site Selection

While the criteria, climate change impact on average lowest groundwater level, is not included in the suitability analysis, it provides insights into the framework's robustness concerning future drought effects. The correlation between suitable areas for DB and MAR and regions expecting significant groundwater level declines highlights the methodology's potential as a decision-support tool for large-scale drought mitigation. Groundwater levels directly affect water availability during droughts, making their consideration crucial for strategically placing DB and MAR to enhance groundwater recharge and storage, supporting overall drought resilience.

Thorough viability assessments are necessary before starting to implement NbS in the field (Ringleb et al., 2016). The suitability maps are crucial for guiding policymakers in early NbS implementation, aiding informed decision-making (Russo et al., 2015). Specialized training is also required for policymakers to effectively utilize the framework. Stakeholder involvement, especially from government and municipal bodies, is essential for validation and practical application (Ahmadisharaf et al., 2016). Engaging stakeholders in the AHP process not only ensures diverse perspectives are considered but also provides indirect training, equipping them with the skills needed for effective framework utilization.

Comparative Analysis of Annual Potential Recharge, Water Demand, and Climate Change Impact

While the annual potential recharge in the three scenarios may not suffice to offset the high rates of water use across all basins, it is essential to acknowledge the presence of groundwater and surface water reserves capable of meeting water demand. Thus, combining MAR and DB or increasing the runoff holding capacity of DB's is needed. Since the annual average runoff in Flanders is relatively small (calculated around 8% of the total precipitation), holding the runoff might not be the best approach. For such groundwater-dominated regions, the use of MAR can be quite relevant and successful. The anticipated decline in the average lowest groundwater level by 2050 and 2100 due to climate change is substantial. It is noteworthy that these declines are projected to remain lower than the annual recharge rates, thus providing a degree of compensation. Understanding the delicate balance between annual recharge rates, water use, and the resilience of groundwater and surface water reserves is crucial for sustainable water resource management, especially in the face of climate change impacts.

Limitations and future directions

Understanding the limitations of this work is crucial. Conflicts between nature conservation, farming, city development, and implementing NbS are inevitable due to limited space. Finding compromises among different stakeholders is essential. Additionally, putting planned NbS ideas into practice faces significant challenges and barriers, including knowledge gaps of effectiveness, lack of awareness, low cost and benefits expertise, poor stakeholder engagement, and insufficient financing (Nelson et al., 2020). Looking ahead, some barriers

can be addressed in future work by performing a cost-benefit analysis and getting stakeholders involved in selecting preferences in the AHP process. Furthermore, uncertainties in input data, particularly regarding groundwater characteristics and recharge data, require further investigation. Validating maps with real field data to ensure accuracy is also important to enhance the effectiveness of NbS strategies in mitigating drought.

6.2.7 Conclusion

- The new framework addresses a literature gap by providing a comprehensive suitability mapping study for drought mitigation.
- The inclusion of drought-specific criteria, such as recharge, is essential for identifying and prioritizing areas requiring NbS implementation to effectively address future drought challenges.
- Suitability mapping requires additional criteria, such as climate change impacts and potential hazards, alongside common factors such as soil, land use, and slope.
- The comparison between the Boolean and Analytical Hierarchy Process (AHP) approaches emphasizes AHP's flexibility in identifying suitable areas for detention basins (DB) and managed aquifer recharge (MAR), surpassing the limitations of the Boolean method.
- Flanders exhibits significant potential for DB and MAR, enhancing regional resilience to drought.
- The alignment of DB and MAR locations with existing data on future drought vulnerability underscores the feasibility of the framework for large-scale implementation to mitigate drought impacts.
- Given the high groundwater use in Flanders, additional recharge from detention basins could partially compensate, emphasizing the importance of integrated NbS strategies.
- Complementary NbSs are crucial for meeting the total water demand and ensuring sustainable water supply for various sectors, including industries, domestic use, cooling, etc.

Chapter 7

Conclusion and Recommendation

7.1 Conclusion

In this thesis, several objectives and sub-objectives have been explored, with the final milestone to use a new coupled surface water–groundwater model to advance the evaluation of the impact of drought on water resources. This final milestone underscores the need to find adaptation/mitigation measures to attenuate drought's severe impact on surface and groundwater reserves. Thus, as a final goal, nature-based solutions (NbS) targeting drought are explored.

The overall conclusion is that the Scheldt basin is highly vulnerable to extreme meteorological, agricultural, and hydrological drought events, with climate change playing a considerable role in aggravating the impacts. To reach this conclusion, the use of a physically-based and fully distributed coupled surface water-groundwater model, SWAT+gwflow is inevitable. Despite the basin being faced with extreme drought events, it is possible to minimize the impact on surface and groundwater resources by utilizing the potential of nature-based solutions.

The major conclusions from each chapter and sub-objectives are the following:

Conclusion from Chapter 3 – objective 1: Groundwater–soil interaction inclusion enhances geohydrological realism in coupled modeling frameworks which is tested with SWAT+gwflow.

The difficulty of modelling geohydrological processes in groundwater-driven watersheds using the standalone SWAT+ model, which has conceptual groundwater representation, drives the first objective's inception. Not only is a physically based and distributed coupled SWAT+gwflow model needed, but crucial groundwater-soil interaction whenever the groundwater is above the soil profile needs to be considered.

Therefore, from Chapter 3, the groundwater-soil interaction modification that is applied to the SWAT+gwflow model has improved the simulation of the geohydrology of a groundwater-dominated watershed. The simulation with the standalone model (SWAT+) has indicated the low performance of the model with a Nash-Sutcliffe Efficiency value (NSE) of less than 0.5, while SWAT+gwflow has NSE value above 0.5 for both calibration and validation periods. In addition, without the modification made in this study, the water balance components are not representative of the reality compared to previous studies. Such interactions are highly recommended to be accounted for in other coupled models, mainly if the intention is to apply a given model in shallow aquifer catchments where dynamic groundwater-soil-surface water interactions are dominant.

Conclusion from Chapter 3 – objective 2: Multi-region testing of an automated SWAT +gwflow toolkit for input, calibration, and output handling proves to ease model development.

The second sub-objective of Chapter 3 is based on the difficulty of generating inputs for the SWAT+gwflow model, which takes hours in a GIS environment. Since the model is new, automating tools did not exist. Therefore, the development of an input generation, post-processing, and calibration (IPPC) toolkit is needed most. The tool is tested with multiple catchments located across the globe with diverse climates, geology, land use, and human influence.

In conclusion, the development of SWAT+gwflow input preparation, post-processing, and calibration tools avoids the extensive GIS manual manipulations required for model development. This was tested with additional watersheds from Spain, Italy, Denmark, and Morocco, on top of seven watersheds inside the regional Scheldt basin in Belgium. Therefore, the toolkit has the advantage of reducing the time required for model development, calibration, and post-processing. It's not only the computational time reduction observed from the catchment modelling, it also validates the model's ability to represent geohydrological processes in different watersheds.

General conclusion from Chapter 4: The SWAT+gwflow's application and ability to represent complex catchment processes is observed.

The primary objective of Chapter 4 is to apply the coupled model and assess its ability to represent complex geohydrological processes. This is tested on two scenarios, one on an intensively drained agriculture-dominated watershed (Kleine Nete, Belgium). In doing so, model calibration strategies are also compared, where the SWAT+gwflow model was calibrated for only streamflow simulation and, on the other hand, with both streamflow and groundwater head. Secondly, the objective is to model the regional Scheldt basin using the new coupled model, which will be used in later chapters to perform drought analysis on the model outputs. In the first objective of modelling the impact of drainage in geohydrology, primarily finding the areas that drain water from the agricultural landscape is needed.

Therefore, a novel methodology combining remote sensing and groundwater level-based techniques is developed to accurately identify agricultural water drainage unit locations.

Conclusion from Chapter 4 – objective 1: The accuracy of agricultural water drainage mapping through a combination of groundwater level-based and remote sensing techniques has improved.

In conclusion, the novel methodology to filter out agricultural water drainage locations proved to increase accuracy; hence, future mapping applications shall include groundwater level-based filtering in addition to the classical remote sensing and decision classification methods. Due to the combination of remote sensing and groundwater level filtering, an additional 19.4 km^2 area is found, which was not mapped by the remote sensing or the decision classification methods. The methodology proved to increase the accuracy of locating drainage units in two catchments, one in Canada and the other in Belgium.

Conclusion from Chapter 4 – objective 2: The SWAT+gwflow captures complex geohydrology under human interventions; calibrating multiple variables improves model fidelity.

The impact of drainage on water balance components is assessed by including the locations of drainage units from the previous objective in the SWAT+gwflow model. The results show that the model can represent the geohydrology (streamflow and groundwater head) of the Kleine Nete watershed and, in general, the model's ability to simulate advanced human interventions in the modelling scheme. The calibration strategy indicated the usefulness of calibrating models for more variables than only one, which can hinder the capturing of the general geohydrology.

Conclusion from Chapter 4 – objective 3: Coupled modeling at the regional scale demonstrates accurate streamflow and groundwater dynamics simulation with implications for drought resilience.

From the third objective of modelling the regional Scheldt basin using the SWAT+gwflow model, it is observed that the Nash-Sutcliffe efficiency is above 0.6 during calibration and validation periods for all the seven watersheds inside the Scheldt basin. Additionally, the simulated groundwater head shows good agreement with observed well data (with a mean absolute error of less than 0.42 m). The higher groundwater-surface water interactions observed in the Scheldt basin indicated the impact of streams on groundwater and vice-versa. This has implications for drought management as the impact of drought on rivers or groundwater can have immense consequences on water availability in respective water bodies. Therefore, water managers and policy-makers need to consider this aspect to cope with extreme drought events and integrated water resources management in the region.

General conclusion from Chapter 5: The developed model was found to be helpful in evaluating historical meteorological, agricultural, and hydrological droughts and their cause in the Scheldt basin.

In Chapter 5, the ability of the coupled model to simulate different water balances (e.g., runoff, soil moisture, ET, streamflow, groundwater head, etc.) helps to assess meteorological, hydrological and agricultural droughts in the Scheldt basin. This chapter has three main parts: firstly, historical drought events are assessed using the model outputs of the calibrated and validated SWAT+gwflow model. This objective aims to select the appropriate distribution function for meteorological, agricultural, and hydrological drought assessment. Additionally, a comparison between standardized index-based and threshold-based methods is made. Also, drought propagation analysis is done to evaluate the impact of meteorological drought on streamflow and groundwater. Secondly, the extent to which climate change plays a role in streamflow drought is investigated. Finally, a similar analysis of groundwater bodies is performed.

Conclusion from Chapter 5 – objective 1: A mix of standardized and threshold-based methods with diverse distribution functions is recommended for robust drought detection. Meteorological droughts propagate swiftly to surface and groundwater systems.

The main conclusion from the historical drought assessment is that the methodology needs careful consideration to capture historical recorded drought events. For example, the standardized-based method is not suitable for agricultural drought assessment due to the lack of a distribution function that best fits soil moisture data. Hence, finding a suitable distribution for a given variable is also an important aspect that can reduce the uncertainty in capturing drought events and increase the accuracy of capturing the spatial and temporal trends. Furthermore, time-lag analysis also revealed the similarity of groundwater and streamflow drought relative to a given meteorological drought in the Scheldt basin. This is attributed to the groundwater-driven nature of the catchments in the Scheldt basin.

Conclusion from Chapter 5 – objective 2: Climate change is observed to create a significant decreasing trend in river flows in the regional Scheldt basin.

In the same chapter, the attribution study in streams in the Scheldt basin outlined the severe impact climate change caused on reducing river discharge. Thus, the inevitable impact needs careful consideration to find mitigation measures such as Nature-based solutions listed in Chapter 6. In addition, the datasets from ISIMIP3a need evaluation before further attribution analysis is made. For example out of the four datasets, only three were able to give reasonable streamflow when forced to the calibrated and validated model.

Conclusion from Chapter 5 – objective 3: Climate change has impacted the Kleine Nete groundwater reserve, with levels decreasing by up to 1.5 meters.

Again, in the same chapter, the attribution study in the groundwater head of the Kleine Nete watershed indicated the possible impact climate change has caused on reducing groundwater reserves. The drought assessment indicated an increase in maximum drought deficit and duration due to climate change. Notably, recent years (from 2010 onwards) have shown a considerable decrease in groundwater heads. Overall, from 1970 onwards, there is an average significant decline of 10 cm in groundwater head, with some locations experiencing a maximum decline ranging between 0.1 and 1.5 meters.

General conclusion from Chapter 6: Nature-based solutions concerning drought are underexplored, and a framework for suitability mapping to find optimum detention basins and managed aquifer recharge areas is needed.

Chapter 6 has two major parts, with the first one aiming to create a review paper on assessing drought-specific nature-based solutions (NbS). The second part of this chapter aimed at creating a framework for finding suitable detention basin (DB) and managed aquifer recharge (MAR) areas that focus on mitigating the impact of drought on water resources. Ultimately, the framework is applied to the Flanders scale by comparing the Boolean and Analytic-Hierarchy Process (AHP) approaches.

Conclusion from Chapter 6 – objective 1: Drought mitigating nature-based solutions are underexplored with a lack of monitoring, modelling, and effectiveness assessment scheme.

From this review paper, three core findings are highlighted. Firstly, the current trend focuses on finding NbS that target flood mitigation sidelining drought. Secondly, most applications lack effectiveness assessment, which is mainly due to the lack of models that can simulate NbS implementations and their impact on geohydrology, biodiversity, ecosystem services, etc. Furthermore, monitoring of NbS is not done mostly; hence, this amplifies the difficulty of model development and calibration. Thirdly, wetlands are found to be most effective in drought mitigation. Hence, focusing on their restoration impact while combining fiscal incentives, strong regulations, and community involvement can drive more equitable and sustainable water management.

Conclusion from Chapter 6 – objective 2: The generic suitability mapping framework has outlined potential MAR and DB areas to minimize the impact that drought can cause on water resources.

The following are the main conclusions: the comparison between the Boolean and Analytic-Hierarchy Process (AHP) approaches emphasizes AHP's flexibility in identifying suitable areas for detention basins and managed aquifer recharge, surpassing the limitations of the Boolean method. Based on both methods, Flanders exhibits significant potential for DB and MAR, enhancing regional resilience to drought. However, complementary NbSs (on top of detention basins) are crucial for meeting the total water demand and ensuring sus-

tainable water supply for various sectors, including industries, domestic use, cooling, etc.

7.2 Recommendations

The PhD dissertation explored the coupled SWAT+gwflow model and then applied the model to different watersheds. Ultimately, the model outputs were used for meteorological, hydrological, and agricultural drought assessment. From each of these milestones, there are numerous lessons learned, and recommendations are set forward as follows.

From chapters 3 and 4:

- The SWAT+gwflow model setup is quite versatile but with limitations on capturing the seasonal variation of the groundwater head, hence, iterations which replace the starting groundwater head need to be implemented for better simulation of groundwater dynamics.
- Additionally, detailed processes such as groundwater wetland interactions must be tried better to represent NbS in riverine wetland-dominated watersheds such as those in the Scheldt basin. If the SWAT+gwflow model setup can simulate the geohydrological condition of wetlands, which are found to be major NbS for drought mitigation, scenario analysis on NbS would have been possible. Hence, fixing the coupled model's structure issue to include wetlands will advance our understanding of wetland's capability to withstand hydroclimatic extremes.
- The calibration should include variables other than river discharge (e.g., Evapotranspiration, groundwater head, etc.) to accurately capture geohydrological processes.
- The calibration should include dense network of groundwater wells to capture the dynamic variability of groundwater head.
- The uncertainty coming from the use of global dataset (aquifer thickness, homogeneous hydraulic conductivity zones), inputs, calibration tool (global vs local), calibration methodology (streamflow vs streamflow and groundwater head), number of paramters used, resolution of the groundwater model (grid size), etc., has to be explored in depth.
- The use of global aquifer dataset has to be evaluated with further modeling analysis done with global and local dataset.
- The comparison between the previous SWAT and the newly structured SWAT+ model for the Kleine Nete indicated contradicting results which shows that there are bugs in the source code of the SWAT+ model, hence, effort to improve the model is needed.
- In general, the coupled model is not yet capable of capturing the full geohydrological processes due to the simplifications made. The aim of this thesis is to capture the general geohydrology rather than the individual wells. However, the model can be

used with limited and global data, obtaining reasonable simulations of water balance components, streamflow and regional groundwater head values. The next researcher can utilize what we have done and widen the optimization to capture the full spectrum of groundwater head variations in the watershed.

From chapter 5:

- The distribution function selection to fit soil moisture data was not possible with all the commonly used distribution functions we tried, hence, future research should consider the use of additional (including three-parameter) distribution functions.
- As for attribution studies, the lack of land use data before 1970 made the analysis purely climate-specific. Thus, future studies should consider using dynamic land cover while performing attribution.
- The attribution dataset from ISIMIP3a has a coarse resolution (0.5^o), which undermines the spatial variability, hence, future studies should consider applying the detrending methodology applied to ISIMIP3a on local observational datasets.
- The groundwater drought attribution results has to be analyzed cautiously due to the lack of mismatch in some of the wells between the measured and factual groundwater head. Additionally, more calibration and the use of local aquifer dataset is required on the coupled model, to ensure better representation of groundwater dynamics in the Kleine Nete watershed and beyond.

From chapter 6:

- Since droughts and floods are seen to happen alternatively, a framework for mapping possible nature-based solution areas shall consider both extremes.
- Nature-based solutions effectiveness assessment is missing due to the lack of tools that accurately can simulate the added value of NbS. Thus, it is recommended that model development be extensively worked on to optimize future nature restoration works.
- Having a model alone that can represent NbS is insufficient as model validation requires data; hence, monitoring NbS implementations to optimize future nature restoration works is vital.
- Local water use, along with the increasing trend of abnormal climate deviations (drought), needs a combination of NbS applications (large-scale and small-scale) to minimize the impact on water resources and economy. Hence, NbS scenarios with multiple options need to be explored in depth.
- Stakeholder engagement in the selection, design, and implementation of NbS is vital. Therefore, tools that can incorporate citizens' opinions at these stages are needed.

- The current NbS mapping results are indicative and should be used cautiously.The inclusion of socio-economic criteria is also required to find realistic and optimized NbS locations. Additionally, weights needs to be adjusted in the AHP method by including stakeholders (governmental bodies – VMM, VLM, INBO, etc., practitioners, citizens, research institutes, etc) which can lead to finding realistic suitable areas.

Chapter 8

Appendix

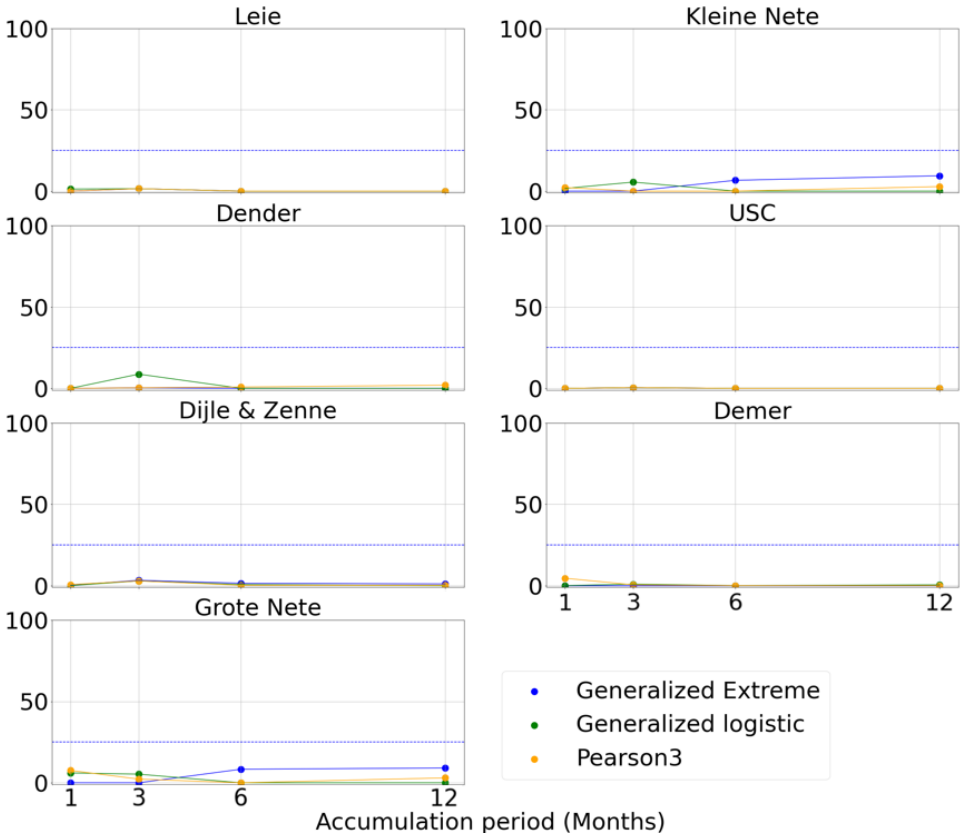


Figure 8.1: Overall rejection frequency plots for meteorological drought for all catchments, horizontal line at 25% represents limit of rejection frequency.

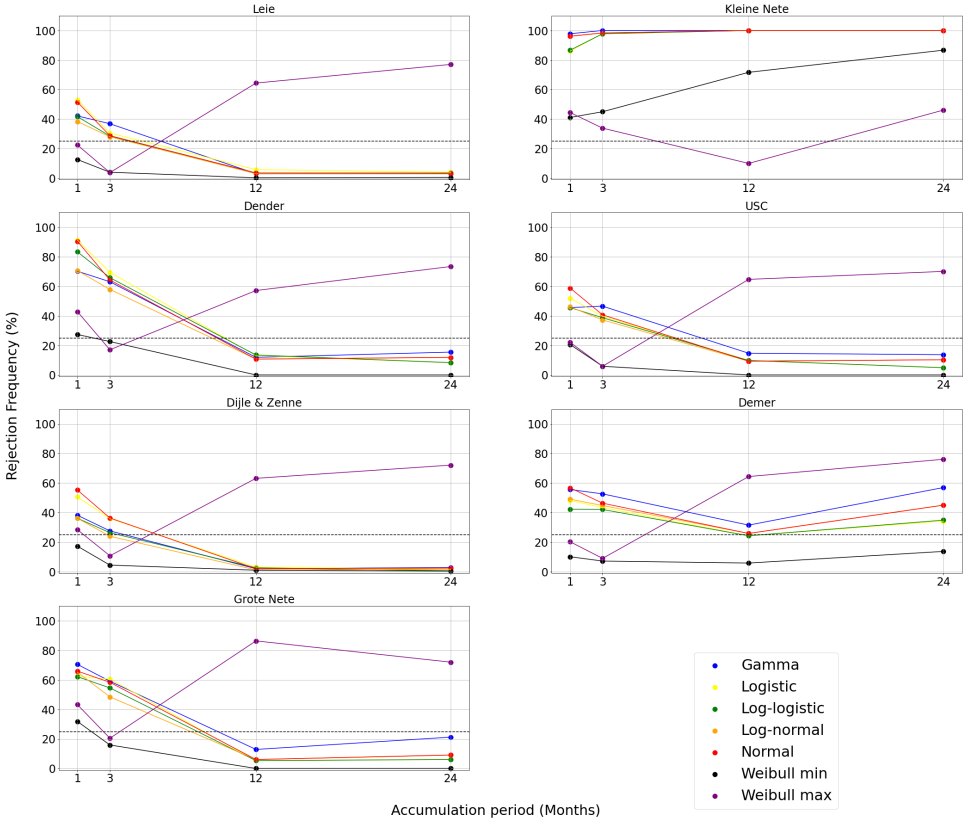


Figure 8.2: Overall rejection frequency plots for soil moisture drought for all catchments, horizontal line at 25% represents limit of rejection frequency.

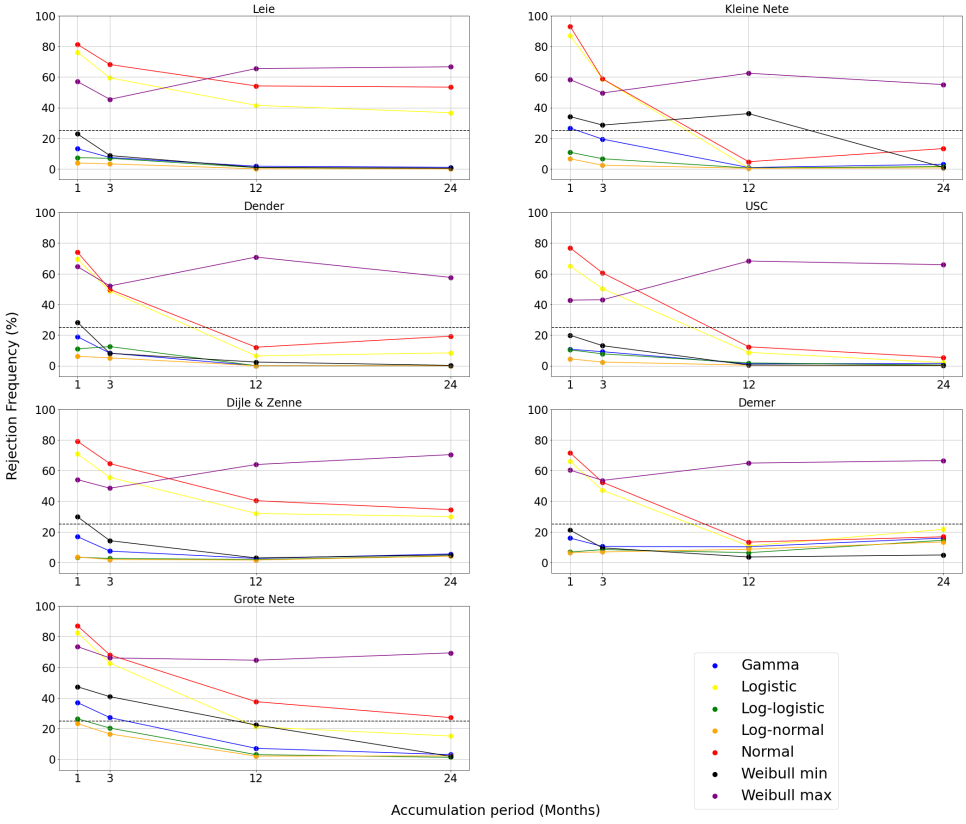


Figure 8.3: Overall rejection frequency plots for all catchments using streamflow, horizontal line at 25% represents limit of rejection frequency.

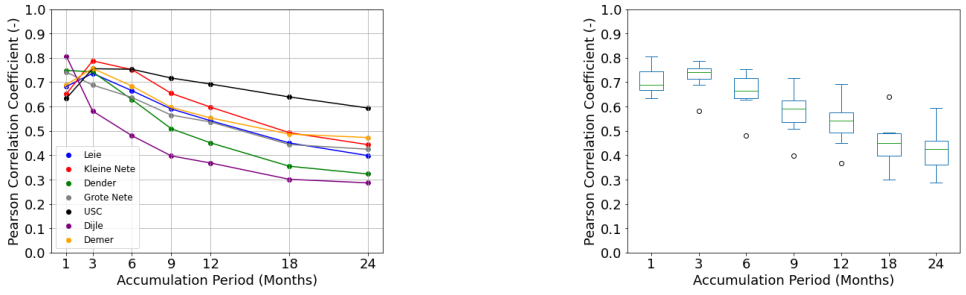


Figure 8.4: Correlation analysis between SSI-1 and SPEI at different accumulation periods on the x-axis

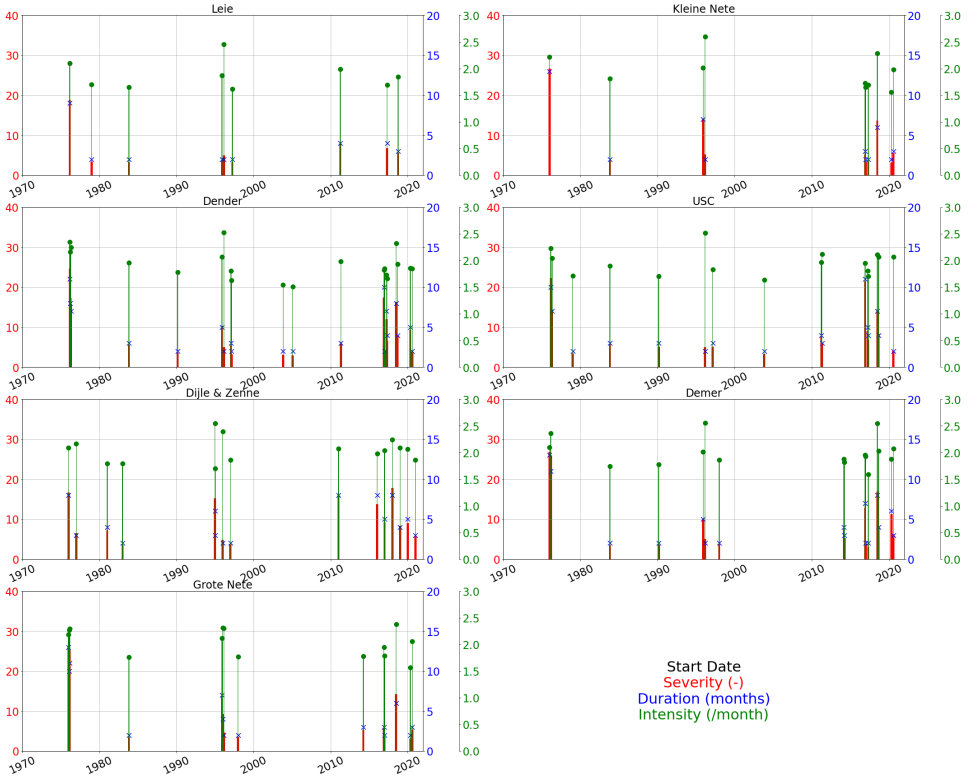


Figure 8.5: Summary of long-term meteorological drought events for all catchments (i.e. 6-month accumulation period).

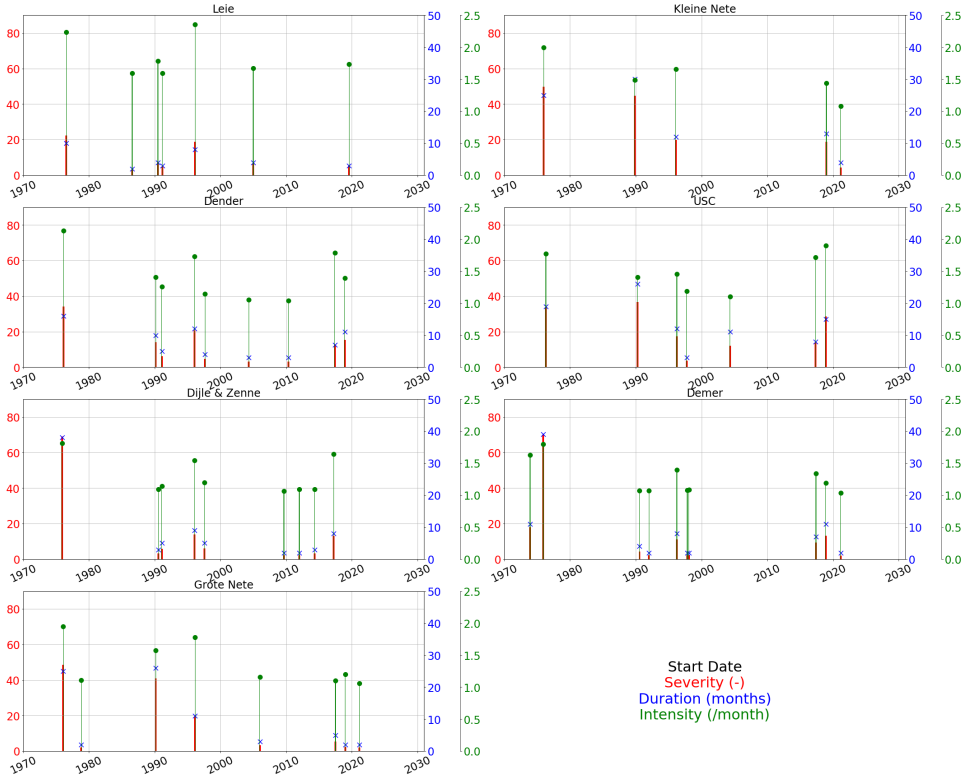


Figure 8.6: Summary of long-term streamflow drought events using SIB for all catchments (12-month accumulation period).

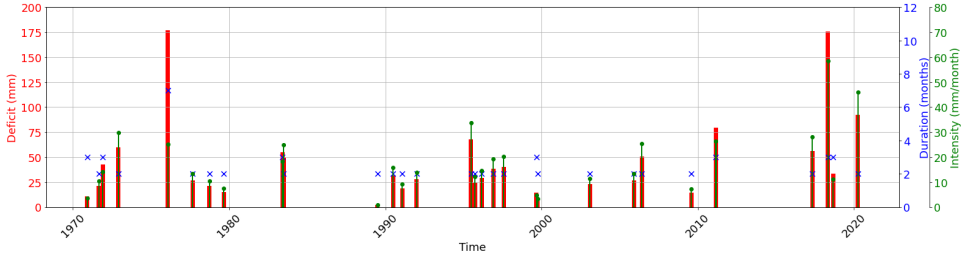


Figure 8.7: Meteorological drought events estimated starting from 1970 using the $80th$ percentile threshold to observe onsets preceding hydrological drought events.

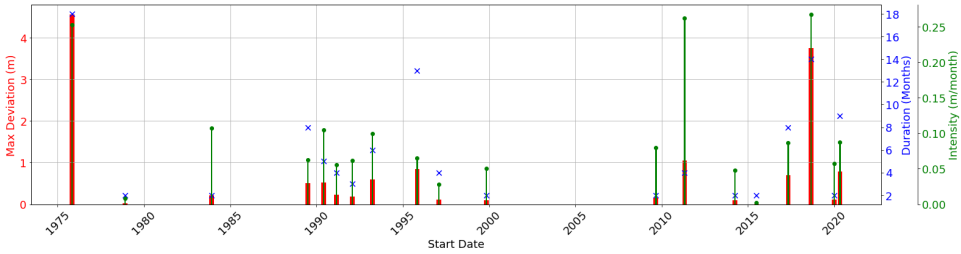


Figure 8.8: Groundwater drought events estimated starting from 1975 using the $80th$ percentile threshold. Location of groundwater head simulated (Herentals) is the closest to the outlet of the streamflow and hydrological subbasin to be spatially consistent.

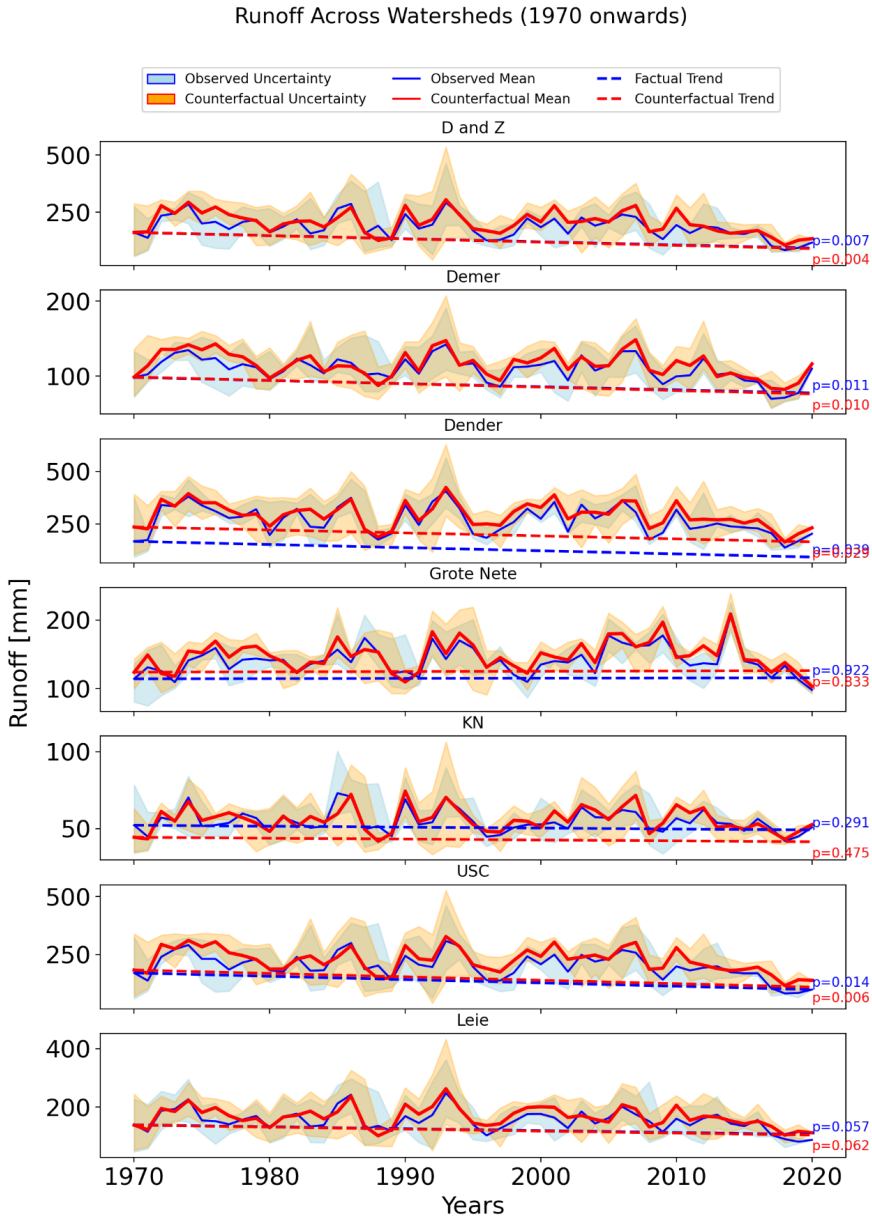


Figure 8.9: Differences between observed and counterfactual mean runoff (mm), averaged across three climate attribution datasets, for various watersheds in the Scheldt basin. Shaded areas represent associated uncertainty ranges, while solid lines indicate mean values. Dashed lines show the observed (blue) and counterfactual (red) trends. P-values indicate the statistical significance of these trends, with values below 0.05 considered significant.

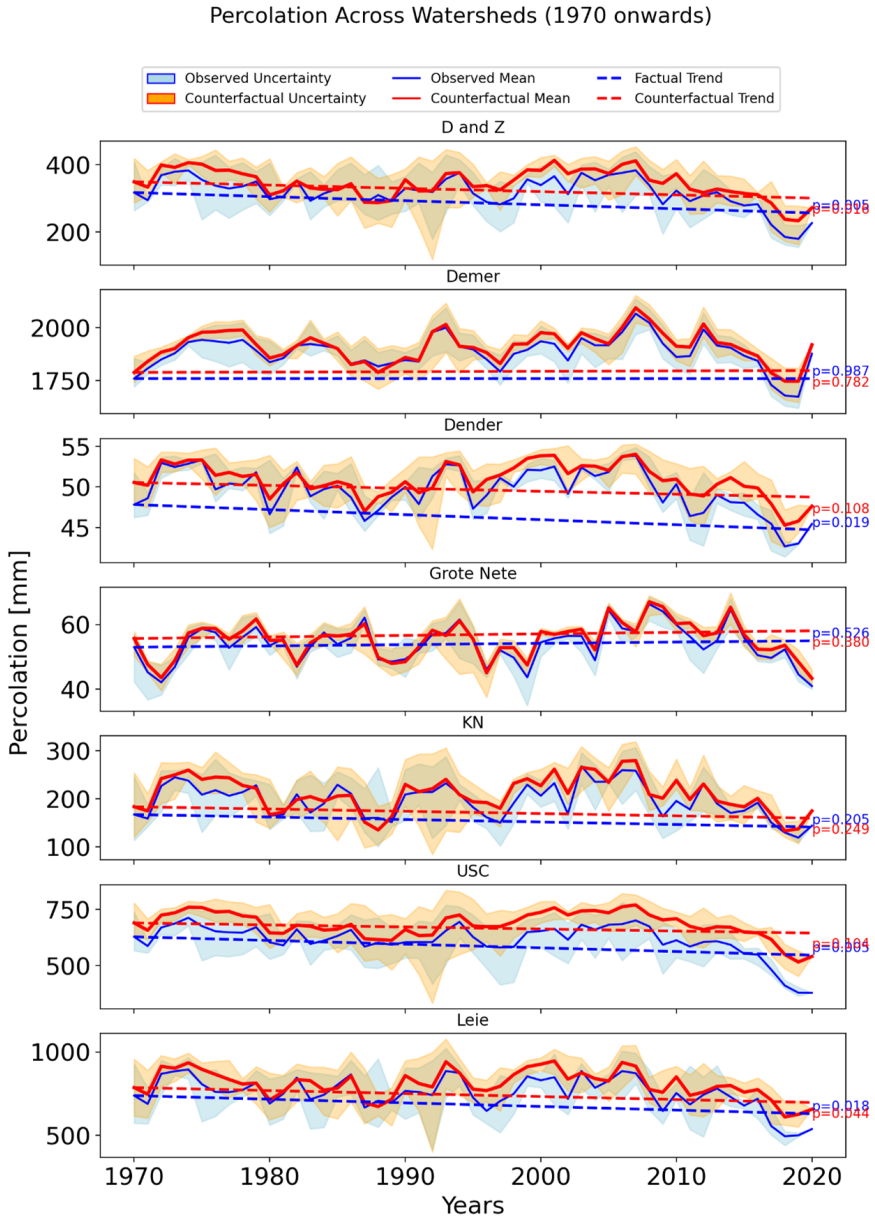


Figure 8.10: Figure 5: Differences between observed and counterfactual mean percolation (mm), averaged across three climate attribution datasets, for various watersheds in the Scheldt basin. Shaded areas represent associated uncertainty ranges, while solid lines indicate mean values. Dashed lines show the observed (blue) and counterfactual (red) trends. P-values indicate the statistical significance of these trends, with values below 0.05 considered significant.

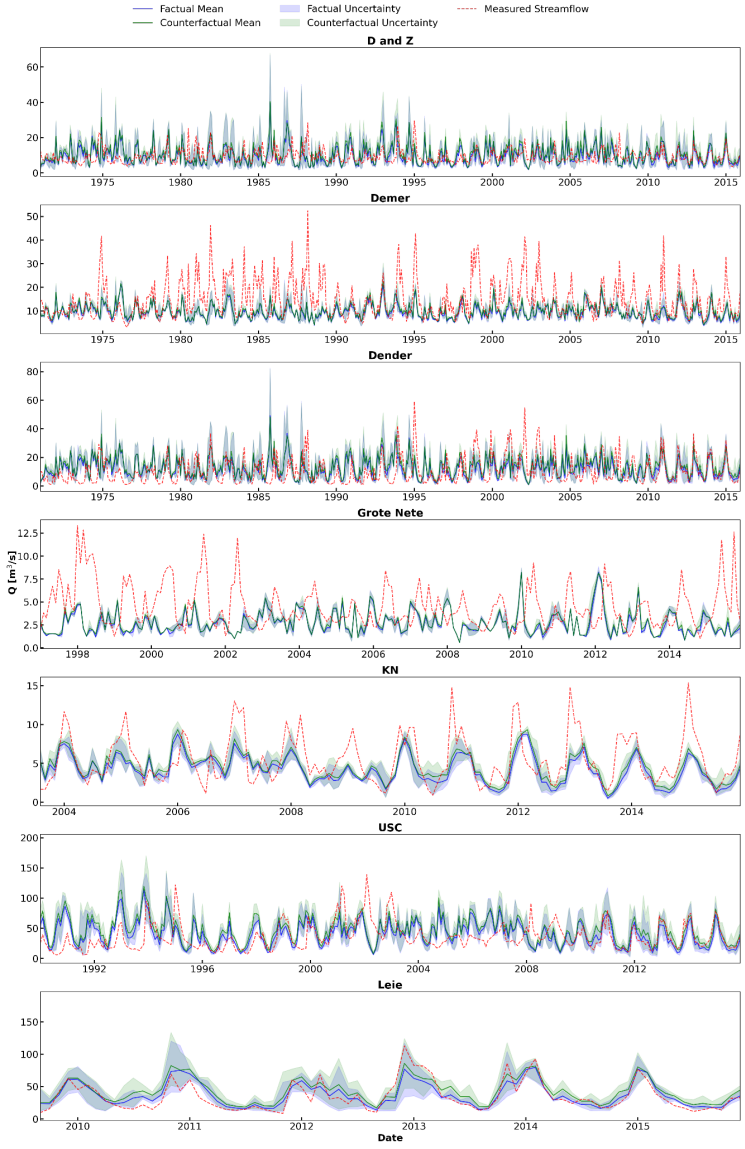


Figure 8.11: Long-term mean streamflow (m³/s) from model simulations using factual and counterfactual climate data, averaged over three climate attribution models. Shaded areas represent uncertainty ranges, and the dashed line represents observed streamflow data for comparison across various watersheds in the Scheldt basin.

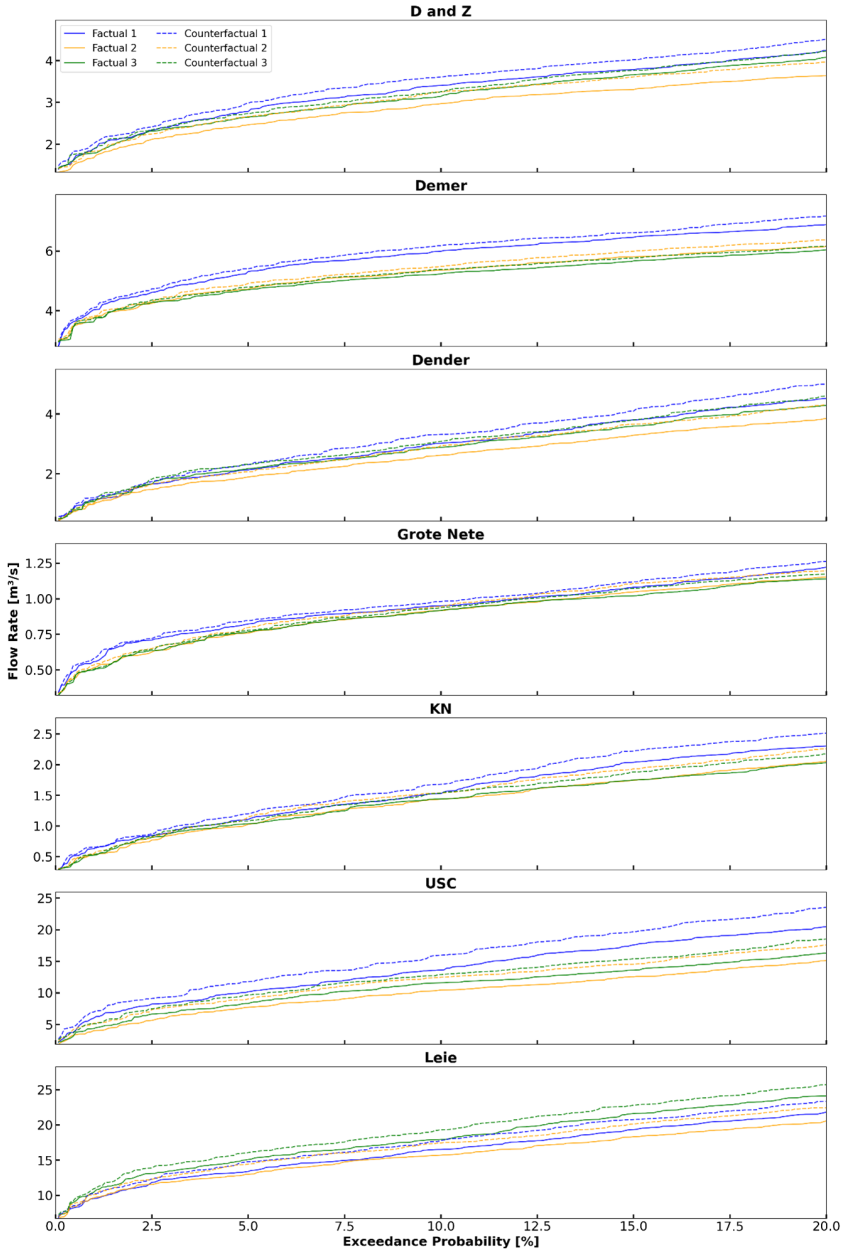


Figure 8.12: Relative differences (deficits) between factual and counterfactual quantiles for low flows, analyzed across three climate attribution dataset and various watersheds in the Scheldt basin. This is to show the low flows (less than 20%).

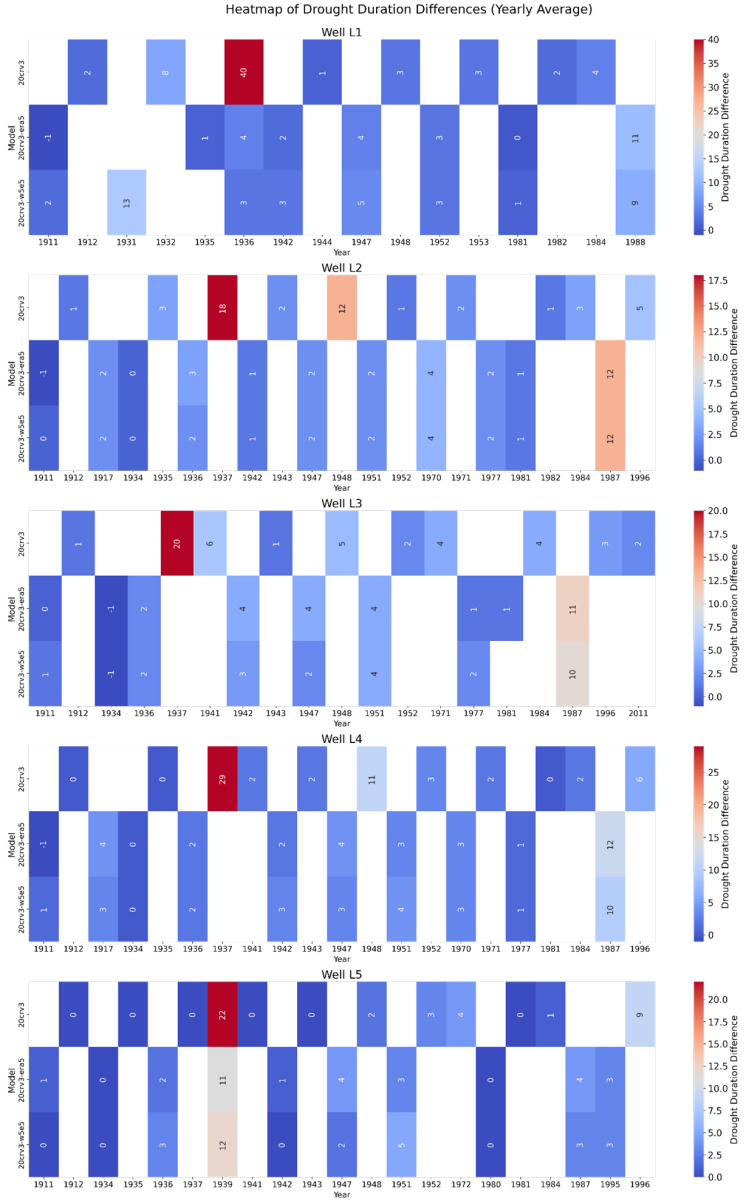


Figure 8.13: Heatmaps showing the yearly drought duration differences (in months) between factual and counterfactual scenarios for drought events at a 12-month accumulation period across three climate attribution models and five wells (L1 to L5). Each panel represents one well, with colours indicating the magnitude of the drought duration difference: blue shades represent shorter drought durations in the factual scenario, while red shades represent longer drought durations in the factual scenario.

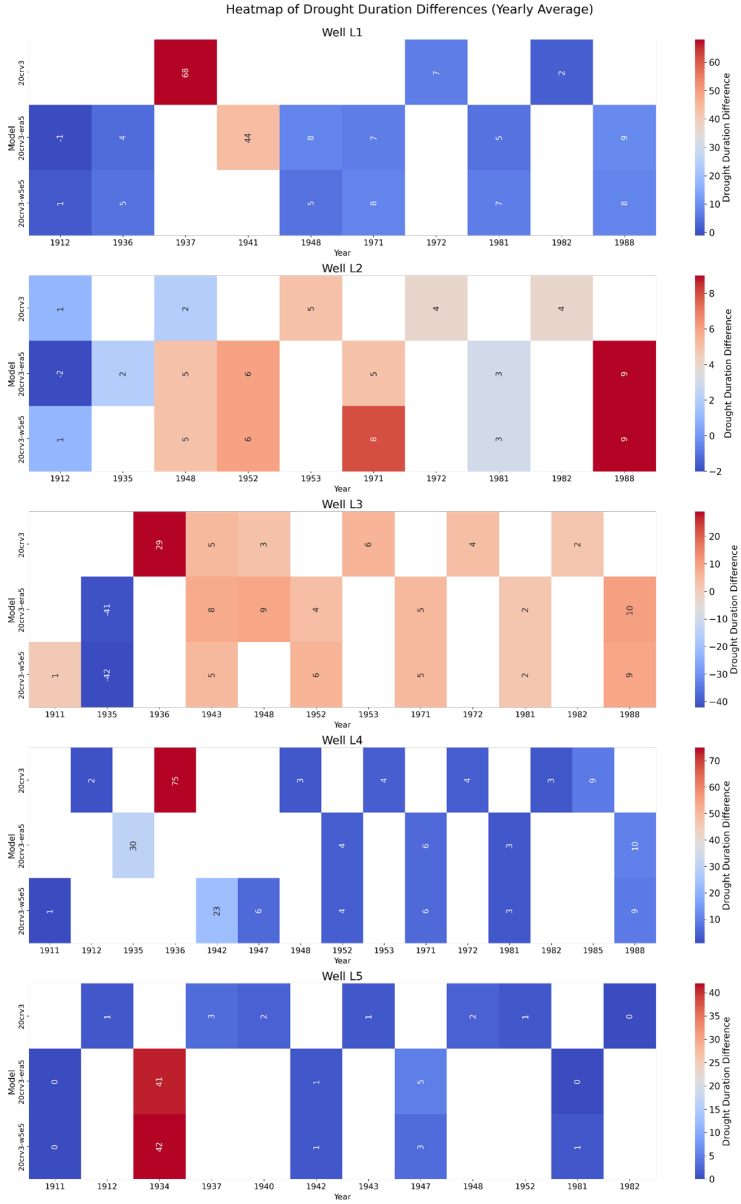


Figure 8.14: Heatmaps showing the yearly drought duration differences (in months) between factual and counterfactual scenarios for drought events at a 24-month accumulation period across three climate attribution models and five wells (L1 to L5). Each panel represents one well, with colours indicating the magnitude of the drought duration difference: blue shades represent shorter drought durations in the factual scenario, while red shades represent longer drought durations in the factual scenario.

List of Outputs

Peer reviewed articles in scientific journals - as first author

1. **Yimer, E. A.**, Van Schaeybroeck, B., Van de Vyver, H., & van Griensven, A. (2022). Evaluating Probability Distribution Functions for the Standardized Precipitation Evapotranspiration Index over Ethiopia. Atmosphere, 13(3), 364. https://doi.org/10.3390/atmos13030364

2. **Yimer, E. A.**, Bailey, R. T., Piepers, L. L., Nossent, J., & Van Griensven, A. (2023). Improved Representation of Groundwater–Surface Water Interactions Using SWAT +gwflow and Modifications to the gwflow Module. Water, 15(18), 3249. https://doi.org/10.3390/w15183249

3. **Yimer, E. A.**, Riakhi, F.-E., Bailey, R. T., Nossent, J., & van Griensven, A. (2023). The impact of extensive agricultural water drainage on the hydrology of the Kleine Nete watershed, Belgium. Science of The Total Environment, 885, 163903. https://doi.org/10.1016/j.scitotenv.2023.163903

4. **Yimer, E. A.**, Yadollahi, S., Riakhi, F.-E., Alitane, A., Weerasinghe, I., Wirion, C., Nossent, J., van Griensven, A., 2023. A groundwater level-based filtering to improve the accuracy of locating agricultural tile drain and ditch networks. International Journal of Applied Earth Observation and Geoinformation 122, 103423

5. **Yimer, E. A.**, Bailey, R. T., Van Schaeybroeck, B., Van De Vyver, H., Villani, L., Nossent, J., & van Griensven, A. (2023). Regional evaluation of groundwater-surface water interactions using a coupled geohydrological model (SWAT+gwflow). Journal of Hydrology: Regional Studies, 50, 101532. https://doi.org/10.1016/j.ejrh.2023.101532

6. **Yimer, E. A.**, De Trift, L., Lobkowicz, I., Villani, L., Nossent, J., van Griensven, A., 2024. The underexposed nature-based solutions: A critical state-of-art review on drought mitigation. Journal of Environmental Management 352, 119903

7. **Yimer, E. A.**, De Trift, L., Dondeyne, S., Speijer, L., Huysmans, M., Cools, J., Nossent, J., van Griensven, A., 2024. Framework for mapping large-scale nature-based solutions for drought

Peer reviewed articles in scientific journals - as contributing author

1. Alitane, A., Essahlaoui, A., Van Griensven, A. **Yimer, E. A.**, Essahlaoui, N., Mohajane, M., Chawanda, C.J., Van Rompaey, A., 2022. Towards a Decision-making approach of sustainable water resources management based on hydrological modeling: a case study in central Morocco. Sustainability 14, 10848.

2. Alitane, A., Essahlaoui, A., **Yimer, E. A.**, The combined use of GIS and water quality indices for environmental assessment of Ouislane River watershed, Morocco. Euro-Mediterr J Environ Integr.

3. Alitane, Abdennabi, Essahlaoui, A., **Yimer, E. A.**, Ousmana, H., Essahlaoui, N., Oumou, A., Hmaidi, A.E., Benyoussef, S., Van Griensven, A., 2024. Hydrogeochemical characterization and statistical approach to assess the quality of the spring water in the Meknes-El Hajeb region, Morocco. Modeling Earth Systems and Environment 10, 6293–6308

4. Nkwasa, A., Getachew, R.E., Lekarkar, K., **Yimer, E. A.**, Martínez, A.B., Tang, T., van Griensven, A., 2024. Can turbidity data from remote sensing explain modelled spatial and temporal sediment loading patterns? An application in the Lake Tana Basin. Environmental Modeling & Assessment 29, 871–882

5. Villani, L., Castelli, G., **Yimer, E. A.**, Chawanda, C.J., Nkwasa, A., Van Schaeybroeck, B., Penna, D., van Griensven, A., Bresci, E., 2024. Impacts of climate change and vegetation response on future aridity in a Mediterranean catchment. Agricultural Water Management 299, 108878

6. Villani, L., Castelli, G., **Yimer, E. A.**, Nkwasa, A., Penna, D., van Griensven, A., Bresci, E., 2024. Exploring adaptive capacities in Mediterranean agriculture: Insights from Central Italy's Ombrone catchment. Agricultural Systems 216, 103903

7. Alemu, M.M., Zaitchik, B.F., Enku, T., Worqlul, A.W, **Yimer, E. A.**, van Griensven, A., 2025. Statistical and hydrological evaluation of remotely sensed rainfall products in the Upper Blue Nile basin, Ethiopia. Modeling Earth Systems and Environment 11, 1–17

8. Elsaidy, A., **Yimer, E. A.**, Mogheir, Y., Huysmans, M., Villani, L., Van Griensven, A., 2025. Groundwater drought and anthropogenic amplifiers: A review of assessment and response strategies in arid and semi-arid areas. Science of the Total Environment 978, 179406

9. Mukama, E.B., **Yimer, E. A.**, Mbungu, W.B., Dondeyne, S., van Griensven, A., 2025. Evaluating the standardized and threshold based drought indices for historical drought detection in the Great Ruaha River Basin, Tanzania. Natural Hazards 1–31.

Articles in draft stage or under submission

1. **Yimer, E. A.**Uncertainty analysis on drought index estimation and impact of climate change on streamflow at Grote Nete watershed (Draft completed and on the process for submission)
2. **Yimer, E. A.**, José, P.T.S., Lorenzo, V., Abdennabi, A., Zakaria, A., Brian, O., Anandita, A., Ryan T. B., Jiri, N.,Ann, V.G, An open source SWAT+gwflow input generation, post-processing and calibration tool for comprehensive assessment of water resources(under review)
3. **Yimer, E. A.**Attributing climate change impact on streamflow decrease at regional scale using coupled surface – groundwater model(Draft)
4. **Yimer, E. A.**Is climate change aggravating groundwater drought? A case study in a groundwater dominated watershed(Draft)
5. **Yimer, E. A.**Introduction to drought, assessment methods, and nature-based solutions(Draft)
6. Mukama, E.B., **Yimer, E.A.**, Mbungu, W.B., Dondeyne, S, & van Grienseven. 2025. Unravelling the hydrologic impact of climate change in the Great Ruaha River Basin, Tanzania.(under review)
7. Mukama, E.B., Ronoh, E., **Yimer, E.A.**, Mbungu, W.B., Dondeyne, S, & van Grienseven. 2025. Future changes in water availability: Insights from CMIP6 model simulations for the Great Ruaha River Basin, Tanzania(Draft)
8. Lorenzo, V., **Yimer, E. A.**, Quantifying future drought overestimation due to neglect of vegetation responses to CO_2(Draft)
9. Elsaidy, A., **Yimer, E. A.**, Mogheir, Y., Huysmans, M., Villani, L., Van Griensven, A., 2025: Temporal and Spatial Patterns of Groundwater Drought in the Bruna River Catchment, Italy(Draft)
10. Melkamu Meseret Alemu, Benjamin F. Zaitchik, Temesgen Enku, Abeyou W. Worqlul, **Yimer, E. A.**, & Ann van Griensven. 2025. Spatiotemporal analysis of drought characteristics across multiple timescales in the Upper Blue Nile basin, Ethiopia (under review)
11. Melkamu Meseret Alemu, Benjamin F. Zaitchik, Temesgen Enku, Abeyou W. Worqlul, **Yimer, E. A.**, & Ann van Griensven. 2025. Evaluating Hydroclimate Dynamics: Trend Analysis and Change Detection for Enhanced Drought Monitoring in the Upper Blue Nile Basin (under review)

Presentations at conferences and workshops

1. SWAT Conference, Prague - July 2022. The application of the SWAT+gwflow model for catchment in irrigation dominated catchment in Morocco. (Oral presentation)
2. ERB 18th Biennial Conference, Portoferraio, Elba Island - June 2022. Assessing the impact of climate change on coastal catchment (Bruna – Italy) using SWAT+gwflow. (Oral presentation)
3. EGU Conference, Vienna May - 2022. Evaluating probability distribution functions for the Standardized Precipitation Evapotranspiration Index over Ethiopia. (Oral presentation)
4. iEMSs Conference, Brussel July - 2022. Improved representation of groundwater-surface water interaction in SWAT+ using the gwflow module and its implication for proper drought characterization. (Oral presentation)
5. EGU Conference, Vienna - April 2022. A novel way of identifying agricultural water drainage systems and their impact on catchment hydrology. (Oral presentation)
6. EGU Conference, Vienna - April 2023. A novel way of identifying agricultural water drainage systems and their impact on catchment hydrology. (Oral presentation)
7. IAHS Conference, Berlin - July 2023. Uncertainty analysis on drought index estimation and impact of climate change on streamflow at Grote Nete watershed. (Oral presentation)
8. SWAT Conference, Aarhus - June 2023. An Open-source Python script to prepare the inputs for the coupled SWAT+gwflow model. (Oral presentation)
9. MedGU Conference, Istanbul - November 2023. The impact of extensive agricultural water drainage on the hydrology of the Kleine Nete watershed, Belgium. (Oral presentation)
10. The first international drought symposium and workshop, Brussels - June 2023. The state of the art drought assessment methodologies using open source R and Python scripts. (Oral presentation and hands on exercise supervision)
11. HydRoData: 2024 Summer School, Ljubljana - Slovenia, September 2024. The state of the art drought assessment methodologies using open source R scripts. (Invited speaker)
12. Capacity development program by “International Training Program (ITP) project, Bahir Dar - Ethiopia, November 2024. The Use of Open-Source Hydrological Models for Water Resources Management: SWAT+GWFLOW. (Invited speaker)
13. A session on Nature-based solutions to protect against hydro-meteorological extremes: the European Geoscience Union (EGU) conference, Vienna -Austria, April 2023. (Convened a session)

Awards and recognitions

1. PhD Strategic Basic (SB) research grant for Assessing the impact of climate change on drought in the Scheldt basin, Belgium, awarded by FWO (2021).

2. Global minds grant for organizing the first international drought symposium in Brussels - Belgium, awarded by VUB international office (2023).

3. Research stay grant for model development in Fort-Collins, Colorado - USA, awarded by FWO (2024).

4. Grant for participation in an international conference abroad, Jeju Island, South Korea, awarded by FWO (2025).

Bibliography

Abbaspour, K. C., Rouholahnejad, E., Vaghefi, S., Srinivasan, R., Yang, H., and Kløve, B.: A continental-scale hydrology and water quality model for Europe: Calibration and uncertainty of a high-resolution large-scale SWAT model, Journal of hydrology, 524, 733–752, https://doi.org/10.1016/j.jhydrol.2015.03.027, 2015.

Abbott, M. B., Bathurst, J. C., Cunge, J. A., O'Connell, P. E., and Rasmussen, J.: An introduction to the European Hydrological System—Systeme Hydrologique Europeen,"SHE", 1: History and philosophy of a physically-based, distributed modelling system, Journal of hydrology, 87, 45–59, https://doi.org/10.1016/0022-1694(86)90114-9, 1986.

Adriaens, D.: shallowgroundwater: estimated zones with shallow groundwater in the Flemish region of Belgium (shallowgroundwater_v1), https://doi.org/10.5281/zenodo.5902881, 2021.

Ahmad, S., Kalra, A., and Stephen, H.: Estimating soil moisture using remote sensing data: A machine learning approach, Advances in water resources, 33, 69–80, iSBN: 0309-1708 Publisher: Elsevier, 2010.

Ahmadisharaf, E., Tajrishy, M., and Alamdari, N.: Integrating flood hazard into site selection of detention basins using spatial multi-criteria decision-making, Journal of Environmental Planning and Management, 59, 1397–1417, https://doi.org/10.1080/09640568.2015.1077104, 2016.

Ahmed, N., Wang, G., Lü, H., Booij, M. J., Marhaento, H., Prodhan, F. A., Ali, S., and Ali Imran, M.: Attribution of changes in streamflow to climate change and land cover change in Yangtze River source region, China, Water, 14, 259, iSBN: 2073-4441 Publisher: MDPI, 2022.

Ahn, K.-H., Merwade, V., Ojha, C. S. P., and Palmer, R. N.: Quantifying relative uncertainties in the detection and attribution of human-induced climate change on winter streamflow, Journal of hydrology, 542, 304–316, iSBN: 0022-1694 Publisher: Elsevier, 2016.

Al Atawneh, D., Cartwright, N., and Bertone, E.: Climate change and its impact on the projected values of groundwater recharge: A review, Journal of Hydrology, 601, 126 602, iSBN: 0022-1694 Publisher: Elsevier, 2021.

Al-Safi, H. I. J., Kazemi, H., and Sarukkalige, P. R.: Comparative study of conceptual versus distributed hydrologic modelling to evaluate the impact of climate change on future runoff in unregulated catchments, Journal of Water and Climate Change, 11, 341–366, iSBN: 2040-2244 Publisher: IWA Publishing, 2020.

Alexander, R. B., Smith, R. A., Schwarz, G. E., Boyer, E. W., Nolan, J. V., and Brakebill, J. W.: Differences in phosphorus and nitrogen delivery to the Gulf of Mexico from the Mississippi River Basin, Environmental science & technology, 42, 822–830, https://doi.org/10.1021/es0716103, 2008.

Alikhani, S., Nummi, P., and Ojala, A.: Urban wetlands: A review on ecological and cultural values, Water (Switzerland), 13, 1–47, https://doi.org/10.3390/w13223301, 2021.

Aliyari, F., Bailey, R. T., Tasdighi, A., Dozier, A., Arabi, M., and Zeiler, K.: Coupled SWAT-MODFLOW model for large-scale mixed agro-urban river basins, Environmental Modelling & Software, 115, 200–210, 2019.

Alley, W. M., Reilly, T. E., and Franke, O. L.: Sustainability of ground-water resources, vol. 1186, US Department of the Interior, US Geological Survey, 1999.

Allred, B., Wishart, D., Martinez, L., Schomberg, H., Mirsky, S., Meyers, G., Elliott, J., and Charyton, C.: Delineation of agricultural drainage pipe patterns using ground penetrating radar integrated with a real-time kinematic global navigation satellite system, Agriculture, 8, 167, https://doi.org/10.3390/agriculture8110167, 2018.

Allred, B., Martinez, L., Fessehazion, M. K., Rouse, G., Williamson, T. N., Wishart, D., Koganti, T., Freeland, R., Eash, N., and Batschelet, A.: Overall results and key findings on the use of UAV visible-color, multispectral, and thermal infrared imagery to map agricultural drainage pipes, Agricultural Water Management, 232, 106 036, https://doi.org/10.1016/j.agwat.2020.106036, 2020.

Allred, B., Martinez, L., Fessehazion, M. K., Rouse, G., Koganti, T., Freeland, R., Eash, N., Wishart, D., and Featheringill, R.: Time of day impact on mapping agricultural subsurface drainage systems with UAV thermal infrared imagery, Agricultural Water Management, 256, 107 071, 2021.

Allred, B. J., Fausey, N. R., Peters, L., Chen, C., Daniels, J. J., and Youn, H.: Detection of buried agricultural drainage pipe with geophysical methods, Applied Engineering in Agriculture, 20, 307, https://doi.org/10.13031/2013.16067, 2004.

Amano, H. and Iwasaki, Y.: Estimation of Groundwater Recharge in Kumamoto Area, Japan in 2016 by Mapping Land Cover Using GIS Data and SPOT 6/7 Satellite Images, Sustainability, 14, 545, https://doi.org/10.3390/su14010545, 2022.

Arnold, J. G., Srinivasan, R., Muttiah, R. S., and Williams, J. R.: Large area hydrologic modeling and assessment part I: model development 1, JAWRA Journal of the American Water Resources Association, 34, 73–89, https://doi.org/10.1111/j.1752-1688.1998.tb05961.x, 1998.

Arnold, J. G., Moriasi, D. N., Gassman, P. W., Abbaspour, K. C., White, M. J., Srinivasan, R., Santhi, C., Harmel, R. D., Van Griensven, A., and Van Liew, M. W.: SWAT: Model use, calibration, and validation, Transactions of the ASABE, 55, 1491–1508, https://doi.org/10.13031/2013.42256, 2012.

Arnold, J. G., Bieger, K., White, M. J., Srinivasan, R., Dunbar, J. A., and Allen, P. M.: Use of decision tables to simulate management in SWAT+, Water, 10, 713, https://doi.org/10.3390/w10060713, 2018.

Atkinson, S. E., Woods, R. A., and Sivapalan, M.: Climate and landscape controls on water balance model complexity over changing timescales, Water Resources Research, 38, 50–1–50–17, https://doi.org/10.1029/2002WR001487, 2002.

Avery, C.: Interaction of ground water with the Rock River near Byron, Illinois, US Department of the Interior, US Geological Survey, 1994.

Baez-Villanueva, O. M., Zambrano-Bigiarini, M., Miralles, D. G., Beck, H. E., Siegmund, J. F., Alvarez-Garreton, C., Verbist, K., Garreaud, R., Boisier, J. P., and Galleguillos, M.: On the timescale of drought indices for monitoring streamflow drought considering catchment hydrological regimes, Hydrology and Earth System Sciences, 28, 1415–1439, iSBN: 1027-5606 Publisher: Copernicus GmbH, 2024.

Bailey, R., Rathjens, H., Bieger, K., Chaubey, I., and Arnold, J.: SWATMOD-Prep: Graphical user interface for preparing coupled SWAT-MODFLOW simulations, JAWRA Journal of the American Water Resources Association, 53, 400–410, https://doi.org/10.1111/1752-1688.12502, 2017.

Bailey, R., Bieger, K., Arnold, J., and Bosch, D.: A New Physically-Based Spatially-Distributed Groundwater Flow Module for SWAT+, Hydrology, 7, 75, https://doi.org/10.3390/hydrology7040075, 2020a.

Bailey, R. T., Wible, T. C., Arabi, M., Records, R. M., and Ditty, J.: Assessing regional-scale spatio-temporal patterns of groundwater–surface water interactions using a coupled SWAT-MODFLOW model, Hydrological Processes, 30, 4420–4433, https://doi.org/10.1002/hyp.10933, 2016.

Bailey, R. T., Park, S., Bieger, K., Arnold, J. G., and Allen, P. M.: Enhancing SWAT+ simulation of groundwater flow and groundwater-surface water interactions using MODFLOW routines, Environmental Modelling & Software, 126, 104 660, https://doi.org/10.1016/j.envsoft.2020.104660, 2020b.

Bailey, R. T., Bieger, K., Flores, L., and Tomer, M.: Evaluating the contribution of subsurface drainage to watershed water yield using SWAT+ with groundwater modeling, Science of The Total Environment, 802, 149 962, https://doi.org/10.1016/j.scitotenv.2021.149962, 2022.

Bailey, R. T., Abbas, S., Arnold, J., White, M., Gao, J., and Čerkasova, N.: Augmenting the National agroecosystem model with physically based spatially distributed groundwater modeling, Environmental Modelling & Software, 160, 105 589, https://doi.org/10.1016/j.envsoft.2022.105589, 2023.

Barendrecht, M. H., Matanó, A., Mendoza, H., Weesie, R., Rohse, M., Koehler, J., de Ruiter, M., Garcia, M., Mazzoleni, M., and Aerts, J. C.: Exploring drought-to-flood interactions and dynamics: A global case review, Wiley Interdisciplinary Reviews: Water, p. e1726, iSBN: 2049-1948 Publisher: Wiley Online Library, 2024.

Barron, O., Barr, A., and Donn, M.: Effect of urbanisation on the water balance of a catchment with shallow groundwater, Journal of Hydrology, 485, 162–176, 2013.

Barthel, R. and Banzhaf, S.: Groundwater and surface water interaction at the regional-scale–a review with focus on regional integrated models, Water resources management, 30, 1–32, 2016.

Bastiaensen, T., Van Wambeke, E., El Bakkali, C., Desair, J., Noël, C., Kenis, K., Vincke, L., and Jacobs, S.: Beyond Biodiversity: Eliciting Diverse Values of Urban Green Spaces in Flanders, Land, 12, 1186, https://doi.org/10.3390/land12061186, 2023.

Bastola, S. and Misra, V.: Evaluation of dynamically downscaled reanalysis precipitation data for hydrological application, Hydrological Processes, 28, 1989–2002, iSBN: 0885-6087 Publisher: Wiley Online Library, 2014.

Basu, N. B., Rao, P. S. C., Winzeler, H. E., Kumar, S., Owens, P., and Merwade, V.: Parsimonious modeling of hydrologic responses in engineered watersheds: Structural heterogeneity versus functional homogeneity, Water resources research, 46, https://doi.org/10.1029/2009WR007803, 2010.

Batelaan, O. and De Smedt, F.: GIS-based recharge estimation by coupling surface–subsurface water balances, Journal of hydrology, 337, 337–355, https://doi.org/10.1016/j.jhydrol.2007.02.001, 2007.

Bauer, P., Gumbricht, T., and Kinzelbach, W.: A regional coupled surface water/groundwater model of the Okavango Delta, Botswana, Water Resources Research, 42, https://doi.org/10.1029/2005WR004234, 2006.

Bauwe, A., Kahle, P., and Lennartz, B.: Hydrologic evaluation of the curve number and Green and Ampt infiltration methods by applying Hooghoudt and Kirkham tile drain equations using SWAT, Journal of Hydrology, 537, 311–321, https://doi.org/10.1016/j.jhydrol.2016.03.054, 2016.

Bayat, B., Zahraie, B., Taghavi, F., and Nasseri, M.: Evaluation of spatial and spatiotemporal estimation methods in simulation of precipitation variability patterns, Theoretical and applied climatology, 113, 429–444, https://doi.org/10.1007/s00704-012-0795-7, 2013.

Bear, J.: Dynamics of fluids in porous media–American Elsevier pub, Comp., inc. New York, 764p, 1972.

Beck, H. E., Zimmermann, N. E., McVicar, T. R., Vergopolan, N., Berg, A., and Wood, E. F.: Present and future Köppen-Geiger climate classification maps at 1-km resolution, Scientific data, 5, 1–12, https://doi.org/10.1038/sdata.2018.214, 2018.

Behrendt, H., Huber, P., Kornmilch, M., Opitz, D., Schmoll, O., Scholz, G., and Uebe, R.: Nutrient emissions into river basins of Germany, Texte, 23, 261, URL https://www.researchgate.net/publication/265222040_Nutrient_Emissions_into_River_Basins_of_Germany, 2000.

Belden, E. and Steele, N.: Green infrastructure and sustainable design for streets: The elmer avenue neighborhood retrofit demonstration, pp. 3166–3173, https://doi.org/10.1061/41173(414)331, 2011.

Belle, J., Collins, N., and Jordaan, A.: Managing wetlands for disaster risk reduction: A case study of the eastern Free State, South Africa, Jamba: Journal of Disaster Risk Studies, 10, https://doi.org/10.4102/jamba.v10i1.400, 2018.

Bhaga, T. D., Dube, T., Shekede, M. D., and Shoko, C.: Impacts of climate variability and drought on surface water resources in Sub-Saharan Africa using remote sensing: A review, Remote Sensing, 12, 4184, iSBN: 2072-4292 Publisher: MDPI, 2020.

Bhatta, B., Shrestha, S., Shrestha, P. K., and Talchabhadel, R.: Evaluation and application of a SWAT model to assess the climate change impact on the hydrology of the Himalayan River Basin, Catena, 181, 104 082, iSBN: 0341-8162 Publisher: Elsevier, 2019.

Bhuiyan, C.: Various drought indices for monitoring drought condition in Aravalli terrain of India, in: Proceedings of the XXth ISPRS Congress, Istanbul, Turkey, vol. 2004, pp. 12–23, 2004.

Bieger, K., Arnold, J. G., Rathjens, H., White, M. J., Bosch, D. D., Allen, P. M., Volk, M., and Srinivasan, R.: Introduction to SWAT+, a completely restructured version of the soil and water assessment tool, JAWRA Journal of the American Water Resources Association, 53, 115–130, https://doi.org/10.1111/1752-1688.12482, 2017.

Bindoff, N. L., Stott, P. A., AchutaRao, K. M., Allen, M. R., Gillett, N., Gutzler, D., Hansingo, K., Hegerl, G., Hu, Y., and Jain, S.: Detection and attribution of climate change: from global to regional, Climate change 2013: the physical science basis, 2014.

Blann, K. L., Anderson, J. L., Sands, G. R., and Vondracek, B.: Effects of agricultural drainage on aquatic ecosystems: a review, Critical reviews in environmental science and technology, 39, 909–1001, https://doi.org/10.1080/10643380801977966, 2009.

Blauhut, V., Stahl, K., Stagge, J. H., Tallaksen, L. M., De Stefano, L., and Vogt, J.: Estimating drought risk across Europe from reported drought impacts, drought indices, and vulnerability factors, Hydrology and Earth System Sciences, 20, 2779–2800, https://doi.org/10.5194/hess-20-2779-2016, 2016.

Blöschl, G. and Montanari, A.: Climate change impacts—throwing the dice?, Hydrological Processes: An International Journal, 24, 374–381, iSBN: 0885-6087 Publisher: Citeseer, 2010.

Boerema, A., Schoelynck, J., Bal, K., Vrebos, D., Jacobs, S., Staes, J., and Meire, P.: Economic valuation of ecosystem services, a case study for aquatic vegetation removal in the Nete catchment (Belgium), Ecosystem Services, 7, 46–56, https://doi.org/10.1016/j.ecoser.2013.08.001, 2014.

Bouabdelli, S., Zeroual, A., Meddi, M., and Assani, A.: Impact of temperature on agricultural drought occurrence under the effects of climate change, Theoretical and Applied Climatology, 148, 191–209, iSBN: 0177-798X Publisher: Springer, 2022.

Brady, A., Faraway, J., and Prosdocimi, I.: Attribution of long-term changes in peak river flows in Great Britain, Hydrological Sciences Journal, 64, 1159–1170, iSBN: 0262-6667 Publisher: Taylor & Francis, 2019.

Brouwers, J., Peeters, B., Van Steertegem, M., van Lipzig, N., Wouters, H., Beullens, J., Demuzere, M., Willems, P., De Ridder, K., and Maiheu, B.: MIRA klimaatrapport 2015: over waargenomen en toekomstige klimaatveranderingen, 2015.

Carluer, N. and De Marsily, G.: Assessment and modelling of the influence of man-made networks on the hydrology of a small watershed: implications for fast flow components, water quality and landscape management, Journal of Hydrology, 285, 76–95, https://doi.org/10.1016/j.jhydrol.2003.08.008, 2004.

Carsel, R. F. and Parrish, R. S.: Developing joint probability distributions of soil water retention characteristics, Water resources research, 24, 755–769, 1988.

Center, P. W. P.: California's Water, PPIC Water Policy Center: San Francisco, CA, USA, 2016.

Chalid, A. and Prasetya, B.: Utilization of a pond in East Jakarta for a sustainable urban drainage system model, vol. 437, Institute of Physics Publishing, https://doi.org/10.1088/1755-1315/437/1/012018, 2020.

Chapman, S. W., Parker, B. L., Cherry, J. A., Aravena, R., and Hunkeler, D.: Groundwater–surface water interaction and its role on TCE groundwater plume attenuation, Journal of Contaminant Hydrology, 91, 203–232, https://doi.org/10.1016/j.jconhyd.2006.10.006, 2007.

Chawanda, C. J., George, C., Thiery, W., Van Griensven, A., Tech, J., Arnold, J., and Srinivasan, R.: User-friendly workflows for catchment modelling: Towards reproducible SWAT+ model studies, Environmental Modelling & Software, 134, 104 812, https://doi.org/10.1016/j.envsoft.2020.104812, 2020.

Chiang, F., Mazdiyasni, O., and AghaKouchak, A.: Evidence of anthropogenic impacts on global drought frequency, duration, and intensity, Nature Communications, 12, 2754, https://doi.org/10.1038/s41467-021-22314-w, 2021.

Choi, W., Kim, S. J., Rasmussen, P. F., and Moore, A. R.: Use of the North American Regional Reanalysis for hydrological modelling in Manitoba, Canadian Water Resources Journal, 34, 17–36, iSBN: 0701-1784 Publisher: Taylor & Francis, 2009.

Christen, E. and Skehan, D.: Design and management of subsurface horizontal drainage to reduce salt loads, Journal of irrigation and drainage engineering, 127, 148–155, https://doi.org/10.1061/(ASCE)0733-9437(2001)127:3(148), 2001.

Christidis, N. and Stott, P. A.: The influence of anthropogenic climate change on wet and dry summers in Europe, Science Bulletin, 66, 813–823, iSBN: 2095-9273 Publisher: Elsevier, 2021.

Chávez, C., Fuentes, C., Brambila, F., and Morales-Durán, N.: Soil salinity control in irrigated land with agricultural drainage systems, in: Agroecology, pp. 101–121, IntechOpen, URL https://www.intechopen.com/chapters/48119, 2015.

CIW: Evaluatierapport droogte 2017, URL https://www.integraalwaterbeleid.be/nl/publicaties/documenten/evaluatierapport-droogte-2017, 2017.

CIW: Evaluatierapport waterschaarste en droogte 2018, URL https://www.integraalwaterbeleid.be/nl/nieuws/downloads-van-nieuwsberichten/evaluatierapport-waterschaarste-en-droogte-2018, 2018.

CIW: Evaluatierapport waterschaarste en droogte 2019, URL https://www.integraalwaterbeleid.be/nl/nieuws/downloads-van-nieuwsberichten/evaluatierapport-waterschaarste-en-droogte-2019, 2019.

Cohen, I., Zandalinas, S. I., Huck, C., Fritschi, F. B., and Mittler, R.: Meta-analysis of drought and heat stress combination impact on crop yield and yield components, Physiologia Plantarum, 171, 66–76, https://doi.org/10.1111/ppl.13203, 2021.

Cohen-Shacham, E., Walters, G., Janzen, C., and Maginnis, S.: Nature-based Solutions to address global societal challenges, URL https://portals.iucn.org/library/sites/library/files/documents/2016-036.pdf, 2016.

Commission, N. C.: BELGIAN NATIONAL CLIMATE CHANGE ADAPTATION STRATEGY, URL https://www.cnc-nkc.be/sites/default/files/report/file/be_nas_2010_0.pdf, 2010.

Conant Jr, B.: Delineating and quantifying ground water discharge zones using streambed temperatures, Groundwater, 42, 243–257, 2004.

Cook, B. I., Mankin, J. S., and Anchukaitis, K. J.: Climate Change and Drought : From Past to Future, Current Climate Change Reports, 4, 164–179, 2018.

Cooper, C. M.: Biological effects of agriculturally derived surface water pollutants on aquatic systems—a review, Journal of environmental quality, 22, 402–408, https://doi.org/10.2134/jeq1993.00472425002200030003x, 1993.

Coordinatiecommissie Integraal Waterbeleid: Ontwerp Stroomgebiedbeheerplannen Schelde en Maas 2022-2027 SGBP sectie: Dijle- en Zennebekken, Tech. rep., 2021.

Cornes, R. C., van der Schrier, G., van den Besselaar, E. J., and Jones, P. D.: An ensemble version of the E-OBS temperature and precipitation data sets, Journal of Geophysical Research: Atmospheres, 123, 9391–9409, iSBN: 2169-897X Publisher: Wiley Online Library, 2018.

Cortinovis, C., Olsson, P., Boke-Olén, N., and Hedlund, K.: Scaling up nature-based solutions for climate-change adaptation: Potential and benefits in three European cities, Urban Forestry and Urban Greening, 67, https://doi.org/10.1016/j.ufug.2021.127450, 2022.

Coustau, M., Rousset-Regimbeau, F., Thirel, G., Habets, F., Janet, B., Martin, E., de Saint-Aubin, C., and Soubeyroux, J.-M.: Impact of improved meteorological forcing, profile of soil hydraulic conductivity and data assimilation on an operational Hydrological Ensemble Forecast System over France, Journal of Hydrology, 525, 781–792, iSBN: 0022-1694 Publisher: Elsevier, 2015.

Coördinatiecommissie Integraal Waterbeleid: Blue Deal: De strijd tegen droogte en waterschaarste, Tech. rep., URL https://www.zuhaldemir.be/sites/parlement.n-va.be/files/generated/files/news-attachment/blue_deal_clean_0.pdf, 2020.

Critchley, A. and Di Prima, F.: Water Harvesting Technologies Revisited. Deliverable 2.1 of the FP7 Project Water Harvesting Technologies: Potentials for Innovations, Improvements and Upscaling in Sub-Saharan Africa, Tech. rep., 2012.

Cui, M., Ferreira, F., Fung, T. K., and Matos, J. S.: Tale of two cities: How nature-based solutions help create adaptive and resilient urban water management practices in singapore and lisbon, Sustainability (Switzerland), 13, 10 427, https://doi.org/10.3390/su131810427, 2021.

Dams, J., Salvadore, E., Van Daele, T., and Batelaan, O.: Case kleine nete: hydrologie: wetenschappelijk rapport-NARA 2009, 2009.

Davamani, V., John, J. E., Poornachandhra, C., Gopalakrishnan, B., Arulmani, S., Parameswari, E., Santhosh, A., Srinivasulu, A., Lal, A., and Naidu, R.: A Critical Review of Climate Change Impacts on Groundwater Resources: A Focus on the Current

Status, Future Possibilities, and Role of Simulation Models, Atmosphere, 15, 122, iSBN: 2073-4433 Publisher: MDPI, 2024.

Davidson, N. C.: How much wetland has the world lost? Long-term and recent trends in global wetland area, Marine and Freshwater Research, 65, 936–941, https://doi.org/10.1071/MF14173, 2014.

Davies, C., Chen, W. Y., Sanesi, G., and Lafortezza, R.: The European Union roadmap for implementing nature-based solutions: A review, Environmental Science and Policy, 121, 49–67, https://doi.org/10.1016/j.envsci.2021.03.018, 2021.

Dayal, K. S., Deo, R. C., and Apan, A. A.: Investigating drought duration-severity-intensity characteristics using the Standardized Precipitation-Evapotranspiration Index: case studies in drought-prone Southeast Queensland, Journal of Hydrologic Engineering, 23, 05017 029, iSBN: 1084-0699 Publisher: American Society of Civil Engineers, 2018.

de Boer, C. and Bressers, H.: Complex and dynamic implementation processes: the renaturalization of the Dutch Regge River, Journal of Thrombosis and Haemostasis, 2011.

De Niel, J. and Willems, P.: Climate or land cover variations: what is driving observed changes in river peak flows? A data-based attribution study, Hydrology and Earth System Sciences, 23, 871–882, iSBN: 1607-7938 Publisher: Copernicus Publications Göttingen, Germany, 2019.

De Ridder, K., Couderé, K., Depoorter, M., Liekens, I., Pourria, X., Steinmetz, D., Vanuytrecht, E., Verhaegen, K., and Wouters, H.: Evaluation of the Socio-Economic Impact of Climate Change in Belgium., Tech. rep., 2020.

Deb, P., Kiem, A. S., and Willgoose, G.: A linked surface water-groundwater modelling approach to more realistically simulate rainfall-runoff non-stationarity in semi-arid regions, Journal of Hydrology, 575, 273–291, https://doi.org/10.1016/j.jhydrol.2019.05.039, 2019.

Debele, S. E., Kumar, P., Sahani, J., Marti-Cardona, B., Mickovski, S. B., Leo, L. S., Porcù, F., Bertini, F., Montesi, D., Vojinovic, Z., and Di Sabatino, S.: Nature-based solutions for hydro-meteorological hazards: Revised concepts, classification schemes and databases, Environmental Research, 179, 108 799, https://doi.org/10.1016/j.envres.2019.108799, 2019.

Decleer, K., Wouters, J., Jacobs, S., Staes, J., Spanhove, T., Meire, P., and van Diggelen, R.: Mapping wetland loss and restoration potential in Flanders (Belgium): An ecosystem service perspective, Ecology and Society, 21, 46, https://doi.org/10.5751/ES-08964-210446, 2016.

Devito, K. J., Hill, A. R., and Roulet, N.: Groundwater-surface water interactions in headwater forested wetlands of the Canadian Shield, Journal of Hydrology, 181, 127–147, 1996.

Didovets, I., Krysanova, V., Nurbatsina, A., Fallah, B., Krylova, V., Saparova, A., Niyazov, J., Kalashnikova, O., and Hattermann, F. F.: Attribution of current trends in streamflow to climate change for 12 Central Asian catchments, Climatic Change, 177, 16, iSBN: 0165-0009 Publisher: Springer, 2024.

Dierickx, W. and Feyen, J.: Drainage development in Belgium, in: Proceedings, Symposium 25th International Course on Land Drainage, p. 141, URL https://edepot.wur.nl/214970, 1987.

Dile, Y., Srinivasan, R., and George, C.: QGIS Interface for SWAT+: QSWAT+ Step by Step Setup for the Robit Watershed, Lake Tana basin Ethiopia, Version, 2, 1–137, 2022.

Dillon, P., Pavelic, P., Page, D., Beringen, H., and Ward, J.: Managed aquifer recharge: An Introduction, Tech. rep., https://doi.org/10.1007/BF01929660, 2009.

Ding, Y., Gong, X., Xing, Z., Cai, H., Zhou, Z., Zhang, D., Sun, P., and Shi, H.: Attribution of meteorological, hydrological and agricultural drought propagation in different climatic regions of China, Agricultural Water Management, 255, 106 996, https://doi.org/10.1016/j.agwat.2021.106996, 2021.

Doherty, J.: PEST user manual part I and II, Watermark Numerical Computing, Brisbane, Australia, 2016.

Dorst, H., van der Jagt, A., Raven, R., and Runhaar, H.: Urban greening through nature-based solutions – Key characteristics of an emerging concept, Sustainable Cities and Society, 49, 8, https://doi.org/10.1016/j.scs.2019.101620, 2019.

Dragoni, W. and Sukhija, B. S.: Climate change and groundwater: a short review, vol. 288, The Geological Society of London London, issue: 1, 2008.

Drought 1976: The drought of 1976, URL https://isgeschiedenis.nl/nieuws/de-droogte-van-1976, n.d.

Du, B., Arnold, J. G., Saleh, A., and Jaynes, D. B.: Development and application of SWAT to landscapes with tiles and potholes, Transactions of the ASAE, 48, 1121–1133, https://doi.org/10.13031/2013.18522, 2005.

Eggermont, H., Balian, E., Azevedo, José Manuel N Beumer, V., Brodin, T., Claudet, J., Fady, B., Grube, M., Keune, H., Lamarque, P., Reuter, K., Smith, M., Van Ham, C., Weisser, W. W., and Le Roux, X.: Nature-based Solutions: New Influence for Environmental Management and Research in Europe Nature-based Solutions, an Emerging Term, Gaia, 24, 243–248, 2015.

Ejaz, F., Wöhling, T., Höge, M., and Nowak, W.: Lumped geohydrological modelling for long-term predictions of groundwater storage and depletion, Journal of Hydrology, 606, 127 347, https://doi.org/10.1016/j.jhydrol.2021.127347, 2022.

Endter-wada, J., Kettenring, K. M., and Sutton-grier, A.: Protecting wetlands for people: Strategic policy action can help wetlands mitigate risks and enhance resilience, Environmental Science and Policy, 108, 37–44, https://doi.org/10.1016/j.envsci.2020.01.016, 2020.

Epelde, A. M., Cerro, I., Sánchez-Pérez, J. M., Sauvage, S., Srinivasan, R., and Antigüedad, I.: Application of the SWAT model to assess the impact of changes in agricultural management practices on water quality, Hydrological Sciences Journal, 60, 825–843, iSBN: 0262-6667 Publisher: Taylor & Francis, 2015.

Ernst, L. F.: Grondwaterstromingen in de verzadigde zone en hun berekening bij aanwezigheid van horinzontale evenwijdige open leidingen, Tech. rep., Centrum voor Landbouwpublikaties en Landbouwdocumentatie, URL https://library.wur.nl/WebQuery/wurpubs/fulltext/188156, 1962.

Essou, G. R., Sabarly, F., Lucas-Picher, P., Brissette, F., and Poulin, A.: Can precipitation and temperature from meteorological reanalyses be used for hydrological modeling?, Journal of Hydrometeorology, 17, 1929–1950, iSBN: 1525-755X, 2016.

Europea, C.: Addressing the challenge of water scarcity and droughts in the European Union, Communication from the Commission to the European Parliament and the Council, COM (2007), 414, 2007.

European Comission: Horizon Europe, URL https://research-and-innovation.ec.europa.eu/funding/funding-opportunities/funding-programmes-and-open-calls/horizon-europe_en, n.d.

European Commission: Towards an EU research and innovation policy agenda for nature-based solutions & re-naturing cities. Final report of the Horizon 2020 expert group on 'Nature-based solutions and re-naturing cities', Tech. rep., 2015.

Ewen, J., Parkin, G., and O'Connell, P. E.: SHETRAN: distributed river basin flow and transport modeling system, Journal of hydrologic engineering, 5, 250–258, https://doi.org/10.1061/(ASCE)1084-0699(2000)5:3(250), 2000.

Faivre, N., Fritz, M., Freitas, T., de Boissezon, B., and Vandewoestijne, S.: Nature-Based Solutions in the EU: Innovating with nature to address social , economic and environmental challenges , Environmental Research, 159, 509–518, https://doi.org/10.1016/j.envres.2017.08.032, 2017.

Fallahi, M. M., Shabanlou, S., Rajabi, A., Yosefvand, F., and IzadBakhsh, M. A.: Effects of climate change on groundwater level variations affected by uncertainty (case study: Razan aquifer), Applied Water Science, 13, 143, iSBN: 2190-5487 Publisher: Springer, 2023.

Fan, Y., Li, H., and Miguez-Macho, G.: Global patterns of groundwater table depth, Science, 339, 940–943, https://doi.org/10.1126/science.1229881, 2013.

Fausey, N. R., Brown, L. C., Belcher, H. W., and Kanwar, R. S.: Drainage and water quality in Great Lakes and cornbelt states, Journal of Irrigation and Drainage Engineering, 121, 283–288, https://doi.org/10.1061/(ASCE)0733-9437(1995)121:4(283), 1995.

Ferreira, V., Barreira, A., Pinto, P., and Panagopoulos, T.: Understanding attitudes towards the adoption of nature-based solutions and policy priorities shaped by stakeholders' awareness of climate change, Environmental Science and Policy, 131, 149–159, https://doi.org/10.1016/j.envsci.2022.02.007, 2022.

Fleckenstein, J. H., Krause, S., Hannah, D. M., and Boano, F.: Groundwater-surface water interactions: New methods and models to improve understanding of processes and dynamics, Advances in Water Resources, 33, 1291–1295, https://doi.org/10.1016/j.advwatres.2010.09.011, 2010.

Foster, S. S. D., Morris, B. L., and Lawrence, A. R.: Effects of urbanization on groundwater recharge, in: Groundwater problems in urban areas: Proceedings of the International Conference organized by the Institution of Civil Engineers and held in London, 2–3 June 1993, pp. 43–63, Thomas Telford Publishing, https://doi.org/10.1680/gpiua.19744.0005, 1994.

Frame, D. J., Rosier, S. M., Noy, I., Harrington, L. J., Carey-Smith, T., Sparrow, S. N., Stone, D. A., and Dean, S. M.: Climate change attribution and the economic costs of extreme weather events: a study on damages from extreme rainfall and drought, Climatic Change, 162, 781–797, https://doi.org/10.1007/s10584-020-02729-y, 2020.

Franken, T. and Wolfs, V.: Effecten van klimaatverandering op de freatische grondwaterstanden synthese rapport, Tech. rep., URL https://edepot.wur.nl/99130, 2022.

Frantzeskaki, N.: Seven lessons for planning nature-based solutions in cities, Environmental Science and Policy, 93, 101–111, https://doi.org/10.1016/j.envsci.2018.12.033, 2019.

Frantzeskaki, N., Vandergert, P., Connop, S., Schipper, K., Zwierzchowska, I., Collier, M., and Lodder, M.: Examining the policy needs for implementing nature-based solutions in cities: Findings from city-wide transdisciplinary experiences in Glasgow (UK), Genk (Belgium) and Poznan (Poland), Land Use Policy, pp. 1–22, 2020.

Frederiksen, R. R. and Molina-Navarro, E.: The importance of subsurface drainage on model performance and water balance in an agricultural catchment using SWAT and SWAT-MODFLOW, Agricultural Water Management, 255, 107 058, https://doi.org/10.1016/j.agwat.2021.107058, 2021.

Freeze, R. A.: A stochastic-conceptual analysis of one-dimensional groundwater flow in nonuniform homogeneous media, Water resources research, 11, 725–741, iSBN: 0043-1397 Publisher: Wiley Online Library, 1975.

Fryar, A. E., Wallin, E. J., and Brown, D. L.: Spatial and temporal variability in seepage between a contaminated aquifer and tributaries to the Ohio River, Groundwater Monitoring & Remediation, 20, 129–146, 2000.

Fröhle, P., Manojlovic, N., Tadesse, Y., Gruhn, A., Dittrich, H., and Ebel, C.: Managing Droughts in Northern Germany—The Reconect NBS Approach and Water Resources Model for Vier- Und Marschlande Area, Hamburg, Germany, in: Springer Water, pp. 529–549, Springer Nature, https://doi.org/10.1007/978-981-19-1600-7_34, 2022.

Fu, G., Crosbie, R. S., Barron, O., Charles, S. P., Dawes, W., Shi, X., Van Niel, T., and Li, C.: Attributing variations of temporal and spatial groundwater recharge: A statistical analysis of climatic and non-climatic factors, Journal of hydrology, 568, 816–834, iSBN: 0022-1694 Publisher: Elsevier, 2019.

Funk, C., Peterson, P., Landsfeld, M., Pedreros, D., Verdin, J., Shukla, S., Husak, G., Rowland, J., Harrison, L., and Hoell, A.: The climate hazards infrared precipitation with stations—a new environmental record for monitoring extremes, Scientific data, 2, 1–21, iSBN: 2052-4463 Publisher: Nature Publishing Group, 2015.

Galbiati, L., Bouraoui, F., Elorza, F. J., and Bidoglio, G.: Modeling diffuse pollution loading into a Mediterranean lagoon: development and application of an integrated surface–subsurface model tool, Ecological Modelling, 193, 4–18, https://doi.org/10.1016/j.ecolmodel.2005.07.036, 2006.

Gao, Q., Zribi, M., Escorihuela, M. J., and Baghdadi, N.: Synergetic use of Sentinel-1 and Sentinel-2 data for soil moisture mapping at 100 m resolution, Sensors, 17, 1966, https://doi.org/10.3390/s17091966, 2017.

Gassman, P. W., Reyes, M. R., Green, C. H., and Arnold, J. G.: The soil and water assessment tool: historical development, applications, and future research directions, Transactions of the ASABE, 50, 1211–1250, https://doi.org/10.13031/2013.23637, 2007.

Gathagu, J. N., Sang, J. K., and Maina, C. W.: Modelling the impacts of structural conservation measures on sediment and water yield in Thika-Chania catchment, Kenya, International Soil and Water Conservation Research, 6, 165–174, https://doi.org/10.1016/j.iswcr.2017.12.007, 2018.

Gelfan, A., Kalugin, A., and Krylenko, I.: Detection, attribution, and specifying mechanisms of hydrological changes in geographically different river basins, Climatic Change, 176, 122, iSBN: 0165-0009 Publisher: Springer, 2023.

Goolsby, D. A. and Battaglin, W. A.: Long-term changes in concentrations and flux of nitrogen in the Mississippi River Basin, USA, Hydrological Processes, 15, 1209–1226, https://doi.org/10.1002/hyp.210, 2001.

Gorissen, L., Spira, F., Meynaerts, E., Valkering, P., and Frantzeskaki, N.: Moving towards systemic change? Investigating acceleration dynamics of urban sustainability transitions in the Belgian City of Genk, Journal of Cleaner Production, 173, 171–185, https://doi.org/10.1016/j.jclepro.2016.12.052, 2018.

Gour, L., Maurya, S., Koutu, G. K., Singh, S. K., Shukla, S., and Mishra, D.: Characterization of rice (Oryza sativa L.) genotypes using principal component analysis including scree plot rotated component matrix, International Journal of Chemical Studies, 5, 975–983, 2017.

Gramlich, A., Stoll, S., Stamm, C., Walter, T., and Prasuhn, V.: Effects of artificial land drainage on hydrology, nutrient and pesticide fluxes from agricultural fields–A review, Agriculture, ecosystems & environment, 266, 84–99, 2018.

Green, C. H., Tomer, M. D., Di Luzio, M., and Arnold, J. G.: Hydrologic evaluation of the soil and water assessment tool for a large tile-drained watershed in Iowa, Transactions of the ASABE, 49, 413–422, https://doi.org/10.13031/2013.20415, 2006.

Greve, P., Gudmundsson, L., and Seneviratne, S. I.: Regional scaling of annual mean precipitation and water availability with global temperature change, Earth System Dynamics, 9, 227–240, iSBN: 2190-4987 Publisher: Copernicus Publications Göttingen, Germany, 2018.

Gudmundsson, L. and Seneviratne, S. I.: Anthropogenic climate change affects meteorological drought risk in Europe, Environmental Research Letters, 11, 044 005, iSBN: 1748-9326 Publisher: IOP Publishing, 2016.

Guevara Ochoa, C., Medina Sierra, A., Vives, L., Zimmermann, E., and Bailey, R.: Spatio-temporal patterns of the interaction between groundwater and surface water in plains, Hydrological Processes, 34, 1371–1392, https://doi.org/10.1002/hyp.13615, 2020.

Guo, T., Gitau, M., Merwade, V., Arnold, J., Srinivasan, R., Hirschi, M., and Engel, B.: Comparison of performance of tile drainage routines in SWAT 2009 and 2012 in an extensively tile-drained watershed in the Midwest, Hydrology and Earth System Sciences, 22, 89–110, https://doi.org/10.5194/hess-22-89-2018, 2018.

Gupta, H. V., Sorooshian, S., Hogue, T. S., and Boyle, D. P.: Advances in automatic calibration of watershed models, Calibration of watershed models, 6, 9–28, https://doi.org/10.1029/WS006, 2003.

Guzman, J. A., Moriasi, D. N., Gowda, P. H., Steiner, J. L., Starks, P. J., Arnold, J. G., and Srinivasan, R.: A model integration framework for linking SWAT and MODFLOW, Environmental Modelling & Software, 73, 103–116, https://doi.org/10.1016/j.envsoft.2015.08.011, 2015.

Gärdenäs, A. I., Šimůnek, J., Jarvis, N., and van Genuchten, M. T.: Two-dimensional modelling of preferential water flow and pesticide transport from a tile-drained field, Journal of Hydrology, 329, 647–660, https://doi.org/10.1016/j.jhydrol.2006.03.021, 2006.

Gómez Martín, E., Máñez Costa, M., Egerer, S., and Schneider, U. A.: Assessing the long-term effectiveness of Nature-Based Solutions under different climate change scenarios,

Science of the Total Environment, 794, 148 515, https://doi.org/10.1016/j.scitotenv.2021.148515, 2021.

Gökkaya, K., Budhathoki, M., Christopher, S. F., Hanrahan, B. R., and Tank, J. L.: Subsurface tile drained area detection using GIS and remote sensing in an agricultural watershed, Ecological Engineering, 108, 370–379, https://doi.org/10.1016/j.ecoleng.2017.06.048, 2017.

Gülbaz, S. and Kazezyilmaz-Alhan, C.: An evaluation of hydrologic modeling performance of EPA SWMM for bioretention, Water Science and Technology, 76, 3035–3043, https://doi.org/10.2166/wst.2017.464, 2017.

Habets, F., Boone, A., Champeaux, J.-L., Etchevers, P., Franchisteguy, L., Leblois, E., Ledoux, E., Le Moigne, P., Martin, E., and Morel, S.: The SAFRAN-ISBA-MODCOU hydrometeorological model applied over France, Journal of Geophysical Research: Atmospheres, 113, iSBN: 0148-0227 Publisher: Wiley Online Library, 2008.

Hani, H. M., Nour El Din, M. M., Khalifa, A., and Elalfy, E.: Development of suitability map for managed aquifer recharge: Case study, West Delta, Egypt, Aqua Water Infrastructure, Ecosystems and Society, 72, 868–884, https://doi.org/10.2166/aqua.2023.177, 2023.

Hankins, K., Welker, A., and Mandarano, L.: An integrated monitoring plan for biolnfiltration BMPs, pp. 1097–1104, https://doi.org/10.1061/40971(310)137, 2008.

Hansen, A. L., Refsgaard, J. C., Christensen, B. S. B., and Jensen, K. H.: Importance of including small-scale tile drain discharge in the calibration of a coupled groundwater-surface water catchment model, Water Resources Research, 49, 585–603, https://doi.org/10.1029/2011WR011783, 2013.

Hao, Z., AghaKouchak, A., Nakhjiri, N., and Farahmand, A.: Global integrated drought monitoring and prediction system, Scientific data, 1, 1–10, iSBN: 2052-4463 Publisher: Nature Publishing Group, 2014.

Harbaugh, A. W.: MODFLOW-2005, the US Geological Survey modular ground-water model: the ground-water flow process, vol. 6, US Department of the Interior, US Geological Survey Reston, VA, USA, URL https://wwwbrr.cr.usgs.gov/hill_tiedeman_book/documentation/MODFLOW-MODPATH-ModelViewer/MF2005-tma6a16.pdf, 2005.

Harris, I., Osborn, T. J., Jones, P., and Lister, D.: Version 4 of the CRU TS monthly high-resolution gridded multivariate climate dataset, Scientific data, 7, 1–18, iSBN: 2052-4463 Publisher: Nature Publishing Group, 2020.

Harvey, J. W. and Bencala, K. E.: The effect of streambed topography on surface-subsurface water exchange in mountain catchments, Water resources research, 29, 89–98, 1993.

Hasselquist, E. M., Lidberg, W., Sponseller, R. A., Ågren, A., and Laudon, H.: Identifying and assessing the potential hydrological function of past artificial forest drainage, Ambio, 47, 546–556, https://doi.org/10.1007/s13280-017-0984-9, 2018.

Hayashi, M. and Rosenberry, D. O.: 6. Effects of groundwater exchange on the hydrology and ecology of surface waters, Journal of groundwater hydrology, 43, 327–341, 2001.

Hein, T., Schwarz, U., Habersack, H., Nichersu, I., Preiner, S., Willby, N., and Weigelhofer, G.: Current status and restoration options for floodplains along the Danube River, Science of the Total Environment, 543, 778–790, https://doi.org/10.1016/j.scitotenv.2015.09.073, 2016.

Heudorfer, B. and Stahl, K.: Comparison of different threshold level methods for drought propagation analysis in Germany, Hydrology Research, 48, 1311–1326, iSBN: 0029-1277 Publisher: IWA Publishing, 2017.

Hidalgo, H. G., Das, T., Dettinger, M. D., Cayan, D. R., Pierce, D. W., Barnett, T. P., Bala, G., Mirin, A., Wood, A. W., and Bonfils, C.: Detection and attribution of streamflow timing changes to climate change in the western United States, Journal of Climate, 22, 3838–3855, iSBN: 0894-8755 Publisher: American Meteorological Society, 2009.

Hisdal, H., Tallaksen, L. M., Gauster, T., Bloomfield, J. P., Parry, S., Prudhomme, C., and Wanders, N.: Hydrological drought characteristics, in: Hydrological drought, pp. 157–231, Elsevier, 2024.

Holden, P. B., Rebelo, A. J., Wolski, P., Odoulami, R. C., Lawal, K. A., Kimutai, J., Nkemelang, T., and New, M. G.: Nature-based solutions in mountain catchments reduce impact of anthropogenic climate change on drought streamflow, Communications Earth and Environment, 3, 51, https://doi.org/10.1038/s43247-022-00379-9, 2022.

Holder, A. J., Rowe, R., McNamara, N. P., Donnison, I. S., and McCalmont, J. P.: Soil & Water Assessment Tool (SWAT) simulated hydrological impacts of land use change from temperate grassland to energy crops: A case study in western UK, GCB Bioenergy, 11, 1298–1317, iSBN: 1757-1693 Publisher: Wiley Online Library, 2019.

Hooghoudt, S. B.: General consideration of the problem of field drainage by parallel drains, ditches, watercourses, and channels, Contribution to the knowledge of some physical parameters of the soil, 7, 1940.

Hoyt, J. C.: Drought of 1936, with Discussion on the Significance of Drought in Relation to Climate, Tech. rep., Government Printing Office,, 1938.

Huang, S., Kumar, R., Flörke, M., Yang, T., Hundecha, Y., Kraft, P., Gao, C., Gelfan, A., Liersch, S., and Lobanova, A.: Evaluation of an ensemble of regional hydrological models in 12 large-scale river basins worldwide, Climatic Change, 141, 381–397, 2017.

Hui, J., Wu, Y., Zhao, F., Lei, X., Sun, P., Singh, S. K., Liao, W., Qiu, L., and Li, J.: Parameter optimization for uncertainty reduction and simulation improvement of hydrological modeling, Remote Sensing, 12, 4069, https://doi.org/10.3390/rs12244069, 2020.

Huscroft, J., Gleeson, T., Hartmann, J., and Börker, J.: Compiling and mapping global permeability of the unconsolidated and consolidated Earth: GLobal HYdrogeology MaPS 2.0 (GLHYMPS 2.0), Geophysical Research Letters, 45, 1897–1904, https://doi.org/10.1002/2017GL075860, 2018.

Hussain, M., Farooq, M., Muscolo, A., and Rehman, A.: Crop diversification and saline water irrigation as potential strategies to save freshwater resources and reclamation of marginal soils—a review, Environmental Science and Pollution Research, 27, 28 695–28 729, https://doi.org/10.1007/s11356-020-09111-6, 2020.

Ibrahim, B., Wisser, D., Barry, B., Fowe, T., and Aduna, A.: Hydrological predictions for small ungauged watersheds in the Sudanian zone of the Volta basin in West Africa, Journal of Hydrology: Regional Studies, 4, 386–397, iSBN: 2214-5818 Publisher: Elsevier, 2015.

Ikenberry, C. D., Soupir, M. L., Helmers, M. J., Crumpton, W. G., Arnold, J. G., and Gassman, P. W.: Simulation of daily flow pathways, tile-drain nitrate concentrations, and soil-nitrogen dynamics using SWAT, JAWRA Journal of the American Water Resources Association, 53, 1251–1266, https://doi.org/10.1111/1752-1688.12569, 2017.

INBO: Effecten van klimaatverandering op bos en natuur in Vlaanderen, URL https://www.vlaanderen.be/publicaties/effecten-van-klimaatverandering-op-bos-en-natuur-in-vlaanderen, publication Title: www.vlaanderen.be, n.d.

Iqbal, J., Su, C., Rashid, A., Yang, N., Baloch, M. Y. J., Talpur, S. A., Ullah, Z., Rahman, G., Rahman, N. U., Earjh, and Sajjad, M. M.: Hydrogeochemical assessment of groundwater and suitability analysis for domestic and agricultural utility in southern Punjab, Pakistan, Water (Switzerland), 13, 3589, https://doi.org/10.3390/w13243589, 2021.

Irfanullah, H. M.: Nature-based solutions should be an integral part of locally-led adaptation, Climate Tribune, 2021.

Jacob, D., Petersen, J., Eggert, B., Alias, A., Christensen, O. B., Bouwer, L. M., Braun, A., Colette, A., Déqué, M., and Georgievski, G.: EURO-CORDEX: new high-resolution climate change projections for European impact research, Regional environmental change, 14, 563–578, iSBN: 1436-3798 Publisher: Springer, 2014.

Jakubínský, J., Pechanec, V., Cudlín, O., Purkyt, J., and Cudlín, P.: Identification of Surface Runoff Source Areas as a Tool for Projections of NBS in Water Management, in: Handbook of Environmental Chemistry, vol. 107, pp. 313–338, Springer Science and Business Media Deutschland GmbH, https://doi.org/10.1007/698_2021_775, 2022.

Jokar, D., Khakzand, M., and Faizi, M.: The application of low impact development approaches toward achieving circularity in the water sector: A case study from Soltan Abad, shiraz, Iran, Journal of Cleaner Production, 320, https://doi.org/10.1016/j.jclepro.2021.128712, 2021.

Jolly, I. D., McEwan, K. L., and Holland, K. L.: A review of groundwater–surface water interactions in arid/semi-arid wetlands and the consequences of salinity for wetland ecology, Ecohydrology: Ecosystems, Land and Water Process Interactions, Ecohydrogeomorphology, 1, 43–58, 2008.

Jones, R. W., Renfrew, I. A., Orr, A., Webber, B. G. M., Holland, D. M., and Lazzara, M. A.: Evaluation of four global reanalysis products using in situ observations in the Amundsen Sea Embayment, Antarctica, Journal of Geophysical Research: Atmospheres, 121, 6240–6257, iSBN: 2169-897X Publisher: Wiley Online Library, 2016.

Jordan, S., Quinn, J., Zaniolo, M., Giuliani, M., and Castelletti, A.: Advancing reservoir operations modelling in SWAT to reduce socio-ecological tradeoffs, Environmental Modelling & Software, 157, 105 527, iSBN: 1364-8152 Publisher: Elsevier, 2022.

Jódar, J., Martos-Rosillo, S., Custodio, E., Mateos, L., Cabello, J., Casas, J., Salinas-Bonillo, M., Martín-Civantos, J., González-Ramón, A., Zakaluk, T., Herrera-Lameli, C., Urrutia, J., and Lambán, L.: The Recharge Channels of the Sierra Nevada Range (Spain) and the Peruvian Andes as Ancient Nature-Based Solutions for the Ecological Transition, Water (Switzerland), 14, https://doi.org/10.3390/w14193130, 2022.

Kabisch, N., Korn, H., Stadler, J., and Bonn, A.: Nature-based Solutions to Climate Change Adaptation in Urban Areas—Linkages Between Science, Policy and Practice, https://doi.org/10.1007/978-3-319-56091-5_8, 2017.

Kalantari, Z., Ferreira, C. S. S., Keesstra, S., and Destouni, G.: Nature-based solutions for flood-drought risk mitigation in vulnerable urbanizing parts of East-Africa, Current Opinion in Environmental Science & Health, 5, 73–78, https://doi.org/10.1016/j.coesh.2018.06.003, 2018.

Kalbus, E., Reinstorf, F., and Schirmer, M.: Measuring methods for groundwater–surface water interactions: a review, Hydrology and Earth System Sciences, 10, 873–887, https://doi.org/10.5194/hess-10-873-2006, 2006.

Kalita, P. K., Cooke, R. A., Anderson, S. M., Hirschi, M. C., and Mitchell, J. K.: Subsurface drainage and water quality: The Illinois experience, Transactions of the ASABE, 50, 1651–1656, https://doi.org/10.13031/2013.23963, 2007.

Karjalainen, M., Kaartinen, H., and Hyyppä, J.: Agricultural monitoring using Envisat alternating polarization SAR images, Photogrammetric Engineering & Remote Sensing, 74, 117–126, https://doi.org/10.14358/PERS.74.1.117, 2008.

Karásek, P. and Nováková, E.: Agricultural tile drainage detection within the year using ground penetrating radar, Journal of Ecological Engineering, 21, https://doi.org/10.12911/22998993/119976, 2020.

Keery, J., Binley, A., Crook, N., and Smith, J. W.: Temporal and spatial variability of groundwater–surface water fluxes: Development and application of an analytical method using temperature time series, Journal of Hydrology, 336, 1–16, 2007.

Keesstra, S., Nunes, J., Novara, A., Finger, D., Avelar, D., Kalantari, Z., and Cerdà, A.: The superior effect of nature based solutions in land management for enhancing ecosystem services, Science of the Total Environment, 610, 997–1009, https://doi.org/10.1016/j.scitotenv.2017.08.077, 2018.

Kendall, M. G.: Rank correlation methods., publisher: Griffin, 1948.

Kidmose, J., Refsgaard, J. C., Troldborg, L., Seaby, L. P., and Escrivà, M. M.: Climate change impact on groundwater levels: ensemble modelling of extreme values, Hydrology and Earth System Sciences, 17, 1619–1634, iSBN: 1607-7938 Publisher: Copernicus Publications Göttingen, Germany, 2013.

Kiesel, J., Fohrer, N., Schmalz, B., and White, M. J.: Incorporating landscape depressions and tile drainages of a northern German lowland catchment into a semi-distributed model, Hydrological Processes: An International Journal, 24, 1472–1486, https://doi.org/10.1002/hyp.7607, 2010.

Kim, N. W., Chung, I. M., Won, Y. S., and Arnold, J. G.: Development and application of the integrated SWAT–MODFLOW model, Journal of hydrology, 356, 1–16, https://doi.org/10.1016/j.jhydrol.2008.02.024, 2008.

Kirkham, D.: Problems and trends in drainage research, mixed boundary conditions, Soil Science, 113, 285–293, 1972.

KMI: De droogte van 2016-2017, URL https://www.meteo.be/nl/info/nieuwsbrief/artikels-2017/de-droogte-van-2016-2017-het-archief, 2017.

Koch, S., Bauwe, A., and Lennartz, B.: Application of the SWAT model for a tile-drained lowland catchment in North-Eastern Germany on subbasin scale, Water Resources Management, 27, 791–805, https://doi.org/10.1007/s11269-012-0215-x, 2013.

Koganti, T., Van De Vijver, E., Allred, B. J., Greve, M. H., Ringgaard, J., and Iversen, B. V.: Mapping of agricultural subsurface drainage systems using a frequency-domain ground penetrating radar and evaluating its performance using a single-frequency multi-receiver electromagnetic induction instrument, Sensors, 20, 3922, 2020.

Koiv-Vainik, M., Kill, K., Espenberg, M., Uuemaa, E., Teemusk, A., Maddison, M., Palta, M. M., Török, L., Mander, , and Scholz, M.: Urban stormwater retention capacity of nature-based solutions at different climatic conditions, Nature-Based Solutions, p. 100038, https://doi.org/10.1016/j.nbsj.2022.100038, 2022.

Kooijman, E. D., McQuaid, S., Rhodes, M. L., Collier, M. J., and Pilla, F.: Innovating with nature: From nature-based solutions to nature-based enterprises, Sustainability (Switzerland), 13, 1263, https://doi.org/10.3390/su13031263, 2021.

Koster, R. D. and Suarez, M. J.: Soil moisture memory in climate models, Journal of hydrometeorology, 2, 558–570, iSBN: 1525-7541, 2001.

Krishnamurti, T. N., Bedi, H. S., and Subramaniam, M.: The summer monsoon of 1987, Journal of Climate, 2, 321–340, iSBN: 1520-0442, 1989.

Kumar, P., Debele, S. E., Sahani, J., Aragão, L., Barisani, F., Basu, B., Bucchignani, E., Charizopoulos, N., Di Sabatino, S., Domeneghetti, A., Edo, A. S., Finér, L., Gallotti, G., Juch, S., Leo, L. S., Loupis, M., Mickovski, S. B., Panga, D., Pavlova, I., Pilla, F., Prats, A. L., Renaud, F. G., Rutzinger, M., Basu, A. S., Shah, M. A. R., Soini, K., Stefanopoulou, M., Toth, E., Ukonmaanaho, L., Vranic, S., and Zieher, T.: Towards an operationalisation of nature-based solutions for natural hazards, Science of the Total Environment, 731, 138 855, https://doi.org/10.1016/j.scitotenv.2020.138855, 2020.

Köhler, M. and Kaiser, D.: Green roof enhancement on buildings of the university of applied sciences in neubrandenburg (Germany) in times of climate change, Atmosphere, 12, https://doi.org/10.3390/atmos12030382, 2021.

Lamontagne, S., Leaney, F. W., and Herczeg, A. L.: Groundwater–surface water interactions in a large semi-arid floodplain: implications for salinity management, Hydrological Processes: An International Journal, 19, 3063–3080, 2005.

Lane, T. P., King, A. D., Perkins-Kirkpatrick, S. E., Pitman, A. J., Alexander, L. V., Arblaster, J. M., Bindoff, N. L., Bishop, C. H., Black, M. T., and Bradstock, R. A.: Attribution of extreme events to climate change in the Australian region–A review, Weather and Climate Extremes, 42, 100 622, iSBN: 2212-0947 Publisher: Elsevier, 2023.

Larocque, M. and Broda, S.: Groundwater–surface water interactions in Canada, vol. 41, Taylor & Francis, URL https://www.tandfonline.com/doi/full/10.1080/07011784.2016.1176537, 2016.

Lassiter, A.: Identifying causal changes in landscape greenness with very high-resolution airborne multispectral imagery and a panel data model, Urban Forestry and Urban Greening, 67, https://doi.org/10.1016/j.ufug.2021.127380, 2022.

Leta, O. T. and Bauwens, W.: Assessment of the Impact of Climate Change on Daily Extreme Peak and Low Flows of Zenne Basin in Belgium, Hydrology, 5, 38, https://doi.org/10.3390/hydrology5030038, 2018.

Levy, J. and Xu, Y.: Groundwater management and groundwater/surface-water interaction in the context of South African water policy, URL http://hdl.handle.net/10566/825, 2011.

Liu, B., Tang, C.-S., Pan, X.-H., Zhu, C., Cheng, Y.-J., Xu, J.-J., and Shi, B.: Potential Drought Mitigation Through Microbial Induced Calcite Precipitation-MICP, Water Resources Research, 57, https://doi.org/10.1029/2020WR029434, 2021.

Liu, H., Jia, Y., and Niu, C.: " Sponge city " concept helps solve China 's urban water problems, Environmental Earth Sciences, 76, 473, https://doi.org/10.1007/s12665-017-6652-3, 2017.

Lloyd, E. A. and Shepherd, T. G.: Environmental catastrophes, climate change, and attribution, Annals of the New York Academy of Sciences, 1469, 105–124, iSBN: 0077-8923 Publisher: Wiley Online Library, 2020.

Loheide II, S. P. and Gorelick, S. M.: A local-scale, high-resolution evapotranspiration mapping algorithm (ETMA) with hydroecological applications at riparian meadow restoration sites, Remote Sensing of Environment, 98, 182–200, 2005.

Ludwig, J. A., Wilcox, B. P., Breshears, D. D., Tongway, D. J., and Imeson, A. C.: Vegetation patches and runoff–erosion as interacting ecohydrological processes in semiarid landscapes, Ecology, 86, 288–297, 2005.

Luo, Y. and Sophocleous, M.: Two-way coupling of unsaturated-saturated flow by integrating the SWAT and MODFLOW models with application in an irrigation district in arid region of West China, Journal of Arid Land, 3, 164–173, 2011.

Mabon, L., Barkved, L., de Bruin, K., and Shih, W.-Y.: Whose knowledge counts in nature-based solutions? Understanding epistemic justice for nature-based solutions through a multi-city comparison across Europe and Asia, Environmental Science & Policy, 136, 652–664, https://doi.org/10.1016/j.envsci.2022.07.025, 2022.

Mackinnon, K., Sobrevila, C., and Hickey, V.: Biodiversity, climate change, and adaptation: nature-based solutions from the World Bank portfolio, 2008.

Maes, D., Vanreusel, W., Herremans, M., Vantieghem, P., Brosens, D., Gielen, K., Beck, O., Van Dyck, H., Desmet, P., and Vlinderwerkgroep Natuurpunt: A database on the distribution of butterflies (Lepidoptera) in northern Belgium (Flanders and the Brussels Capital Region), ZooKeys, 585, 143–156, https://doi.org/10.3897/zookeys.585.8019, 2016.

Mallik, S., Mishra, U., and Paul, N.: Groundwater suitability analysis for drinking using GIS based fuzzy logic, Ecological Indicators, 121, 107 179, https://doi.org/10.1016/j.ecolind.2020.107179, 2021.

Mann, H. B.: Nonparametric tests against trend, Econometrica: Journal of the econometric society, pp. 245–259, 1945.

Martina, M. L. V., Todini, E., and Liu, Z.: Preserving the dominant physical processes in a lumped hydrological model, Journal of Hydrology, 399, 121–131, iSBN: 0022-1694 Publisher: Elsevier, 2011.

Maré, H. G., Rademeyer, J. I., and Sami, K.: Application on Groundwater/Surface water Interaction Modeling in the Schoonspruit Catchment, URL https://www.miya-water.com/fotos/artigos/02_application_on_groundwater_surface_water_interaction_modeling_in_the_schoonspruit_catchment_19810471915a326afa23030_9880970755f1842df3c636.pdf, 2007.

Maskey, S. and Trambauer, P.: Hydrological modeling for drought assessment, in: Hydro-Meteorological Hazards, Risks and Disasters, pp. 263–282, Elsevier, 2015.

McCauley, L., Bradford, J., Robles, M., Shriver, R., Woolley, T., and Andrews, C.: Landscape-scale forest restoration decreases vulnerability to drought mortality under climate change in southwest USA ponderosa forest, Forest Ecology and Management, 509, https://doi.org/10.1016/j.foreco.2022.120088, 2022.

Mehan, S., Aggarwal, R., Gitau, M. W., Flanagan, D. C., Wallace, C. W., and Frankenberger, J. R.: Assessment of hydrology and nutrient losses in a changing climate in a subsurface-drained watershed, Science of the Total Environment, 688, 1236–1251, https://doi.org/10.1016/j.scitotenv.2019.06.314, 2019.

Meilinger, V. and Monstadt, J.: The material politics of integrated urban stormwater management in Los Angeles, California, Local Environment, 27, 847–862, https://doi.org/10.1080/13549839.2022.2078292, 2022.

Memarian, H., Balasundram, S. K., Abbaspour, K. C., Talib, J. B., Boon Sung, C. T., and Sood, A. M.: SWAT-based hydrological modelling of tropical land-use scenarios, Hydrological sciences journal, 59, 1808–1829, iSBN: 0262-6667 Publisher: Taylor & Francis, 2014.

Mendonça, R., Roebeling, P., Fidélis, T., and Saraiva, M.: Policy instruments to encourage the adoption of nature-based solutions in urban landscapes, Resources, 10, 81, https://doi.org/10.3390/resources10080081, 2021.

Mengel, M., Treu, S., Lange, S., and Frieler, K.: ATTRICI v1. 1–counterfactual climate for impact attribution, Geoscientific Model Development, 14, 5269–5284, iSBN: 1991-9603 Publisher: Copernicus GmbH, 2021.

Menking, K. M., Syed, K. H., Anderson, R. Y., Shafike, N. G., and Arnold, J. G.: Model estimates of runoff in the closed, semiarid Estancia basin, central New Mexico, USA, Hydrological sciences journal, 48, 953–970, 2003.

Meyer, A. D., Tirry, D., Gulinck, H., and Orshoven, J. V.: Actualisatie MIRA Achtergronddocument Bodem - Thema Bodemafdichting, 2011.

Milieumaatschappij, V.: IMPACT-tool: verken de gevolgen van klimaatverandering. Klimaatportaal Vlaanderen, Tech. rep., URL https://klimaat.vmm.be/tools/impact, 2021.

Minnig, M., Moeck, C., Radny, D., and Schirmer, M.: Impact of urbanization on groundwater recharge rates in Dübendorf, Switzerland, Journal of Hydrology, 563, 1135–1146, https://doi.org/10.1016/j.jhydrol.2017.09.058, 2018.

Mishra, V., Cherkauer, K. A., and Shukla, S.: Assessment of drought due to historic climate variability and projected future climate change in the midwestern United States, Journal of Hydrometeorology, 11, 46–68, 2010.

Mitsch, W. J., Day, J. W., Gilliam, J. W., Groffman, P. M., Hey, D. L., Randall, G. W., and Wang, N.: Reducing Nitrogen Loading to the Gulf of Mexico from the Mississippi River Basin: Strategies to Counter a Persistent Ecological Problem: Ecotechnology—the use of natural ecosystems to solve environmental problems—should be a part of efforts to shrink the zone of hypoxia in the Gulf of Mexico, BioScience, 51, 373–388, https://doi.org/10.1641/0006-3568(2001)051[0373:RNLTTG]2.0.CO;2, 2001.

Modarres, R.: Streamflow drought time series forecasting, Stochastic Environmental Research and Risk Assessment, 21, 223–233, iSBN: 1436-3240 Publisher: Springer, 2007.

Moeskops, S.: River Kleine Nete: Creating ecological flooding zones at recreation areas, Tech. rep., Flanders Environmental Ageny, 2018.

Mohd Zaini, J. C., Saraf, N. M., Naharudin, N., Abdul Rasam, A. R., and Hashim, N.: Identifying Suitable Areas for Plantation of Organic Products Using GIS and AHP, IOP Conference Series: Earth and Environmental Science, 767, 012 009, https://doi.org/10.1088/1755-1315/767/1/012009, 2021.

Mondal, A. and Mujumdar, P. P.: On the basin-scale detection and attribution of human-induced climate change in monsoon precipitation and streamflow, Water Resources Research, 48, iSBN: 0043-1397 Publisher: Wiley Online Library, 2012.

Moore, W. S.: The effect of submarine groundwater discharge on the ocean, Annual review of marine science, 2, 59–88, URL https://www.annualreviews.org/doi/abs/10.1146/annurev-marine-120308-081019, 2010.

Morales, F. F. and de Vries, W. T.: Establishment of Natural Hazards Mapping Criteria Using Analytic Hierarchy Process (AHP), Frontiers in Sustainability, 2, 667 105, https://doi.org/10.3389/frsus.2021.667105, 2021.

Moriasi, D. N., Arnold, J. G., Van Liew, M. W., Bingner, R. L., Harmel, R. D., and Veith, T. L.: Model evaluation guidelines for systematic quantification of accuracy in watershed simulations, Transactions of the ASABE, 50, 885–900, https://doi.org/10.13031/2013.23153, 2007.

Moriasi, D. N., Gowda, P. H., Arnold, J. G., Mulla, D. J., Ale, S., Steiner, J. L., and Tomer, M. D.: Evaluation of the Hooghoudt and Kirkham tile drain equations in the Soil and Water Assessment Tool to simulate tile flow and nitrate-nitrogen, Journal of Environmental Quality, 42, 1699–1710, https://doi.org/10.2134/jeq2013.01.0018, 2013.

Moriasi, D. N., Gitau, M. W., Pai, N., and Daggupati, P.: Hydrologic and water quality models: Performance measures and evaluation criteria, Transactions of the ASABE, 58, 1763–1785, https://doi.org/10.13031/trans.58.10715, 2015.

Mubeen, A., Ruangpan, L., Vojinovic, Z., Sanchez Torrez, A., and Plavšić, J.: Planning and Suitability Assessment of Large-scale Nature-based Solutions for Flood-risk Reduction, Water Resources Management, 35, 3063–3081, https://doi.org/10.1007/s11269-021-02848-w, 2021.

Muenich, R. L., Kalcic, M., and Scavia, D.: Evaluating the impact of legacy P and agricultural conservation practices on nutrient loads from the Maumee River Watershed, Environmental Science & Technology, 50, 8146–8154, https://doi.org/10.1021/acs.est.6b01421, 2016.

Mukaka, M. M.: Statistics corner: A guide to appropriate use of correlation coefficient in medical research, Malawi Medical Journal, 24, 69–71, 2012.

Muma, M., Rousseau, A. N., and Gumiere, S. J.: Assessment of the impact of subsurface agricultural drainage on soil water storage and flows of a small watershed, Water, 8, 326, https://doi.org/10.3390/w8080326, 2016.

Naffees Gowsar, S., Nirmaladevi, M., Radha, M., Kumaraperumal, R., and Vishnu Shankar, S.: Characterization of Groundwater Quality using Principal Component Analysis of Andipalayam and Neruperichel blocks of Tiruppur District, International Archieve of Applied Sciences and Technology, 10, 76–83, https://doi.org/10.15515/iaast.0976-4828.10.2.7683, 2019.

NAIAD: NAIAD Case Studies: Medina del Campo Aquifer demonstration site \textbar Connecting Nature, URL https://connectingnature.eu/oppla-case-study/20457, n.d.

Nash, J. E. and Sutcliffe, J. V.: River flow forecasting through conceptual models part I—A discussion of principles, Journal of hydrology, 10, 282–290, https://doi.org/10.1016/0022-1694(70)90255-6, 1970.

Naz, B. S. and Bowling, L. C.: Automated identification of tile lines from remotely sensed data, Transactions of the ASABE, 51, 1937–1950, https://doi.org/10.13031/2013.25399, 2008.

Naz, B. S., Ale, S., and Bowling, L. C.: Detecting subsurface drainage systems and estimating drain spacing in intensively managed agricultural landscapes, Agricultural water management, 96, 627–637, https://doi.org/10.1016/j.agwat.2008.10.002, 2009.

Neitsch, S. L., Arnold, J. G., Kiniry, J. R., and Williams, J. R.: Soil and water assessment tool theoretical documentation version 2009, Tech. rep., Texas Water Resources Institute, URL https://oaktrust.library.tamu.edu/bitstream/handle/1969.1/128050/TR-406_SoilandWaterAssessmentToolTheoreticalDocumentation.pdf?sequence=1, 2011.

Nelson, D. R., Bledsoe, B. P., Ferreira, S., and Nibbelink, N. P.: Challenges to realizing the potential of nature-based solutions, Current Opinion in Environmental Sustainability, 45, 49–55, https://doi.org/10.1016/j.cosust.2020.09.001, 2020.

Nesshöver, C., Assmuth, T., Irvine, K. N., Rusch, G. M., Waylen, K. A., Delbaere, B., Haase, D., Jones-Walters, L., Keune, H., Kovacs, E., Krauze, K., Külvik, M., Rey, F., van Dijk, J., Vistad, O. I., Wilkinson, M. E., and Wittmer, H.: The science, policy and practice of nature-based solutions: An interdisciplinary perspective, Science of the Total Environment, 579, 1215–1227, https://doi.org/10.1016/j.scitotenv.2016.11.106, 2017.

Nguyen, T. T., Keupers, I., and Willems, P.: Conceptual river water quality model with flexible model structure, Environmental Modelling & Software, 104, 102–117, iSBN: 1364-8152 Publisher: Elsevier, 2018.

Nguyen, T. T., Ngo, H. H., Guo, W., Wang, X. C., Ren, N., Li, G., Ding, J., and Liang, H.: Implementation of a specific urban water management - Sponge City, Science of the Total Environment, 652, 147–162, https://doi.org/10.1016/j.scitotenv.2018.10.168, 2019.

Nguyen, T. V., Dietrich, J., Dang, T. D., Tran, D. A., Van Doan, B., Sarrazin, F. J., Abbaspour, K., and Srinivasan, R.: An interactive graphical interface tool for parameter calibration, sensitivity analysis, uncertainty analysis, and visualization for the Soil and Water Assessment Tool, Environmental Modelling & Software, 156, 105 497, https://doi.org/10.1016/j.envsoft.2022.105497, 2022.

Nichols, P. and Lucke, T.: Local level stormwater harvesting and reuse: A practical solution to the water security challenges faced by urban trees, Sustainability (Switzerland), 7, 8635–8648, https://doi.org/10.3390/su7078635, 2015.

Nkwasa, A., Chawanda, C. J., Schlemm, A., Ekolu, J., Frieler, K., and Van Griensven, A.: Historical climate impact attribution of changes in river flow and sediment loads at selected gauging stations in the Nile basin, Climatic Change, 177, 42, iSBN: 0165-0009 Publisher: Springer, 2024.

Nolan, R., Vesk, P., and Robinson, D.: Recovery potential of microwetlands from agricultural land uses, Ecological Management and Restoration, 19, 81–84, https://doi.org/10.1111/emr.12283, 2018.

Northcott, W. J., Verma, A. K., and Cooke, R. A.: Mapping subsurface drainage systems using remote sensing and GIS., Mapping subsurface drainage systems using remote sensing and GIS., pp. 1–10, 2000.

Nossent, J.: Sensitivity and uncertainty analysis in view of the parameter estimation of a SWAT model of the River Kleine Nete, URL https://researchportal.vub.be/en/publications/sensitivity-and-uncertainty-analysis-in-view-of-the-parameter-est, 2012.

Nossent, J., Elsen, P., and Bauwens, W.: Sobol'sensitivity analysis of a complex environmental model, Environmental Modelling & Software, 26, 1515–1525, https://doi.org/10.1016/j.envsoft.2011.08.010, 2011.

Ntegeka, V., Willems, P., Baguis, P., Roulin, E., Vansteenkiste, T., and Holvoet, K.: Climate change impacts on hydrological extremes (floods, low flows) along catchments in the Scheldt river basin, in: EGU General Assembly Conference Abstracts, p. 11048, 2010.

NWS, V.: VRT NWS, URL https://www.vrt.be/vrtnws/en/2024/05/30/past-six-months-were-the-wettest-since-records-began/, 2017.

NWS, V.: VRT NWS, URL https://www.vrt.be/vrtnws/nl/2017/06/08/stevenen_we_af_opeendrogezomerzoalsin1976-1-2998362/, 2022.

Nyquist, J. E., Freyer, P. A., and Toran, L.: Stream bottom resistivity tomography to map ground water discharge, Groundwater, 46, 561–569, 2008.

Odongo, R. A., De Moel, H., and Van Loon, A. F.: Propagation from meteorological to hydrological drought in the Horn of Africa using both standardized and threshold-based indices, Natural Hazards and Earth System Sciences, 23, 2365–2386, iSBN: 1684-9981 Publisher: Copernicus Publications Göttingen, Germany, 2023.

OECD: Nature-based solutions for adapting to water-related climate risks: Policy perspectives, Organization for Economic Cooperation and Development Paris, France, 2020.

Oosterbaan, R. J.: Agricultural drainage criteria, Drainage principles and applications, 16, 1–49, URL https://waterlog.info/pdf/chap17.pdf, 1994.

Oral, H. V., Carvalho, P., Gajewska, M., Ursino, N., Masi, F., van Hullebusch, E. D., Kazak, J. K., Exposito, A., Cipolletta, G., Andersen, T. R., Finger, D. C., Simperler, L., Regelsberger, M., Rous, V., Radinja, M., Buttiglieri, G., Krzeminski, P., Rizzo, A., Dehganian, K., Nikolova, M., and Zimmermann, M.: A review of nature-based solutions for urban water management in European circular cities: a critical assessment based on case studies and literature, Blue-Green Systems, 2, 112–136, https://doi.org/10.2166/bgs.2020.932, 2020.

Ouled Belgacem, A., Ben Salem, F., Gamoun, M., Chibani, R., and Louhaichi, M.: Revival of traditional best practices for rangeland restoration under climate change in the dry areas: A case study from Southern Tunisia, International Journal of Climate Change Strategies and Management, 11, 643–659, https://doi.org/10.1108/IJCCSM-02-2018-0019, 2019.

Oxtobee, J. P. and Novakowski, K.: A field investigation of groundwater/surface water interaction in a fractured bedrock environment, Journal of Hydrology, 269, 169–193, https://doi.org/10.1016/S0022-1694(02)00213-5, 2002.

Park, S., Nielsen, A., Bailey, R. T., Trolle, D., and Bieger, K.: A QGIS-based graphical user interface for application and evaluation of SWAT-MODFLOW models, Environmental modelling & software, 111, 493–497, https://doi.org/10.1016/j.envsoft.2018.10.017, 2019.

Pechlivanidis, I. G., Jackson, B. M., Mcintyre, N. R., and Wheater, H. S.: Catchment scale hydrological modelling: A review of model types, calibration approaches and uncertainty analysis methods in the context of recent developments in technology and applications, Global NEST journal, 13, 193–214, 2011.

Pellicer-Martínez, F., González-Soto, I., and Martínez-Paz, J. M.: Analysis of incorporating groundwater exchanges in hydrological models, Hydrological Processes, 29, 4361–4366, iSBN: 0885-6087 Publisher: Wiley Online Library, 2015.

Perkins, S. P. and Sophocleous, M.: Development of a comprehensive watershed model applied to study stream yield under drought conditions, Groundwater, 37, 418–426, https://doi.org/10.1111/j.1745-6584.1999.tb01121.x, 1999.

Perkins-Kirkpatrick, S. E., Stone, D. A., Mitchell, D. M., Rosier, S., King, A. D., Lo, Y. T. E., Pastor-Paz, J., Frame, D., and Wehner, M.: On the attribution of the impacts of extreme weather events to anthropogenic climate change, Environmental Research Letters, 17, 024 009, https://doi.org/10.1088/1748-9326/ac44c8, 2022.

Peters, E., Van Lanen, H. A. J., Torfs, P., and Bier, G.: Drought in groundwater—drought distribution and performance indicators, Journal of hydrology, 306, 302–317, iSBN: 0022-1694 Publisher: Elsevier, 2005.

Peterson, J. R. and Hamlett, J. M.: Hydrologic Calibration Of The Swat Model In A Watershed Containing Fragipan Soils 1, JAWRA Journal of the American Water Resources Association, 34, 531–544, https://doi.org/10.1111/j.1752-1688.1998.tb00952.x, 1998.

Piani, C., Weedon, G. P., Best, M., Gomes, S. M., Viterbo, P., Hagemann, S., and Haerter, J. O.: Statistical bias correction of global simulated daily precipitation and temperature for the application of hydrological models, Journal of hydrology, 395, 199–215, iSBN: 0022-1694 Publisher: Elsevier, 2010.

Pilliod, D. S., Rohde, A. T., Charnley, S., Davee, R. R., Dunham, J. B., Gosnell, H., Grant, G. E., Hausner, M. B., Huntington, J. L., and Nash, C.: Survey of Beaver-related Restoration Practices in Rangeland Streams of the Western USA, Environmental Management, 61, 58–68, https://doi.org/10.1007/s00267-017-0957-6, 2018.

Poelmans, L. and Van Rompaey, A.: Detecting and modelling spatial patterns of urban sprawl in highly fragmented areas: A case study in the Flanders-Brussels region, Landscape and Urban Planning, 93, 10–19, https://doi.org/10.1016/j.landurbplan.2009.05.018, 2009.

Possemiers, M., Huysmans, M., Peeters, L., Batelaan, O., and Dassargues, A.: Relationship between sedimentary features and permeability at different scales in the Brussels Sands, Geologica Belgica, URL https://popups.uliege.be/1374-8505/index.php?id=3627&gathStatIcon=true&lang=fr, 2012.

Putthividhya, A. and Laonamsai, J.: SWAT and MODFLOW modeling of spatio-temporal runoff and groundwater recharge distribution, in: World Environmental and Water Resources Congress 2017, pp. 51–65, https://doi.org/10.1061/9780784480618.006, 2017.

Quintana-Segui, P., Le Moigne, P., Durand, Y., Martin, E., Habets, F., Baillon, M., Canellas, C., Franchisteguy, L., and Morel, S.: Analysis of near-surface atmospheric variables: Validation of the SAFRAN analysis over France, Journal of applied meteorology and climatology, 47, 92–107, iSBN: 1558-8432, 2008.

Radonic, L.: Re-conceptualising Water Conservation: Rainwater Harvesting in the Desert of the Southwestern United States, Water Alternatives, 12, 699–714, 2019.

Raimonet, M., Oudin, L., Thieu, V., Silvestre, M., Vautard, R., Rabouille, C., and Le Moigne, P.: Evaluation of gridded meteorological datasets for hydrological modeling, Journal of Hydrometeorology, 18, 3027–3041, iSBN: 1525-755X, 2017.

Raymond, C. M., Frantzeskaki, N., Kabisch, N., Berry, P., Breil, M., Nita, M. R., Geneletti, D., and Calfapietra, C.: A framework for assessing and implementing the co-benefits of nature-based solutions in urban areas, Environmental Science and Policy, 77, 15–24, https://doi.org/10.1016/j.envsci.2017.07.008, 2017.

Rejani, R., Rao, K. V., Srinivasa Rao, C. H., Osman, M., Sammi Reddy, K., George, B., Pratyusha Kranthi, G. S., Chary, G. R., Swamy, M. V., and Rao, P. J.: Identification of Potential Rainwater-Harvesting Sites for the Sustainable Management of a Semi-Arid Watershed, Irrigation and Drainage, 66, 227–237, https://doi.org/10.1002/ird.2101, 2017.

Reynolds, E. P.: An automated method of identifying the location of agricultural field drainage tiles in northwest Ohio, The University of Toledo, URL https://etd.ohiolink.edu/apexprod/rws_etd/send_file/send?accession=toledo1404730697&disposition=inline, 2014.

Ricart, S. and Rico-amoros, A. M.: Constructed Wetlands to Face Water Scarcity and Water Pollution Risks: Learning from Farmers' Perception in Alicante, Spain, Water, 13, 2431, https://doi.org/10.3390/w13172431, 2021.

Ricciardiello, L., Leja, M., and Ollivier, M.: Horizon Europe, the new programme for research & innovation: Which opportunities for GI research in the years to come?, United European Gastroenterology Journal, 9, 407–409, 2021.

Richardson, C. M., Davis, K. L., Ruiz-González, C., Guimond, J. A., Michael, H. A., Paldor, A., Moosdorf, N., and Paytan, A.: The impacts of climate change on coastal groundwater, Nature Reviews Earth & Environment, 5, 100–119, iSBN: 2662-138X Publisher: Nature Publishing Group UK London, 2024.

Ringleb, J., Sallwey, J., and Stefan, C.: Assessment of managed aquifer recharge through modeling-A review, Water (Switzerland), 8, 579, https://doi.org/10.3390/w8120579, 2016.

Ritzema, H. P., Satyanarayana, T. V., Raman, S., and Boonstra, J.: Subsurface drainage to combat waterlogging and salinity in irrigated lands in India: Lessons learned in farmers' fields, Agricultural water management, 95, 179–189, https://doi.org/10.1016/j.agwat.2007.09.012, 2008.

Rocha, A. K. P., de Souza, L. S. B., de Assunção Montenegro, A. A., de Souza, W. M., and da Silva, T. G. F.: Revisiting the application of the SWAT model in arid and semi-arid regions: A selection from 2009 to 2022, Theoretical and Applied Climatology, 154, 7–27, iSBN: 0177-798X Publisher: Springer, 2023.

Roelens, J., Rosier, I., Dondeyne, S., Van Orshoven, J., and Diels, J.: Extracting drainage networks and their connectivity using LiDAR data, Hydrological processes, 32, 1026–1037, https://doi.org/10.1002/hyp.11472, 2018.

Rogé, P., Friedman, A., Astier, M., and Altieri, M.: Farmer Strategies for Dealing with Climatic Variability: A Case Study from the Mixteca Alta Region of Oaxaca, Mexico, Agroecology and Sustainable Food Systems, 38, 786–811, https://doi.org/10.1080/21683565.2014.900842, 2014.

Romano, G., Dal Sasso, P., Trisorio Liuzzi, G., and Gentile, F.: Multi-criteria decision analysis for land suitability mapping in a rural area of Southern Italy, Land Use Policy, 48, 131–143, https://doi.org/10.1016/j.landusepol.2015.05.013, 2015.

Roy, S.: Remote sensing & GIS applications for drainage detection and modeling in agricultural watersheds, PhD Thesis, URL https://scholarworks.iupui.edu/handle/1805/4086, 2014.

Rozemeijer, J. C., Van Der Velde, Y., McLaren, R. G., Van Geer, F. C., Broers, H. P., and Bierkens, M. F. P.: Integrated modeling of groundwater–surface water interactions in a tile-drained agricultural field: The importance of directly measured flow route contributions, Water Resources Research, 46, https://doi.org/10.1029/2010WR009155, 2010.

Ruangpan, L., Vojinovic, Z., Di Sabatino, S., Leo, L., Capobianco, V., Oen, A., Mcclain, M., and Lopez-Gunn, E.: Nature-based solutions for hydro-meteorological risk reduction: a state-of-the-art review of the research area, Natural Hazards and Earth System Sciences, 20, 243–270, https://doi.org/10.5194/nhess-20-243-2020, 2020.

Russo, T. A., Fisher, A. T., and Lockwood, B. S.: Assessment of managed aquifer recharge site suitability using a GIS and modeling, Groundwater, 53, 389–400, https://doi.org/10.1111/gwat.12213, 2015.

Saaty, T.: The Analytic Hierarchy Process, McGraw-Hill, New York, 1980.

Sahani, J., Kumar, P., Debele, S., Spyrou, C., Loupis, M., Aragão, L., Porcù, F., Shah, M., and Di Sabatino, S.: Hydro-meteorological risk assessment methods and management by nature-based solutions, Science of the Total Environment, 696, https://doi.org/10.1016/j.scitotenv.2019.133936, 2019.

Sallwey, J., Bonilla, J., Lopez, F., Junghanns, R., and Stephan, C.: Suitability maps for managed aquifer recharge: a review of multi-criteria decision analysis studies, Environmental Reviews, 27, 2018.

Sayl, K. N., Mohammed, A. S., and Ahmed, A. D.: GIS-based approach for rainwater harvesting site selection, IOP Conference Series: Materials Science and Engineering, 737, 012 246, https://doi.org/10.1088/1757-899X/737/1/012246, 2020.

Schilling, K. E., Gassman, P. W., Arenas-Amado, A., Jones, C. S., and Arnold, J.: Quantifying the contribution of tile drainage to basin-scale water yield using analytical and numerical models, Science of the Total Environment, 657, 297–309, https://doi.org/10.1016/j.scitotenv.2018.11.340, 2019.

Schober, P., Boer, C., and Schwarte, L. A.: Correlation coefficients: appropriate use and interpretation, Anesthesia & analgesia, 126, 1763–1768, iSBN: 0003-2999 Publisher: LWW, 2018.

Schoukens, H.: The Conservation of Aquifers in Flanders as a Regulatory Challenge: How to Avoid a Death by a Thousand Cuts?, Chinese Journal of Environmental Law, 6, 323–347, https://doi.org/10.1163/24686042-12340090, 2022.

Scibek, J., Allen, D. M., Cannon, A. J., and Whitfield, P. H.: Groundwater–surface water interaction under scenarios of climate change using a high-resolution transient groundwater model, Journal of Hydrology, 333, 165–181, https://doi.org/10.1016/j.jhydrol.2006.08.005, 2007.

Secci, D., Tanda, M. G., D'Oria, M., Todaro, V., and Fagandini, C.: Impacts of climate change on groundwater droughts by means of standardized indices and regional climate models, Journal of Hydrology, 603, 127 154, iSBN: 0022-1694 Publisher: Elsevier, 2021.

Sechu, G. L., Nilsson, B., Iversen, B. V., Greve, M. B., and Greve, M. H.: Historical Loss of Groundwater-Dependent Terrestrial Ecosystems in Undrained and Artificially Drained Landscapes in Denmark, Water, 15, 946, https://doi.org/10.3390/w15050946, 2023.

Seddon, N., Chausson, A., Berry, P., Girardin, C. A., Smith, A., and Turner, B.: Understanding the value and limits of nature-based solutions to climate change and other global challenges, Philosophical Transactions of the Royal Society B: Biological Sciences, 375, 20190 120, https://doi.org/10.1098/rstb.2019.0120, 2020.

Shangguan, W., Hengl, T., Mendes de Jesus, J., Yuan, H., and Dai, Y.: Mapping the global depth to bedrock for land surface modeling, Journal of Advances in Modeling Earth Systems, 9, 65–88, https://doi.org/10.1002/2016MS000686, 2017.

Siad, S. M., Iacobellis, V., Zdruli, P., Gioia, A., Stavi, I., and Hoogenboom, G.: A review of coupled hydrologic and crop growth models, Agricultural Water Management, 224, 105 746, https://doi.org/10.1016/j.agwat.2019.105746, 2019.

Silliman, S. E. and Booth, D. F.: Analysis of time-series measurements of sediment temperature for identification of gaining vs. losing portions of Juday Creek, Indiana, Journal of Hydrology, 146, 131–148, 1993.

Singh, J., Knapp, H. V., Arnold, J. G., and Demissie, M.: Hydrological modeling of the Iroquois river watershed using HSPF and SWAT 1, JAWRA Journal of the American

Water Resources Association, 41, 343–360, https://doi.org/10.1111/j.1752-1688.2005.tb03740.x, 2005.

Sivapalan, M.: Process complexity at hillslope scale, process simplicity at watershed scale: Is there a connection?, in: EGS-AGU-EUG Joint Assembly, p. 7973, 2003.

Sloan, B. P., Basu, N. B., and Mantilla, R.: Hydrologic impacts of subsurface drainage at the field scale: Climate, landscape and anthropogenic controls, Agricultural Water Management, 165, 1–10, https://doi.org/10.1016/j.agwat.2015.10.008, 2016.

Smedema, L. K., Abdel-Dayem, S., and Ochs, W. J.: Drainage and agricultural development, Irrigation and Drainage Systems, 14, 223–235, https://doi.org/10.1023/A:1026570823692, 2000.

Smith, D. R., Livingston, S. J., Zuercher, B. W., Larose, M., Heathman, G. C., and Huang, C.: Nutrient losses from row crop agriculture in Indiana, Journal of Soil and Water Conservation, 63, 396–409, https://doi.org/10.2489/jswc.63.6.396, 2008.

Smith, L. and Freeze, R. A.: Stochastic analysis of steady state groundwater flow in a bounded domain: 2. Two-dimensional simulations, Water Resources Research, 15, 1543–1559, iSBN: 0043-1397 Publisher: Wiley Online Library, 1979.

Sobol', I. M.: On sensitivity estimation for nonlinear mathematical models, Matematicheskoe modelirovanie, 2, 112–118, URL http://computeroptics.ru/KO/PDF/KO39-4/390403.pdf, 1990.

Soliman, K., Sallam, O. M., and Schüth, C.: Delineating MAR Sites Using GIS-MCDA for Nuweiba Alluvial Fan Aquifer, Sinai, Egypt, Water (Switzerland), 14, 475, https://doi.org/10.3390/w14030475, 2022.

Sophocleous, M. A., Koelliker, J. K., Govindaraju, R. S., Birdie, T., Ramireddygari, S. R., and Perkins, S. P.: Integrated numerical modeling for basin-wide water management: The case of the Rattlesnake Creek basin in south-central Kansas, Journal of Hydrology, 214, 179–196, 1999.

Spinoni, J., Naumann, G., Carrao, H., Barbosa, P., and Vogt, J.: World drought frequency, duration, and severity for 1951-2010: WORLD DROUGHT CLIMATOLOGIES FOR 1951-2010, International Journal of Climatology, 34, 2792–2804, https://doi.org/10.1002/joc.3875, 2014.

Spinoni, J., Vogt, J. V., Naumann, G., Barbosa, P., and Dosio, A.: Will drought events become more frequent and severe in Europe?, iSBN: 0899-8418 Publisher: John Wiley & Sons Ltd, 2018.

Spruill, C. A., Workman, S. R., and Taraba, J. L.: Simulation of daily and monthly stream discharge from small watersheds using the SWAT model, Transactions of the ASAE, 43, 1431, https://doi.org/10.13031/2013.3041, 2000.

Sreedevi, S., Kunnath-Poovakka, A., and Eldho, T. I.: Comparison of Conceptual and Distributed Hydrological Models for Runoff Estimation in a River Basin, in: The Ganga River Basin: A Hydrometeorological Approach, pp. 135–148, Springer, 2021.

Sridhar, V., Billah, M. M., and Hildreth, J. W.: Coupled surface and groundwater hydrological modeling in a changing climate, Groundwater, 56, 618–635, 2018.

Srivastava, P., McNair, J. N., and Johnson, T. E.: COMPARISON OF PROCESS-BASED AND ARTIFICIAL NEURAL NETWORK APPROACHES FOR STREAMFLOW MODELING IN AN AGRICULTURAL WATERSHED 1, JAWRA Journal of the American Water Resources Association, 42, 545–563, https://doi.org/10.1111/j.1752-1688.2006.tb04475.x, 2006.

Stagge, J. H., Tallaksen, L. M., Gudmundsson, L., Van Loon, A. F., and Stahl, K.: Candidate distributions for climatological drought indices (SPI and SPEI), International Journal of Climatology, 35, 4027–4040, https://doi.org/https://doi.org/10.1002/joc.4267, 2015.

Stagge, J. H., Kingston, D. G., Tallaksen, L. M., and Hannah, D. M.: Observed drought indices show increasing divergence across Europe, Scientific Reports, 7, 1–10, iSBN: 2045-2322 Publisher: Nature Publishing Group, 2017.

Stefania, G. A., Rotiroti, M., Fumagalli, L., Simonetto, F., Capodaglio, P., Zanotti, C., and Bonomi, T.: Modeling groundwater/surface-water interactions in an Alpine valley (the Aosta Plain, NW Italy): the effect of groundwater abstraction on surface-water resources, Hydrogeology Journal, 26, 147–162, https://doi.org/10.1007/s10040-017-1633-x, 2018.

Stillman, J. S., Haws, N. W., Govindaraju, R. S., and Rao, P. S. C.: A semi-analytical model for transient flow to a subsurface tile drain, Journal of Hydrology, 317, 49–62, https://doi.org/10.1016/j.jhydrol.2005.04.028, 2006.

Stoll, S., Hendricks Franssen, H.-J., Butts, M., and Kinzelbach, W.: Analysis of the impact of climate change on groundwater related hydrological fluxes: a multi-model approach including different downscaling methods, Hydrology and Earth System Sciences, 15, 21–38, iSBN: 1027-5606 Publisher: Copernicus GmbH, 2011.

Stott, P. A., Gillett, N. P., Hegerl, G. C., Karoly, D. J., Stone, D. A., Zhang, X., and Zwiers, F.: Detection and attribution of climate change: a regional perspective, Wiley interdisciplinary reviews: climate change, 1, 192–211, iSBN: 1757-7780 Publisher: Wiley Online Library, 2010.

Streck, N. A., Rundquist, D., and Connot, J.: Estimating residual wheat dry matter from remote sensing measurements, Photogrammetric Engineering and Remote Sensing, 68, 1193–1202, URL https://www.asprs.org/wp-content/uploads/pers/2002journal/november/2002_nov_1193-1201.pdf, 2002.

Sugg, Z.: Assessing US farm drainage: Can GIS lead to better estimates of subsurface drainage extent, World Resources Institute, Washington, DC, 20002, 2007.

Sun, W., Ishidaira, H., Bastola, S., and Yu, J.: Estimating daily time series of streamflow using hydrological model calibrated based on satellite observations of river water surface width: Toward real world applications, Environmental research, 139, 36–45, iSBN: 0013-9351 Publisher: Elsevier, 2015.

Sun, X., Wang, J., Ma, M., and Han, X.: Attribution of Extreme Drought Events and Associated Physical Drivers across Southwest China Using the Budyko Framework, Remote Sensing, 15, 2702, https://doi.org/10.3390/rs15112702, 2023.

Sung, J. H. and Chung, E.-S.: Development of streamflow drought severity–duration–frequency curves using the threshold level method, Hydrology and Earth System Sciences, 18, 3341–3351, iSBN: 1027-5606 Publisher: Copernicus GmbH, 2014.

Sur, C., Park, S.-Y., Kim, J.-S., and Lee, J.-H.: Prognostic and diagnostic assessment of hydrological drought using water and energy budget-based indices, Journal of Hydrology, 591, 125 549, iSBN: 0022-1694 Publisher: Elsevier, 2020.

Sy, M., Baguian, H., and Gahi, N.: Multiple Use of Green Spaces in Bobo-Dioulasso, Burkina Faso, Urban Agriculture, 27, 33–36, 2014.

Tabari, H., Taye, M. T., and Willems, P.: Water availability change in central Belgium for the late 21st century, Global and planetary change, 131, 115–123, iSBN: 0921-8181 Publisher: Elsevier, 2015.

Tallaksen, L. M., Hisdal, H., and Van Lanen, H. A.: Space–time modelling of catchment scale drought characteristics, Journal of Hydrology, 375, 363–372, iSBN: 0022-1694 Publisher: Elsevier, 2009.

Tam, V. T. and Nga, T. T. V.: Assessment of urbanization impact on groundwater resources in Hanoi, Vietnam, Journal of environmental management, 227, 107–116, 2018.

Tarek, M., Brissette, F., and Arsenault, R.: Uncertainty of gridded precipitation and temperature reference datasets in climate change impact studies, Hydrology and Earth System Sciences, 25, 3331–3350, iSBN: 1027-5606 Publisher: Copernicus GmbH, 2021.

Taylor, R. G., Scanlon, B., and Döll, P.: Ground water and climate change Nature Climate Change, 2013.

Thayn, B. J., Campbell, M., Deloriea, T., Thayn, B. J., Campbell, M., and Deloriea, T.: Mapping Tile-Drained Agriculture Land, The Institute for Geospatial Analysis and Mapping (GEOMAP), Illinois State University Institute, 2011.

Thompson, J.: Identifying subsurface tile drainage systems utilizing remote sensing techniques, PhD Thesis, University of Toledo, URL http://rave.ohiolink.edu/etdc/view?acc_num=toledo1290141705, 2010.

Tigabu, T. B., Wagner, P. D., Hörmann, G., and Fohrer, N.: Modeling the spatio-temporal flow dynamics of groundwater-surface water interactions of the Lake Tana Basin, Upper Blue Nile, Ethiopia, Hydrology Research, 51, 1537–1559, 2020.

Tilahun, T. and Seyoum, W. M.: High-resolution mapping of tile drainage in agricultural fields using unmanned aerial system (UAS)-based radiometric thermal and optical sensors, Hydrology, 8, 2, https://doi.org/10.3390/hydrology8010002, 2020.

Tomer, M. D., Moorman, T. B., and Rossi, C. G.: Assessment of the Iowa River's South Fork watershed: part 1. Water quality, journal of soil and water conservation, 63, 360–370, https://doi.org/10.2489/jswc.63.6.360, 2008.

Topuz, M. and Deniz, M.: Application of GIS and AHP for land use suitability analysis: case of Demirci district (Turkey), Humanities and Social Sciences Communications, 10, 115, https://doi.org/10.1057/s41599-023-01609-x, 2023.

Trémolet, S., Favero, A., Karres, N., Toledo, M., Makropoulos, C., Lykou, A., Hanania, S., Rebollo, V., and Anton, B.: Investing in Nature for Europe Water Security, Tech. rep., 2019.

Tuohy, P., Humphreys, J., Holden, N. M., and Fenton, O.: Runoff and subsurface drain response from mole and gravel mole drainage across episodic rainfall events, Agricultural Water Management, 169, 129–139, https://doi.org/10.1016/j.agwat.2016.02.020, 2016.

UN: Drought in Numbers, URL https://reliefweb.int/attachments/56b8b7cc-cb67-374a-b79a-8a593360b5c8/Drought%20in%20Numbers.pdf, 2022.

Uniyal, B., Jha, M. K., and Verma, A. K.: Assessing climate change impact on water balance components of a river basin using SWAT model, Water resources management, 29, 4767–4785, iSBN: 0920-4741 Publisher: Springer, 2015.

Valayamkunnath, P., Barlage, M., Chen, F., Gochis, D. J., and Franz, K. J.: Mapping of 30-meter resolution tile-drained croplands using a geospatial modeling approach, Scientific data, 7, 1–10, https://doi.org/10.6084/m9.figshare.12668234, 2020.

Valipour, M., Krasilnikof, J., Yannopoulos, S., Kumar, R., Deng, J., Roccaro, P., Mays, L., Grismer, M. E., and Angelakis, A. N.: The evolution of agricultural drainage from the earliest times to the present, Sustainability, 12, 416, https://doi.org/10.3390/su12010416, 2020.

Van Camp, M., Coetsiers, M., Martens, K., and Walraevens, K.: Effects of multi-annual climate variability on the hydrodynamic evolution (1833 to present) in a shallow aquifer system in northern Belgium, Hydrological sciences journal, 55, 763–779, iSBN: 0262-6667 Publisher: Taylor & Francis, 2010.

Van der Kamp, G. and Hayashi, M.: Groundwater-wetland ecosystem interaction in the semiarid glaciated plains of North America, Hydrogeology Journal, 17, 203, 2009.

Van der Velde, Y., De Rooij, G. H., and Torfs, P.: Catchment-scale non-linear groundwater-surface water interactions in densely drained lowland catchments, Hydrology and Earth System Sciences, 13, 1867–1885, https://doi.org/10.5194/hess-13-1867-2009, 2009.

Van Der Zee, S., Stofberg, S. F., Yang, X., Liu, Y., Islam, M. N., and Hu, Y. F.: Irrigation and drainage in agriculture: a salinity and environmental perspective, Current perspective on irrigation and drainage, pp. 1–21, https://doi.org/10.5772/66046, 2017.

Van Huijgevoort, M. H., Hazenberg, P., Van Lanen, H. A., and Uijlenhoet, R.: A generic method for hydrological drought identification across different climate regions, Hydrology and Earth System Sciences, 16, 2437–2451, iSBN: 1027-5606 Publisher: Copernicus GmbH, 2012.

Van Lanen, H. A. and Peters, E.: Definition, effects and assessment of groundwater droughts, in: Drought and drought mitigation in Europe, pp. 49–61, Springer, 2000.

Van Loon, A. F.: On the Propagation of Drought.: How Climate and Catchment Characteristics Influence Hydrological Drought Development and Recovery, Wageningen University and Research, 2013.

Van Loon, A. F.: Hydrological drought explained, WIREs Water, 2, 359–392, https://doi.org/10.1002/wat2.1085, 2015.

Van Loon, A. F., Van Huijgevoort, M. H. J., and Van Lanen, H. A. J.: Evaluation of drought propagation in an ensemble mean of large-scale hydrological models, Hydrology and Earth System Sciences, 16, 4057–4078, iSBN: 1027-5606 Publisher: Copernicus GmbH, 2012.

Van Loon, A. F., Tijdeman, E., Wanders, N., Van Lanen, H. J., Teuling, A. J., and Uijlenhoet, R.: How climate seasonality modifies drought duration and deficit, Journal of Geophysical Research: Atmospheres, 119, 4640–4656, iSBN: 2169-897X Publisher: Wiley Online Library, 2014.

Van Oldenborgh, G. J., Van Der Wiel, K., Kew, S., Philip, S., Otto, F., Vautard, R., King, A., Lott, F., Arrighi, J., Singh, R., and Van Aalst, M.: Pathways and pitfalls in extreme event attribution, Climatic Change, 166, 13, https://doi.org/10.1007/s10584-021-03071-7, 2021.

Van Oost, K., Verstraeten, G., Doetterl, S., Notebaert, B., Wiaux, F., Broothaerts, N., and Six, J.: Legacy of human-induced C erosion and burial on soil–atmosphere C exchange, Proceedings of the National Academy of Sciences, 109, 19 492–19 497, https://doi.org/10.1073/pnas.1211162109, 2012.

Vandersteen, K., Gedeon, M., and Beerten, K.: A synthesis of hydraulic conductivity measurements of the subsurface in Northeastern Belgium, Geologica Belgica, URL https://popups.uliege.be/1374-8505/index.php?id=4592&file=1&pid=4587, 2014.

Vansteenkiste, T., Tavakoli, M., Ntegeka, V., De Smedt, F., Batelaan, O., Pereira, F., and Willems, P.: Intercomparison of hydrological model structures and calibration approaches in climate scenario impact projections, Journal of Hydrology, 519, 743–755, iSBN: 0022-1694 Publisher: Elsevier, 2014.

Varner, B. L., Gress, T. A., and White, S. E.: The effectiveness and economic feasibility of image-based agricultural tile maps., in: Proceedings of the 6th International Conference on Precision Agriculture and Other Precision Resources Management, Minneapolis, MN, USA, 14-17 July, 2002, pp. 1450–1464, American Society of Agronomy, 2003.

Verma, A. K., Cooke, R. A., and Wendte, L.: Mapping subsurface drainage systems with color infrared aerial photographs, Urbana-Champaign: Department of Agricultural Engineering, University of Illinois, 1996.

Vicente-Serrano, S. M., Beguería, S., and López-Moreno, J. I.: A multiscalar drought index sensitive to global warming: the standardized precipitation evapotranspiration index, Journal of climate, 23, 1696–1718, https://doi.org/https://doi.org/10.1175/2009JCLI2909.1, 2010.

Vicente-Serrano, S. M., Peña-Angulo, D., Beguería, S., Domínguez-Castro, F., Tomás-Burguera, M., Noguera, I., Gimeno-Sotelo, L., and El Kenawy, A.: Global drought trends and future projections, Philosophical Transactions of the Royal Society A: Mathematical, Physical and Engineering Sciences, 380, 20210 285, https://doi.org/10.1098/rsta.2021.0285, 2022.

VITO: 1 in 4 Flemish people work in a water-intensive sector, URL https://vito.be/en/news/1-4-flemish-people-work-water-intensive-sector, 2022.

VMM: Uitwerking van een reactief afwegingskader voor prioritair watergebruik tijdens waterschaarste, Tech. rep., VMM, De Vlaamse Waterweg, KU Leuven, Department of Environment, & Department of Agriculture and Fisheries, URL https://www.vmm.be/bestanden/VRAG-Eindrapport_TW.pdf, 2021.

Voeckler, H. M., Allen, D. M., and Alila, Y.: Modeling coupled surface water–Groundwater processes in a small mountainous headwater catchment, Journal of Hydrology, 517, 1089–1106, https://doi.org/10.1016/j.jhydrol.2014.06.015, 2014.

Vriens, L., Van Hove, M., Paelinckx, D., and Heirman, J.: Biologische Waarderingskaart, Kaartbladen 15, Tech. rep., Rapport van het Instituut voor Natuur- en Bosonderzoek INBO.R.2006.10, Brussel, 2006.

Vu, M. T., Raghavan, S. V., and Liong, S.-Y.: SWAT use of gridded observations for simulating runoff–a Vietnam river basin study, Hydrology and Earth System Sciences, 16, 2801–2811, iSBN: 1027-5606 Publisher: Copernicus GmbH, 2012.

Wagner, W., Lemoine, G., and Rott, H.: A method for estimating soil moisture from ERS scatterometer and soil data, Remote sensing of environment, 70, 191–207, https://doi.org/10.1016/S0034-4257(99)00036-X, 1999.

Waibel, M. S., Gannett, M. W., Chang, H., and Hulbe, C. L.: Spatial variability of the response to climate change in regional groundwater systems–Examples from simulations in the Deschutes Basin, Oregon, Journal of Hydrology, 486, 187–201, 2013.

Wang, H., Chen, Y., Pan, Y., Chen, Z., and Ren, Z.: Assessment of candidate distributions for SPI/SPEI and sensitivity of drought to climatic variables in China, International Journal of Climatology, 39, 4392–4412, https://doi.org/https://doi.org/10.1002/joc.6081, 2019.

Wang, M., Zhang, Y., Lu, Y., Gao, L., and Wang, L.: Attribution analysis of streamflow changes based on large-scale hydrological modeling with uncertainties, Water Resources Management, 37, 713–730, iSBN: 0920-4741 Publisher: Springer, 2023.

Wang, Y. and Chen, N.: Recent progress in coupled surface–ground water models and their potential in watershed hydro-biogeochemical studies: A review, Watershed Ecology and the Environment, 3, 17–29, 2021.

Ward, M., Poleacovschi, C., and Perez, M.: Using AHP and spatial analysis to determine water surface storage suitability in Cambodia, Water (Switzerland), 13, 367, https://doi.org/10.3390/w13030367, 2021.

Warsta, L., Karvonen, T., Koivusalo, H., Paasonen-Kivekäs, M., and Taskinen, A.: Simulation of water balance in a clayey, subsurface drained agricultural field with three-dimensional FLUSH model, Journal of hydrology, 476, 395–409, https://doi.org/10.1016/j.jhydrol.2012.10.053, 2013.

Welderufael, W. A., Woyessa, Y. E., and Edossa, D. C.: Impact of rainwater harvesting on water resources of the modder river basin, central region of South Africa, Agricultural Water Management, 116, 218–227, https://doi.org/10.1016/j.agwat.2012.07.012, 2013.

White, M. J., Harmel, R. D., Arnold, J. G., and Williams, J. R.: SWAT check: A screening tool to assist users in the identification of potential model application problems, Journal of environmental quality, 43, 208–214, https://doi.org/10.2134/jeq2012.0039, 2014.

Wilhite, D. and Glantz, M.: Understanding the drought phenomenon: The role of definitions, Water International, 10, 111–120, https://doi.org/10.4324/9780429301735-2, 1985.

Williams, M. R., King, K. W., and Fausey, N. R.: Drainage water management effects on tile discharge and water quality, Agricultural water management, 148, 43–51, https://doi.org/10.1016/j.agwat.2014.09.017, 2015.

Winchell, M., Srinivasan, R., Di Luzio, M., and Arnold, J.: ArcSWAT interface for SWAT 2005, User's guide, pp. 1–436, 2007.

Woessner, W. W.: Stream and fluvial plain ground water interactions: rescaling hydrogeologic thought, Groundwater, 38, 423–429, https://doi.org/10.1111/j.1745-6584.2000.tb00228.x, 2000.

Woldeamlak, S. T.: Spatio-temporal impacts of climate and land-use changes on the groundwater and surface water resources of a lowland catchment, PhD Thesis, PhD Thesis, Vrije Universiteit Brussels, Belgium, 2007.

Woo, D. K., Song, H., and Kumar, P.: Mapping subsurface tile drainage systems with thermal images, Agricultural Water Management, 218, 94–101, https://doi.org/10.1016/j.agwat.2019.01.031, 2019.

Wossenyeleh, B. K., Worku, K. A., Verbeiren, B., and Huysmans, M.: Drought propagation and its impact on groundwater hydrology of wetlands: a case study on the Doode Bemde nature reserve (Belgium), Natural Hazards and Earth System Sciences, 21, 39–51, https://doi.org/10.5194/nhess-21-39-2021, 2021.

Wu, R., Zhang, C., Li, Y., Zhu, C., Lu, L., Cui, C., Zhang, Z., Wang, S., Chu, J., and Li, Y.: Assessment of variability and attribution of drought based on GRACE in China from three perspectives: Water storage component, climate change, water balance, Remote Sensing, 15, 4426, iSBN: 2072-4292 Publisher: MDPI, 2023.

Wu, W.-Y., Lo, M.-H., Wada, Y., Famiglietti, J. S., Reager, J. T., Yeh, P. J.-F., Ducharne, A., and Yang, Z.-L.: Divergent effects of climate change on future groundwater availability in key mid-latitude aquifers, Nature communications, 11, 3710, iSBN: 2041-1723 Publisher: Nature Publishing Group UK London, 2020.

Wunsch, A., Liesch, T., and Broda, S.: Deep learning shows declining groundwater levels in Germany until 2100 due to climate change, Nature communications, 13, 1221, iSBN: 2041-1723 Publisher: Nature Publishing Group UK London, 2022.

WWAP (United Nations World Water Assessment Programme) and UN-Water: The United Nations World Water Development Report 2018: Nature-Based Solutions for Water, URL www.unwater.org/publications/%0Aworld-water-development-report-2018/, 2018.

Yatagai, A., Arakawa, O., Kamiguchi, K., Kawamoto, H., Nodzu, M. I., and Hamada, A.: A 44-year daily gridded precipitation dataset for Asia based on a dense network of rain gauges, Sola, 5, 137–140, iSBN: 1349-6476 Publisher: Meteorological Society of Japan, 2009.

Yen, H., Park, S., Arnold, J. G., Srinivasan, R., Chawanda, C. J., Wang, R., Feng, Q., Wu, J., Miao, C., and Bieger, K.: IPEAT+: A built-in optimization and automatic calibration tool of SWAT+, Water, 11, 1681, https://doi.org/10.3390/w11081681, 2019.

Yevjevich, V. M.: An objective approach to definitions and investigations of continental hydrologic droughts, vol. 23, Colorado State University Fort Collins, CO, USA, 1967.

Yimer, E. A., Van Schaeybroeck, B., Van De Vyver, H., and Van Griensven, A.: Evaluating Probability Distribution Functions for the Standardized Precipitation Evapotranspiration Index over Ethiopia, Atmosphere, 13, 364, https://doi.org/10.3390/atmos13030364, 2022.

Yimer, E. A., Bailey, R. T., Piepers, L. L., Nossent, J., and Van Griensven, A.: Improved Representation of Groundwater–Surface Water Interactions Using SWAT+gwflow and Modifications to the gwflow Module, Water, 15, 3249, https://doi.org/10.3390/w15183249, 2023a.

Yimer, E. A., Riakhi, F.-E., Bailey, R. T., Nossent, J., and van Griensven, A.: The impact of extensive agricultural water drainage on the hydrology of the Kleine Nete watershed, Belgium, Science of The Total Environment, 885, 163 903, https://doi.org/10.1016/j.scitotenv.2023.163903, 2023b.

Yimer, E. A., T. Bailey, R., Van Schaeybroeck, B., Van De Vyver, H., Villani, L., Nossent, J., and Van Griensven, A.: Regional evaluation of groundwater-surface water interactions using a coupled geohydrological model (SWAT+gwflow), Journal of Hydrology: Regional Studies, 50, 101 532, https://doi.org/10.1016/j.ejrh.2023.101532, 2023c.

Yimer, E. A., De Trift, L., Dondeyne, S., Speijer, L., Huysmans, M., Cools, J., Nossent, J., and Van Griensven, A.: Framework for mapping large-scale nature-based solutions for drought mitigation: Regional application in Flanders, Water Research, 261, 122 003, https://doi.org/10.1016/j.watres.2024.122003, 2024a.

Yimer, E. A., De Trift, L., Lobkowicz, I., Villani, L., Nossent, J., and van Griensven, A.: The underexposed nature-based solutions: A critical state-of-art review on drought mitigation, Journal of Environmental Management, 352, 119 903, https://doi.org/10.1016/j.jenvman.2023.119903, 2024b.

Ying, Z., Tetzlaff, D., Comte, J.-C., Wu, S., and Soulsby, C.: Storage Dynamics and Groundwater–Surface Water Interactions in a Drought Sensitive Lowland Catchment: Process-Based Modelling as a Learning Tool, Hydrological Processes, 39, e70 141, 2025.

You, Q., Min, J., Zhang, W., Pepin, N., and Kang, S.: Comparison of multiple datasets with gridded precipitation observations over the Tibetan Plateau, Climate Dynamics, 45, 791–806, iSBN: 1432-0894 Publisher: Springer, 2015.

Yuan, X., Jiao, Y., Yang, D., and Lei, H.: Reconciling the attribution of changes in streamflow extremes from a hydroclimate perspective, Water Resources Research, 54, 3886–3895, iSBN: 0043-1397 Publisher: Wiley Online Library, 2018.

Zaitchik, B. F., Rodell, M., Biasutti, M., and Seneviratne, S. I.: Wetting and drying trends under climate change, Nature Water, 1, 502–513, iSBN: 2731-6084 Publisher: Nature Publishing Group UK London, 2023.

Zambrano-Bigiarini, M. and Rojas, R.: A model-independent Particle Swarm Optimisation software for model calibration, Environmental Modelling & Software, 43, 5–25, https://doi.org/10.1016/j.envsoft.2013.01.004, 2013.

Zare, M., Azam, S., and Sauchyn, D.: A modified SWAT model to simulate soil water content and soil temperature in cold regions: a case study of the south saskatchewan river basin in Canada, Sustainability, 14, 10 804, iSBN: 2071-1050 Publisher: MDPI, 2022.

Zelenhasić, E. and Salvai, A.: A method of streamflow drought analysis, Water resources research, 23, 156–168, iSBN: 0043-1397 Publisher: Wiley Online Library, 1987.

Zhang, H., Yang, L., and Li, M.: A novel comprehensive model of suitability analysis for matching area in underwater geomagnetic aided inertial navigation, Mathematical Problems in Engineering, 2019, 1–11, https://doi.org/10.1155/2019/9740812, 2019.

Zhang, H., Xu, Y., and Kanyerere, T.: A review of the managed aquifer recharge: Historical development, current situation and perspectives, Physics and Chemistry of the Earth, 118-119, 102 887, https://doi.org/10.1016/j.pce.2020.102887, 2020.

Zhang, J., Fu, D., and Zevenbergen, C.: Moving Towards Water Sensitive Cities: A Planning Framework, Underlying Principles, and Technologies—Case Study Kunshan Sponge City, in: Encyclopedia of Inland Waters, Second Edition, vol. 4, pp. 399–416, Elsevier, https://doi.org/10.1016/B978-0-12-819166-8.00185-7, 2022.

Zhang, X., Srinivasan, R., Zhao, K., and Liew, M. V.: Evaluation of global optimization algorithms for parameter calibration of a computationally intensive hydrologic model, Hydrological Processes: An International Journal, 23, 430–441, https://doi.org/10.1002/hyp.7152, 2009.

Zhaoqiang, Z., Ping, W., Linqi, L., Qiang, F., Yibo, D., Peng, C., Ping, X., Tian, W., and Haiyun, S.: Recent development on drought propagation: A comprehensive review, Journal of Hydrology, p. 132196, iSBN: 0022-1694 Publisher: Elsevier, 2024.

Zhou, Z., Wang, P., Li, L., Fu, Q., Ding, Y., Chen, P., Xue, P., Wang, T., and Shi, H.: Recent development on drought propagation: A comprehensive review, Journal of Hydrology, 645, 132 196, https://doi.org/10.1016/j.jhydrol.2024.132196, 2024.

Zhu, Y., Wang, W., Singh, V. P., and Liu, Y.: Combined use of meteorological drought indices at multi-time scales for improving hydrological drought detection, Science of the Total Environment, 571, 1058–1068, iSBN: 0048-9697 Publisher: Elsevier, 2016.

Zhu, Y., Liu, Y., Wang, W., Singh, V. P., and Ren, L.: A global perspective on the probability of propagation of drought: From meteorological to soil moisture, Journal of Hydrology, 603, 126 907, iSBN: 0022-1694 Publisher: Elsevier, 2021.

Zomlot, Z., Verbeiren, B., Huysmans, M., and Batelaan, O.: Spatial distribution of groundwater recharge and base flow: Assessment of controlling factors, Journal of Hydrology: Regional Studies, 4, 349–368, https://doi.org/10.1016/j.ejrh.2015.07.005, 2015a.

Zomlot, Z., Verbeiren, B., Huysmans, M., and Batelaan, O.: Spatial distribution of groundwater recharge and base flow: Assessment of controlling factors, Journal of Hydrology: Regional Studies, 4, 349–368, https://doi.org/10.1016/j.ejrh.2015.07.005, iSBN: 2214-5818 Publisher: Elsevier, 2015b.